Institute of Crop Science
University of Hohenheim
Department of Product Quality of Specialty Crops
PD Dr. Götz M. Reustle

Analysis of the interaction between the helper component proteinase (HC-Pro) of *Zucchini yellow mosaic virus* (ZYMV) and the plant RNA methyltransferase Hua enhancer 1 (HEN1)

Dissertation

Submitted in fulfilment of the requirements for the degree 'Doktor der Agrawissenschaften´ (Dr. sc. agr. / Ph.D in Agricultural Sciences)

To the

Faculty of Agricultural Sciences

Presented by

Rana M. Jamoos
Nablus (Palestine)

2012

This thesis was accepted as a doctoral dissertation in fulfillment of the requirements for the degree “Doktor der Agrawissenschaften” by the Faculty of Agricultural Sciences at University of Hohenheim. On 7 August 2012

Date of Examination: 7 August 2012

Examination Committee

Supervisor and Review	Dr. G. Reustle
Co-Reviewer	Prof. Dr. G. Weber
Additional examiner	Dr: M. Wassenegger
Vice Dean and Head of Committee	Prof. Dr. A. Fangmeier

Abbreviations

Aa	Amino acids
AbA	Aureobasidin A
ACLSV	Apple chlorotic leaf spot virus
ACMV	African cassava mosaic virus
Ade	Adenosine
AGO	Argonaute
BiMoV	Bidens mottle virus
BNYVV	Beet necrotic yellow vein virus
Bp	Base pair
BSA	Bovine serum albumin
BSMV	Barley stripe mosaic virus
BtMV	Beet mosaic virus
BWYV	Beet western yellows virus
BYMV	Bean yellow mosaic virus
BYV	Beet yellows virus
CABMV	Cowpea aphid-borne mosaic virus
Caf	Carpelfactory
CaMV	Cauliflower mosaic virus
cDNA	Complementary DNA strand
CHS	chalcone synthase gene
CIRV	Carnation Italian ringspot virus
CIYVV	Clover yellow vein virus
CMV	Cucumber mosaic virus
CP	Coat protein
DCL1	Dicer-like protein
DMSO	Dimethyl sulfoxide
DMTase	DNA methyltransferases
dNTPs	Deoxynucleoside triphosphates
DRM	Domain rearranged methyltransferases
dsRBD	double-stranded RNA binding domain
dsRNA	Double-stranded RNA
DTT	Dithiothreitol
ECL	Enhanced chemiluminescence
EDTA	Ethylene diamine tetracteic acid
EF1-α	Eukaryotic elongation factor 1-α
eIF4a	Eukaryotic initiation factor 4-A
ELISA	Enzyme-linked immunosorbent assay
ER	Endoplasmic reticulum
EtBr	Ethidium bromide
GUS	Beta-glucoronidase
HC-Pro	Helper-component proteinase
HDA6	Histone deacetylase
HEN 1	HUA ENHANCER 1
His	Histidine
Hr	Hour
IPTG	Isopropyl-β-D-1-thiogalactopyranoside
IR-PTGS	Inverted-repeat transgenes
kDa	Kilo dalton
LB	Luria-Bertani
Leu	Leucine
LMV	Lettuce mosaic virus
MBP	Maltose-binding protein
MES	2-morpholinoethanesulfonic acid
MET1	DNA methyltransferase
miRNA	microRNA
MS	Murashige & Skoog
nat-siRNAs	Natural antisence transcript siRNAs
NLS	Nuclear localization sequences
Nt	Nucleotide
OD_{600}	Optical density at 600nm
ON	Over night
PAV	Potato A potyvirus

PBS	Phosphate buffered saline
PBST	Phosphate buffered saline tween
PCR	Polymerase chain reaction
PCV	Peanut clump virus
PDR	Pathogen-derived resistance
PepMV	Pepper mottle virus
PLD	PPIase-like domain
Pol IV	Polymerase IV
PoLV	Pothos latent virus
PPV	Plum pox virus
PRSV	Papaya ringspot virus
PSTVd	Potato spindle tuber viroid
PTGS	Post-transcriptional gene silencing
PVDF	Polyvinylidine difluoride
PVX	Potato virus X
PVY	Potato virus Y
qRT-PCR	Real-time PCR on RNA
RdDM	RNA directed DNA Methylation
RDR	RNA dependent RNA polymerase
rgs-CaM	Regulator of gene silencing-calmodulin-like protein
RHBV	Rice hoja blanca virus
RISC	RNA-induced silencing complex
RITS	RNA-induced transcriptional silencing complex
RNAi	RNA interference
Rpm	Rounds per minute
RSS	RNA silencing suppressor
RT-PCR	Reverse transcription-polymerase chain reaction
RYMV	Rice yellow mottle virus
SAM	S-adenosyl methionine
SDE1	Silencing Defective1
SDS	Sodium dodecyl sulfate
SDS-PAGE	Sodium dodecyl sulfate polyacrylamide gel electrophoresis
SGS2	Suppressor of Gene Silencing2
sin1	Short integuments1
siRNA	Small interfering RNAs
SKP1	S-phase kinase related protein 1
SPCSV	Sweet potato chlorotic stunt virus
ssRNA	Single stranded RNA
sus1	Suspensor1
TAE	Tris-acetate-EDTA
ta-siRNAs	Trans-acting siRNAs
TAV	Tomato aspermy virus
TBE	Tris-Borate-EDTA
TBSV	Tomato bushy stunt virus
TCV	Turnip crinkle virus
TEG	Tris-EDTA-glycin
TEMED	Tetramethylene-ethylenediamine
TEV	Tobacco etch virus
TGS	Transcriptional gene silencing
Tris	Tris(hydroxymethyl) aminomethane
Trp	Tryptophan
TSWV	Tomato spotted wilt virus
TVMV	Tobacco vein mottling virus
TYLCV-C	Tomato yellow leaf curl virus-China
TYMV	Turnip yellow mosaic virus
U	Unit
vd-sRNA	Viroid-derived small RNAs
VIGS	Virus-induced gene silencing
Vol	Volume
X-α-Gal	5-bromo-4-chloro-3-indolyl alpha-D-galactopyranoside
ZYMV	Zucchini Yellow Mosaic Virus

List of Figures

List of Tables

Dedication

To

My family for their love, kindness, encouragement, and endless support

Acknowledgments

I can find no words to express my sincere appreciation and gratitude to my source of inspiration my Palestinian supervisor Prof Mohammed S. Ali-Shtayeh for providing me with the possibility to work on this project and for his endless support, continual encouragement and help throughout the course of this study.

I would like to express my sincere gratitude and thanks to my supervisor Dr. habil Michael Wassenegger for his guidance, patience, critical reading of the thesis and valuable suggestions. Special thanks for the effort you put into the corrections of this thesis and your valuable suggestions.

I am grateful for Dr. Gabi Krczal who gave me the opportunity to carry out this work at the AlPlanta-Institute.

I would like to thank Dr. Götz Reustle for his help in getting the acceptance for me at the University of Hohenheim.

A special thanks goes to Dr. Kajohn Boonrod, your suggestions and help has really enriched the work.

I would like to send my thanks and gratitude for Dr. Marc Fuellgrabe, Dr. Mirko Moser, and Dr. Athanasias Dalakouras, for being there for me when I needed their help.

Thanks to all employees at the AlPlanta-Institute specially the epigenetic group: Michele, Nora, and Britta for collaboration and the nice working climate.

I do not have the words to thank my friend Muna and her family for their endless help with non-scientific matters just as important as the scientific ones.

My thanks also go to all people who have in some way helped me to continue this work.

1 General Introduction

1.1 Discovery of RNA silencing

RNA silencing phenomena were first described in petunia, where over-expression of flower pigmentation genes resulted in suppression of transgene and endogenous RNA. In order to obtain increased flower pigmentation, petunia plants were transformed with chalcone synthase (CHS) transgene constructs that should have led to over-expression. As a result reduction in flower pigmentation or even the complete absence of pigmentation was reported. The phenomenon was called co-suppression since it involves sequence-specific degradation of transcripts from both transgenes and their homologous endogenous counterparts (Van der Krol *et al*., 1990).

Several groups were investigating whether transgenic forms of virus resistance could be obtained according to the concept of “pathogen-derived resistance” (PDR). This concept was first described by Grumet and co-workers (1987), who proposed the possibility to investigate pathogen-derived genes as a means to obtain resistance in a variety of host-parasite systems. It was suggested that intentional expression of such genes in altered form, level or developmental stage, could interfere with pathogen replication resulting in specific host resistance. Among possible targets for PDR-mediated virus resistance, the most broadly exploited viral genes were those that code for the coat protein (CP), replicase and movement protein (Baulcombe, 1996). For several years this phenomenon was referred to as RNA-mediated resistance, and only in 1993 Dougherty and co-workers (Lindbo *et al*., 1993) linked this phenomenon to “co-suppression” in plants. The observations they made on co-suppression phenomena were in transgenic tobacco plants expressing either a full-length of the Tobacco etch virus (TEV) CP or a form truncated at the N-terminus of the TEV CP. After infection of these plants with TEV, typical systemic symptoms developed. However, 3 to 5 weeks post infection, transgenic plants "recovered". Surprisingly, in recovered tissue, transgene mRNA levels were less than transgene mRNA levels in non-inoculated transgenic tissue of the same developmental stage, while the transgene transcription rates were the same (Lindbo *et al*., 1993).

The observation of English and co-workers (1996), that a silenced GUS transgene (beta-glucuronidase) could prevent virus accumulation of Potato virus X (PVX) carrying *GUS* sequences, pointed toward an actual role of what was then called post-transcriptional gene silencing (PTGS), as a sequence specific antiviral defense mechanism. Supporting evidence of the more general nature of this plant response to viral infection was provided by the finding that the recovered parts of virus-infected plants would not only be resistant against the initially inoculated virus, but would also cross-protect the plant against other viruses carrying homologous sequences (Ratcliff *et al*., 1999). In addition, this work showed that viral RNA-mediated cross protection

was caused by the same mechanism as transgene-induced PTGS. These phenomena are now generally known as virus-induced gene silencing (VIGS).

A crucial discovery was the finding of short virus-derived double stranded RNA (dsRNA) molecules in infected host plants, explaining the sequence specificity of the RNA breakdown mechanism (Hamilton and Baulcombe, 1999). Plants containing a silenced transgene indeed accumulated small dsRNA molecules whose sequence was identical to the transgene. These small dsRNA species are commonly referred to as small interfering RNAs (siRNAs).

Next to the discovery of virus-specific siRNAs, it was demonstrated that plants that are deficient in essential RNA silencing genes, show enhanced viral pathogenicity (Morel *et al*., 2002). These findings, and the fact that all tested plant viruses encode proteins that interfere with and suppress the RNA silencing pathway, supported the idea that RNA silencing acts as a native antiviral defense system in plants. The viral proteins counteracting RNA silencing, often already known as "virulence factors", are commonly referred to as RNA silencing suppressor (RSS) proteins (Brigneti *et al*., 1998; Kasschau and Carrington, 1998). RSS proteins will be discussed in detail in subsequent paragraphs.

Silencing of endogenous and viral genes has now become a commonly used method. Transgene constructs can be arranged as inverted repeats (IRs), producing dsRNA, which efficiently trigger silencing of homologous genes (Smith *et al*., 2000). This approach can be used to generate transgenic virus resistant or endogenous gene knock-down plants. For gene knock-down VIGS is often preferred over the production of transgenic plants, as this fast method can give a first indication on whether a gene knock-down produces the expected phenotype (Lu *et al*., 2003).

A next step to an increased general concept of RNA silencing was achieved in animal research. In *Caenorhabditis elegans*, sense and anti-sense transcripts were already being used for quite some time to knock-down gene expression. However the real break-through came when Fire and co-workers (Fire *et al*., 1998) discovered that injection of very low amounts of dsRNA into *C. elegans* could induce what they called RNA interference (RNAi). Like in plants, this method of RNA silencing was much more efficient than just using single-stranded (ss) sense or anti-sense RNA. Building blocks of the gene silencing pathway proved to have remarkable similarities in different organisms and hence suggest an ancient role of RNA silencing in development, gene regulation, pathogen resistance, and chromatin structure.

1.2 RNA Silencing

RNA silencing represents a widespread mechanism of gene regulation found in a broad range of eukaryotic organisms. It plays an important role in development and maintenance of

genome integrity. RNA silencing also operates as an adaptive inducible antiviral defense mechanism (Ding, 2010; Ding and Voinnet, 2007). The combined features of RNA silencing phenomena are the production of small RNAs (sRNAs) that act as specificity determinants for down regulation of gene expression, and they are required for one or more members of the Argonaute (AGO) family proteins (Llave, 2010; Ruiz-Ferrer and Voinnet, 2009; Voinnet, 2009).

Genetic and biochemical experiments have established a general mechanistic model for these related pathways and identified factors that are required for RNA silencing in a variety of organisms (Fig. 1.1). The process is initially triggered by dsRNA, which can be introduced experimentally, as in the case of transgenes, or arise from endogenous genes, including transposons, or from replicating RNA viruses. The dsRNA trigger is cleaved by a ribonuclease III (RNase III)-like enzyme termed Dicer (Dcr) (in plants, Dicer-like (DCL)) into 21–24 nucleotide long siRNAs (Bernstein *et al*., 2001; Zamore *et al*., 2000). In another step, the siRNAs are denatured and incorporated into a multi-subunit endonuclease silencing complex called RNA-induced silencing complex (RISC) (Hammond *et al*., 2000). Within the activated RISC, ss siRNAs act as guides to bring the complex into contact with complementary RNAs and thereby cause their degradation (Bernstein *et al*., 2001; Zamore *et al*., 2000).

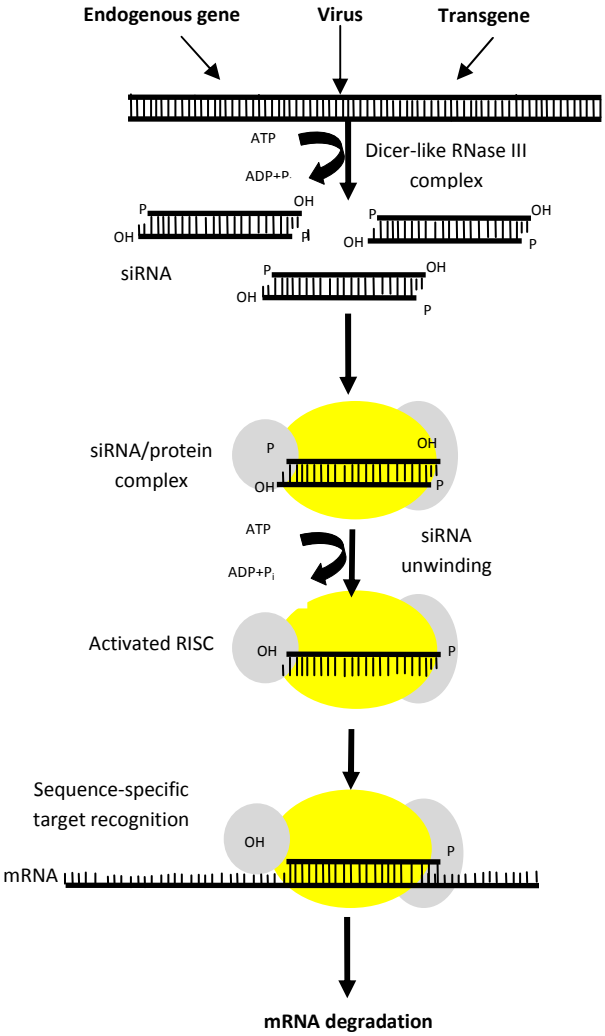

Figure 1.1: Schematic illustration of RNA silencing pathway (adapted from Roth *et al*., 2004).

RNA silencing and related pathways are not involved only in the response to viruses, but also act on transposon silencing through transcriptional gene silencing (TGS) that is based on sequence specific DNA methylation, chromatin condensation. Moreover, RNA silencing involves (developmental) gene regulation by micro RNAs (miRNAs) (see below) (Bartel, 2004; Baulcombe, 2004). These processes play an important role in plants and other multicellular organisms.

1.2.1 The plant defense mechanisms against invading viruses

The viral defense mechanism is considered as one of the main biological roles of RNA-silencing in plants. It plays an important role in identifying and inactivating invading nucleic acid molecules (Voinnet, 2005). The natural response of plants to viral infection is adaptive and requires the recognition of foreign nucleic acids for initiation. The dsRNA which is formed as an intermediate in the replication of RNA viruses is the initiator of RNA silencing (Smith *et al*., 2000; Voinnet, 2005), and their ss genomic RNAs are the targets of the silencing function. Three classes of viral siRNA molecules are recognized depending on the origin: 1. Primary siRNAs are produced from dsRNA molecules produced during the replication of viral genomes; 2. Secondary siRNAs originating from dsRNA molecules, deriving from aberrant derivatives of viral ssRNA genomes that are transcribed by host-encoded RNA-directed RNA polymerases (RDRs) (Gazzani *et al*., 2004); 3. Structural siRNAs that result directly from complex structured regions of the viral genome (Mlotshwa *et al*., 2008). In plants, antiviral defense is preferably guided by RISC-mediated cleavage of the viral target RNA rather than by inhibiting its translation (Pantaleo *et al*., 2007). Benefits of the RNA silencing-based defense system are, for instance, its adaptability and elasticity. The defense-specificity is not pre-formed, but is determined by the invading RNA sequence, and therefore the defense can be directed against any invading virus. In this sense, the system resembles the immune system of vertebrates (Voinnet, 2001).

Another benefit of the silencing system is that it is effectively amplified by the very presence of its trigger (Brodersen and Voinnet, 2006), and also transmitted from its initial induction site into neighboring cells, and systemically throughout the whole plant. This stipulation of remote tissues may significantly enhance the plants' defense-potential against the spreading viral infection.

1.2.2 Transcriptional gene silencing

Wassenegger and co-workers were the first to give the indication that RNA is involved in *de novo* DNA methylation in the nucleus (Wassenegger *et al*., 1994). *De novo* DNA methylation was first discovered in tobacco plants transformed with T-DNAs containing viroid cDNA sequences. Upon viroid infection, plant genome–integrated cDNA copies of the viroid became methylated, while other parts of the T-DNA insertion remained unaffected. This suggests that replication of viroids initiates methylation of the homologous DNA copies. The phenomenon was termed RNA-directed DNA Methylation (RdDM) (Wassenegger *et al*., 1994). The role of RNA silencing in RdDM was shown upon expression of dsRNA of promoter sequences in plants. Methylation of the promoter and subsequent TGS were observed (Mette *et al*., 2000). RdDM is limited to the region of homology between DNA and RNA and results in the methylation of cytosines (Wassenegger, 2000) by domain rearranged methyltransferases (DRM1 and DRM2),

chromomethylase3 (CMT3) and DNA methyltransferase MET1 in *Arabidopsis thaliana* (Cao and Jacobson, 2002). Later, it has been reported that the siRNA–dependent *de novo* methylation of DNA in plants is maintained by histone modifications (Zilberman *et al*., 2003). Recently several components of the RdDM pathway have been identified; the DNA methyltransferases (DMTase) MET1 and the putative histone deacetylase HDA6 maintain or enhance methylation. Recruitment of HDA6 then reinforces methylation and finally heterochromatin is formed at the specific targeted loci (Aufsatz *et al*., 2002; Aufsatz *et al*., 2004). Recent reports suggest that AGO4 is also involved in 24 nt siRNA-directed DNA methylation and its maintenance (Zilberman *et al*., 2003), while DCL1, which is required for miRNA processing, was shown not to be required for TGS (Finnegan *et al*., 2003). The fact that siRNA-induced TGS has also been found in human cell lines confirmed the importance of RNA silencing in gene regulation through TGS (Morris, 2009).

The accumulation of 24 nt repeat associated siRNA from transposons and centromeric repeats is dependent on DCL3 and RDR2 action (Chan *et al*., 2005), and probably serves to protect the genome against damage caused by transposons (Xie *et al*., 2004). Endogenous repeat-associated sRNAs possess the ability to trigger *de novo* methylation of cognate genomic DNA sequences and may thereby contribute to heterochromatin formation (Xie *et al*., 2004; Zilberman *et al*., 2004).

1.2.3 Transposon and endogenous repeat-associated gene silencing

Transposons are sequences of DNA that can move to new insertion sites within the genome of a single cell. This movement can cause major damage to the plant genome (Wicker *et al*., 1950). Transposons, like viruses, represent a nucleic acid-based threat to plants. Plants have evolved a defense system to fight against transposons that is based on RNA silencing. They produce transposon-derived 24 nt siRNAs (Hamilton *et al*., 2002; Xie *et al*., 2004). These siRNAs cause TGS of the transposons upon sequence-specific RdDM. Studies on *Arabidopsis* mutants revealed the involvement of RDR2 and other RNA processing factors to be required for transposon silencing (Bender, 2004). Similarly, work conducted in *C. elegans* revealed that several factors involved in RNAi are required for transposon silencing (Sijen and Plasterk, 2003). RNAi is heritable in *C. elegans*; the progeny of *C. elegans* exposed to dsRNA inherit the ability to silence genes that were targeted by RNAi in the previous generation (Alcazar *et al*., 2008; Vastenhouw *et al*., 2006). A recent study conducted to investigate the mechanism of RNAi inheritance in *C. elegans*, showed that exposure of animals to dsRNA results in the heritable expression of siRNAs and the heritable deposition of histone 3 lysine 9 methylation (H3K9me) marks in progeny (Burton *et al*., 2011). The detection of siRNAs before the appearance of H3K9me marks, suggested that chromatin marks are not directly inherited but, rather, reestablished in inheriting progeny. Furthermore, H3K9me marks appear more prominently in

inheriting progeny than in animals directly exposed to dsRNA, suggesting that germ-line transmission of silencing signals may enhance the efficiency of siRNA-directed H3K9me (Burton *et al*., 2011).

1.3 The biochemistry of the RNA silencing machinery

The RNA silencing machinery involves different pathways and target molecules, each of which is mediated by specific enzymes. The main enzymatic steps in silencing processes are the conversion of ssRNAs into dsRNAs by RDRs, followed by the cleavage of the dsRNAs by the Dcr or DCL complexes, sequence-specific cytoplasmic degradation of RNA molecules by the RISC, *de novo* DNA-methylation by RdDM complexes and different histone-modifying and chromatin-remodeling activities. According to various mutant analyses, also several accessory proteins are required in reactions mediated by RNA silencing (Matzke *et al*. 2004).

1.3.1 RNA–directed/dependent RNA polymerases (RDRs/RdRps)

The RNA-directed/dependent RNA polymerases (RDRs/RdRps) play a key role in RNA silencing, heterochromatin formation and natural gene regulation. RNA silencing is triggered by dsRNA as mentioned before. Hence, conversion of ssRNA sequences to ds form is required for silencing of endogenous transcripts.

The activity of a RDR was first discovered in 1971 (Astier-Manifacier and Cornuet, 1971) and its polymerase activity was studied *in vitro* (Schiebel *et al*., 1993). *Arabidopsis* encodes six RDRs (RDR1-RDR6) ranging from approximately 100 to 130 kDa in size. Based on phylogenetic analysis of all identified RDRs, it was suggested to rename the *Arabidopsis* genes as AtRDR1, AtRDR2, AtRDR3a, AtRDR3b, AtRDR3c and AtRDR6 (Wassenegger and Krczal 2006). Viruses produce their own RNA-dependent RNA polymerase (RdRp) (Wassenegger and Krczal 2006). It was reported that RDR1 is induced upon viral and viroid infection (Khan *et al*., 1986).

RDR2 and RDR6 were studied in detail and are linked to some RNA silencing pathways in plants. One of the silencing pathways leading to DNA methylation is mediated by RNA Polymerase IV (PolIV), PolV, RDR2 and DCL3. In this pathway PolIV, PolV and RDR2 would synthesize dsRNA which is then cleaved by DCL3 to generate 24 nt siRNAs (Xie *et al*., 2004; Zilberman *et al*., 2003). In one other pathway, PolIV acts together with AGO4 and one of the RDRs to produce specific siRNAs. These two silencing pathways are independent in leaves but interdependent in flowers (Herr *et al*., 2005).

RDR6, also known as Silencing Defective1 (SDE1) and Suppressor of Gene Silencing 2 (SGS2), was one of the first to be identified as a component of the RNA silencing machinery in plants by screening plant mutants deficient in RNA silencing (Mourrain *et al*., 2000; Tang *et al*., 2003). Without RDR6, RNA silencing can still be triggered through introduction of dsRNA-

producing systems, e.g. IRs and viruses. However, initiation of silencing by ssRNA requires RDR6 activity, indicating that this enzyme is responsible for converting ssRNA into dsRNA by synthesizing a complementary strand. RDR6 is also required for the reception, but not the production, of long-range RNA silencing signals, while having no effect on short-range signals (Schwach *et al*., 2005). It has been suggested that RDR6 is involved in antiviral defense because it enables systemic signaling that can inhibit viral spread by targeting the virus in the early stages of its infection cycle (Schwach *et al*., 2005). RDR6 has also been implied in the biosynthesis of endogenous trans-acting siRNAs (ta-siRNAs), which have a role in developmental regulation (Peragine *et al*., 2004).

1.3.2 Plant DCL proteins

Dcr and DCL proteins are multi-domain proteins and ranging in sizes from 135-200 kDa (Shi *et al*., 2006). DCL is a dsRNA-specific ribonuclease III-like endonuclease which cleaves the dsRNAs into 21-24 nt long siRNAs, having 5′ phosphates, 3′ hydroxyl groups, and 2 nt 3′ overhangs at the termini of the duplex (Bernstein *et al*., 2001; Lau *et al*., 2001).

Dcr was first discovered in *Drosophila* (Bernstein *et al*., 2001). Interestingly, many animals encode only one dicer, *Drosophila* encodes two (Lee *et al*., 2004), *Arabidopsis* encodes at least DCL1, DCL2, DCL3 and DCL4 (Finnegan *et al*., 2003), while *Oriza sativa* encodes six DCL proteins (DCL1, DCL2a, DCL2b, DCL3a, DCL3b, and DCL4) (Margis *et al*., 2006). It is reasonable to assume that the multiple roles dicer plays in the different branches of RNA silencing in animals are divided over the different homologues in plants.

Different Dcr orthologues are involved in the production of distinct siRNAs, and are active in different cellular compartments (cytoplasmic vs. nuclear) (Finnegan *et al*., 2003; Lee and Ambros, 2001). DCL1 is required for the accumulation of miRNAs and ta-siRNAs (Bartel, 2004; Chen, 2005; Park *et al*., 2002). In plants, DCL2 is involved in cleaving natural antisense transcripts into siRNAs generating the natural antisense transcripts siRNAs (nat-siRNAs) (Deleris *et al*., 2006). In virus-infected plants, DCL2 is also involved in cleaving the invading RNAs. Similar to RDR2, DCL3 plays a role in the accumulation of endogenous 24 nt siRNAs which are involved in DNA methylation and heterochromatin formation (Xie *et al*., 2004).

DCL4 has multiple roles in plants, it generates 21 nt RNAs which are associated with ta-siRNA biosynthesis and siRNAs involved in RNAi. In addition, DCL4 is involved in cleavage of invading RNAs in virus-infected plants (Blevins *et al*., 2006). Two things support the idea that DCL4 is involved in RNA silencing pathways: first the size of siRNAs produced by DCL4 is similar to that of RNA silencing associated siRNAs (21 nt). Second, it was reported that DCL4 is required for the accumulation of siRNA-derived from moderately expressed IRs (Dunoyer *et al*., 2006).

The crucial role of the Dcr/DCL enzymes in developmental regulation was validated by morphological disorders caused by various Dcr/DCL mutants. Well characterized mutants of DCL1, including short integuments1 (sin1), suspensor1 (sus1) and carpelfactory (caf), produced malformed flowers with non-fused carpels, abnormal stamen and ectopic floral meristem cells in the center, indicating that DCL1 is involved in the regulation of organ development and in meristem cell identity and differentiation (Kasschau *et al*., 2003; Park *et al*., 2002; Reinhart *et al*., 2002). These data also indicated that DCL2-4 do not compensate for the function of DCL1, but function in separate dsRNA cleavage pathways. For instance, the PTGS pathway is operating normally in the caf/dcl1-9 mutant plants, indicating that this siRNA-guided function is not mediated by DCL1 (Finnegan *et al*., 2003). Yet, DCL1 may help DCL3 and DCL4 to produce siRNAs from IRs associating DCL1 with other RNA silencing pathways (Dunoyer *et al*., 2007).

1.3.3 RNA methyltransferase HUA ENHANCER 1 (HEN1)

Associated with DCL1 and miRNA biogenesis is HUA ENHANCER 1 (HEN1). HEN1 was first identified in a genetic screen as a floral pattering gene and later found to be essential for *Arabidopsis* miRNA accumulation *in vivo* (Chen *et al*., 2002; Park *et al*., 2002). HEN1 mutants showed multifaceted developmental defects in *Arabidopsis* (Boutet *et al*., 2003; Park *et al*., 2002). A subset of sRNAs, such as miRNAs and siRNAs in plants (Yu *et al*., 2005), Piwi-interacting RNAs in animals (Kirino and Mourelatos, 2007) and siRNAs in *Drosophila* (Horwich *et al*., 2007), require an additional crucial step for their maturation, namely 2′-O-methylation at the 3′ terminal nucleotide. The RNA methyltransferase HEN1, and its homologues catalyze this specific modification (Kurth and Mochizuki, 2009; Yu *et al*., 2005). HEN1 has a S-Adenosyl Methionine (SAM) binding pocket, methylates miRNA/miRNA* duplexes *in vitro* (Yu *et al*., 2005) and does not require guide RNAs to methylate its targets (Omer *et al*., 2002). In *Arabidopsis*, HEN1 (AtHEN1) methylates double-stranded sRNAs (Yu *et al*., 2005), probably before they are loaded onto AGO proteins (Ramachandran and Chen, 2008). Unlike plant HEN1, *Drosophila* HEN1 specifically acts on ssRNA. In homozygous *Drosophila* HEN1 mutants, both the length and abundance of piRNAs were decreased. In *Arabidopsis*, the 2′-O-methylation protects miRNAs and siRNAs from 3′-end uridylation and from 3′- to 5′-exonuclease-mediated degradation (Chen, 2007; Li *et al*., 2005). Loss of this modification causes a general reduction in the levels of sRNAs in plants (Boutet *et al*., 2003; Li *et al*., 2005). HEN1 methylation might also prevent miRNAs from being used as primers, thus disabling undesirable miRNA-induced transitivity on endogenous targets (Yu *et al*., 2005) (for transitivity, see below). It is also involved in siRNA production, at least in the case of begomovirus silencing (Akbergenov *et al*., 2006).

The plant HEN1 and its animal homologues share a highly conserved methyltransferase (MTase) domain (Chen, 2007) that is not closely related to any known RNA 2′-O-MTase

according to a phylogenetic analysis (Tkaczuk *et al*., 2006). Two putative RNA binding domains, a dsRNA binding domain (dsRBD) and a La motif have been identified in the amino-terminal region of HEN1 (Tkaczuk *et al*., 2006). The HEN1 protein consists of five structural domains, four of which directly interact with sRNA substrates and the PPIase-like domain (PLD) which shows a high degree of structural similarity to well characterized FK506-binding proteins (Kang *et al*., 2008).

1.3.4 Argonaute proteins

AGO proteins comprise a highly conserved protein family that is involved in a variety of RNA silencing phenomena in a diverse set of organisms. AGO proteins are encoded by multigene families, which comprise ten members in *Arabidopsis*, five in *Drosophila*, more than 20 in *C. elegans*, and eight in human (Carmell *et al*., 2002; Mallory and Vaucheret, 2010). They are about 100 kDa in size, contain a PAZ domain and a unique PIWI domain. The PAZ domain consists of approximately 130 amino acids. PAZ and PIWI domains are responsible for 3′-2 nt-overhang recognition and endonucleolytic activities, respectively (Hammond *et al*., 2000; Song and Joshua-Tor, 2006). Due to their basic character AGO proteins bind RNAs (e.g. siRNAs), and guide them to functional complexes (Matzke *et al*., 2004; Tang *et al*., 2003; Vaucheret *et al*., 2004). In addition to the PAZ and PIWI domains, in AGO proteins, an N-terminal and middle domain are present. The 5′-region of the target is positioned between the PAZ and N-terminal domain in such a way that the catalytic core of the PIWI domain is able to cleave the phosphodiester bond between position 10 and 11 measured from the 5′-end of siRNAs, which is recognized by AGO (Rivas *et al*., 2005).

Only a small subset of AGO proteins has been functionally characterized. However, increasing evidence indicates that different subsets of the AGO family members are involved in different kinds of gene silencing and have diverse functions in cells. AGO proteins have been characterized as slicer proteins, because the first characterized AGO protein catalyzed targeted RNA cleavage (Song and Joshua-Tor, 2006). However, this term is not accurate to describe all AGO proteins since not all are capable of slicing and, instead, may repress gene expression by other mechanisms (Mallory and Vaucheret, 2010). Sequence comparisons indicated that *Arabidopsis* AGO1, 4, 5, 7 and 10 all have a conserved ‘slicer’ catalytic motif, the DDH triad that was identified in human AGO2 (Rivas *et al*., 2005, Qi *et al*., 2006). The DDH amino acid core is not sufficient to indicate the cleavage activity of AGO proteins (Mallory and Vaucheret, 2010). In *Arabidopsis*, the replacement of the MID PIWI domain of AGO1 with the MID PIWI domain of AGO10, both possess DDH catalytic core, doesn’t restore silencing activity of in AGO1 hypomorphic mutation (Mallory *et al*., 2009). The exact “slicer” activity of each individual AGO protein, however, needs further experimental testing. Among the ten members of the *Arabidopsis*

AGO (AtAGO) family, AtAGO1, AtAGO4 and AtAGO7 were tested and showed slicer activity (Baumberger and Baulcombe, 2005, Qi *et al*., 2006). The AtAGO1 is required for both miRNA regulated plant development and DNA methylation triggered by sense transgene-induced PTGS (S-PTGS) but not IR transgene-induced PTGS (IR-PTGS) (Baumberger and Baulcombe, 2005; Boutet *et al*., 2003; Vaucheret *et al*., 2004). AtAGO7 seems to work as a surrogate slicer in the absence of AtAGO1, it was assumed that AtAGO1 is capable of targeting viral RNAs with more compact structure, while AtAGO7 favours less structured RNA targets (Qu *et al*., 2008). Furthermore miRNA390 is the unique miRNA that binds to AtAGO7 to guide cleavage of ta-siRNA from *TAS3* locus (Montgomery *et al*., 2008). AtAGO10 is required for translational control of several miRNA targets including AtAGO1 (Brodersen *et al*., 2008; Mallory *et al*., 2009). AtAGO2 has antiviral mechanism against viruses that suppress AtAGO1 (Harvey *et al*., 2011). AtAGO4, AtAGO6, and AtAGO9 are involved in TGS and associated with 24 nt sRNAs (reviewed in Mallory and Vaucheret, 2010). AtAGO4 is widely expressed and is essential for DNA and histone methylation in *Arabidopsis* and more likely plays a role in the RNA-induced transcriptional silencing (RITS) pathway (Havecker *et al*., 2010; Mi *et al*., 2008; Zilberman *et al*., 2004). The expression of AtAGO6 is largely confined to the shoot and root growing points and the connecting vascular tissue (Eun *et al*., 2011; Havecker *et al*., 2010). Recently, AtAGO6 was identified to be involved in PolV-mediated steps of RNA-mediated TGS in shoot and root meristems (Eun *et al*., 2011).

1.3.5 Effector complexes

RNA-induced effector complexes include the RITS complex guiding methylation and chromatin modifications, and RISC causing cleavage of homologous sequences and translational arrest (Li and Ding, 2006). RISCs are multi-protein complexes of which several components have been identified. They are large assemblies of 250-500 kDa, associated with the single-stranded fragments of siRNAs and miRNAs (Nykänen *et al*., 2001; Omarov *et al*., 2007). SRNA molecules provide sequence-specificity to RISC. Like these sRNAs, AGO proteins have been found to be part of effector complexes in all organisms studied, which is, in the case of the *Arabidopsis* RITS, AtAGO4, and in the case of RISC, AtAGO1.

In *Drosophila*, AGO2 (DmAGO2) is part of RISC and essential for siRNA-directed RNA silencing. DmAGO2 is not required for the miRNA biogenesis but a role for DmAGO1 was indicated (Okamura *et al*., 2004). R2D2, a DmDicer-2 associated protein, was shown to play an important role in RNA binding and strand discrimination of siRNAs and miRNAs for incorporation of the proper RNA strands into RISC (Liu *et al*., 2003). Though R2D2 is not involved in endonucleic cleavage of dsRNA, it stabilizes the association of DmDicer-2 and siRNAs.

Generally, it can be concluded that most if not all AGO proteins are involved in different parts of RNA silencing and possibly define the mode of action of RISC in which they are incorporated (Baulcombe, 2004). Regardless of the way different Dicer enzymes produce siRNAs and miRNAs, single strands of siRNA or miRNA duplexes are incorporated into RISC, the effector of RNA silencing. RISC provides the different (catalytic) functions such as mRNA cleavage and translational inhibition. In plants, it was shown that, the loading of siRNA into a particular AGO complex is preferentially, but not exclusively, directed by their 5'-terminal nucleotides (Mi *et al*., 2008).

1.4 Small RNA biogenesis in plants

Over the years, a number of sRNA classes that have different functions, have been discovered. These sRNAs (21-25 nt long) which are homologous to the target RNA sequences, are the trademark of activated silencing systems (Dugas and Bartel, 2004). Two main classes of sRNA molecules - the siRNAs and miRNAs - have been reported. Lee and co-workers (1993) were the first to report on miRNAs which they detected in animals. In plants, miRNAs were first discovered by Hamilton and Baulcombe (1999). Later, various miRNAs and siRNAs have been reported from different plants, animals, yeast and fungi (Brodersen and Voinnet, 2006; Li and Ding, 2006; Lleave *et al*., 2002a and 2002b; Vaucheret *et al*., 2006).

MiRNAs and siRNAs were categorized depending on their mode of synthesis. MiRNAs are derived from local ds hairpin structures formed by specific precursor transcripts (Fig. 1.2). In contrast, siRNAs arise from long dsRNAs that derive from aberrant transcripts of transgenes, transposons, heterochoromatic DNA or from ds replication intermediates of RNA-viruses and viroids (Fig. 1.2). MiRNAs are composed of one specific ssRNA deriving from one arm of hairpin loop-structured precursors. SiRNAs are composed of a set of multiple RNAs which are processed from dsRNAs over the full length. Notably and generally in contrast to miRNAs, Dicer-processed siRNAs can be loaded onto RISC in sense and antisense orientation. Thus, miRNAs are targeting RNAs at specific sites while siRNAs are targeting any RNA sequence sharing homology with the initial processed dsRNA (Dugas and Bartel, 2004; Mallory and Vaucheret, 2004; Zamore, 2002).

Besides these two main classes of sRNAs, different species of endogenous sRNAs have been found. The 24 nt nat-siRNAs are produced from dsRNAs formed by bidirectional transcription of overlapping genes (Borsani *et al*., 2005). The 21 nt ta-siRNAs are produced from non-coding, ss ta-siRNA precursors (TAS RNA genes) *via* conversion into dsRNAs by RDR6 (Brodersen and Voinnet 2006; Li and Ding 2006; Vaucheret *et al*., 2006). Finally, endogenous 24 nt siRNAs which are involved in the RdDM mechanism are generally produced from

heterochromatic DNA involving the activity of PolIV, PolV and RDR2 (Chan *et al.*, 2005; He *et al.*, 2011).

Interestingly, both ta-siRNA and miRNAs can guide degradation of homologous target sequences of different members of the same gene family. So far, the ta-siRNA-generating loci, TAS1, 2 and 4 RNA genes, have been identified only in *Arabidopsis* (Brodersen and Voinnet, 2006; Vaucheret, 2006). However, TAS3 was also found in other plant species (Shen *et al.*, 2009). Due to their important role in development and antiviral defense miRNAs and siRNAs will be discussed in details in the following section.

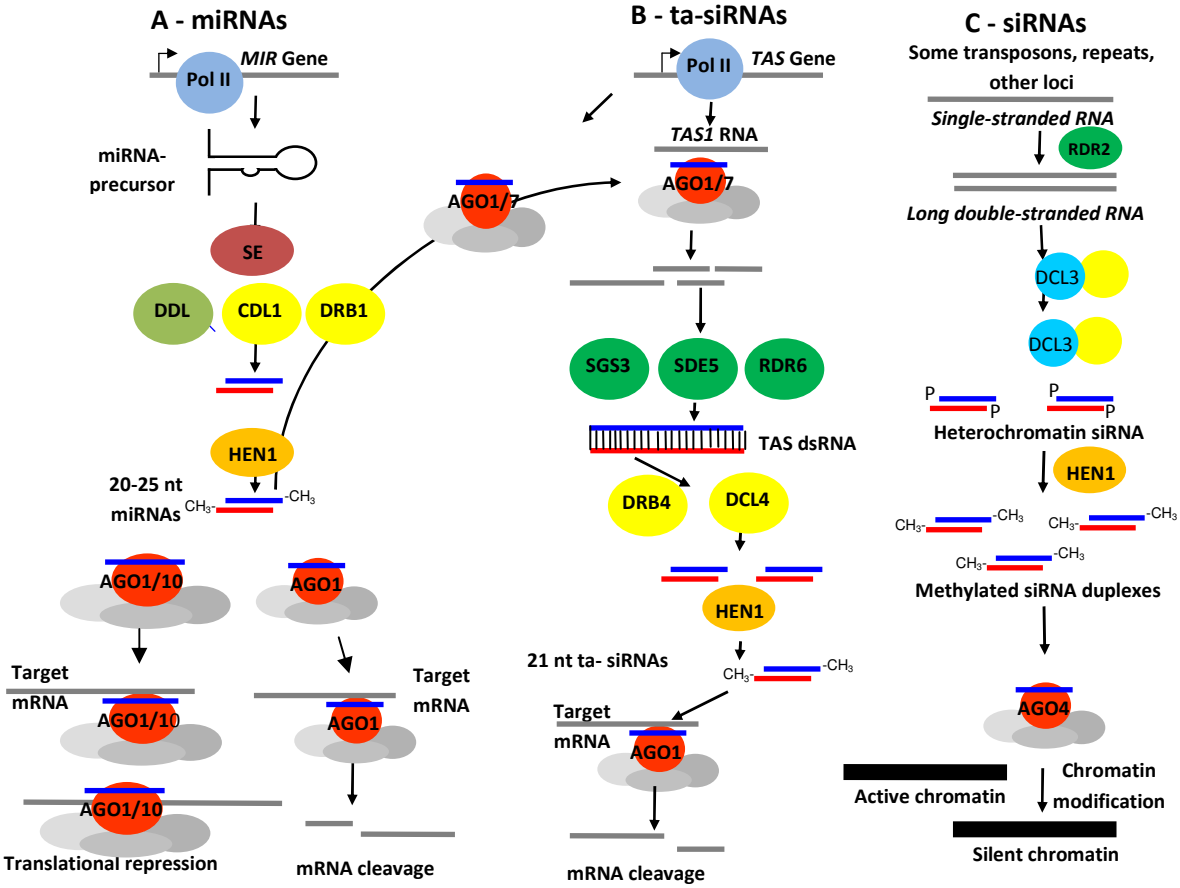

Figure 1.2: Schematic illustration of different small RNA pathways in plants (adapted from Mallory and Vaucheret, 2010; Johnes-Roades *et al.*, 2006). A = miRNA mechanism; B = ta-siRNA mechanism; C = siRNA mechanism.

1.4.1 Micro RNAs (miRNAs)

MiRNAs are endogenous 21-25 nt long RNAs that play important regulatory roles in animals and plants. They comprise one of the more abundant classes of gene regulatory molecules in multicellular organisms and likely influence the output of many protein-coding genes (Bartel, 2004). MiRNAs mediate either the cleavage or the translational arrest of their target mRNAs. This mode of action was assumed to be determined by their level of complementarity to their target sequences. Imperfect base pairing between the miRNA and the target RNA predominantly leads

to translational arrest. Full complementarity between miRNAs with their targets leads to RNA cleavage and subsequent degradation by other cellular nucleases (Bartel and Bartel, 2003; Carrington and Ambros, 2003; Tang *et al*., 2003). However, in plants, fully complementary miRNAs and siRNAs were associated with translational repression (Dalakouras *et al*., 2011; Voinnet, 2009; Aukerman and Sakai 2003; Chen, 2004). Moreover, several plant miRNAs comprising nucleotide mismatches in the recognition sites mediate cleavage of their targets (Jones-Rhoades and Bartel, 2004; Kasschau *et al*., 2003; Palatnik *et al*., 2003). As some plant miRNAs function through translational arrest, some animal miRNAs function via target RNA cleavage (Yekta *et al*., 2004) indicating that no general rules can be applied (Ambros, 2003; Bartel, 2004).

In plants and animals, numerous mRNAs that are targeted by the silencing machinery code for transcription factors. Developmental differentiation of organisms requires accurate temporal and spatial regulation of multiple gene functions. It has been shown that the regulation of many of these genes happens *via* RNA silencing, mediated by specific miRNAs which can regulate multiple target genes simultaneously. Correlating with the regulatory role, various miRNAs are expressed in specific tissues and at specific stages of development (Alvarez *et al*., 2006; Mallory *et al*., 2004; Valoczi *et al*., 2006). In *Arabidopsis*, AtDCL1 is regulated by miR162 and miR838 (Xie *et al*., 2003) and AtAGO1 is regulated by miR168 (Vaucheret *et al*., 2004). A single mutation in the miR168 binding site caused hyper-accumulation of AtAGO1 mRNA and a strong phenotype (Vaucheret, 2006). Well-known mutants of these dominant regulatory genes are due to small nucleotide changes in the miRNA target sites of their mRNAs and not due to the altered protein functions (Dugas and Bartel, 2004; Mallory and Vaucheret, 2004).

Localization of these miRNAs in actively dividing cells and young organs indicated their crucial role in cell differentiation (Valoczi *et al*., 2006). Further evidence for the central role of miRNAs in developmental differentiation came from the analysis of mutants, such as *ago1*, *hen1*, *caf1/dcl1-9* or *hyl1* in *Arabidopsis* (Bouche *et al*., 2006; Henderson *et al*., 2006; Vaucheret *et al*., 2004). Each of these mutants is related to gene functions required for miRNA biosynthesis or miRNA function. For example, *dcl1* mutants are associated with floral organ morphogenesis defects and altered ovule development, suggesting a critical role of miRNAs in these developmental processes. Also, mutations in miRNA genes or miRNA target sequences themselves cause very clear development defects (Kasschau *et al*., 2003).

1.4.2 Short interfering RNAs (siRNAs)

A major difference between the miRNA and siRNA molecules is given by their biosynthesis pathways. SiRNA may be cleaved from dsRNAs of external origin, such as replicating virald RNAs, from synthetic dsRNAs or from dsRNA synthesized from aberrant cellular transcripts by

RDR6 (Han and Grierson, 2002; Reinhart *et al*., 2002). SiRNA targets include highly expressed transgenes and transposons. Evidently, siRNA production is a defense mechanism against different invading nucleic acids (Waterhouse *et al*., 2001; Zamore, 2002). In plants, siRNAs fall into two distinct size classes (Hamilton *et al*., 2002; Mallory *et al*., 2002; Tang *et al*., 2003). The 21-22 nt siRNAs function in silencing of target RNAs by sequence specific cleavage or translational arrest. The 24-25 nt siRNAs appear to mediate silencing related functions that are associated with DNA methylation and systemic silencing (Aufsatz *et al*., 2002; Hamilton *et al*., 2002). SiRNAs of different sizes are apparently produced by different DCL proteins which can be separately induced under different conditions (Hamilton *et al*., 2002; Tang *et al*., 2003).

Along with DCL, RDR1, RDR2 and RDR6 proteins are also involved in siRNA biogenesis (Mourrain *et al*., 2000; Xie *et al*., 2004; Yu *et al*., 2003). For example, DCL3 and RDR2 generate 24 nt siRNAs from retroelements, transposons and from direct and inverted repeats (Xie *et al*., 2004; Zilberman *et al*., 2003). RDR6 is involved in PTGS of transgenes, in silencing of viral RNAs and in silencing of endogenous mRNAs that are targets of ta-siRNAs and nat-siRNAs (Parizotto *et al*., 2004; Peragine *et al*., 2004; Yu *et al*., 2003).

The silencing process, i.e. degradation of target RNAs, can be effectively amplified by a self-reinforcing loop. Primary siRNAs produced from initial silencing-inducing dsRNAs mediate RNA cleavage but may also prime copying of target RNAs by RDR6. Processing of the resulting secondary dsRNA serves as a substrate for DCL proteins producing secondary siRNAs (Tang *et al*., 2003; Vaistij *et al*., 2002).

1.5 Silencing Suppressor Proteins

One of the major roles of RNA silencing in plants is to provide a defense system against viruses (Anandalakshmi *et al*., 1998; Ding, 2010). The fact that viruses effectively infect their specific host plants indicates that they successfully counteract the host defenses. Viruses have various means to protect their genomes against the silencing process. They often replicate inside vesicles or in proteinaceous inclusions which protect them from the intracellular enzymes. DsRNA viruses isolate their entire dsRNA stage inside capsid particles and thus avoid the exposure of the dsRNA to the RNAi machinery. Moreover, all viruses encapsidate their ssRNA genomes into ribonucleoprotein complexes to protect them from degradation (Csorba *et al*., 2010; Li and Ding, 2006; Voinnet *et al*., 2005a). However, many, if not all, plant viruses and at least some animal viruses encode proteins that suppress gene silencing (Levy *et al*., 2008; Merai *et al*., 2005; Nayak *et al*., 2010).

In 1998, researchers discovered the first RSS - the helper-component proteinase (HC-Pro) of TEV - providing the strongest experimental support for a role of RNA silencing in host immunity against viruses (Anandalakshmi *et al*., 1998; Kasschau and Carrington, 1998; Li *et al*., 1999).

Other well characterized silencing suppressor proteins include 2b proteins of cucumoviruses, P19 of tombusviruses and P25 of potexviruses (Roth *et al*., 2004). Currently more than a dozen RSSs that are encoded by RNA- and DNA-viruses are known (Table 1.1).

1.5.1 Functional assays to identify RNA silencing suppressors

After the discovery of HC-Pro as a RSS many other viruses were shown to express proteins capable of inhibiting the plant antiviral mechanism. The establishment of relatively simple and reliable functional assays to detect RSS activity greatly accelerated their discovery. Three major approaches have been widely used to identify plant viral RSS: (1) transient expression assays, (2) the reversal of silencing assays, and (3) stable expression assays.

1.5.1.1 Transient expression assays - *Agrobacterium* coinfiltration

The *Agrobacterium* coinfiltration (agro-coinfiltration) approach provides a rapid and easy test of suppressor activity and is currently one of the most commonly used methods for the identification of potential viral RSS. The assay is based on the transient, simultaneous expression of two transgenes in leaves using *Agrobacterium tumefaciens* (bacterial pathogen of plants) (Johansen and Carrington, 2001; Lleave *et al*., 2000; Voinnet *et al*., 2000). In this assay, two *A. tumefaciens* strains are used. One strain induces RNA silencing of a reporter gene (e.g. green fluorescent protein (GFP)) and another strain is used to express the putative RSS. Mixtures of the two *A. tumefaciens* strains are co-infiltrated into plant leaves (e.g. *Nicotiana benthamiana*). In the infiltrated patches, silencing of the reporter is then monitored.

1.5.1.2 Reversal of silencing assay

The ‘reversal of silencing assay’ is flexible and can be used to immediately identify candidate viruses that may suppress silencing (Brigneti *et al*., 1998). A modification of the same technique can then be used to identify the specific viral gene product that suppresses silencing. In the assay, GFP- or GUS-silenced transgenic plants are used for infections with different viruses or virus constructs. In the infected plants, reversal of silencing is monitored by detection of re-expression of GFP or GUS (Ruiz *et al*., 1998). Reversal of silencing indicates that the tested virus encodes a RSS (Voinnet *et al*., 1999). PVX encodes a RSS that cannot derepress reporter gene expression in this assay. Thus, PVX is a good vector to test other viral genes for their silencing suppression capability by introducing the gene of interest into the PVX genome and by expressing it through infection with the recombinant virus (Brigneti *et al*., 1998).

Table 1.1 RNA silencing suppressors (RSS) of plant viruses

Genome	Virus Genus	Virus	RNAi Suppressor	Evidence	Reference
DNA	Geminivirus	African cassava mosaic virus (ACMV)	AC2	Infection with ACMV, PVX-AC2, or PVX-C2 reverses silencing	Dong *et al*., 2003
		Tomato yellow leaf curl virus-China (TYLCV-C)	C2	Blocks sense induced silencing in agro-coinfiltration assays; AC2 and C2 are homologs	Bisaro, 2006; Dong *et al*., 2003
+ ssRNA	Aureusvirus	Pothos latent virus (PoLV)	P14	P14 prevents the accumulation of hairpin transcript-derived siRNAs; binding of dsRNAs without size specificity	Merai *et al*., 2005
+ ssRNA	Carmovirus	Turnip crinkle virus (TCV)	CP	TCV infection does not reverse silencing; in agro-coinfiltration assays, CP blocks sense and antisense induced local silencing and prevents systemic silencing	Dunoyer *et al*., 2004 ; Qu *et al*., 2003
+ ssRNA	Closterovirus	Beet yellows virus (BYV)	P21	Suppresses inverted repeat (IR) induced local silencing in agro-coinfiltration assay	Reed *et al*., 2003
+ ssRNA	Crinivirus	Sweet potato chlorotic stunt virus (SPCSV)	P22	RNase III with dsRNA-specific endonuclease activity that enhances the RNA-silencing suppression activity	Kreuze *et al*., 2005; Valverde *et al*., 2007
+ ssRNA	Cucumovirus	Cucumber mosaic virus (CMV) Tomato aspermy virus (TAV)	2b	Infection with CMV or with PVX-2b vector blocks silencing; interferes with systemic signal	Li *et al*., 2002; Roth *et al*., 2004
+ ssRNA	Furovirus	Beet necrotic yellow vein virus (BNYVV)	P14	Agro-coinfiltration assay with sense induced silencing; BNYVV P14 corresponds to PCV P15	Dunoyer *et al*., 2002
+ ssRNA	Hordeivirus	Barley stripe mosaic virus (BSMV)	γb	RNA mediated cross protection between PVX-GFP and Tobacco mosaic virus (TMV) -GFP vectors is eliminated when γb is expressed from the PVX vector	Yelina *et al*., 2002
+ ssRNA	Pecluvirus	Peanut clump virus (PCV)	P15	PCV infection blocks silencing; p15 blocks local and delays systemic sense-induced silencing in agro-coinfiltration assays	Dunoyer *et al*., 2002
+ ssRNA	Polerovirus	Beet western yellows virus (BWYV)	PO	BWYV PO suppresses local but not systemic sense-induced silencing in agro-coinfiltration assays	Pfeffer *et al*., 2002
+ ssRNA	Potexvirus	Potato virus X (PVX)	P25	PVX infection does not suppress silencing; in agro-coinfiltration, P25 blocks systemic but not always local silencing	Roth *et al*., 2004
+ ssRNA	Potyvirus	Potato virus Y (PVY) Tobacco etch virus (TEV)	HC-Pro	Does not block systemic silencing in stable expression grafting assay but does in agro-coinfiltration assays	Roth *et al*., 2004
+ ssRNA	Sobemovirus	Rice yellow mottle virus (RYMV)	P1	Infection with PVX-P1 viral vector reverses silencing	Voinnet *et al*., 1999
+ ssRNA	Tombusvirus	Tomato bushy stunt virus (TBSV)	P19	Limited activity in reversal of silencing; strong activity in agro-coinfiltration	Voinnet *et al*., 2003
+ ssRNA	Trichovirus	Apple chlorotic leaf spot virus (ACLSV)	P50	Suppress systemic silencing induced by both ss and dsRNA, but do not have any effect on local silencing; does not affect the accumulation of either short (20-23 nt) or long (24-26 nt) sRNAs	Yaegashi *et al*., 2007
+ ssRNA	Tymovirus	Turnip yellow mosaic virus (TYMV)	P69	Suppress the siRNA pathway but promote the miRNA-guided inhibition of host gene expression	Chen *et al*., 2004
- ssRNA	Tenuivirus	Rice hoja blanca virus (RHBV)	NS3	Agro-coinfiltration assay of sense induced local silencing	Bucher *et al*., 2003
- ssRNA	Tospovirus	Tomato spotted wilt virus (TSWV)	NSs	TSWV infection reverses silencing; in agro-coinfiltration, NSs suppressed sense- but not IR-induced local and systemic silencing	Bucher *et al*., 2003

1.5.1.3 Stable expression assay

In the 'stable expression assay', transgenic plants are generated that constitutively express a RSS. A significant drawback of this method is that (high) expression of RSS proteins often leads to developmental defects in the plants. The transgenic plants can be genetically crossed with well-characterized transgenic lines carrying silenced reporter genes. Progeny of such genetic crosses are then be assayed for expression of the RSS and monitored for reporter gene expression (Anandalakshmi *et al*., 1998).

The 'stable expression assay' is also suitable to investigate suppression of systemic silencing (Guo and Ding, 2002; Mallory *et al*., 2001, 2003). In this assay, the ability of a plant to send a mobile silencing signal is assayed by grafting a reporter gene-expressing scion onto a rootstock expressing the RSS and carrying the same (but due to the presence of the RSS) re-expressed reporter gene (Palauqui *et al*., 1997). If the RSS in the rootstock blocks the production or movement of the systemic silencing signal, the transgene in the scion will be continuously expressed. If the suppressor does not block systemic silencing, the transgene will become silenced in the scion.

1.5.2 Mechanism of silencing suppression

According to their mode of function, RSS proteins can be divided into different groups (Alvarado and Scholthof, 2009; Burgyán and Havelda, 2011). In the following sections, examples of how plant viral suppressors affect different steps of the RNA silencing pathway are given. Some viral proteins can multifunctionally act at different stages in the silencing process which reaffirms the efficient and pleiotropic nature of many virus proteins. Several virus-encoded suppressors have an RNA binding property and often display preference for specific molecules (Lakatos *et al*., 2006; Merai *et al*., 2006).

1.5.2.1 Suppressors affecting the processing of dsRNA

Two viral proteins were shown to inhibit processing of dsRNA to siRNA: the P14 of Pothos latent aureuvirus and P38 of Turnip crinkle virus (TCV). The two proteins also bind dsRNA in a size–independent way (Merai *et al*., 2006; Merai *et al*., 2005). SiRNAs that derived from S- or IR-PTGS were undetectable in TCV-infected plants indicating that P38 suppressed DCL activity (Qu *et al*., 2003). In single, double and triple *Arabidopsis dcl* mutants, the accumulation of siRNA was monitored after infection with a P38-deficient TCV. In this virus, P38 was replaced by GFP (TCV-GFPΔp38) (Deleris *et al*., 2006). In TCV-GFPΔp38-infected *dcl4* mutants, 22 nt but no 21 nt siRNAs were predominantly found and the virus titer was low. In *dcl2/dcl4* plants, the RNA levels of TCV-GFPΔp38 and TCV were almost identical. This corroborated that P38 suppression may mainly act on DCL4 and DCL2 activity. However, it was shown that P38 binds AGO1,

thereby interfering with the AGO1-dependent homeostatic network. This in turn leads to the inhibition of DCLs resulting in changes in miRNA levels creating a virus-favorable environment in the plant (Azevedo *et al*., 2010).

The P6 of the Cauliflower mosaic virus (CaMV) has been shown to interfere with viral siRNA processing. P6 has two importin-alpha-dependent nuclear localization signals, which are mandatory for CaMV infectivity. One of the nuclear functions of P6 is to suppress RNA silencing by interacting with the dsRNA binding protein 4, which is required for the functioning of DCL4 (Haas *et al*., 2008).

1.5.2.2 Suppressors of the silencing signal amplification

In plants infected with viruses, host proteins such as RDR1 and RDR6 are involved in the synthesis of viral siRNAs. These secondary viral siRNAs play an essential role in silencing-based antiviral immunity (Garcia-Ruiz *et al*., 2010; Wang *et al*., 2010). The 2b of CMV inhibits the production of secondary viral siRNA (Diaz-Pendon *et al*., 2007). The mechanism by which 2b inhibits secondary viral siRNA function has been unraveled (see below). The suppressor of gene silencing 3 (SGS3) is a coiled-coil protein involved in siRNA signal amplification. Previous studies suggest that SGS3 binds and stabilizes RNA templates to initiate RDR6-mediated dsRNA synthesis. The V2 protein of Tomato yellow leaf curl virus (TYLCV) binds to SGS3 and by that interferes with RNA silencing through blocking of the RDR6 activity (Glick *et al*., 2008). A point mutation on V2 that impairs its binding to SGS3 also abolishes its ability to suppress silencing indicating that the V2/SGS3 interaction is important for suppression (Glick *et al*., 2008; Fukunaga and Doudna, 2009).

1.5.2.3 Suppressors of the stabilization of sRNAs

1.5.2.3.1 Sequestration of sRNAs

Sequestration of ds sRNAs preventing the assembly of RISC effector is the most common suppression strategy evolved by several viral genera (Csorba *et al*., 2007; Ding and Voinnet, 2007; Wu *et al*., 2010). The P19 protein of the genus Tombusvirus is a very strong and efficient RSS. It blocks transgene-induced PTGS and VIGS and is essential for systemic virus infection. P19 prevents RNA silencing by sRNA sequestration through binding of ds sRNAs with high affinity (Silhavy *et al*., 2002). During Cymbidium ringspot virus (CymRSV) infections the concentration of free siRNAs decreases through formation of P19/siRNA complexes thereby sequestering siRNAs for the programming of active RISC (Lakatos *et al*., 2004). The NS3 protein of Rice hoja blanca virus (RHBV) suppressed GFP silencing apparently by affecting the accumulation of GFP siRNAs (Bucher *et al*., 2003). NS3 binds siRNAs *in vitro* without sequence preference but exhibiting the highest affinity for 21 nt siRNAs with or without 2-nt overhangs and

a low affinity for 26 nt siRNAs (Hemmes *et al*., 2007). Two siRNA binding RSS (HC-Pro and P38) require the ethylene-inducible host transcription factor (RAV2) for the suppression of RNA silencing but the mechanistic role of this plant cofactor is unclear (Endres *et al*., 2010).

1.5.2.3.2. Interference with methyltransferase HEN1

2'-O methylation is essential for the biogenesis of sRNAs (see above) (Yu *et al*., 2005). P21 of Beet yellows virus (BYV), P19 of Tomato bushy stunt virus (TBSV), and P1/HC-Pro of Turnip mosaic virus (TuMV) interfere with sRNA stabilization, including miRNAs, by blocking HEN1-mediated methylation (Lozsa *et al*., 2008; Yu *et al*., 2006). It is probable that sRNA-binding RSS have a higher affinity to siRNA and miRNAs than the HEN1 methyltransferase has (Burgyan and Havelda, 2011). The 126 kDa replicase protein of Tobacco mosaic virus (TMV) exhibits suppressor activity by the interference with HEN1 methylation of siRNAs (Vogler *et al*., 2007). The effect of the TMV replicase protein could be on sRNA demethylation., since the enzyme has methyltransferase activity. Alternatively, the protein may bind sRNAs, thereby excluding these from HEN1 methylation (Vogler *et al*., 2007). However, inhibition of the methylation step requires the temporal and spatial coexpression of the suppressor, endougenous or viral siRNAs and miRNAs (Lozsa *et al*., 2008).

1.5.2.4 Suppressors of RISC activity

The P0 protein of Beet western yellows virus (BWYV) contains a conserved minimal F-box motif that interacts with homologues of the S-phase kinase-related protein 1 (SKP1), a core subunit of the multi-component SCF family of ubiquitin E3 ligases. The P0 functions as an F-box protein that targets a key component of the RNA silencing machinery (Pazhouhandeh *et al*., 2006). In plants, it physically interacts with AGO1 to trigger AGO1 protein degradation (Bortolamiol *et al*., 2007; Csorba *et al*., 2010). It has been found that the P0 cannot interfere with the slicer activity of preprogrammed siRNA/miRNA containing AGO1, but can prevent the *de novo* formation of siRNA/miRNA-loaded AGO1 (Csorba *et al.,* 2010). The RSS of Potato chlorotic stunt crinivirus (SPCSV) encoded RNase III endonuclease cleaves 21, 22 and 24 vsiRNAs into 14 bp products, which are inactive in the RNA-silencing pathways, thus preventing RISC assembly (Cuellar *et al*., 2009).

1.5.2.5 Suppressors interfering with the epigenetic modification of the viral genome

The Begomovirus Tomato golden mosaic virus (TGMV)-encoded AL2 protein and the closely related Curtovirus Beet curly top virus (BCTV) L2 act as silencing suppressors. The two RSS modulate endogenous biochemical pathways for the benefit of viruses. They interact with and inactivate the adenosine kinase (ADK), a cellular enzyme important for adenosine salvage and methyl cycle maintenance (Wang *et al.,* 2003). Plants infected with the L2 mutant BCTV and other

unrelated viruses display increased ADK activity, suggesting that ADK could be a part of the response of a plant to viral infection. ADK plays a role in sustaining the methyl cycle. By inhibiting ADK, the AL2 and L2 proteins indirectly block this cycle and thereby could interfere with the epigenetic modification of the viral genome (Bisaro, 2006; Wang *et al.,* 2005). It has been previously shown that *in vitro* methylated TGMV cannot replicate in protoplasts, suggesting that methylation of the viral genome could be a valid mode for combating geminivirus infections (Bisaro, 2006).

The geminivirus nuclear protein AC2, functions as a transactivator of viral transcription and a suppressor of RNA silencing. Characterization of and the relationship between these two functions for AC2 from Mungbean yellow mosaic virus-Vigna (MYMV) and African cassava mosaic geminivirus have been investigated (Trinks *et al*., 2005). Evidence for the transcription-dependent activity of AC2 has also been found. Several promoters cloned from *Arabidopsis* were strongly induced by both AC2 proteins. These results suggested that silencing suppression and transcription activation by AC2 are functionally connected and that some of the AC2-inducible host genes may code for components of an endogenous network that controls silencing (Trinks *et al*., 2005).

1.5.2.6 Viral suppressors with unspecified function

In addition to the above mentioned groups of the RSS proteins with specific interactions, there is another group of viruses encoding RSS proteins with still unknown functions. Among the most studied are the Tobravirus 16K, the Hordeivirus γb and the Pecluvirus P15 proteins. In an *Agrobacterium*-mediated transient assay, the 16K protein of Tobacco rattle virus (TRV) suppresses RNA silencing in transgenic GFP-expressing *N. benthamiana* plants. The 16K protein slightly reduced the accumulation of GFP-derived siRNA suggesting that it may interfere with the initiation and/or maintenance of RNA silencing (Ghazala *et al*., 2008). Another study indicated that the 16K protein operates downstream of dsRNA formation since its effect was compromised when dsRNA inducers were present in high amounts suggesting oversaturation of the 16K protein (Martínez-Priego *et al*., 2008).

The γb protein of Barley stripe mosaic virus (BSMV) (Hordeivirus) is involved in viral pathogenesis but not needed for virus replication (Petty *et al*., 1990). Its suppressor activity was demonstrated by *Agrobacterium*-mediated transient assays (Bragg and Jackson, 2004). The γb protein of a related Hordeivirus localized in the cytoplasm and peroxisome, but its suppressor activity was not associated with its presence in the peroxisome. Similarly to γb, the cysteine-rich Pecluviral P15 suppressor forms coiled-coil structures required for protein-protein interaction and silencing activity. The coiled-coil sequence rather than the peroxisome localization motif is essential for its silencing suppression activity (Alvarado and Scholthof, 2009).

1.5.3 Comparison of different suppressors

The mode of function of six different silencing suppressors encoded by six unrelated RNA-viruses were studied and compared in two independent studies (Dunoyer *et al*., 2004; Chapman *et al*., 2004). Among the tested suppressors were the P1/HC-Pro of TuMV, the P38 of TCV, the P19 of TBSV, the P25 of PVX, the P15 of Peanut clump pecluvirus (PCV) and the 2b of CMV.

Most plant viruses have (+) ssRNA genomes and during viral replication their dsRNA replication intermediates are recognized by the RNA silencing machinery (Ahlquist, 2002). Alternatively or in addition, secondary structures in regions of the ssRNA molecules can be recognized (Szittya *et al*., 2002). No obvious sequence homology was found between the different silencing suppressors and they might act by inhibiting the generation of sRNAs preventing the incorporation of sRNAs into RISC or by interfering with RISC function as described above (Burgyán and Havelda, 2011). Four of the most studied RSS proteins, HC-Pro, P19, 2b, and P25 will be discussed in more detail.

1.5.3.1 Potyviral helper-component protease

The potyviral HC-Pro protein is one of the first identified and well studied plant viral RSS (Anandalakshmi *et al*., 1998; Brigneti *et al*., 1998). HC-Pro proteins of Potyviruses are multifunctional proteins with roles in different crucial steps of the viral infection process (Saenz *et al*., 2002; Stenger *et al*., 2005). The different functions of HC-Pro have been mapped, including cleavage of the viral polyprotein (Verchot *et al*., 1992), insect vector transmission (Pirone and Blanc, 1996), capsid binding (Blanc *et al*., 1997), RNA binding (Urcuqui-Inchima *et al*., 2000), viral movement and replication (Kasschau and Carrington, 1995) and virus synergism (Shi *et al*., 1997; Wang *et al*., 2002).

A first indication how HC-Pro actually suppresses RNA silencing was reported by Anandalakshmi and co-workers (1998) who showed that crossing a GUS-silenced plant line and a HC-Pro expressing plant line could restore GUS expression. HC-Pro was shown to be a strong silencing suppressor. It inhibits effectively initiation of silencing and reverses already established silencing, while it failed to block systemic silencing (Brigneti *et al*., 1998; Lleave *et al*., 2000; Mallory *et al*., 2001, 2003). It appears to interfere with RNA silencing in different ways depending on how silencing is initiated and whether silencing is mediated by miRNAs or siRNAs. HC-Pro specifically sequesters sRNA duplexes by binding sRNAs (<24 nt) and blocking their assembly into RISC (Lakatos *et al*., 2006; Shiboleth *et al*., 2007). Accumulation of specific miRNAs and their target RNAs was enhanced in HC-Pro-expressing plants indicating that the function of miRNAs was repressed (Kasschau *et al*., 2003; Mallory *et al*., 2002). HC-Pro also displays different modes of action when acting as a viral RSS, including possible interference with DCL proteins (Dunoyer *et al*., 2004).

Over-expression of HC-Pro in *Arabidopsis* caused developmental defects similar to those observed in *Arabidopsis caf/dcl1-9, dcl-1, ago-1* and *hen-1* mutants. These defects, disturbance of organ differentiation and polarity, appeared to be related to HC-Pro interference with miRNA accumulation and/or with reduced miRNA function (Dunoyer *et al*., 2004; Kasschau *et al*., 2003; Syller, 2006). Interference with the RNA-regulatory pathways may also be related to viral symptoms which comprise various organ malformations and growth reduction.

A conserved FRNK box located within the central region of HC-Pro was found to be involved in siRNA and miRNA duplex sequestration and a mutation of the ZYMV HC-Pro^{FRNK} to FINK (HC-Pro^{FINK}) caused attenuation of symptoms upon infection and a decrease in miRNA accumulation (Shiboleth *et al*., 2007). Although HC-Pro^{FINK} has a lower affinity for miRNA duplexes than the wild type HC-Pro^{FRNK}, it still retains its suppressor capacity (Shiboleth *et al*., 2007). Similarly, studies on other Potyvirus spp. with mutated HC-Pro have clarified the role of this protein in pathogenicity and symptom development (Gonzalez-Jara *et al*., 2005; Torres-Barcelo *et al*., 2008; Wu *et al*., 2010; Yambao *et al*., 2008). The FRNK box is responsible for viral genome amplification, RNA binding and suppression of PTGS/VIGS (Plisson *et al*., 2003). Recently, Torres-Barcelo and co-workers (2008) showed that mutations randomly distributed on three different regions of HC-Pro affect its pathogenicity and suppression ability for S-PTGS suggesting that regions outside the HC-Pro central domain are also important for PTGS.

1.5.3.2 Tombusvirus P19

The P19 of Tombusvirus is the best understood viral RSS. The function of P19 varied in different assays of silencing suppression. It can reverse silencing when applied on established silencing but this occurs only in regions close to veins (Voinnet *et al*., 1999). However, when applied simultaneously with silencing inducers (in a transient silencing suppression assay) it effectively obstructs local and systemic silencing (Hamilton *et al*., 2002; Silhavy *et al*., 2002; Voinnet *et al*., 2003). *In vitro*, P19 binds PTGS-generated 21 nt siRNAs, 21 nt miRNAs and 21 nt synthetic dsRNAs with 2 nt 3′-overhanging end(s). It only very inefficiently binds ssRNAs, long dsRNAs and blunt-ended 21 nt dsRNAs (Dunoyer *et al*., 2004; Lakatos *et al*., 2004; Ye *et al*., 2003). Crystallographic studies have shown that P19 forms homodimers, which act like a molecular ruler, measuring the length of siRNA duplexes and binding them in a sequence-independent way (Vargason *et al*., 2003; Ye *et al*., 2003). Due to this specificity for 21 nt sRNAs, P19 proteins of different Tombusviruses can function as silencing suppressors in a wide range of organisms. They were demonstrated to even function in insects and mammalian cells (Dunoyer *et al*., 2004; Lakatos *et al*., 2004). It was found that P19 activity inhibit siRNA-directed RNA cleavage and prevents siRNAs from being incorporated into RNA silencing effectors such as RISC in the heterologous *in vitro* system based on *Drosophila* embryo extracts (Lakatos *et al*.,

2006). Moreover, the alteration of leaf morphology in P19-expressing plants may indicate that the PTGS pathway is also important in the regulation of plant development (Silhavy *et al*., 2002).

1.5.3.3 Cucumber mosaic virus 2b

The 2b protein of CMV is a small protein composed of only 110 amino acids. Initially, it was identified as a pathogenicity determinant by Ding and co-workers (1994, 1996). This role is associated with its activity as a RSS (Brigneti *et al*., 1998; Lucy *et al*., 2000). The suppressor activity of 2b is different among different CMV strains. Based on viral RNA sequence data and 2b suppressor activity three subgroups were identified in CMV: IA, IB, and II (Lewsey *et al*., 2007; Shi *et al*., 2002). A surprising effect of CMV 2b has been demonstrated recently. The 2b facilitates epigenetic modifications through the transport of siRNA into the nucleus (Kanazawa *et al*., 2011).

In plants, CMV 2b is considered a multifunctional protein as it has roles in viral long-distance movement, viral symptom severity, and intercellular RNA silencing suppression (Hemera *et al*., 2011). The CMV 2b interferes with local and systemic silencing. It was further reported that 2b interferes with AGO1-containing RISC activity by directly interacting with its PAZ and PIWI domains, and inhibiting AGO1 slicer activity (Zhang *et al*., 2006). González and co-workers (2010) showed that the 2b protein is present in the nucleolus and that it interacts with AGO1 and AGO4 *in vivo*. Using a series of mutants, they showed that the putative nuclear localization signals (NLS) and phosphorylation motif of 2b are not required for self-interaction or for interaction with AGO proteins. Neither protein/protein interactions nor nucleolar targeting was sufficient to provide local silencing suppression activity. In contrast, the ability of 2b to bind sRNAs appeared to be indispensable for its silencing suppressor function. Nuclear targeting of 2b is thought to be required for its function as a silencing suppressor, as the loss of the NLS in some mutants also abolished its silencing suppressor activity (Lucy *et al*., 2000; Wang *et al*., 2004).

The mode of action of CMV 2b on RdDM was explored by Hamera and coworkers (2011). The 2b exists in a complex of 24 nt repeat-associated siRNAs (rasiRNA) *in vivo,* which regulate genomic DNA methylation. The 2b can also bind siRNA and miRNA with single and duplex forms with equal affinity (Goto *et al*., 2007; Hamera *et al*., 2011). Sequencing data demonstrated that 2b preferentially binds sRNAs with a 5'-adenosines which are loaded onto AGO4 (Hamera *et al*., 2011). The interaction of 2b with AGO4 was shown by the transient assay of Bimolecular florescence complementation (BiFC) (Gonzalez *et al*., 2010). Furthermore, Hamera and coworkers (2011) showed that CMV 2b interacts directly with the PAZ and Piwi domains of AGO4, and caused the attenuation of AGO4 slicer activity and subsequent hypomethylation of AGO4-related loci. Interestingly, it was also found that 2b can cause hypomethylation of AGO4 targets independently of its catalytic activity (Hamera *et al*., 2011).

1.5.3.4 Potato Virus X P25

The PVX P25 protein is essential for cell-to-cell movement of PVX. However, using agro-coinfiltration experiments it was shown that a P25 transgene construct blocked systemic silencing (Roth *et al*., 2004; Hamilton *et al*., 2002; Voinnet *et al*., 2000). P25 turned out to be a multifunctional silencing suppressor (Bayne *et al*., 2005; Voinnet *et al*., 2000) with nucleotide binding, RNA helicase activity (Kalinina *et al*., 2002) and the ability to induce plasmodesmata gating (Howard *et al*., 2004). P25 appeared to be a very weak suppressor because it did not block siRNA biogenesis and had no effect on endogenous miRNA accumulation. It may block the silencing pathway by interfering with RISC (Bayne *et al*., 2005). The possibility that P25 may target AGO proteins was investigated by Chiu and coworkers (2010). Their biochemical data indicated a strong interaction between P25 and AtAGO1 when these proteins were transiently co-expressed in *N. benthamiana*. P25 also interacts with AtAGO2, AtAGO3 and AtAGO4 but not with AtAGO5 and AtAGO9 (Chiu *et al*., 2010). These findings are consistent with the idea that RNA silencing is an antiviral defense mechanism and that the counter-defense role of P25 acts through the degradation of AGO proteins *via* the proteasome pathway.

1.6 Application of RNA silencing suppressors in biotechnology.

Viral RSS proteins provided a new tool for technologies using genetically modified plants. Many biotechnological applications are impaired by RNA silencing and suppressors of silencing can be used to attain consistent, high-level expression of transgenes in plants (Mallory *et al*., 2002; Voinnet *et al*., 2003). With silencing under control, transgenic plants can be engineered to produce a range of transgene products, moderate levels of expression to produce desired plant traits or very high-level expression to use plants as bioreactors for the production of pharmaceuticals, vaccines or other high-value products (Roth *et al*., 2004). Also, viral RSS proteins provide unique tools to understand the mechanism of RNA silencing. Much of what is currently known about the RNA silencing pathways came from *in vitro* and genetic studies in organisms other than plants (Tijsterman *et al*., 2002).

In plants, traditional genetic approaches have led to the identification of a number of cellular genes required for RNA silencing (Mourrain *et al*., 2000). Surprisingly, however, all of these genes are required for sense-, but not for IR-transgene induced silencing (Boutet *et al*., 2003). The plant viral suppressors, many of which appear to work downstream of dsRNA, provide a novel means of entry into parts of the silencing pathway that are not easily accessible by genetic screens. The currently known suppressors appear to work at different steps in silencing, thereby providing access to a number of points in the pathway where silencing can be controlled. Identifying host proteins that interact with a viral RSS is one very promising approach that is being used to elucidate silencing pathways. The yeast two-hybrid system has been used to identify

tobacco proteins that interact with HC-Pro, including the rgs-CaM that suppresses RNA silencing when over-expressed (Anandalakshmi *et al*., 2000). This result suggests that a calcium controlled signal transduction pathway involving rgs-CaM is one of the mechanisms regulating RNA silencing. The identification of a viral suppressor that works in animal cells (Li *et al*., 2002) offers the possibility that such proteins may provide a similar tool to understand silencing pathways in other organisms as well.

1.7 Aims of the Work

The main goal of this work is to uncover the molecular mechanism of HC-Pro as RNA silencing suppressor, and to understand how positive-strand RNA viruses cause disease symptoms. The ZYMV silencing suppressor is the only HC-Pro of which the functions of silencing suppression and symptom induction have been dissected. Previous results suggested that HC-Pro exhibits two independent RSS activities. One RSS function is based on sRNA binding whereas the second one appeared to interfere with sRNA stability. In the present study, I have specifically aimed to elucidate the following:

1. Determination of the sub-cellular localization of the ZYMV HC-Pro^{FRNK} protein and its HC-Pro^{FINK} mutant.
2. Comparison of developmental abnormalities caused by HC-Pro^{FRNK} and HC-Pro^{FINK} in transgenic *N. benthamiana* and *A. thaliana* plants.
3. Investigation if HC-Pro^{FINK} produces phenotypes in *N. benthamiana* and *A. thaliana* when targeted into the nucleus.
4. Analysis of the interaction between HC-Pro and plant proteins involved in the stability of sRNAs.
5. Investigation if HC-Pro^{FRNK} and HC-Pro^{FINK} interfere with HEN1 methyltransferase activity *in vitro*.
6. Analysis of self interaction of HC-Pro^{FRNK} and HC-Pro^{FINK}

2 Materials and Methods

2.1 Materials

Chemical substances, unless otherwise stated in the text, were purchased from the following companies: Applied Biosystems (www.appliedbiosystems.com), Bio-Rad (www.bio-rad.com), Biozym (www.biozym.com), Duchefa (www.duchefa.com), Fisher Scientific (www.fishersci.com), GE Healthcare (www.gehealthcare.com), Invitrogen (www.invitrogen.com), Merck (www.merck-chemicals.de), Neolab (www.neolab.de), Perkin Elmer (www.perkinelmer.com), Roche (www.roche.com), Roth (www.carl-roth.de), Sigma-Aldrich (www.sigmaaldrich.com), Qiagen (www.qiagen.com), and Thermo Fisher (www.thermofisher.com). Restriction enzymes and other DNA modifaying enzymes were purchased from New England Biolabs (www.neb-online.de) and Fermentas (www.fermentas.de). Membranes, X-ray films and other laboratory equipment was purchased from the following companies: 3M (solutions.3mdeutschland.de), Axon (www.axon.com), Biometra (www.biometra.de), Brand (www.brand.de), Braun (www.bbraun.de), Eppendorf (www.eppendorf.de), Fisher Scientific, GE Healthcare, Greiner (www.greinerbioone.com), LHG (www.lhg-karlsruhe.de), Medical Market (Hofheim, Germany), Merck, Millipore (www.millipore.com), Sarstedt (www.sarstedt.com), Sartorius (www.sartorius.de), Schleicher & Schull (www.schleicher-schuell.com).

2.1.1 Plant material

The plant material used in this study are presented in Table 2.1.

Table 2.1 List of plant material used in this study.

Scientific name
Nicotiana benthamiana
Arabidopsis thaliana (Line Col-0)
Solanum lycopersicom (Hellfrucht/Fruehstamm)

2.1.2 Bacterial and yeast strains

Bacterial and yeast strains used in this study are presented in Tables 2.2 and 2.3.

Table 2.2 Bacterial strains, their genotypes and sources.

Species	Strain	Genotype	Source
Agrobacterium tumefaciens	ATHV	C58C1 Rif^r	(Hellens *et al*., 2000)
A. tumefaciens	GV3101	pMP90RK Gm^r, Km^r, Rif^r	(Koncz and Schell, 1986)
Escherichia coli	BL21 (DE3) *codon plus*	F- *omp*T *hsd*SB(rB- mB-) *gal dcm rne*131 (DE3), (*argU,ileY*, and *leuW*)	Stratagene (www.stratagene.com)
E. coli	INVα	F´ *end*A1 *rec*A1 *hsd*R17 (rk-, mk+) *sup*E44 *thi*-1 *gyr*A96 *rel*A1 φ80*lac*ZΔM15 Δ(*lac*ZYA-*arg*F)U169 λ-	Invitrogen

Table 2.3 Yeast host strain, their genotypes, reporter genes, transformation markers and refernces.

Species	Strain	Genotype	Reporters	Transformation Markers	Reference
Saccharomyces cerevisiae	Y2H Gold: b, d	*MATa, trp1-901, leu2-3, 112, ura3-52, his3-200, gal4Δ, gal80Δ, LYS2: GAL1UAS–Gal1TATA–His3, GAL2UAS–Gal2TATA–Ade2 URA3 : MEL1UAS–Mel1TATA AUR1-C MEL1*	*AbAr, HIS3, ADE2, MEL1*	*trp1, leu2*	Nguyen, unpublished
S. cerevisiae	Y187c	*MATα, ura3-52, his3-200, ade2-101, trp1-901, leu2-3, 112, gal4Δ, gal80Δ, met–, URA3 : GAL1UAS–Gal1TATA–LacZ, MEL1*	*MEL1, LacZ*	*trp1, leu2*	(Harper *et al*., 1993)

2.1.3 Antibodies, oligonucleotides

2.1.3.1 Antobodies

Antibodies used for the detection of proteins in western blot analysis are listed in Table 2.4.

Table 2.4 List of antibodies, their origin, mode of dilutions and sources.

Antibody	Organism	Dilution	Source
anti-GFP	Rabbit	1:1,000	Santa-Cruz (www.scbt.com)
anti-GFP-HRP	Mouse	1:10,000	Miltenyi Biotec (www.miltenyibiotec.com)
anti-HA	Mouse	1:10,000	Sigma-Aldrich
anti-HA-Peroxidase	Mouse	1:1,000	Roche
anti-rabbit peroxidise	Goat	1:1,000	Santa-Cruz
anti-mouse IgG peroxidise	Goat	1:1,000	Sigma-Aldrich
anti-MBP	Mouse	1:10,000	New England Biolabs
HC-Pro antiserum	Rabbit	1:10,000	S.D.Yeh, Taiwan

2.1.3.2 Oligonucleotide

2.1.3.2.1 RNA oligonucleotides

Lyophilized synthetic RNA oligonucleotides (Sigma-Aldrich) (Table 2.5) were diluted in H_2O at a concentration of 1 µg/µl stock solution.

Table 2.5 Overview and sequences of the RNA oligonucleotides.

Designation	Sequense (5'→3')
ath-miR173	UUC GCU UGC AGA GAG AAA UCA C
ath-miR173*	GAU UCU CUG UGU AAG CCG AAA G
ath-miR168	TTC CCG ACC TGC ACC AAG CGA
ath-miR168*	ATT CAG TTG ATG CAA GGC GGG
ath-miR159	AGG AGC TCC CTT CAA TCC AAA
ath-miR159*	GTT TTG GAG GAA GGG AGC TC
ath-miR156	GTG CTC ACT CTC TTC TGT CA
ath-miR156*	CTG ACA GAT AGA GCA GTG AGC
ath-miR162	TCG ATA AAC CTC TGC ATC CAG
ath-miR162*	CTG GAT GCA GAG GTT TAT CGA
ath-miR171c	CGT GAT ATT GGC ACG GCT CAA
ath-miR171c*	GAT TGA ACC GCA CTA ATA TCT
ath-miR160a	TGG CAT ACA GGG AGC CAG GCA
ath-miR160a*	TGC ATG GCT CCT CAT ACG CCA
ath-miR390a	GGC GCT ATC CCT CCT GAG CTT
ath-miR390a*	TGA AAC TCA GGA TGG ATA GCG

2.1.3.2.2 DNA oligonucleotides

The DNA oligonucleotides were purchased from Sigma-Aldrich and Invitrogen (Table 2.6). The oligonucleotides were stored as 100 µM stock solution at -20°C.

Table 2.6 Overview and sequences of DNA oligonucleotides used.

Description	Sequence (5′→ 3′)
5pMal-fwd seq2	TGA AAT CAT GCC GAA CAT CC
pGADT7 seq for	TAA TAC GAC TCA CTA GG
pGADT7 seq rev	AGA TGG TGC ACG ATG CAC AG
pGBKT7 seq for	GTA ATA CGA CTC ACT ATA GG
pGBKT7 seq rev	TTT TCG TTT TAA AAC CTA AGA
5'-delta-N2-Mal-FRNK	CTC AGA ATC TCG AGC TCT CAT CTG
3'-delta-N2-Mal-FRNK	CAG ATG AGA GCT CGA GAT TCT GAG
5'-delta-N3-Mal-FRNK	CAT CAA CAC GGA GCT CAT GAA AG
3'-delta-N3-Mal-FRNK	CTT TCA TGA GCT CCG TGT TGA TG
NcoI delete C-F	CAA TAT TTT CCT CGC CAT GGA TGA AC
NcoI delete C-R	GTT CAT CCA TGG CGA GGA AAA TAT TG
HEN1p1 for	GGD GAT GCA RTH TTR KCD WMY RTW GG
HEN1p1 rev	CTW CCA GAW CCR CAK CCM AAR TC
HEN1p2 for	GAY TTK GGM TGY GGW TCT GGW AG
HEN1p2 rev	AGT DAT YTG VGA RGC RAA KCC KCG
HEN1-EcoRI-PI-F	CTC AGT GTA GGA TTT GAA TTC TTA TAA G
HEN1-HindIII-PI-R	CTG AGG AAG CTT TGC CAA TAG TC
HEN1-HindIII-P2-F	GAC TAT TGG CAA AGC TTC CTC AG
HEN1-StuI-P2-R	GAG AGA ATA AGG CCT GTT CCA TTC
HEN1-StuI-P3-F	GAA TGG AAC AGG CCT TAT TCT CTC
HEN1-BamHI-P3-R	CTT CTG GAT CCC ACA TCA CTA ACC
HEN1-BamHI-FRET-R	CTC TGG ATC CTC TTT ATT GTC ACT ACT CC
Linker pPCV A-F	GAT CTT CCC CTG CAG GAG CTC GGC GCG CCT GTA CAG TTA ATT AAC T
Linker pPCV B-R	CTA GAG TTA ATT AAC TGT ACA GGC GCG CCG AGC TCC TGC AGG GGA A
HC-Pro -Y2H NdeI-F	CGC CAT ATG GCG TCG TCA CAA CCG GAA G
HC-Pro -Y2H XmaI-R	CCC CCG GGG GTC AGC CAA CTC TGT AAT GTT TC
Hc-Pro-int-seq-F	GCT TCT TGA AAT GAC TCA GTG G
Hc-Pro XbaI –R	GCT CTA GAG CTT AGC CAA CTC TGT AAT GTT TC
PSTVd-for1	CGG GGA AAC CTG GAG CGA ACT
PSTVd-rev1	GGG ATC CCT GAA GCG CTC CTC
GFP BamHI-F	CGG GAT CCC GAT GGG TAA AGG AGA AGA AC
GFP XbaI-R	GCT CTA GAG CTT TGT ATA GTT CAT CCA TGC C
Hc-Pro XbaI- F	GCT CTA GAG ATG TCG TCA CAA CCG GAA GTT C
HA-AscI-F	GGC GCG CCA TGT ATC CAT ATG ATG TTC C
GFP-XbaI stop-R	ACT CTA GAG GAT CCT TAT TTG TAT AGT TCA TCC
AGO1-EcoRI-P1-F	GTG AAT TCC CCA TGG TGC GGA AGA AG
AGO1-EcoRI-P1-R	CAA GGG GAA TTC GTC TAG AGA GC
AGO1-EcoRI-PII-F	GCT CTC TAG ACG AAT TCC CCT TG
AGO1-BamHI-PII-R	GGA TCC CTA ACA ATA AAA CAT AAC CCT C

2.1.4 Vectors and expression plasmids

The binary vectors used for the expression of genes in plant and bacteria are listed in Table 2.7.

Table 2.7 Overview of generated vectors and plasmids.

Plasmid	Comment	Resistance	Reference
pBin19:HA-HC-Pro^{FINK}	pBin19 binary vector with HA-HC-Pro FINK gene in T-DNA under the control of CaMV 35S promotor and poly(A)-signals	Km	(Shiboleth *et al.*, 2007)
pBin19:HA-HC-Pro^{FRNK}	pBin19 binary vector with HA-FRNK HC-Pro gene in T-DNA under the control of the CaMV 35S promoter and poly (A) signals	Km	(Shiboleth *et al.,* 2007)
pKB:biNLS-GFP	pKB binary vector with GFP fused with the nuclear localization signal	Sm/Sp	(Boonrod *et al*., 2004)
pKB:biNLS-HC-Pro-GFP	pKB binary vector with HC-Pro GFP fused with the nuclear localization signal	Sm/Sp	(Fuellgrabe, Unpublished data)
pPCV702SM-MC:HA-NLS-HC-Pro	pPCV binary vector with HC-Pro fused with the nuclear localization signal	Sm/Sp	This work
pPCV702SM-MC:HC-Pro-GFP	pPCV702SM-MC binary vector with GFP fused to the C-terminus of HC-Pro	Sm/Sp	This work
pPCV702SM:GFP-HC-Pro	pPCV702SM binary vector with GFP fused to the N-terminus of HC-Pro	Sm/Sp	This work
pTPCR-SlHEN1	pTPCR cloning vector containing SlHEN1 cDNA with *EcorI* and *BamHI* restriction sites	Cb	This work
pPCV702SM: HEN1-GFP	pPCV702SM binary vector with GFP fused to the C-terminus of SlHEN1	Sm/Sp	This work
pPCV702SM: HEN1-mRFP	pPCV702SM binary vector with RFP fused to the C-terminus of SlHEN1	Sm/Sp	This work
pMAL.c2X	Vector encoding malE gene for expression of fusion proteins with N-terminal MBP	Cb	(Di Guan *et al*., 1988)
pMAL.c2X:HA-HC-Pro ΔN1	HC-ProFRNK lacking 93 aa from the N-terminus fused with the N-terminus of MBP proteins	Cb	(Fuellgrabe, 2010)
pMAL.c2X:HA-HC-Pro ΔN2	See section 2.2.1.24	Cb	This work
pMAL.c2X:HA-HC-Pro ΔN3	See section 2.2.1.24	Cb	This work
pMAL.c2X:HA-HC-Pro ΔC7	See section 2.2.1.24	Cb	This work
pMAL.c2X:HA-HC-Pro ΔC8	See section 2.2.1.24	Cb	This work
pMAL.c2X:HA-HC-Pro ΔC9	See section 2.2.1.24	Cb	This work
pMAL.c2X:HA-HC-Pro^{FINK}	HC-Pro^{FINK} fused with the N-terminus of MBP proteins	Cb	(Fuellgrabe *et al.,* 2011)
pMAL.c2X:HA-HC-Pro^{FRNK}	HC-Pro^{FRNK} fused with the N-terminus of MBP proteins	Cb	(Fuellgrabe *et al.,* 2011)
pGADT:HC-Pro^{FRNK}	pGADT7 vector with HC-Pro^{FRNK} fused inframe with GAL4 DNA-AD (Activation domain)	Cb	This work
pGBKT:HC-Pro^{FRNK}	pGBKT7 vector with HC-Pro^{FRNK} fused inframe with GAL4 DNA-BD (Binding domain)	Km	This work
pGADT:HC-Pro^{FINK}	pGADT7 vector with HC-Pro^{FINK} fused inframe with GAL4 DNA-AD	Cb	This work
pGBKT:HC-Pro^{FINK}	pGBKT7 vector with HC-Pro^{FINK} fused inframe with GAL4 DNA-BD	Km	This work
pGADT:SlHEN1	pGADT7 vector with HEN1 fused inframe with GAL4 DNA-AD (Activation domain)	Km	This work
pGADT:NbAGO1	pGADT7 vector with AGO1 fused inframe with GAL4 DNA-AD (Activation domain)	Km	This work

Plasmid	Comment	Resistance	Reference
pGADT7-T	Control vector	Cb	Clontech (www.clontech.com)
pGBKT7-53	Control vector	Km	Clontech (www.clontech.com)
pGBKT7-Lam	Control vector	Km	Clontech (www.clontech.com)
pPCV702SM-MC	Modified pPCV702SM plasmid with streptomycin/spectinomycin resistance gene; additional polylinker between 35S promoter and p (A) nos sequence	Sm/Sp	This work
pPCV702SM:GpG	pPCV vector encoding a GFP-hairpin from a 143 bp fragment of the cDNA GFP5 composed in both sense and in antisense orientation. The two fragments are separated by a 90 bp spacer of the Potato spindle tuber viroid (PSTVd)	Sm/Sp	(Dalakouras *et al*., 2009)
pKB:GUS-GFP	pKB vector encoding GUS fused to the GFP protein; locolizes the protein in the cytosol	Sm/Sp	Kindly provided by Dr. Kajohn Boonrod
pPCV702SM:GFP5	pPCV vector encoding GFP protein which possesses an N-terminal leader sequence that localizes the protein to the endoplasmic reticulum (ER)	Sm/Sp	(Vogt *et al.*, 2004)

2.2 Methods

2.2.1 Cloning and general work with nucleic acids

2.2.1.1 Preparation of competent *E. coli* cells

The production of chemocompetent bacteria of the *E. coli* strains INVα, SM10 and BL21 (DE3 codon) plus was carried out according to the protocol of Inoue and co-workers (1990).

E. coli strains were spread out from a stock culture on LB plates. The next day, a few colonies from the plate were inoculated with a sterile inoculation loop in 247.5 ml SOB medium with 2.5 ml Mg^{2+} solution in a l l Erlenmeyer flask. The cells were incubated at 18°C and 190 rpm until they reach an optical density of OD_{600} = 0.4-0.5. Flasks were chilled for 10 min on ice and the cell cultures were transferred to refrigerated centrifuge tubes. Cells were centrifuged at 4,000 x g for 10 min at 4°C. The cell pellet was resuspended in 80 ml ice-cold transformation buffer (Appendix C) and incubated for 10 min on ice. After centrifugation (4,000 x g, 10 min, 4°C) the cell pellet was resuspended in 20 ml transformation buffer solution, DMSO was added to a final concentration of 7% and the cells were incubated for 10 min on ice. The cell suspension was divided into 100 µl aliquots and frozen in liquide nitrogen (LN). Chemocompetent cells were stored at -80°C until use.

2.2.1.2 Transformation of bacteria

100 µl aliquots of chemocompetent cells *E. coli* (INFα) were thawed on ice and 10 µl ligation mixtures or 10-50 ng plasmid DNA were added. Mixtures were incubated for 30 min

on ice and then incubated for 45 sec at 42°C. Mixtures were cooled on ice for 2 min, mixed with 200 µl SOC-medium (Appendix C) and incubated for 1 h at 37°C with 190 rpm shaking.

After one-hour incubation, 200 µl of the reaction mixtures were plated on LB agar media plates supplemented with the appropriate antibiotics for selection of recombinant clones and incubated at 37°C overnight (ON). Positive colonies were screened by plasmid minipreparation procedures (miniprep) followed by digestion with specific restriction enzymes. Table 2.8 lists the concentrations of antibiotics, which were needed for selection of recombinant clones. After cooling of the LB medium to ~60°C, the respective antibiotics were added (Table 2.8).

Table 2.8 Overview of the antibiotics used for selection of recombinant *E. coli* clones. The final concentrations and the respective resistance genes are indicated.

Antibiotic	Final concentration	Resistance gene
Ampicillin	100 µg/ml	amp^r and. $bla_{(TEM-1)}$
Carbenicillin	50 µg/ml	amp^r and. $bla_{(TEM-1)}$
Kanamycin	50 µg/ml	*nptI*
Streptomycin	20 µg/ml	*AadA* (Strep/$Spec^R$)-Gen
Spectomycin	25 µg/ml	*AadA* (Strep/$Spec^R$)-Gen

2.2.1.3 Isolation of plasmid DNA using the alkaline method

The method is based on the selective alkaline denaturation of linear DNA, while circular plasmid DNA remains stable (Birnboim and Doly, 1979). This involves culturing of the corresponding bacterial clones in 1 ml LB medium with appropriate antibiotics ON at 37°C with shaking. The next day, cells were centrifuged for 5 min at 10,000 x g in a tabletop centrifuge. Pellets were dissolved in 100 µl P1 (50 mM Tris-HCl, pH = 7.5, 10 mM EDTA, 5% Glycerol (volume (v)/v), 100 g/ml RNase A). After that, 200 µl P2 (200 mM NaOH, 1% (weight (w)/v) SDS) were added, the reaction tubes were repeatedly inverted and incubated 5 min at room temperature (RT). 150 µl P3 (3 M $NaCH_3COO$, pH = 5.5) were added, samples were mixed and incubated for 10 min at -20°C for nucleic acids precipitation. The mixtures were centrifuged for 5 min at 17,900 x g and supernatants were transferred into new reaction tubes already containing 500 µl ice-cold 100% ethanol. After mixing, the mixtures were incubated for 2 min at RT, followed by centrifugation for 5 min at 17,900 x g. Pellets were washed with 500 µl cold ethanol (70%) and samples were centrifuged as mentioned in the previous step. After drying, pellets were resuspended in 15 µl ddH_2O.

2.2.1.4 Plasmid preperation using QIAprep Spin Miniprep Kit

For plasmid DNA isolation the QIAprep Spin Miniprep Kit (Qiagen) was used. The method is based on the principle of the binding of plasmid DNA with a high salt buffer to a silica membrane. Bacterial clones were cultured ON in 5-10 ml LB medium with the appropriate antibiotics at 37°C with shaking. After the centrifugation of the culture at 17,900 x g. for 5 min, plasmids were recovered according to the manufacturer's protocol. Plasmid

concentrations were measured by using the NanoDrop ND-1000® Spectrophotometer (PEQLAB Biotechnologie, www.peqlab.de). The quality of the DNA was analysed by agarose gel electrophoresis.

2.2.1.5 Transformation of *A. tumefaciens* competent cells

Transformation of *A. tumefaciens* cells was done either by using electroporation or the freeze and thaw methods.

2.2.1.5.1 Transformation of competent *A. tumefaciens* cells by electroporation

50 µl of a electrocompetent *A. tumefaciens* (strain ATHV) cultures were thawed on ice (Rakesh, 1996), mixed with 10-15 ng of binary plasmids in pre-cooled kuvette tubes and incubated on ice for 5 min. Electroporation was carried out at 2,50 kV, 25 µF, and 200 Ω for 5 sec using the Gene Pulser II (Bio-Rad). Immediately, 450 µl SOC medium were added and tubes were incubated at 28°C with shaking (160 rpm) for 1 h. 50 and 100 µl of the *Agrobacterium* cultures were plated onto LB plates with appropriate antibiotics. The plates were incubated at 28°C for 2 days.

2.2.1.5.2 Transformation of *A. tumefaciens* by the freeze and thaw method

50 µl of a chemically competent *A. tumefaciens* (strain GV3101) cultures were thawed on ice and mixed with 1 µg of plasmid DNA (Jyothishwaran *et al*., 2007). Suspension were frozen for 1 min in LN and then incubated for 5 min at 37°C. 200 µl of SOC medium were added and the mixtures were incubated for 1 h at 28°C with shaking at 160 rpm. Suspension were completely plated onto LB plates containing appropriate antibiotics. The plates were incubated upside down for 1-2 days at 28°C.

2.2.1.6 Selection of the transformed *A. tumefaciens* cells

Only cells that have incorporated a recombinant plasmid with the corresponding resistance gene can grow on the antibiotic-containing medium. The concentrations of antibiotics, which were needed for selection of recombinant clones are presented in Table 2.9.

Table 2.9 List of the antibiotics used for selection of recombinant *A. tumefaciens* clones. The final concentrations, abbreviations and the respective resistance genes are indicated.

Antibiotic	Final Concentration	Abbreviation	Resistant gene
Kanamycin	50 µg/ml	LB_{Km50}	*nptII*
Rifampicin	100 µg/ml	LB_{Rif100}	*rpoB*-Mutation
Streptomycin	100 µg/ml	LB_{Sm100}	*AadA* (Strep/$Spec^R$)-Gen
Spectomycin	100 µg/ml	LB_{Sp100}	*AadA* (Strep/$Spec^R$)-Gen

2.2.1.7 Isolation of recombinant plasmid DNA from *A. tumefaciens* cells

The isolation of plasmid DNA from *A. tumefaciens* cells was performed using the Wizard Plus SV Miniprep DNA Purification System (Promega, Mannheim). *Agrobacterium* clones were cultured in 10 ml of LB medium with appropriate antibiotics for 1-2 days at

28°C. Cultures were centrifuged for 5 min at 4,000 x g and the plasmid extraction was carried out according to the manufacturer's instructions. The extracted plasmid DNA was re-transformed into *E. coli* to obtain a pure plasmid for further analysis (sequencing, restriction analysis). 10 µl of plasmid DNA were used for the re-transformation.

2.2.1.8 Production of bacterial-stock cultures

Glycerol stock cultures were prepared for long term storage of bacterial cultures. The addition of glycerol prevent damaging of the cells by deep freezing and enables the cultivation of cells after thawing. To prepare stock cultures 800 µl of a bacterial culture and 200 µl sterile glycerol (87%) were mixed, frozen in LN and stored at -80°C.

2.2.1.9 Restriction analysis of DNA

Plasmid DNA was digested with restriction enzymes according to the manufacturers' protocols (New England Biolabs, Fermentas). Restriction endonucleases cut DNA by hydrolysis, recognizing a short, defined nucleotide sequence. The digestions were carried out in the buffer provided by the manufacturers. For restriction analyses reactions were carried out in a total volume of 10 µl. For cloning experiments restrictions were performed in 50-100 µl. Reaction mixtures were incubated for 30-90 min at 37°C.

2.2.1.10 Dephosphorylation of linearized DNA fragments

In order to prevent the re-circularization of linearized plasmids, the 5'-phosphate groups were removed from the DNA with alkaline phosphatase. To a 50 µl restriction sample containing 1 µg of plasmid DNA 1 U of FastAP™ Alkaline Phosphatase (Fermentas) was added. Reaction mixtures were incubated for 30-60 min at 37°C and incubated for 5 min at 75°C to inactivate the enzyme. Phenol-chloroform-extraction followed by ethanol precipitation was carried out to remove the residual enzyme. The nucleic acids were resuspended in 12 µl ddH_2O and 2 µl of the solutions were separated on an agarose gel to determine the DNA concentration.

2.2.1.11 Phenol-chloroform extraction and ethanol precipitation

Phenol-chloroform extraction is a standard method for the removal of proteins from nucleic acid solutions. The phenol acts as hydrogen bridge and forms hydrophobic interactions with amino acid side chains. The phenol dissociates the protein/nucleic acid complexes into free components and the denatured proteins accumulate in the phenol phase. Phenol at a pH value of 7.8 prevents the DNA to pass into the phenol phase. A mixture of phenol and chloroform 1:1 ratio was used. The chloroform denatures the proteins and thus facilitates the phase formation.

For the purification of nucleic acids reaction mixtures, equal volumes of a phenol-chloroform (1:1) solution were added and mixed vigorously for 30 sec. After the mixtures were centrifuged at 17,900 x g for 5 min, the aqueous phases (upper phases) were transferred into new reaction tubes, mixed with equal volumes of chloroform and centrifuged for 5 min at 17,900 x g. The aqueous phases with the nucleic acids were then transferred into new reaction tubes and nucleic acids were precipitated with ethanol.

Ethanol precipitation is used to purify and concentrate nucleic acids. Nucleic acids are less soluble in alcohol than in water and addition of salt decreases its solubility. 2.5 volumes of 100% ethanol and 1/10 volume of 3 M sodium acetate (pH = 5.2) were added to the reaction tubes containing the nucleic acids in the aqueous phase. After incubation for 30 min at -20°C, samples were centrifuged for 10 min at 4°C and 17,900 x g. Nucleic acids pellets were washed with 500 µl ethanol (70%) and were again centrifuged for 5 min. Pellets were dried at RT for 10-15 min and resuspended in 15 µl ddH_2O.

2.2.1.12 Agarose gel electrophoresis and documentation

Agarose gel electrophoresis is used to determine the sizes of linear DNA fragments. For the separation of fragments smaller than 1 kilo bases (kb), 1.5-2% agarose gels were used. For fragments up to 8 kb, 1% agarose gels and for fragments larger than 8 kb, 0.8% agarose gels were used. Agarose suspensions were heated in a microwave oven to enable agarose melting and then cooled to 50-60°C. For visualization of separated nucleic acids, 50 ng/ml of EtBr were added to agarose suspensions. Agarose solutions were poured into gel trays carrying a comb for formation of wells. After gel solidification, combs were removed and gels were placed in horizontal gel chambers filled with 1x TAE buffer.

The DNA samples were mixed with 6x DNA sample buffer (Fermentas) and loaded into the wells from the cathode side. Electrophoresis was carried out at 80-100 V. Electrophoresis was stopped after the desired seperation was reached and nucleic acids were visualized on a transilluminator under UV light. The GeneRuler DNA Ladder Mix (Fermentas) was used as a size marker.

2.2.1.13 Extraction of DNA from agarose gels with Nucleo Spin® Extract II kit

DNA fragments were extracted from agarose gels using the Nucleo Spin® Extract II kit (Macherey-Nagel, www.mn-net.com) according the manufacture's instructions. Gel pieces containing the DNA fragments were cut with a scalpel and the DNA fragments were resolved in the extraction buffer at 55°C for 10 min. The DNA was then bound to a silica membrane and impurities such as agarose, salts, proteins, and the EtBr were removed by washing steps. The DNA was eluted either with elution buffer provided with the kit or with ddH_2O. To

analyze the quality and concentration of the purified fragments, 5 µl of the elution fractions were applied to agarose gel electrophoresis as mentioned in the previous section. The putified DNA was then stored at -20°C unitl it was used for ligation or probing.

2.2.1.14 Ligation of linear DNA fragments.

It is possible to combine complementary 5'- or 3'-overhanging DNA ends and blunt DNA ends with other blunt DNA ends by covalent bonds using T4 DNA ligase. This DNA ligation involves creating a phosphodiester bond between the 3'-hydroxyl group of one nucleotide and the 5'-phosphate of another nucleotide. Ligation reactions were performed in a total volume of 20 µl according to the manufacturer's protocol (Fermentas).

Typical reaction mixtures for ligations:

5-10	µl	DNA-fragment
2	µl	purified linearized vector
2	µl	10x ligation buffer
1	µl	T4 DNA-ligase
x	µl	nuclease-free H_2O
20	**µl**	

Reaction tubes were incubated for 1 h at RT or at 8°C ON before 10 µl of the ligation mixtures were used for transformation of *E. coli* cells.

2.2.1.15 5'-end labeling of DNA

Radiolabelling of DNA/RNA oligonucleotides for sRNA-Northern blot hybridization was performed using [γ-^{32}P]-ATP (Perkin Elmer). T4 polynucleotide kinase transfers the γ-phosphate group of ATP to the 5'-terminal hydroxyl group of the oligodeoxynucleotide. The reaction was conducted with the mirVANA Probe & Marker Kit (Applied Biosystems) according to the manufacturer's instructions.

Reaction mixtures for 5'-end labeling.

0.1-20	Pmol	DNA/RNA-oligonucleotid
1-40	Pmol	[γ-^{32}P]-ATP
1	µl	10 x kinase-buffer
1	µl	T4-polynucleotidkinase (10 U/µl)
X	µl	nuclease-free H_2O
10	**µl**	

The components were mixed and incubated for 1 h at 37°C. Reactions were either stopped by adding 1 mM of EDTA or by heating at 95°C for 2 min. Unincorporated radiolabeled nucleotides were removed by purification with the columns contained in the kit. Reaction mixtures were mixed with 350 µl Binding/Washing buffer, drawn through purification columns and centrifuged for 30 sec (10,000 x g, RT). After the flow-through was discarded, a second washing step with 300 µl Bindings/Washing puffer was performed. Columns were transferred into new 1.5 ml centrifuge tubes and 20 µl of hot elution buffer (10 mM Tris-HCL, pH = 7.0, 0.1 mM EDTA) (95°C) were pipetted onto the columns. Labeled

DNA/RNA oligonucleotides were recovered from the columns by centrifugation (30 sec, 10,000 x g, RT). The elution step was repeated with 20 µl elution buffer.

2.2.1.16 Circular mutagenesis and *DpnI* selection of mutants

With this mutagenesis method it is possible to introduce mutations into plasmids with sizes up to 10 kb (Laibel and Boonrad, 2009; Weiner *et al*., 1994). The method does not require additional cloning steps. Using PCR with two mutagenesis primers and a Pfu polymerase new mutated plasmids are produced from denatured DNA templates. The original DNA templates are cleaved with *DpnI* before the PCR products are transformated into *E. coli*. *DpnI* is added directly to the PCR product and specifically cleaves methylated sequences, such as the bacterial DNA template. PCR products are not methylated and are thus not cleaved by the enzyme.

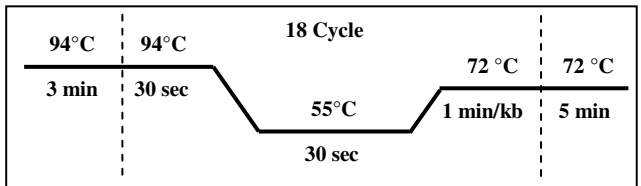

temperature program for directed mutagenesis

Mutagenesis primers must be complementary to each other and require a length of 25-45 nt. Mutated sequences should be in the middle of the primers and should be flanked by at least 8 matching nucleotides. Furthermore, the GC content should be greater than 40% and the melting temperature should be above 60°C.

Reaction mixtures were pipetted on ice into sterile PCR tubes and the tubes were transferred into a thermocycler.

Reaction mixture of the directed mutagenesis approach

5	µl	10x *Pfu*-buffer with $MgSO_4$
5	µl	dNTP-mix (2 mM each)
1,5	µl	primer A (10 mM)
1,5	µl	primer B (10 mM)
10-50	ng	template-DNA
0,5	µl	*Pfu* DNA-polymerase (2,5 U/µl)
x	µl	nuclease-free H_2O
50	**µl**	

PCR products were analyzed on agarose gels and template plasmids were removed by incubation of the samples with 2 µl of *DpnI* for 1 hour at 37°C. For *E. coli* transformation 5 µl of the samples were used.

2.2.1.17 Reverse transcription

In the reverse transcription process, a specific RNA sequence is transcribed into a complementary DNA strand (cDNA) by an enzyme termed reverse transcriptase (Baltimore, 1970; Temin and Mizutani, 1970). Primers that are complementary to the 3'-end of RNA templates are extended and the resulting cDNA strands are directly used in a PCR (RT-PCR).

This method is suitable for the detection of small amounts of RNA molecules and for the synthesis of double stranded cDNA molecules that can be directly cloned.

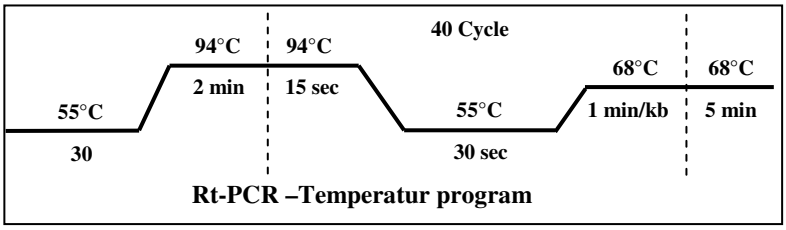

The SuperScript III One-Step RT-PCR System with Platinum® Taq DNA Polymerase (Invitrogen) with a temperature optimum of 55°C and reduced RNase H activity was used in this work.

Reaction mix:

12.5	µl	2x reaction mix
(0.01 pg- 0.1 µg)	µl	template RNA
1	µl	sense primer (10 µM)
1	µl	anti-sense primer (10 µM)
1	µl	SuperScript. III RT/Platinum® Taq Mix
X	µl	nuclease-free H_2O
25	**µl**	

2.2.1.18 Purification of PCR products

Purification of PCR products was performed with the QIAquick PCR Purification Kit (Qiagen) according to the manufacturer's instructions. The DNA was bound to a silica membrane column and impurities such as salts, primers, dNTPs and DNA polymerase were removed by washing steps. The DNA was eluted with 30-50 µl H_2O from the column and subsequently used for cloning and other applications or stored at -20°C.

2.2.1.19 DNA purification using DNeasy Plant Mini Kit

For cellular DNA extraction the DNeasy Plant Mini Kit (Qiagen) was used according to the manufacturer's protocol. DNeasy Plant Kits use advanced silica-gel–membrane technology and simple spin procedures to isolate highly pure total cellular DNA from plant tissues and cells or fungi. For this purpose samples are mechanically disrupted in LN and chemically lysed. RNA is removed by RNase digestion during lysis. Cell debris is removed and samples are filtered and homogenized by centrifugation through a QIAshredder spin column. Buffering conditions are adjusted, precipitating proteins and polysaccharides, and lysates are loaded onto the DNeasy Plant spin columns. During a brief spin, DNA selectively binds to the silica-gel membrane while contaminants pass through. Remaining contaminants and enzyme inhibitors are removed in one or two efficient wash steps. Pure DNA is eluted in water or low-salt buffer and DNA concentration was measured using the NanoDrop ND-1000® Spectrophotometer (PEQLAB Biotechnologie). The quality of the DNA was analysed by agarose gel electrophoresis.

2.2.1.20 RNA extraction from plant with the Tri-Reagent

RNA extraction was carried out using the Trizol reagent solution (Ambion, www.ambion.com). Total RNA was isolated for Northern blot analysis and reverse transcription reactions.

RNA extraction with Tri-reagent solution is based on the principle of guanidine thiocyanate-phenol-chloroform method and allows for the simultaneous extraction of RNA, DNA and proteins (Chomczynski and Sacchi, 1987). The extraction of RNA was carried out according to the manufacturer's guidelines. 0.2 g of leaf material were transferred (without the main leaf vein) into 2 ml safe lock reaction tubes with a tungsten-carbon-metal ball and frozen immediately in LN. The tissue was homogenized for 1 min in a cell mill at 30 Hz and put back into LN. 1 ml Tri-reagent solution was added to the crushed tissue and homogenized by pipetting mixtures up and down. Samples were incubated for 5 min at RT, mixed with 1/5 volumes of chloroform and incubated for 10 min at RT with mixing of the samples every 2 min. Samples were centrifuged for 15 min at 12,000 x g and the supernatant was transferred into a 1.5 ml reaction tubes. 1.5 volumes isopropanol were added and the tubes were incubated for 30 min at RT. For RNA precipitation, samples were centrifuged at 12,000 x g for 30 min at 4°C and supernatants were discarded. Pellets were washed with 500 µl ethanol (70%). After removing the supernatant, pellets were dried for 15 min at RT and resuspended in 20-50 µl RNA Storage Solution (Applied Biosystems). The quality of the RNA was analyzed by electrophoresis on 1% Tris-Borate-EDTA (TBE) gels and stored at -80°C. The quantification of the RNA was carried out by using the NanoDrop ND-1000® Spectrophotometer (PEQLAB Biotechnologie).

2.2.1.21 Detection of sRNA molecules by Northern blot analysis

The detection of sRNA molecules was carried out by sRNA-Northern blot analysis. 10 µg of total RNA were mixed with 1 volume of TBE-urea buffer (Appendix C) and denatured at 80°C for 5 min. Samples were loaded onto 20% TBE acrylamide gels (Anamed, www.anamed-gele.com) at 80 V for 4 h in 1x TBE buffer using the XCell SureLock™ Mini-Cell system (Invitrogen). RNA was transferred onto positively charged nylon membranes (Ambion) by electro-blotting at 300 mA for 1 h at 4°C with the Mini Trans-Blot electrophoretic transfer cell system (Bio-Rad). Membrane were washed with 2x SSC and the semidried membranes were UV-cross-linked (312 nm and 300 µJ/cm^2). Hybridizations were carried out in 25 ml PerfectHyb™ Plus Hybridization Buffer (Sigma-Aldrich). After addition of radioactively-labeled DNA oligonucleotides (see Section 2.2.1.15), hybridizations were run ON at 42°C in an hybridization oven. The next day, membranes were washed three times for 30 min with 25 ml wash buffer at 50°C (Appendix C). Membranes were exposed to Fujifilm

Imaging Plates (Fujifilm, www.fujifilm.com) for 24 h and scanned using PharosFX Plus PhosphorImager (Bio-Rad).

2.2.1.22 The detection of mRNA molecules by Northern blot analysis

For Northern blot analysis, 10 µg of total RNA were mixed with 1 volume of denaturizing buffer (Appendix C) and samples were heated at 65°C for 10 min for denaturation. Samples were mixed with 1/10 volumes of RNA-loading dye and electrophorized on 1.2% agarose formaldehyde gels at 90 V for 4 h. Gels were washed with ddH_2O for 20 min and then with 10x SSC for 20 min. Capillary transferred onto a positively charged BioBond Plus membranes (Sigma-Aldrich) was performed ON with 10x SSC. Membranes were dried at RT for 10 min and RNA was UV-cross-linked (254 nm and 240 µJ/cm^2). Random-primed [α-^{32}P]dCTP-labeled PCR fragments (Random Primed DNA Labeling Kit; Roche) were used as probes. The PerfectHyb Plus 1x (Sigma-Aldrich) was used for ON-hybridizations at 64^{o}C. The next day, membranes were washed at 64^{o}C with buffer 1 (2x SSC, 0.1% SDS, w/v) for 30 min and with buffer 2 (0.5x SSC, 0.1% SDS, w/v) for 15 min. Membranes were exposed as mentioned in the previous section.

2.2.1.23 Construction of the expression vectors

2.2.1.23.1 Modification of the pPCV702SM binary vector

A polylinker was inserted into the multiple cloning site of the pPCV702SM binary vector to introduce new restriction sites to enable cloning of HC-Pro constructs. The polylinker was generated by annealing the two primers, Linker pPCV A-F and Linker pPCV B-R (Table 2.6). The linker was 46 bp length and contained several restriction sites, including *SacI, SalI, AscI*. The pPCV702SM binary vector was cleaved with *BglII* and *XbaI*, and ligated to the annealed oligonucleotides. Restriction analysis with *AscI* and *StuI* revealed several clones that were composed of a 3,000 and a 8,150 bp fragment. Fragment sizes were as expected by calculation indicating that the cloning was successful. One of the clones (pPCV702SM-MC) was used for further experiments (Fig. B-1).

2.2.1.23.2 Production of HC-Pro fusion proteins

For the preparation of binary vectors which were used to express HC-Pro-GFP fusion proteins, the GFP was fused either to the C- or the N-terminus of the HC-Pro.

2.2.1.23.2.1 Production of pPCV702SM:GFP-HC-Pro

The GFP was N-terminally fused to the HC-Pro by cloning the GFP coding sequence into the multiple cloning site of the pPCV702SM. For this purpose a PCR with the Phusion polymerase and the pKB:biNLS-GFP (Table 2.7) was performed and the complete open reading frame of the GFP without stop codon was amplified. The 5'-primer (GFP-BamHI-F)

spanning 29 bp of the 5'-end of the GFP coding sequence contained a *BamHI* site. The 31 nt long 3'-primer (GFP-XbaI-R) was complementary to the 3'-end of the GFP coding region but lacked the stop codon and contained an *XbaI* site (Table 2.6). The amplified 724 bp long PCR product was cleaved with *BamHI* and *XbaI* and cloned into the pPCV702SM linearized with *BamHI* and *XbaI*. For the fusion of the HC-Pro at the C-terminus of the GFP coding sequence, the HC-Pro was amplified by PCR using the Phusion polymerase, plasmids, pBin19:HA-HC-Pro^{FINK} and pBin19:HA-HC-Pro^{FRNK}, as templates (Table 2.7) and the primer pair, Hc-Pro XbaI-F/Hc-Pro XbaI-R (Table 2.6). The 5'-primer spanning 31 bp of the 5'-end of the HC-Pro coding sequence contained an *XbaI* site. The 32 nt long 3'-primer was complementary to the 3'-end of the HC-Pro coding region, contained a stop codon and an *XbaI* site. The amplified 1,391 bp long PCR product was cleaved with *XbaI* and cloned into the *XbaI*-linearized pPCV702SM producing the pPCV702SM:GFP-HC-Pro construct (Fig. B-2). Restriction anlysis with *BamHI* and *SalI* revealed several clones that were composed of a 1,944 bp, 174 bp, and a 1,1065 bp fragment. The fragment sizes were as expected by calculation indicating the correct orientation of the HC-Pro cDNA.

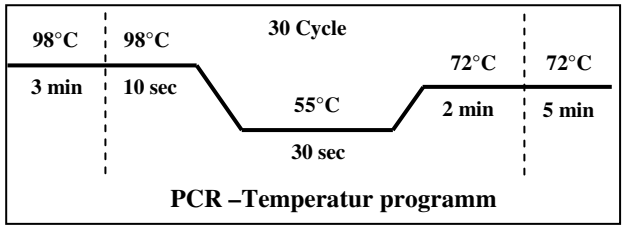

2.2.1.23.2.2 Production of pPCV702SM:HC-Pro-GFP

For the GFP fused to the C-terminus of the HC-Pro, the HC-Pro coding sequence was amplified by PCR using the Phusion polymerase, the primer pair, HC-Pro-AscI-F/GFP-XbaI stop-R (Table 2.6), and the pKB:biNLS-HC-Pro-GFP plasmid as a template (Table 2.7). The 5'-primer spanning 19 bp of the 5'-end of the HA-HC-Pro coding sequence contained an *AscI* site and the 19 nt long 3'-primer that was complementary to the 3'-end of the GFP coding region contained a stop codon and an *XbaI* site. The amplified 2,147 bp long PCR product was cloned into the pJET1.2/blunt cloning vector, and sequenced. After confirmation of the correct sequence the NLS-HC-Pro-GFP fragment was cleaved from the cloning plasmid with *AscI* and *XbaI* and ligated after purification into pPCV702SM–MC linearized with the same enzymes producing the pPCV702SM-MC:HC-Pro-GFP (Fig. B-3).

2.2.1.23.3 Production of pPCV702SM:HA-NLS-HC-Pro

In order to direct the HC-Pro into the nucleus, a nuclear localization signal (NLS) sequence was fused to the N-terminus of the HC-Pro. A PCR was carried out using the pKB-biNLS-HcPro-GFP (Table 2.7) and the primer pair HA-AscI-F/Hc-Pro XbaI-R (Table 2.6) to amplify the complete open reading frame of and to introduce a stop codon at the C-terminus of the NLS-HC-Pro. The 5'-primer spanning 22 bp of the 5'-end of the HA-NLS coding

sequence contained an *AscI* restriction site. The 19 nt long 3'-primer was complementary to the 3'-end of the HC-Pro coding region and contained a stop codon and an XbaI site. The 1467 bp long PCR product was cloned into the pPCV702SM-MC linearized wih *AscI* and *XbaI*. After cloning restriction analysis with *AscI* and *XbaI* revealed that the HA-NLS-HC-Pro fragment was successfully cloned in pPCV702SM-MC giving the pPCV702SM-MC:HA-NLS-HC-Pro vector. As expected, two fragments with sizes of 1,467 bp and 1,1095 bp were detectable.

2.2.1.24 Deletion constructs in HC-Pro pMAL.c2X vectors

To identify the HEN1-binding domain of HC-Pro, N- and C-terminal deletion mutants (Δ) of the HC-Pro were generated (Fig. 2.1). The MBP:HA:HC-Pro^{FRNK} carrying a *SacI* site at its 5´-end was used for the production of ΔN deletions. A second *SacI* site was introduced at position 271 (ΔN1, previously produced, see below), at position 341 (ΔN2) and at position 417 (ΔN3), repsectively. The sites were introduced *via* site-directed mutagenesis as mentioned in section 2.2.1.16 (Laible and Boonrod, 2009) using the primers presented in Table 2.6. The ΔN1 was kindly provided by Dr. Fuellgrabe (Fuellgrabe, 2010). The generation of the ΔN2 (MBP:HA:HC-ProΔN2) and ΔN3 (MBP:HA:HC-ProΔN3) mutatants were also generated *via* site-directed mutagenesis using MBP:HA:HC-Pro^{FRNK} as a template and the primers pairs HC-Pro mut N2_F/HC-Pro mut N2_R and HC-Pro mut N3_F/HC-Pro mut N3_R, respectively (Table 2.10). The PCR products were digested with *DpnI,* and transfotmed into chemocompetent *E. coli* cells (INFα). MBP:HA:HC-ProΔN2 and MBP:HA:HC-ProΔN3 were finally produced by cleavage with *SacI* and religation (Fig. 2.1).

The generation of the C-terminal mutants, ΔC7 (deletion of 411 bp), ΔC8 (deletion of 332 bp) and ΔC9 (deletion of 272), was previously described (Fuellgrabe, 2010). *NcoI* sites were introduced into the pMal.c2X:HA:HC-Pro-ΔC7-ΔC9/GFP *via* site-directed mutagenesis using the pair primers, *NcoI* delete C-F/*NcoI* delete C-R (Table 2.6). After digestion of PCR products with *DpnI* and transformation into INFα cells, the plasmids were cleaved with *NcoI* resulting in the deletion of the C-terminal GFP. By religation of the cleaved plasmids the final clones, MBP:HA:HC-ProΔC7, MBP:HA:HC-ProΔC8 and MBP:HA:HC-ProΔC9 were generated (Table 2.10 and Fig. 2.1).

Table 2.10 Summary of plasmids generated by mutagenesis, the output vectors, the primer pairs used, N- and C-temini deletions, new restriction sites, and mutated plasmids.

Starting plasmid	Primer	Mutation	Restriction site	mutated plasmid
pMAL-HA-HC-Pro	HC-Pro mut N2_F HC-Pro mut N2_R	Δ1-114	+ *SacI*	MBP:HA-HC-ProΔN2
pMAL-HA-HC-Pro	HC-Pro mut N3_F HC-Pro mut N3_R	Δ1-139	+ *SacI*	MBP:HA-HC-ProΔN3
pMAL-HA-HC-Pro-mut C7-GFP	NcoI delete C-F NcoI delete C-R	Δ322-456	+ *NcoI*	MBP:HA-HC-ProΔC7
pMAL-HA-HC-Pro-mut C8-GFP	NcoI delete C-F NcoI delete C-R	Δ350-456	+ *NcoI*	MBP:HA-HC-ProΔC8
pMAL-HA-HC-Pro-mut C9-GFP	NcoI delete C-F NcoI delete C-R	Δ373-456	+ *NcoI*	MBP:HA-HC-ProΔC9

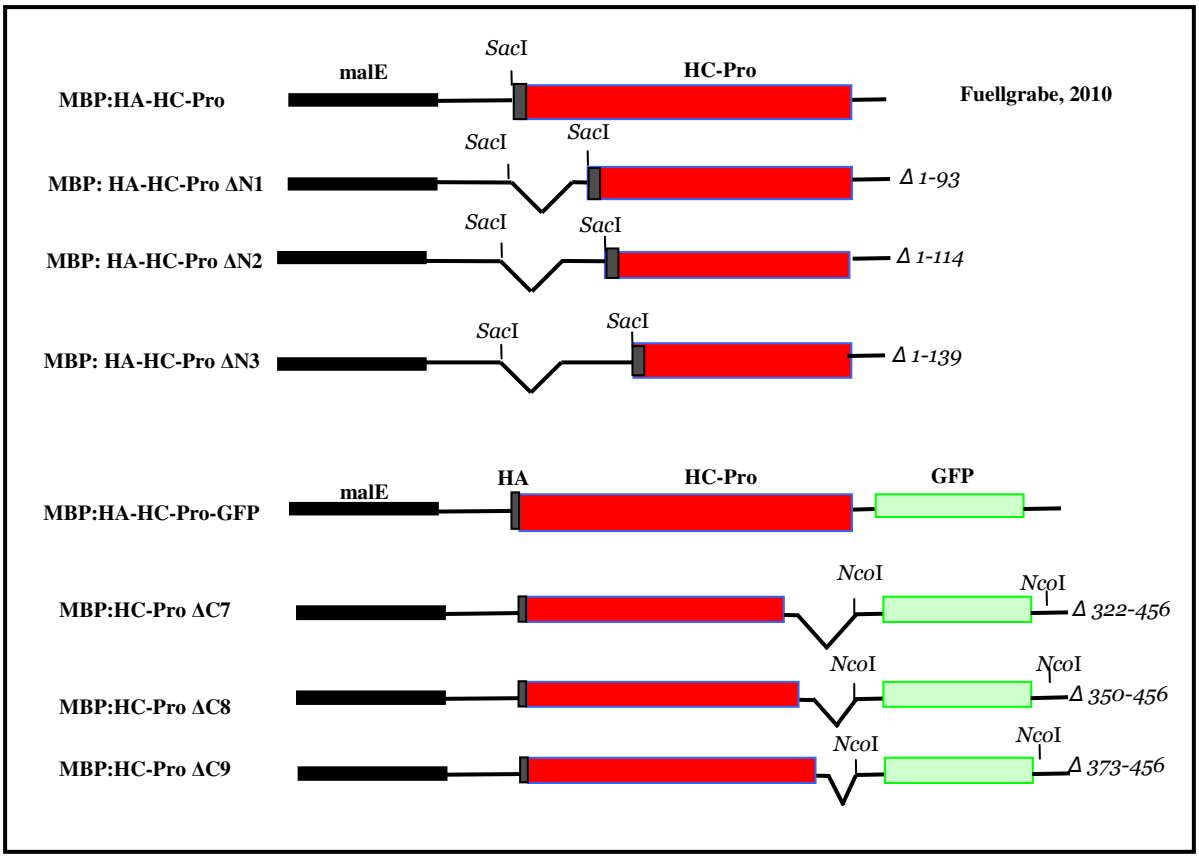

Figure 2.1: Schematic overview of the mutagenesis constructs. HA = HA-tag; HC-Pro = helper component protease; GFP = green fluorescent protein; triangles indicate the mutated regions.

2.2.1.25 Cloning of the *Solanum lycopersicon HEN1* cDNA into pPCVMC702SM

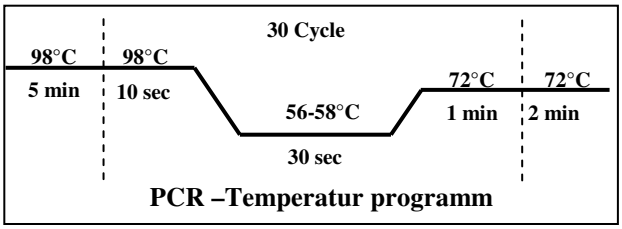

Using the sequence data of *Arabidopsis thaliana* (AAL05056), *Vitis vinifera* (emb-AM454387.2), *Solanum lycopersicum* (gb-AC215448.2), *Physcomitrella patens* subsp *Patens* (XM-001780574), and *Oryza sativa* Japonica (dbj-AK111609.1) *HENI* genes (Fig. A-1), two degenerate primers pairs (HEN1p1 for/HEN1p1 rev and HEN1p2 for/HEN1p2 rev) (Table 2.6) were synthesized to amplify two fragments of the *SlHEN1* gene. PCR was carried out with genomic DNA of tomato (Hellfruit). The amplified fragments were sequenced to

confirm the amplification of the *SlHEN1* gene. Subsequently, six specific primers (HEN1-EcoRI-PI-F/HEN1-HindIII-PI-R, HEN1-HindIII-P2-F/HEN1-StuI-P2-R, and HEN1-StuI-P3-F/HEN1-BamHI-P3-R) (Table 2.6) were used to amplify the full length *SlHEN1* cDNA. Table 2.11 shows the length of each fragment, the restriction sites and the primers that were used for their amplification. Reverse transcription was performed with 5'- and 3'-primers on total tomato RNA as described in section 2.2.1.17. The three cDNA products were cloned into the pJET1.2/blunt cloning vector and sequenced. After confirmation of the correct sequences, the three fragments were ligated together to obtain the full length *HEN1* cDNA. Ligation was conducted as follows: i) the third fragment (818 bp) was cleaved from the pJET vector using *StuI* and *BamHI*, and the purified fragment was ligated with the pTPCR vector digested with the same enzymes; ii) the pTPCR containing the third fragment (as confirmed by restrition analysis using *StuI* and *BamHI*) was digested with *HindIII* and *StuI* and ligated with the second, *HindIII*/*StuI* fragment (1196 bp) cleaved from the pJET vector; iii) the pTPCR containing the two fragments (as confirmed by restrition analysis using *HindIII* and *BamHI*) was digested with *EcoRI* and *HindIII* and ligated with the first fragment (971bp) cleaved from the pJET vector using the same enzymes. At the end of this cloning the full length *HEN1* cDNA was generated in the pTPCR vector as an *EcoRI*/*BamHI* fragment. This 2938 bp long fragment was subsequently used for cloning into the pGADT7 yeast expression vector, and into pPCV702SM fused to the GFP and RFP reporter genes.

Table 2.11 Amplification of the HEN1 cDNA from *S. lycopersicon* using RT-PCR, primers used for the amplification, length of each fragment, and restriction sites.

Primer	Fragment length	Restriction site
HEN1-EcoRI-PI-F/ HEN1-HindIII-PI-R	971 bp	EcoRI- HindIII
HEN1-HindIII-P2-F/ HEN1-StuI-P2-R	1196 bp	HindIII- StuI
HEN1-StuI-P3-F/ HEN1-BamHI-P3-R	818 bp	StuI-BamHI

To produce the pGADT:SlHEN1 (Fig. B-4), the *SlHEN1* cDNA was excised from the pTPCR:SlHEN1 cloning vector with *EcoRI* and *BamHI*, and ligated into the *EcoRI* and *BamHI*-cleaved pGADT7. According to this cloning step the *SlHEN1* cDNA was in frame with the GAL4-DNA activation domain and could be used as a prey in the yeast-two hybrid system.

The SlHEN1 cDNA was also fused in frame to the N-terminus of the GFP/dtomatoRFP reporter genes. The corresponding fusion products were introduced into the pPCV702SM binary vector. For this purpose the full length *SlHEN1* cDNA was amplified using the primer pair HEN1-EcorI-F/HEN1-BamHI–FRET-R (Table 2.6) and the pGADT:SlHEN1 as a template. PCR products were analyzed by electrophoreses to validate

that the sizes of the products corresponded to the full length SlHEN1 cDNA (data not shown). They were then directly cloned into the pJET1.2/blunt-vector. After confirmation of successful cloning, the *SlHEN1* cDNAs was excised from the cloning vector by digestion with *EcoRI* and *BamHI*. Introduction of the cDNA into the *EcoRI* and *BamHI*-cleaved pPCV702SMGFP/RFP binary vectors finally produced pPCV702SM:HEN1-GFP and pPCV702SM:HEN1-RFP (Fig. B-5) .

2.2.1.26 Cloning of the *N. benthamiana* Argonaute-1 cDNA into pGADT7

Cloning of the AGO1 gene from *N. benthamiana* was performed analogous to the cloning of the SlHEN1 gene. Two specific primer pairs, AGO1-EcoRI-P1-F/ AGO1-EcoRI-P1-R and AGO1-EcoRI-PII-F/AGO1-BamHI-PII-R (Table 2.6), were used to amplify the full length NbAGO1 cDNA. Table 2.12 show the length of each fragment, their unique restriction sites and the primers that were used for their amplification. Reverse transcription reactions were performed with the 5'- and 3'-primers and with total RNA from *N. benthamiana* as described in section 2.2.1.17. The two PCR products were cloned into the pJET1.2/blunt-vector and were then sequenced. After confirmation of the correct sequences, the 3'-fragment (937 bp) was excised from pJET cloning vector by digestion with *EcoRI* and *BamHI* and the purified fragment was ligated into the *EcoRI/BamHI*-cleaved pGADT7. Successful cloning of the 3'-fragment of NbAGO1 cDNA into the pGADT7 plasmid was confirmed by enzymatic digestion with *EcorI* and *BamHI* and by sequencing. After confirmation of successful cloning, the 5'-fragment of the NbAGO1 cDNA (2262 bp) was excised from the pJET cloning vector with *EcoRI*. The fragment was ligated into the *EcoRI*-linearized pGADT7 plasmid, containing the 3'-fragment of the NbAGO1. The resulting pGADT:NbAGO1 (Fig. B-6) clones were sequenced to screen for the correct orientation of the 5' fragment of the *NbAGO1* cDNA.

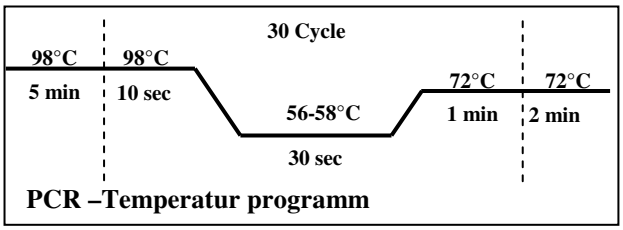

Table 2.12 RT-PCR amplification of the *N. benthamiana* AGO1 cDNA, primers used for their amplification, length of each fragment, and their unique restriction sites .

Primer	Fragment length	Restriction site
AGO1-EcoRI-P1-F AGO1-EcoRI-P1-R	2262 bp	EcoRI-EcoRI
AGO1-EcoRI-PII-F AGO1-BamHI-PII-R	937 bp	EcoRI-BamHI

2.2.2 Transient transformation of *N. benthamiana* plants

The *Agrobacterium*-infiltration method was used for transient transformation of 4-6 weeks old *N. benthamiana* plants (Schob *et al,.* 1997). Plants were grown without irrigation

24 h prior to infiltration. 15 ml of *Agrobacterium* cultures containing the required binary vector were incubated in a 50 ml flask for 1-2 days at 28°C with shaking. The *Agrobacterium* cultures were transferred into a 50 ml Falcon tube and centrifuged for 5 min at 2,700 x g at RT. *Agrobacterium* pellets were resuspended in induction medium (10 mM MES, pH = 5.8, 10 mM $MgCl_2$, 200 mM Acetosyringon). The OD_{600} was adjusted to 0.5–1.0 and suspensions were incubated at RT for 2-4 h.

Infiltrations were performed with 2 ml syringes without needles. Syringes were filled with *Agrobacterium* suspensions, placed on the lower side of the leaves and suspensions were injected under slight pressure. After 3-5 days, leaf samples were taken and the corresponding proteins or RNA were analyzed.

2.2.2.1 Cultivation of *N. benthamiana* plants under sterile conditions

N. benthamiana seeds were transferred into 1.5 ml tubes, 500 µl ethanol (70%) were added and seeds were incubated at RT for 1 min. Thereafter, seeds were soaked with 1 ml of 5% sodium hypochlorite, incubated for 10 min with shaking and washed 3 times with 1 ml of sterile H_2O. Seeds were spread onto 1/2 MS agar plates and cultured in climate chambers. For transgenic seeds the appropriate antibiotics were added to the 1/2 MS agar plates.

2.2.3 Stable plant transformation

2.2.3.1 Stable transformation of *N. benthamiana* with Hc-Pro

For *Agrobacterium*-mediated plant transformation the pBINPLUS binary vector (van Engelen *et al*., 1995) was used to express the HC-Pro$^{FRNK/FINK}$ constructs. The pPCV702SM binary vector (Wassenegger *et al*., 1994) was used to introduce the NLS-HC-Pro$^{FRNK/FINK}$ constructs. The recombinant binary plasmids were introduced into the *A. tumefaciens* strain GV3011 by the freeze and thaw method (2.2.1.5.2). *N. benthamiana* plants were transformed using the leaf disc transformation method (Horsch *et al*., 1985). *N. benthamiana* leaves were carefully cut from four sides with a scalpel and inoculated with *Agrobacterium* suspensions for 30 seconds. Leaves were blotted on sterile filter paper and transferred onto 1/2 MS medium without antibiotics. Plates were incubated in climate chambers at 22^{o}C in the dark for 2 days. After the incubation period, leaves were washed twice with 1/2 MS medium supplemented with carbenicillin (500 mg/ml), transferred onto a regeneration medium (1/2 MS medium) supplemented with kanamycin (200 mg/ml) for selection of transformed plant cells, with carbenicillin (500 mg/ml) to kill the *Agrobacteria* and with the growth regulaters, 1-naphthaleneacetic acid (NAA) (0.01 mg/l) and 6-Benzylaminopurine (BAP) (1 mg/l). The leaf discs were incubated for 4 days in climate chambers and subsequently transferred onto fresh medium every 2 weeks. Putative transformants were transferred for rooting onto 1/2 MS

medium supplemented with kanamycin (200 mg/ml), carbenicillin (500 mg/ml) and NAA (0.01 mg/l). Transformed shoots (T_0) were screened by PCR for the presence of the transgene constructs. For seed production, transformed plants were grown in the greenhouse.

T_0 plants were self-pollinated and the T_1 progeny plants were subjected to biological and molecular analysis after selection on kanamycin. Transgene constructs were detected by PCR with total genomic DNA extracted from each kanamycin-resistant seedling. PCR was performed in 25 µl containing 2 µl of target-DNA with the pair primer Hc-Pro-int-seq-F/Hc-Pro XbaI–R (Table 2.6). PCR conditions were: 30 cycles of 30s at 94°C, 30s at 55°C and 30s at 72°C.

2.2.3.2 Floral dip transformation of *A. thaliana*

Stable *A. thaliana* transformants were produced using the *A. tumefaciens*-mediated floral dip transformation procedure (Clough and Bent, 1998). Plants were cultivated until flowering started. The optimal stage for transformation was achieved when only 2-3 flowers were open. At this developmental stage the majority of buds were still closed. GV3101 strains carrying the designated binary vectors were grown in 10 ml LB medium containing appropriate antibiotics at 28°C ON. 2 ml of each ON culture were inoculated into 50 ml LB medium with appropriate antibiotics and incubated at 28°C for 20–24 h. *Agrobacterium* suspensions were centrifuged at 2,700 x g for 15 min at RT. Pellets were resuspended in equal volumes of infiltration medium. Plants were dipped into the suspensions for 90 sec. Subsequent to floral dipping, plants were kept horizontally under a cover to maintain high humidity. After 24 h, the plants were uncovered and set to dry. Seed collection started three weeks after transformation.

2.2.3.3 Seed sterilization and selection of transformants

Seeds were incubated for 5 min in ethanol (70%) and then 20 min in (10%) sodium hypochlorite (NaOCl) with overhead shaking. After washing 3 times with sterile water, they were dried and placed on solid 1/2 MS medium supplemented with appropriate antibiotics. Seeds were incubated at 4°C for 48 h. After approximately two weeks, transgenic plants were selected.

2.2.3.4 Genomic DNA extraction from plants

Genomic DNA extraction from wild type and transgenic plants was performed according to Edwards and co-workers (1991). Leaf material (~100 mg) was transferred into a 2 ml safe lock reaction tube with a tungsten-carbon-metal ball and frozen immediately in LN. The tissue was homogenized for 1 min in a cell mill at 30 Hz and put back into LN. 400 µl of extraction buffer (200mM Tris-HCl, pH = 7.5, 250mM NaCl, 25 mM EDTA, 0,5% SDS)

were added to the leaf tissue and incubated at 65°C for 30 min. The same volume of chloroform was added, mixed for 5 sec, and centrifuged at 10,000 x g for 5 min. The upper phase ~300 µl was transferred into a 1.5 ml tube, an equal volume of isopropanol was added, carefully mixed, incubated 2 min at RT and centrifuged at 10,000 x g for 5 min. The pellet was then washed in 500 µl of 70% ethanol by centrifuging at 10,000 x g for 5 min, The supernatant was discarded and the pellet was air dried for 15 min. The pellet was resuspended in 200 µl of TE buffer (10 mM Tris-HCl, pH = 8.0, 0,1 mM EDTA) containing 0.02 µg RNase A and incubated at 65°C for 1 h. To fully dissolve the DNA, samples were incubated at 4°C ON. The next day, 5 µl of the DNA sample were separated on 1% TAE gel to analyze the quantity and quality of the DNA.

2.2.4 Analysis of the rgs/Cam (calmoduline) expression level in transgenic *N. benthamiana* plants

The analysis of the rgs/Cam (calmoduline) expression level was carried out using the SYBR Green I®-based quantitative reverse transcription PCR (qRT-PCR). The SYBR Green I® molecule binds specifically dsDNA. In this state and under excitation at 492 nm, it emits a fluorescence signal at 513 nm. The emitted signal is proportional to the quantity of DNA-bound SYBR Green I® and therefore to the DNA quantity and length. In association with PCR DNA synthesis and the reaction kinetic can be followed measuring the intensity of the emitted fluorescence. The Superscript III Platinum® SYBR® Green I One-Step qRT-PCR kit (Invitrogen) was employed in the qRT-PCR and the detection of the fluorescent signal was performed with the Chromo4™ Real-Time detector (Bio-Rad). Eukaryotic elongation factor 1-α (EF1-α) and eukaryotic initiation factor 4-A (eIF4a) were used as internal controls for data normalization.

2.2.4.1 Real-Time PCR on RNA

The gene expression analysis was directly performed with plant total RNA (2.2.1.20). 10 µg of total RNA were treated with RNase free DNaseI (New England Biolabs) by mixing the total RNA with 10 µl 10x RNase free DNase buffer, 1 µl RNase free DNase and DEPC water to 100 µl. After incubation for 30 min at 37°C, 1 µl EDTA (final concentration 5 mM) was added and the DNase was heat-deactivated for 15 min at 70°C. The RNA sample was directly used as template in the one-step qRT-PCR. The reaction mix was prepared in a final volume of 20 µl as follows:

0.3 µl gene specific primer forward (10 µM)
0.3 µl gene specific primer reverse (10 µM)
10 µl 2x SYBR Green I PCR mix (Invitrogen)
0.4 µl RT/Platinum Taq mix (Invitrogen)
7.5 µl H_2O
1 µl DNase-treated total RNA

The sequences of primers used in the qRT-PCR are reported in Table 2.13.

Table 2.13 Primers for the qRT-PCR analysis.

Gene	Primer code	**5′-3′ sequences**
Eukaryotic translation initiation factor 4A	eIF4a–F	GAC CAG TTA GAC CTC CAG CAA C
	eIF4a–R	CAA CAC ACT GCA AAG CTT CAT C
Elongation factor-1 α	EF1-α –F	TGG TTA TGT TGC CTC AAA CTC C
	EF1-α –R	CTT ACC AGA ACG CCT GTC AAT C
Rgs/Cam (Calmoduline)	rgs-CaM_F	TAC GTG CAA CAT GTG CAT GG
	rgs-CaM_R	CCC TCC ATT TCA TAC ATT CC

Parameters for the qRT-PCR were:

55°C, 5 min
95°C, 30 sec
60°C, 25 sec
72°C, 23 sec
Plate read, 10 sec
} 40 cycles
72°C, 4 min
Melting curve analysis 55 to 95°C, 1°C/min 10 sec read
16°C ∞

2.2.4.2 Analysis of the qRT-PCR data

The data analysis was carried out as described by Moser (2010). The procedure was based on the DART-PCR (Peirson *et al*., 2003) and the LinRegPCR methods (Ruijter *et al*., 2009) where the fluorescence data obtained from qRT-PCR are analysed to calculate the reaction efficiency value (E) associated to each specific primer. Further, the E values are subjected to a one-way analysis of variance (ANOVA) in order to determine if a single average E value can be adopted for all primers in all the samples. In the case that the ANOVA hypothesis is rejected (the variance between samples and primers is too large), an E value for each primer is calculated. A further parameter necessary for the analysis is the cycle (Ct) at which the fluorescence value reach a threshold point. This value is determined from the analysis based on the fluorescence curve region where the reaction kinetic reaches its maximum. Once the E and the Ct values are known it is possible to calculate the initial fluorescence of a specific target through the equation:

$I_o = I_{Ct}/E^{Ct}$ (Peirson *et al*., 2003). Where:

I_o = fluorescence at cycle 0
I_{Ct} = fluorescence at cycle Ct (corresponds to the threshold value)
Ct= cycle at which the fluorescence in the reaction reaches the threshold value
E = efficiency value (between 1 and 2)

2.2.5 Crossing of transgenic Nb-HC-Pro^{FRNK} plants with plants expressing a PSTVd cDNA construct

Genetic crossing between a Nb-HC-Pro^{FRNK} plant and transgenic plants expressing an infectious Potato spindle tuber viroid (PSTVd) cDNA construct (Nb-PSTVd-Nb) were carried out to analyze the effect of HC-Pro on the accumulation of PSTVd-derived siRNAs.

Reciprocal crosses were made between the two transgenic *N. benthamiana* lines. Emasculation (removal of the anthers) of immature flowers that do not contain mature pollen was conducted to avoid self-pollinated. Using a brush or forceps, the pollens from mature flowers were transferred to the stigma of the emasculated flower and the pollinated flowers were covered. Seeds were collected from these flowers after maturation. The T1 hybrids were checked by PCR for the presence of the two genes using specific primer pairs for the PSTVd (PSTVd-for1/PSTVd-rev1) and HC-Pro (Hc-Pro-int-seq-F/Hc-Pro XbaI–R) transgenes (Table 2.6).

2.2.6 Protein extraction from plants

For the isolation of total proteins from plants, initially 100 mg of leaf material were transferred into a 1.5 ml reaction tube. The leaf material was mixed with 1 volume of extraction buffer containing protease inhibitors Complete, EDTA free (Roche) and was homogenized using a micropistill. Samples were centrifuged (10,000 x g) for 15 min at 4°C, and separated from cellular debris. Protein concentrations were determined according to the Bradford protein assay (Bradford, 1976, see below) and the protein quality was analyzed by SDS-PAGE and Coomassie blue-staining or by Western blot analysis. Protein extracts were stored at -20°C.

2.2.6.1 Bradford protein assay

The concentration of native proteins was measured according to the method of Bradford (1976) using the Bradford Reagent (Sigma-Aldrich). Proteins and Coomassie Brilliant Blue G-250 form a complex which causes a shift in the maximum absorption of the dye from 465 to 595 nm. The increase of absorbance at 595 nm is proportional to the amount of protein present in the sample. The concentration of proteins is determined by comparison with a BSA protein-based standard curve.

The reaction for the Bradford assay was prepared by mixing 5 µl of total protein extracts with 795 µl H_2O and 200 µl Bradford Reagent. Samples were transferred into 1.5 ml cuvettes and the absorption was determined by using a spectrophotometer.

2.2.6.2 SDS-polyacrylamide gel electrophoresis (SDS-PAGE)

Proteins can be separated according to their molecular weight toward the anode by sodium dodecyl sulfate polyacrylamide gel-electrophoresis (SDS-PAGE) (Laemmli, 1970). The presence of SDS and the denaturing step cause proteins to be separated solely based on their molecular size. Besides the addition of SDS, proteins may be briefly heated at 95°C in the presence of reducing agents, such as dithiothreitol (DTT) or β–mercaptoethanol (β-ME), which denature proteins by reducing disulfide linkages. A pre-stained molecular weight

marker (PageRuler® Plus Prestained Protein Ladder, Fermentas) is used to monitor protein separation and to evaluate transfer efficiency in subsequent Western blotting.

In this work, ready-to-use 9% SDS-polyacrylamide gels (Anamed) in an XCell Mini-Cell SureLock™ (Invitrogen) or 10% handmade mini-polyacrylamide gels in PROTEAN® 3 Cell (Bio-Rad) were used and electrophoresis was conducted according to the manufactures instructions. The gel compositions of the 10% concentration handmade gels with dimensions of 0.75 mm x 7.3 cm x 8.3 cm and 10% concentration was: 2.1 ml of 30% acrylamid-solution, 1.6 ml of separation gel collection buffer, 1.95 ml H_2O, 60 µl 10% APS and 8 µl TEMED).

10 µg of total protein extract were mixed with 1 volume of 3x protein loading buffer (Appendix C) and denatured by heating for 10 min at 95°C. Gels used for electrophoresis were prepared according to the manufacturer's instructions. Gels were rinsed with running buffer, and samples were pipetted into the wells. Electrophoresis was carried out at constant voltage (130-180 V) for approximately 1 h in 1x Tris-glycine running buffer. As a size standard PageRuler ™ Prestained Protein Ladder (Fermentas) was used (Fig. 2.2).

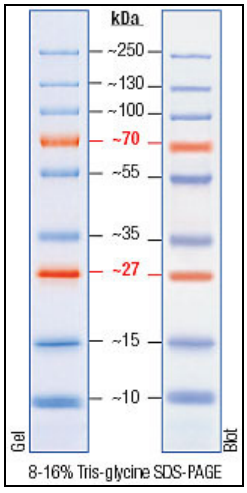

Figure 2.2: Overview of migration of PageRuler ™ Prestained Protein Ladder SDS-PAGE.

2.2.6.3 Coomassie blue staining

For detection of proteins in polyacrylamide gels, the dye Coomassie Brilliant Blue G-250 was used. The detection limit of the staining is 200-400 ng protein per band. In this work the PageBlue protein staining solution (Fermentas) was used.

Gels were placed in a container with 50 ml of water and heated for about 1 min in a microwave oven (do not heat to boiling) and then washed 4 min with H_2O. The washing step was repeated twice. H_2O was removed and 20 ml PageBlue protein staining solution was added. After brief heating in a microwave (30 sec), the gel was incubated for 20 min in the staining solution. Further washing steps in 50 ml H_2O were followed until gels reached the desired decolorization. Subsequently, gels were photographed and dried.

2.2.6.4 Western blot analysis and immunodetection of proteins

2.2.6.4.1 Western blot analysis

The Western blot technique describes the electrophoretic protein transfer from the SDS-PAGE gels onto nitrocellulose or PVDF (polyvinylidene) membranes and the subsequent immunodetection of the specific proteins (Burnette, 1981).

After electrophoresis, gels were cut into appropriate sizes (8×9 cm^2 at maximum) and washed briefly with ddH_2O. Membranes (Roche) were cut into the size of the gels and washed with methanol for 20 sec. Then they were washed 4 times with H_2O and incubated in transfer buffer until use. For blotting, 2 pieces of Whatman 3MM paper were placed onto the tray, the gel was laid on top, the membrane was placed onto the gel and 2 pieces of Whatman 3MM paper were finally placed onto the membrane. Electro-blotting was carried out in the vertical buffer reservoir Mini Trans-Blot® Electrophoretic Transfer Cell (Roche) as described in the manual for 1 h at 300 mA in the cold room.

After protein transfer, membranes were blocked to prevent high background due to unspecific binding of the primary or secondary antibody. Membranes were subsequently washed with 1x Marvel buffer and blocked in 10 ml of milk solution (5%) for 2 h. The primary antibody with the appropriate dilution was added and incubated overnight at 4°C with shaking. The next day, membranes were washed once with 1x PBST and 3 times with 1x PBS, 10 min each time. Membranes were then incubated for 2 h at RT under shaking with 10 ml of milk solution (5%) containing the secondary antibody with the appropriat dilution. Membranes were washed 4 times as described above. The anti-GFP antibody bound to GFP fused proteins were visualised by using a secondary anti-rabbit peroxidise, while the HA-tagged proteins were visualised using anti-HA-Peroxidase. The recommended (1-1000) dilution was used to avoid unspecific signals.

2.2.6.4.2 Protein detection by chemiluminescence method

The detection of target proteins was performed using the enhanced chemiluminescence detection method (Kricka and Whitehead, 1987; Thorpe and Kricka, 1986). The chemiluminescence is a fast and sensitive method for the detection of enzyme antibody conjugates. Chemiluminescence detection allows multiple exposures to be made in order to obtain optimal images. The detection reagents can be removed and the blot can be reprobed to visualize proteins or to optimize detection of the first proteins. The enzyme horseradish peroxidise catalyses the oxidation of luminol in the presence of hydrogen peroxide (H_2O_2) to amino phthalate ions which is an energetically excited state. The decay of this product to the ground state, sets energy free in form of light. A strong enhancement of the light emission is achieved by the agent p-hydroxy coumaric acid which is contained in the solution B. P-

hydroxy coumaric acid acts as a radical transmitter between the formed oxygen radical and luminol.

Immunoblots were visualized according to a homemade enhanced chemiluminescence (ECL) protocol (Laborjornal 5/2005, page 66/67 LJ Verlag). The chemiluminescence substrate gives rise to products that spontaneously emit light at the enzyme's location. This was recorded by using a photographic film. Membranes were placed in a detection cassette (Hypercassette™, GE Healthcare). High sensitive films (Lumi Film Chemiluminescence Detection film®, Roche) were placed onto the membranes and incubated from 30 sec up to 5 min in the dark. Films were developed by gently shaking in the developing solution for 2-3 minutes, rinsed in ddH_2O and fixed by shaking in the fixing solution for 1-2 min. Fixed films were again rinsed in ddH_2O and dried at RT.

2.2.6.4.3 Stripping and re-probing ECL membranes

In the cases where ECL probed membranes had to be incubated with a second set of antibodies, the first set of antibodies had to be removed. For this purpose, ECL membranes were submerged in stripping buffer (62.5 mM Tris-HCl, pH = 6.7, 100 mM β-mercaptoethanol, 2% (w/v) SDS) and incubated at 50°C for 30 min under occasional agitation. After that membranes were washed twice for 15 min in 1x PBST at RT with shaking. To verify that all antibodies were removed membranes were exposed to a detection film as desvribes above. Subsequently, membranes were blocked with 5% (w/v) non-fat dried milk in 1x Marvel buffer for 15 min at RT. The immuno-detection protocol was repeated as described above.

2.2.7 Gene expression in *E. coli* - production of recombinant proteins

With the help of suitable expression systems large quantities of a foreign gene can be produced in living cells. Such expression systems include expression vectors that encode different selection markers, promoters and fusion partners, and organisms or cell lines in which the expression vectors are introduced. The expression of genes depends on the type of promoter. Constitutive expression during the entire cultivation time and inducible promoter systems are available. After the expression, it is necessary to separate and purify recombinant proteins from host cell proteins.

The vector pMAL-C2X (New England Biolabs) encodes a maltose-binding protein (MBP). The desired genes will be expressed as a fusion protein with the MBP and purified using amylose magnetic particles. The vector has a tac promoter which is induced by the addition of isopropyl-b-D-thiogalactopyranoside (IPTG).

The *E. coli* strain BL21 (DE3) codon plus was transformed with expression plasmids. The next day, 25 ml LB-selective medium were inoculated with single bacterial colonies and grown overnight at 37°C and 190 rpm. Subsequently, 1 l of LB-selective medium was inoculated with 10 ml of the ON cultures and incubated at 37°C until OD_{600} = 0.5-0.6 was reached. Protein expression was induced by adding 1 mM of IPTG. After incubation at 14°C for 16 h bacterial cultures were transferred into a centrifuge tube and centrifuged at 4,000 x g for 15 min at 4°C. The bacterial pellets were used for protein extraction or stored at -20°C.

2.2.7.1Protein extraction from *E. coli*

Bacterial pellets from the 1 l culture volumes were mixed with 15 ml BugBuster® Protein Extraction Reagent, 5 µl Benzonase (Merck) and one tablet of protease inhibitors Complete, EDTA free (Roche) and incubated for 1 h at 4°C with gentle shaking. The mixture were then centrifuged for 15 min at 9,000 x g and 4°C. Supernatants with the soluble proteins and sediments were both analyzed.

For the analysis of smaller quantities, 1 ml of bacterial cultures were used, and a volume of 100 µl BugBuster® Protein Extraction Reagent with 0.5 µl Benzonase were added to the bacterial pellets. Mixture were then incubated at 37°C for 30 min or at 4°C for 1 hour.

2.2.7.2 Purification of the bacterial expressed MBP fusion proteins

The purification of MBP-fusion proteins was performed using amylose magnetic beads (New England Biolabs) according to the manufacture's protocol. 500 µl of the magnetic beads suspension were washed with MBP buffer (20 mM Tris-HCl, pH = 7.4, 200 mM NaCl, 1 mM EDTA, 1 mM DTT) and then added to the bacterial protein extracts. After incubation for 1 h at 4°C with shaking, the magnetic particles with bound MBP fusion proteins were isolated using a magnetic field, followed by three washing steps with 1 ml of MBP buffer. For the elution of MBP-fusion proteins, 500 µl of MBP-buffer containing 10 mM maltose were added to the beads and samples were incubated for 15 min at 4°C. Eluted proteins were analyzed on denaturing protein gels. Gels were stained with Coomassie blue.

2.2.8 The yeast two-hybrid system

The Matchmaker™ Gold Yeast Two-Hybrid System kit (Clontech Laboratories, www.clontech.com) was used to study *in vitro* protein-protein interactions.

2.2.8.1 Cloning into the yeast two-hybrid system vectors

In a Matchmaker GAL4-based two-hybrid assay, a bait protein is expressed as a fusion with the Gal4 DNA-binding domain (DNA-BD) of the pGBKT7 vector. The prey proteins are expressed as fusions with the Gal4 activation domain (AD) of the pGADT7 vector (Fields and Song, 1989; Chien *et al.*, 1991).

2.2.8.1.1 Preperation of the pGBKT:HC-Pro$^{FRNK/FINK}$

To generate GAL4 DNA-BD/HC-Pro fusion proteins, the coding regions of HC-Pro constructs were cloned in frame to the C terminus of the GAL4 DNA binding domain into the pGBKT7 vector. In order to amplify the complete HC-Pro open reading frames with stop codons, PCRs with the pBin19:HA-HC-Pro^{FINK} and pBin19:HA-HC-Pro^{FRNK} were performed. The 5'–primer, HC-Pro-Y2H NdeI-F (Table 2.6), spanning 22 bp of the HC-Pro coding sequence contained a *NdeI* site. The 3'–primer, HC-Pro-Y2H XmaI-R (Table 2.6), spanning 19 bp of the HC-Pro gene contained a stop codon an *XmaI* site. PCR products were cloned directly into the pJET1.2/blunt-cloning vector and the resulting plasmids were sequenced. After confirmation of the correct sequences, the HC-Pro$^{FRNK/FINK}$ cDNA fragments were excised from the pJET plasmids with *NdeI* and *XmaI*. The purified 1391 bp fragments were cloned into the *NdeI*/*XmaI*-cleaved pGBKT7 producing pGBKT:HC-Pro^{FRNK} and pGBKT:HC-Pro^{FINK} (Fig. B-7). According to the applied cloning strategy, the HC-Pro proteins were inframe with the GAL4-DNA binding domain.

2.2.8.1.2 Cloning of the pGADT-HC-Pro $^{FRNK/FINK}$

To generate GAL4 DNA-AD fusion proteins the HC-Pro$^{FRNK/FINK}$ cDNAs were cloned in frame with the GAL4 DNA activation domain into the pGADT7 vector. Fusion to the GAL4 DNA-AD was conducted following the same strategy that was used for cloning of HC-Pro$^{FRNK/FINK}$ into pGBKT7 (see above). This cloning produced pGADT:HC-Pro^{FRNK} and pGADT:HC-Pro^{FINK} (Fig. B-8).

The production of chemocompetent cells of the *Saccharomyces cerevisiae* Y2H Gold and Y187 strains was carried out according to the manufacturer's manual (Clonetech, Yeastmaker^{TM} Yeast transformation system user manual, 2008).

The *S. cerevisiae* strains were spread out on YPDA plates from a frozen yeast stock and were incubated at 30^{o}C for 3 days. From each strain 3 colonies were inoculated in 3ml of sterile YPD medium in 15 ml culture tubes and cells were incubated at 30^{o}C with shaking at 250 rpm for 12 h. 5 µl of the cultures were transferred into 50 ml of YPD in a 250 ml flasks and the cultures were incubated with shaking until the optical density of OD_{600} = 0.3 was reached. Cells were centrifuged at 700 x g for 5 min at RT, pellets were resuspended in 100 ml of fresh YPD medium and cultures were incubated with shaking until the optical density of OD_{600} = 0.4-0.5 was reached (about 4 h). Culture were divided into two 50 ml sterile Falcon tubes and centrifuged at 700 x g for 5 min at RT. Superenatants were discarded and pellets were resuspended in 1.5 ml of 1.1x TE/LiAc. Suspensions were transferred into 1.5 reaction tubes and centrifuged at 17,900 x g for 5 sec. Pellets were resuspended in 600 µl of 1.1x TE/LiAc and cells were directly used for transformation with plasmid DNA.

2.2.8.3 Transformation of competent yeast cells

Yeast cells were transformed according to the Yeastmaker^{TM} Yeast Transformation System 2 small-scale protocol (Clontech).

50 µl of freshly prepared competent cells were mixed in a pre-chilled sterile 1.5 ml tubes with 100 ng of Plasmid DNA (Table 2.14), 5 µl of denatured yeastmaker carrier DNA (5 µg/µl) and 500 µl PEG/LiAc. Samples were incubated at 30^{o}C for 30 min with gentle mixing every 10 min. 20 µl of dimethyl sulfoxide (DMSO) were added and mixures were incubated at 42^{o}C in a water bath for 15 min. Mixtures were then centrifuged at 17,900 x g for 15 sec to pellet the yeast cells. Pellets were resuspended in 1 ml YPD plus medium and incubated for 30 min at 30^{o}C. Cells were centrifuged as above and pellets were resuspended in 1 ml of 0.9% (w/v) NaCl solution.

Table 2.14 Yeast isolates and plasmid DNA used for transformation.

Yeast Strain	Plasmid DNA
Y2H Gold	pGBKT7-53 Control Vector
	pGBKT7-Lam Control Vector
	pGBKT:HC-Pro^{FRNK}
	pGBKT:HC-Pro^{FINK}
	pGBKT:Empty Vector
Y187	pGADT7-T Control Vector
	pGADT:SlHEN1
	pGADT:NbAGO1
	pGADT:HC-Pro^{FRNK}
	pGADT:HC-Pro^{FINK}
	pGADT7 Empty Vector

2.2.8.4 Plating and determination of transformation efficiency

100 µl of 1/10 and 1/100 transformed yeast cells were spread on appropriate SD selection medium (for pGBKT7, SD/-Trp and for pGADT7, SD/-Leu). Plates were incubated upside down at 30^{o}C for 3 days.

2.2.8.5 Selection of transformed yeast cells

Two methods were used for the selection of transformed yeast cells. Transformed colonies were plated on SD medium lacking either leucine (Leu) or tryptophan (Trp) according to the yeast strain used. In the case of yeast strain Y187, SD/-Leu was used while for the Y2H Gold strain, SD/-Trp was used. In addition, PCR with DNA extracted from yeast cells was performed to validate successful transformation.

2.2.8.6 Total DNA extraction from transformed yeast cells

Single colonies of transformed yeast cells were inoculated in 5 ml YPD medium and incubated ON at 30^{o}C with shaking. Cells were harvested by centrifugation at 10,000 x g for 5 min. 1 ml of 1 M sorbitol was added to the pellets and resuspended pellts were transferred into

1.5 ml tubes. 20 µl of lyticase (5 U/ul) were added and samples were incubated 30 min at 30°C. Mixtures were centrifuged at 17,900 x g for 10 sec and pellets were resuspended in 0.5 ml EDTA-SDS (50 mM EDTA and 0.2% SDS). Samples were incubated at 70°C for 15 min, 50 µl of 5 M KAc were added, mixtures were incubated on ice for 30 min and then centrifuged. Supernatants were transferred into 2 ml tubes and extracted 2 times with phenol/chlorophorm and centrifuged for 5 min. Then samples were extracted twice with chlorophorm. Supernatants were transferred into 2 ml tubes and 1 volume 100% EtOH was added. Samples were centrifuged for 10 sec and supernatants were discarded. Pellets were washed with 500 µl 70% EtOH, mixed and incubated at RT for 5 min. Samples were then centrifuged for 10 sec and supernatants were discarded. Finally, pellets were dried and resuspended in 100 µl TE buffer for 1 hour.

2.2.8.7 Bait auto activation and cytotoxicity

2.2.8.7.1 Testing bait for autoactivation.

It is important to confirm that in the absence of a prey protein, the bait does not autonomously activate the reporter genes in Y2H Gold cells. For this purpose HC-Pro$^{FRNK/FINK}$ were cloned in frame with the *GAL4* DNA-BD into the pGBKT7 plasmid. 100 ng of the pGBKT:Hc-Pro$^{FRNK/FINK}$ were transformed into the Y2H Gold strain as described above (2.2.8.3). 100 µl of 1/10 dilutions and 1/100 dilutions of the transformation mixtures were spread onto separate plates, as follows:

• SD/–Trp plates = SDO
• SD/–Trp/X-α-Gal = SDO/X plates
• SD/–Trp/X-α-Gal/AbA = SDO/X/A plates

Plates were incubated for 3-5 days at 30°C.

2.2.8.7.2 Testing bait for toxicity.

In the yeast two-hybrid system, the bait protein should be tested for toxicity when expressed in yeast. For this purpose 100 µl of 1/10 and 1/100 dilutions of Y2H Gold cells transformed with pGBKT:Hc-Pro$^{FRNK/FINK}$ and pGBKT7 (empty) were spread onto SD/–Trp agar plates and incubated for 3-5 days at 30°C.

2.2.8.8 Protein extraction from transformed yeast cells

2.2.8.8.1 Preparation of yeast cultures for protein extraction

In order to validate recombinant protein expression in the transformed yeast cells, each transformed yeast strain was applied to Western blot analysis.

A single colony (1–2 mm in diameter and not older than 4 days) from each transformed yeast strain was cultured in 5 ml of SD selection medium (4 individual colonies were cultured

for each strain). In addition, as a negative control, 10 ml cultures of untransformed yeast cells were grown in YPD medium. Cultures were incubated ON at 30°C with shaking at 250 rpm. The next day, 50 ml aliquots of YPD medium were mixed with the ON cultures and samples were incubated at 30°C with shaking (220–250 rpm) until OD_{600} = 0.4–0.6 was reached. The OD_{600} of a 1 ml sample was multiplied by the culture volume (i.e., 55 ml) to obtain the total number of OD_{600} units. This number will be used in the next section, for example, 0.6 x 55 ml = 33 total OD_{600} units. Cultures were then quickly poured into prechilled 50 ml centrifuges, placed in a prechilled rotor and centrifuged at 1,000 x g for 5 min at 4°C. Supernatants were discarded and cell pellets were resuspended in 50 ml of ice-cold H_2O. Cells were recovered by centrifugation at 1,000 x g for 5 min at 4°C. Cell pellets were immediately frozen in LN and stored at –70°C for protein extraction.

2.2.8.8.2 Preparation of protein extracts using Urea/SDS method

For protein extractios from yeast cells cracking buffer was prepared and pre-warmed to 60°C. Cell pellets were quickly thawed by separately resuspending each one in the pre-warmed cracking buffer. 100 µl of cracking buffer were used per 7.5 OD_{600} units of cells. Cell suspensions were then transferred into 1.5 ml screw-cap microcentrifuge tubes containing 80 µl of glass beads per 7.5 OD_{600} units of cells. Samples were vigorously mixed for 1 min, heated at 70°C for 10 min and centrifuged at 1,000 x g for 5 min at 4°C to remove pellet debris and unbroken cells. Supernatants were transferred into 1.5 ml tubes and samples were immediately analyszed by SDS/Urea PAGE.

2.2.8.9 Mating between bait and prey plasmids

Mating between transformed yeast strains was conducted according to the yeast two-hybrid system. Yeast strains were transformed with different DNA plasmids using the prey and bait vectors (Table 2.15) as described above (section 2.2.8.3).

Table 2.15 Yeast transformants for mating experiments, DNA plasmids and plating media.

Yeast strain	DNA plasmid	Plating medium
Y2H Gold	pGBKT7-53	SD/–Trp with Agar
Y2H Gold	pGBKT7-Lam	SD/–Trp with Agar
Y187	pGADT7-T	SD/–Leu with Agar
Y2H Gold	pGBKT:HC-Pro^{FRNK}	SD/–Trp with Agar
Y187	pGADT:HC-Pro^{FINK}	SD/–Leu with Agar
Y2H Gold	pGBKT:HC-Pro^{FRNK}	SD/–Leu with Agar
Y187	pGADT:HC-Pro^{FINK}	SD/–Leu with Agar
Y187	pGADT:NbAGO1	SD/–Leu with Agar

After a 3 days incubation period at 30°C, single colonies of each type used in the mated yeast strain (Table 2.16) were transferred into 2 ml centrifuge tubes containing 500 µl of 2x YPD. Tubes were incubated with shaking at 200 rpm at 30°C ON (20–24 h). The next day, 100 µl of the cultures were examined under the microscope to check for budding of the yeat

cells. From the mated cultures (0.5 ml), 100 µl of 1/10 and 1/100 dilutions were spread on each of the following agar plates:

- SD/–Trp (SDO)
- SD/–Leu (SDO)
- SD/–Leu/–Trp (DDO)
- SD/-Leu/-Trp/-His (TDO)
- SD/–Leu/–Trp/X-α-Gal/AbA (=DDO/X/A)
- SD/-Leu/-Trp/-His/-Ade (QDO)

Table 2.16 Mated yeast strains.

	Mated strains
Positive Control Mating	Y2H Gold (pGBKT7-53) & Y187 (pGADT7-T)
Negative Control Mating	Y2H Gold (pGBKT7-Lam) & Y187 (pGADT7-T)
Check for dimerization	Y2H Gold (pGBKT:HC-Pro^{FRNK}) & Y187 (pGADT:HC-Pro^{FRNK})
Check for dimerization	Y2H Gold (pGBKT:HC-Pro^{FINK}) & Y187 (pGADT:HC-Pro^{FINK})
Check for protein-protein interaction	Y2H Gold (pGBKT:HC-Pro^{FRNK}) & Y187 (pGADT:NbAGO1)
Check for protein-protein interaction	Y2H Gold (pGBKT:HC-Pro^{FINK}) & Y187 (pGADT:NbAGO1)

Plates were incubated (colony side facing downward) at 30°C for 3–5 days. After that plates were examined to check for the activaton of reporter genes as a result of protein-protein interactions.

2.2.9 Protoplast preparation from infiltrated *N. benthamiana* leaves

Protoplasts were prepared from infiltrated *N. benthamiana* leaves by enzymatic digestion of the plant cell wall. Infiltrated leaves were harvested 2 days post infiltration (dpi), cut with a scalpel into small pieces and incubated in the enzyme solution for protoplast preparation at RT in the dark with gentle agitation for 3 h. Protoplast suspensions were carefully transferred into 1.5 ml reaction tubes and gently centrifuged for 10 min at 300 g. Protoplasts were resuspended in 1 ml of W5 solution.

To identify protein localization *in vivo* a confocal laser-scanning microscope (Carl Zeiss, www.zeiss.de) was used with magnification ranges from 5x to 40x. To validate fluorescence, two different filters including Cy3 (detect red fluorescence of necrotic tissues) and FITC (chlorophyll emit red, GFP green fluorescence) were applied.

2.2.10 Nuclear localization assay of HEN1 fused to GFP/RFP reporter genes

Protein localization of HEN1 was examined by fusion of SlHEN1 to GFP/RFP reporter genes, generating SlHEN1-GFP and SlHEN1-RFP fusion proteins. The corresponding transgene constructs were cloned into the pPCV702SM binary vector. SlHEN1-GFP/RFP were expressed in *N. benthamiana* leaves by transient transformation as described above (2.2.2). Three dpi plant material was monitored by fluorescence microscopy to ceck for the

expression of the fusion proteins using two different filters, including CY3 (Carl Zeiss) and FITC (Carl Zeiss). Subsequently, protoplasts were prepared from infiltrated *N. benthamiana* leaves by enzymatic digestion of the plant cell wall and examined as described above.

2.2.11 *In vitro* binding of HEN1 with HC-Pro

Microtiter plates were coated with 50 units of AtHEN1 RNA methyltransferase (cloned from *Arabidopsis* plants with a physical purity of 95%, New England Biolabs) diluted in100 µl of 3% BSA in PBS buffer and incubated at 4°C ON. Non-specific binding was blocked with 3% BSA in PBS buffer for 1 h. Plates were washed 3 times with PBS buffer and equal amounts (2 µg) of MBP:HA-Hc-Pro proteins diluted in 100 µl of 3% BSA in PBS buffer were added next day. Plates were incubated at RT for 2 h. Unbound proteins were washed out with 0.001% Tween-PBS buffer 4 times and 1 time with PBS buffer. Binding of AtHEN1 to HC-Pro was detected by ELISA with 1:10000 of anti-MBP HRP conjucate (New England Biolabs) and 1:2000 of anti-mouse antibody conjugated with alkaline phosphatase (Sigma-Aldrich). Finally fresh substrate was added to the plates followed by incubation at 37^{o}C for 15 min. The absorbance was measured using a plate reader (Multiscan Ascent) at 405 nm for the detection of protein-protein interactions.

2.2.12 Methyltransferase inhibition assay

The methyltransferase inhibition assay was carried out to examine whether the ZYMV HC-Pro affects the activity of AtHEN1. The inhibition assay was performed according to Yu and co-worker (2005) with some modifications. The reaction was carried out in a total reaction volume of 100 µl which contained 1x NEB 2 buffer (New England Biolabs), 1 µg miRNA 173 duplex, 2 µl Ribo Lock (40 U/µl) RNase-Inhibitor (Fermentas), 2 µl of AtHEN1 (New England Biolabs), 4 µl S-adenosyl-L-[methyl-14C] methionine (58.0 mCi/mmole; GE Healthcare), 5 µg of protein (MBP:HA-HC-Pro$^{FRNK/FINK}$) and MBP as well as MBP buffer as negative controls. After 1 h of incubation at 37°C, the reaction was stopped by the addition of 100 µl of the stopping solution (100 mM Tris-HCl, pH = 8.0), 10 mM EDTA, 150 mM NaCl, 2% SDS, and 0.4 mg/ml proteinase K) and followed by incubation for 15 min at 65°C. The reaction was extracted with phenol/chloroform and the RNA was precipitated by adding 3 µl glycogen and 300 µl isopropanol/10 M ammonium acetate (10:2). For precipitation, samples were incubated for 1 h at -20°C and centrifuged at 17,900 x g for 5 min. Supernatants were discarded, the pellets were washed with cold 70% ethanol, dried for 10 min at RT and resuspended in 10 µl RNAs free H_2O. RNA samples were electrophoresed at 80 V in 1x TBE buffer using 20% TBE-polyacrylamide gel (Anamed). Gels were then dried at 65°C for 1 h, exposed to FujiFilm Imaging Plates (FujiFilm) for up to 3 months and scanned using the PharosFX Plus PhosphorImager (Bio-Rad).

3. Results

3.1 Subcellular localization of HC-Pro protein of the ZYMV

3.1.1 Modification of the pPCV702SM binary vector

A modification of the pPCV702SM binary vector was carried out by the introduction of new restriction sites into the multiple cloning site of the vector producing the binary vector pPCV702SM-MC. This new polylinker was 46 bp in length and contained several restriction sites, including *SacI*, *SalI*, *AscI*. Modification of the polylinker was carried out by annealing the primer pair Linker pPCV A-F/Linker pPCV B-R (Table 2.6). After cloning, restriction analysis with *AscI* and *StuI* confirmed the insertion of the polylinker.

3.1.2 Cloning of HC-Pro fused to GFP

To study the intracellular localization of HC-Pro (HC-Pro^{FRNK}) and its mutant, FINK (HC-Pro^{FINK}), in living cells, we used the green fluorescent protein (GFP) as a reporter. GFP was translational fused to either the N- or C-termini of HC-Pro^{FRNK} and HC-Pro^{FINK}. The HA-HC-Pro$^{FINK/FRNK}$-GFP clones were generated by PCR using the primer pair HA-AscI-F/GFP-XbaI stop-R. The resulting plasmids were checked by restriction analysis using *AscI* and *XbaI*. The GFP-HC-Pro$^{FRNK/FINK}$ clones were generated by PCR using the primer pair, GFP BamHI-F/GFP XbaI-R amplifying the GFP, and the primer pair, Hc-Pro XbaI-F/Hc-Pro XbaI–R amplifying the HC-Pro cDNAs. After cloning, restriction analysis with *BamHI* and *SalI* indicated that the cloning of GFP-HC-Pro^{FRNK}, GFP-HC-Pro^{FINK}, HA-HC-Pro^{FRNK}-GFP, and HA-HC-Pro^{FINK}-GFP was successful.

All constructs were transiently expressed in epidermal cells of *N. benthamiana* leaves by agroinfiltration. The binary vectors pPCV702SM and pPCV702SM-MC were used for cloning the fusion proteins' coding sequences under the control of the cauliflower mosaic virus (CaMV) promoter (P35S) and the nopaline polyadenylation signal sequence (pAnos). Binary vectors were introduced into the *A. tumefaciens* strain GV3101 by the freeze and thaw method giving the GV-GFP-HC-Pro^{FRNK}, GV-HC-Pro^{FRNK}-GFP, GV-GFP-HC-Pro^{FINK} and GV-HC-Pro^{FRNK}-GFP.

3.1.3 Western blot analysis and Chemiluminescence Immunodetection

HC-Pro has an autocatalytic activity that cleaves its carboxyl terminus (Carrington *et al*., 1989), and this will cleave any protein fused to the C-terminus of the HC-Pro. To investigate transgene expression and to analyze the size of the fusion proteins transient expression and Western blot experiments were performed. Samples of *N. benthamiana* plants that were infiltrated with the GV-GFP-HC-Pro and GV-HC-Pro-GFP strains were taken at different time points. The day of infiltration was considered as day 0 and samples were taken 1 to 4 days post infiltration (dpi). Western blot analysis using chemiluminescence immunodetection procedure was applied to confirm the expression of the HC-Pro/GFP fusion proteins. Immunodetection specific for the HA-POD antibody showed accumulation of proteins of about 81 kDa corresponding to the full-size of HC-Pro$^{FRNK/FINK}$-GFP and proteins of approximately 54 kDa representing the size of the HC-Pro protein (Fig. 3.1a). Stripping and immunodetection using GFP-specific antibodies on the same membrane showed the accumulation of a protein of about 27 kDa corresponding to the full-length of the GFP, in addition to the full length HC-Pro-GFP, and some lower molecular mass fragments probably representing proteolytic cleavage products of the HC-Pro-GFP (Fig. 3.1B). For the membrane with the N-terminal GFP-Hc-Pro$^{FRNK/FINK}$ fusion proteins, immunodetection with GFP-specific antibodies showed accumulation of a 81 kDa protein corresponding to the size of the full-length GFP-HC-Pro proteins. No GFP cleaved product was detectable (Fig. 3.1C).

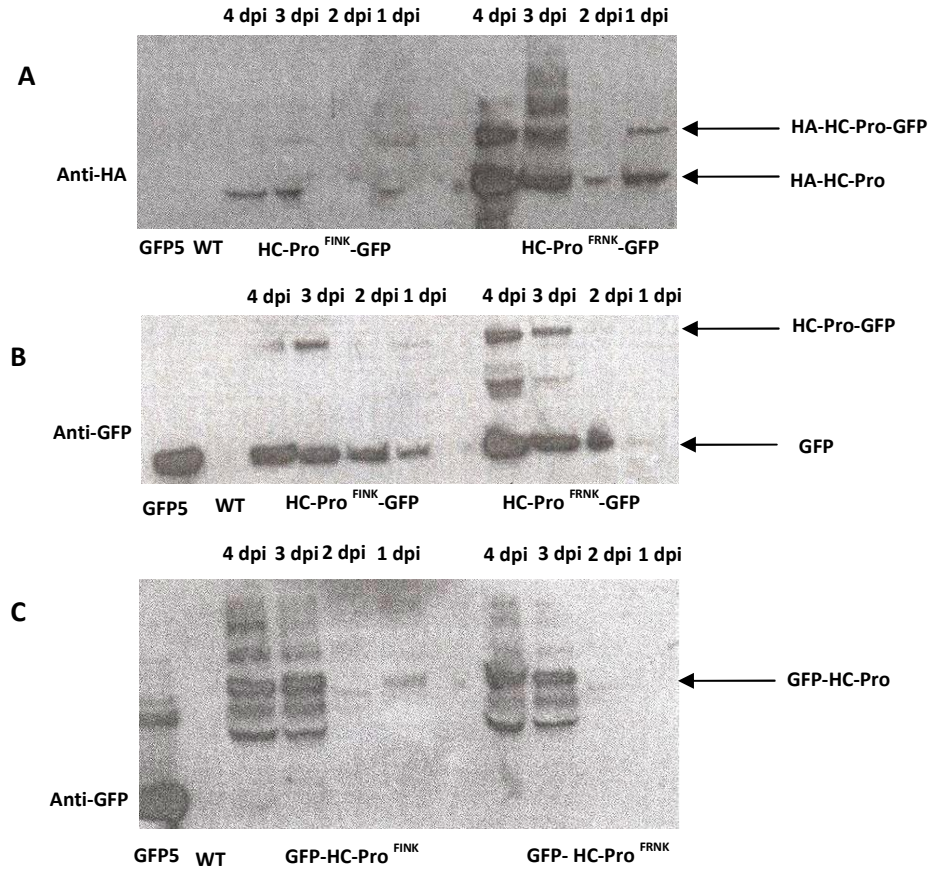

Figure 3.1: Western blot analysis of transiently expressed HC-Pro/GFP fusion proteins: *N. benthamiana* leaves were infiltrated with GV-HC-Pro/GFP strains. Leaf material was harvested at 1 to 4 dpi. GFP5 = total protein from *N. benthamiana* 16c (positive control); WT = total protein from a *N. benthamiana* wild type plant (negative control). Arrows indicate proteins with sizes corresponding to the HC-Pro/GFP (81 kDa), the HC-Pro (54 kDa) and the GFP (27 kDa). (**A**) HC-Pro-GFP fusion proteins, immunodetection using HA-POD antibodies, (**B**) HC-Pro-GFP fusion proteins, immunodetection using GFP-specific antibodies, (**C**) GFP-HC-Pro fusion proteins, immunodetection using GFP-specific antibodies.

3.1.4 Subcellular localization of ZYMV HC-Pro

Subcellular localization of the ZYMV HC-Pro was tested by transient expression of the GFP-HC-Pro^{FRNK}, GFP-HC-Pro^{FINK}, HA-HC-Pro^{FRNK}-GFP, and HA-HC-Pro^{FINK}-GFP as described above. Infiltrated plants were examined 3 dpi by fluorescent microscopy to monitor GFP expression. Protoplasts were isolated from fluorescing leaves and were visualized by confocal laser-scanning microscopy. Subcellular accumulation sites for these proteins were compared with the localization of a ß-glucurodinase (GUS)–GFP fusion protein (cytosolic control), GFP5 (endoplasmic reticulum (ER) control) and NLS–GFP (nuclear control). Our results indicated that the HC-Pro of ZYMV is predominantly associated with the ER (Fig. 3.2).

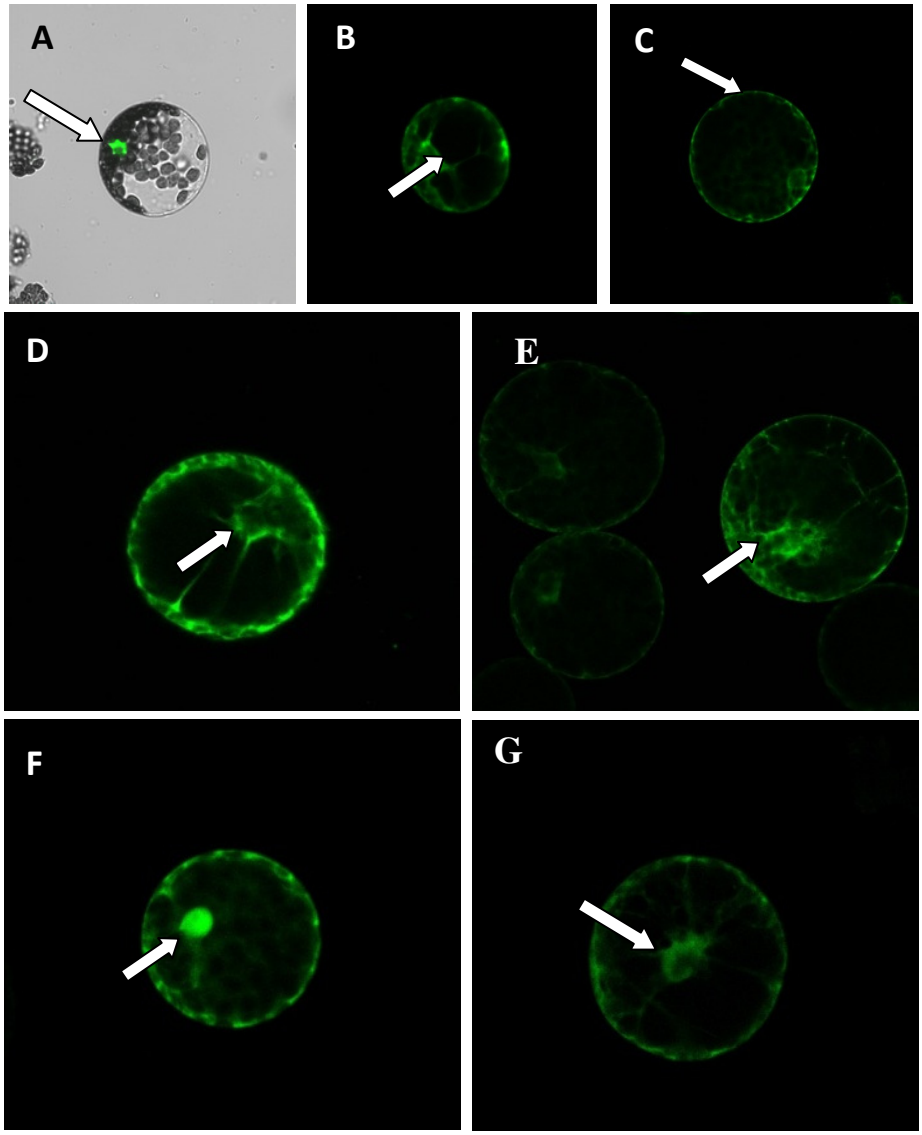

Figure 3.2: Cellular localization of HC-Pro^{FRNK} and HC-Pro^{FINK}. Protoplasts of infiltrated *N. benthamiana* leaves were analyzed by fluorescence microscopy 3 dpi. Arrows indicate localization of GFP. A = NLS-GFP (nuclear control); B = GFP5 (ER control); C = GUS-GFP (cytoplasm control); D = GFP-HC-Pro^{FRNK}; E = GFP-HC-Pro^{FINK}; F = HC-Pro^{FRNK}-GFP; G = HC-Pro^{FINK}-GFP. Images were taken using a confocal laser-scanning microscope.

3.2 Generation of transgenic *N. benthamiana* and *A. thaliana* plants expressing HC-Pro

In order to investigate if stable expression of the ZYMV HC-Pro produces symptoms, *N. benthamiana* and *A. thaliana* plants were transformed with the ZYMV HC-Pro$^{FRNK/FINK}$ transgene constructs. These constructs were constitutively expressed in all cells and through the different developmental stages of the transgenic plants.

We hypothesized that the ZYMV HC-Pro^{FINK} lacking sRNA-binding activity would produce symptoms if targeted into the nucleus. Thus, the ZYMV HC-Pro^{FRNK} and ZYMV HC-Pro^{FINK} were fused to a nuclear localization signal (NLS) resulting in the NLS-HC-Pro^{FRNK} and NLS-HC-Pro^{FINK} transgene constructs, which were used for stable

transformation of *A. thaliana* and *N. benthamiana* plants. The NLS-HC-Pro$^{FRNK/FINK}$ clones were generated by PCR using the primer pair HA-AscI-F/Hc-Pro XbaI-R (Table 2.6). The resulting plasmids were checked by restriction analysis using *AscI* and *XbaI*.

3.2.1 Molecular analysis of transgenic plants expressing ZYMV HC-Pro

A. thaliana and *N. benthamiana* plants were transformed with the ZYMV HC-Pro$^{FRNK/FINK}$ and NLS-HC-Pro$^{FRNK/FINK}$ transgenes which were under the control of the P35S. Transgenic *N. benthamiana* and *A. thaliana* plants were generated by *Agrobacterium*-mediated leaf disc transformation and floral dip transformation, respectively.

For each construct (HA-HC-Pro^{FRNK}, HA-HC-Pro^{FINK}, NLS-HC-Pro^{FRNK}, and NLS-HC-Pro^{FINK}) between 11-13 independent *N. benthamiana* lines were screened for the presence of the HC-Pro gene by PCR using the primer pair Hc-Pro-int-seq-F/Hc-Pro XbaI-R. From these lines, seeds were produced by self-pollination. Two progeny plants (T1 generation) of each of these lines were again screened for the presence of the transgene by PCR and used for further studies. Expression of the HC-Pro in all lines was first confirmed by Northern blot analysis. The membrane was hybridized with a 920 bp long ^{32}P-labeled HC-Pro cDNA fragment that was complementary to the 3'-end of the HC-Pro RNA. Subsequently, Western blot analysis was applied using a polyclonal rabbit anti-ZYMV-HC antiserum (Fig. 3.3a). To avoid any possible tissue culture effects, for each transgene, two independent T1 lines were screened that germinated to 100% on kanamycin-containing medium.

Transgenic *A. thaliana* lines were screened by germinating seeds of the T0 generation on 1/2 MS medium supplemented with 50 mg kanamycin. The percentage of germinating seeds was very low (1%). Only 2 independent transgenic lines were used for further molecular analysis. In all lines, expression of the HC-Pro was confirmed as described for *N. benthamiana* (Fig. 3.3b).

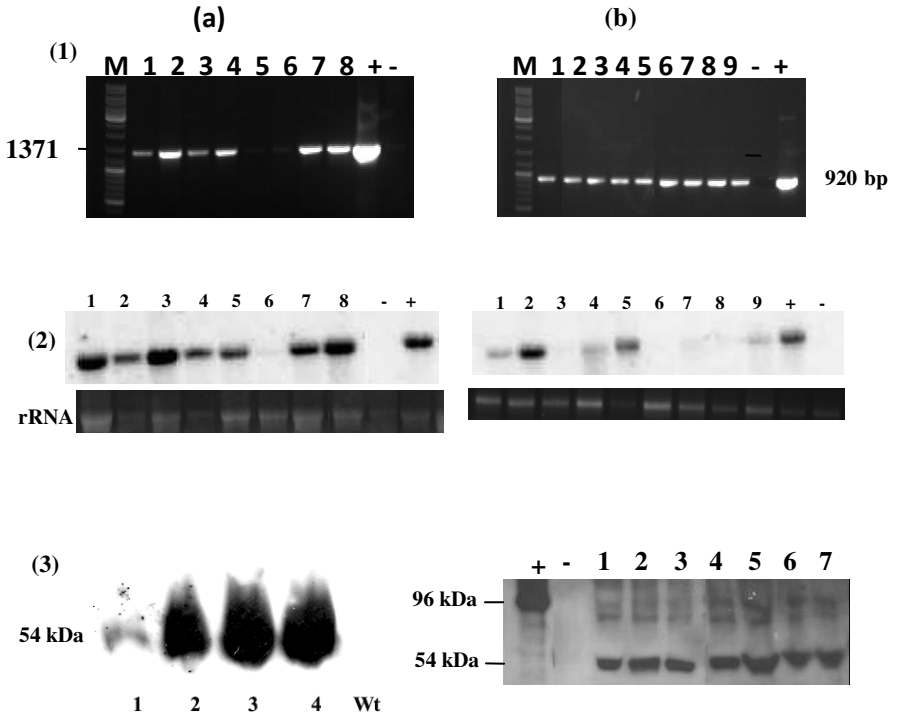

Figure 3.3: Molecular analysis of transgenic plants expressing ZYMV HC-Pro genes. (a) Transgenic *N. benthamiana* lines; (b) Transgenic *A. thaliana* lines; **1=** PCR-mediated detection of the transgene DNA in transformed *N. benthamiana* and *A. thaliana*; **2=** Northern hybridization with a ^{32}P-labeled HC-Pro-specific cDNA probe for the detection of the transgene mRNA; **3=** Western blot analysis to detect the ZYMV HC-Pro in *N. benthamiana* (left panel), and *A. thaliana* (right panel), using antiserum against ZYMV HC-Pro (1:10,000 dilution). **1-4** (left panel) = independent *N. benthamiana* transformants, WT = *N. benthamiana* wild type (negative control), right panel, + = positive control, - = *A. thaliana* non-transformed (negative control), **1-7 =** independent *A. thaliana* transformants.

3.2.2 Phenotypes of transgenic plants

Phenotypes were observed in transgenic plants expressing HC-Pro proteins. *A. thaliana* displayed more disturbed phenotypes than *N. benthamiana* (Tables 3.1). These phenotypes greatly varied between the two plant species and the different constructs. Phenotypic alterations produced by the HC-Pro^{FRNK} and HC-Pro^{FINK} were minor in *N. benthamiana* plants. Some individuals of the HC-Pro^{FRNK}- and HC-Pro^{FINK}-expressing lines showed morphological changes. Generally, reduced growth rates and slight leaf shape alterations were observed (Fig. 3.4). However, several lines showed normal growth rate and no morphological changes. Generally, T0 lines produced seeds after self-pollination and T1 seedlings grown under kanamycin selection germinated at a 90-100% rate.

Table 3.1: Most pronounced phenotypes observed in independent transgenic *N. benthamiana* and *A. thaliana* lines expressing HC-Pro^{FRNK} and HC-Pro^{FINK}, respectively.

Plant species	***N. benthamiana***		***A. thaliana***	
Suppressor construct	**FRNK**	**FINK**	**FRNK**	**FINK**
Leaves	Line 1: normal Line 2: thick, short, wrinkled	Line 1: normal Line 2: thick, short, wrinkled	Line 1 & 2: small, thick, short, de-formed (wrinkled)	Line 1 & 2: normal
Growth	Line 1: normal Line 2: low growth rate	Line 1: normal Line 2: low growth rate	Line 1 & 2: low growth rate	Line 1 & 2: normal
Flowers	Line 1 & 2: normal	Line 1 & 2: normal	Line 1 & 2: late flowering, some flowers did not form capsules, reduced number	Line 1 & 2: normal
Seeds	Line 1 & 2: normal	Line 1 & 2: normal	Line 1 & 2: reduced number	Line 1 & 2: reduced number
Suppressor construct	**HA-NLS-FRNK**	**HA-NLS-FINK**	**HA-NLS-FRNK**	**HA-NLS-FINK**
Leaves	Line 1: normal Line 2: deformed, thick	Line 1: normal Line 2: deformed, thick	Abnormal seedling formation	Normal
Growth	Normal	Normal	Growth rate low	Normal
Flowers	Some flowers deformed, no capsule formation, petals short and bent	Some flowers deformed, no capsule formation	Late flowering, deformations, reduced number, not fully developing	Deformations, not fully developing
Seeds	Some plants were sterile, reduced number	Some plants were sterile, reduced number	Reduced number	Reduced number

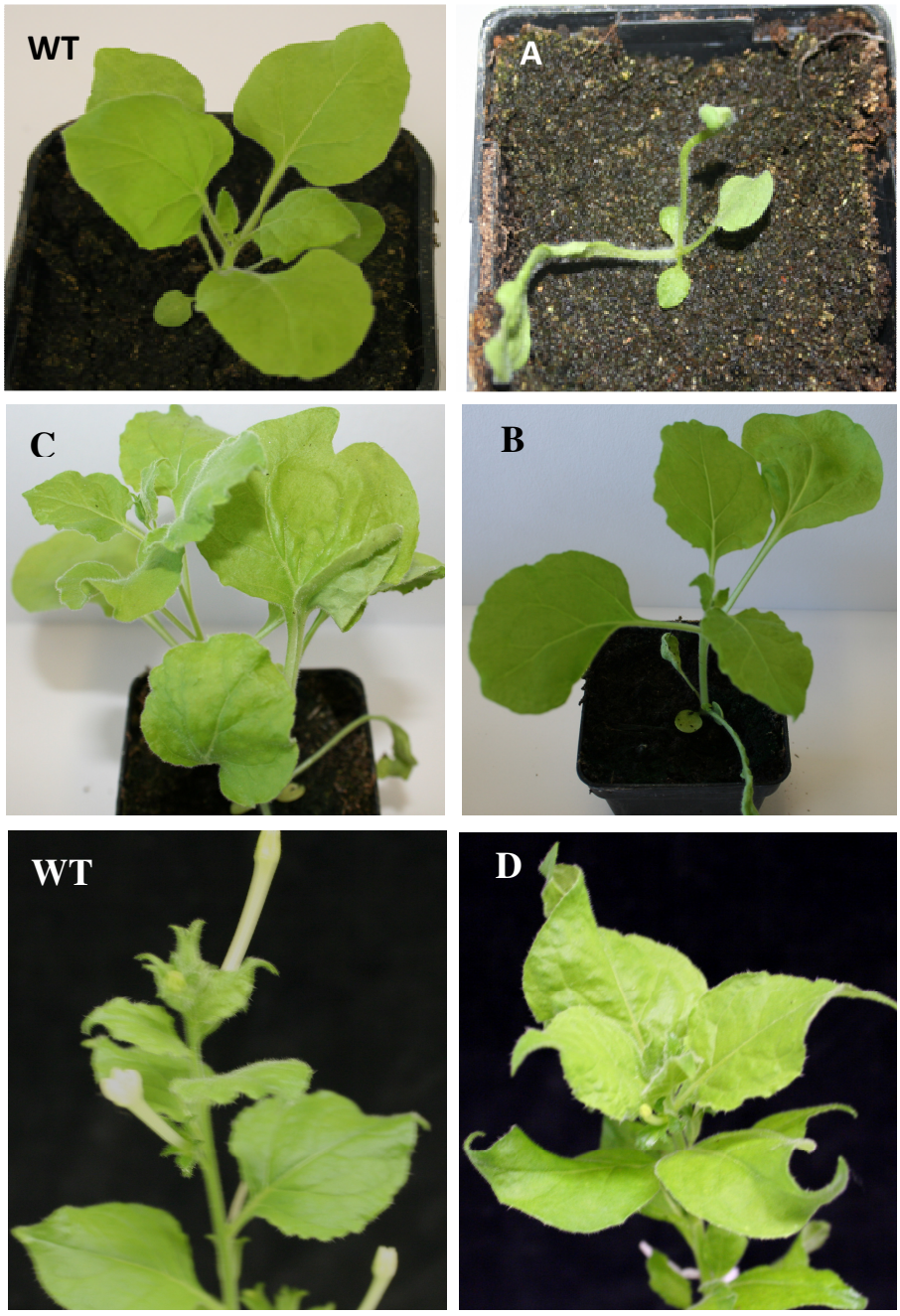

Figure 3.4: Phenotypes observed in *N. benthamiana* plants expressing HC-Pro$^{FRNK/FINK}$. WT = wild type *N. benthamiana.* A = low growth rate, deformed seedlings in a HC-Pro^{FRNK} line; B and C = deformed leaves in HC-Pro^{FRNK} – (B) and HC-Pro^{FINK}- (C) expressing plants; D = leaf rolling in HC-Pro^{FRNK}-expressing plant.

The phenotypes in *A. thaliana* were more obvious and varied among HC-Pro^{FRNK}- and HC-Pro^{FINK}–expressing lines (Table 3.1). In HC-Pro^{FRNK}-expressing lines, the growth rate was very low, with a rosette growth form and short, deformed, thick leaves (Fig. 3.5). In contrast, growth rate and leaf morphology were normal in HC-Pro^{FINK}–expressing lines (Fig. 3.5). However, seed production was reduced in both, the HC-Pro^{FRNK}- and HC-Pro^{FINK}-expressing lines.

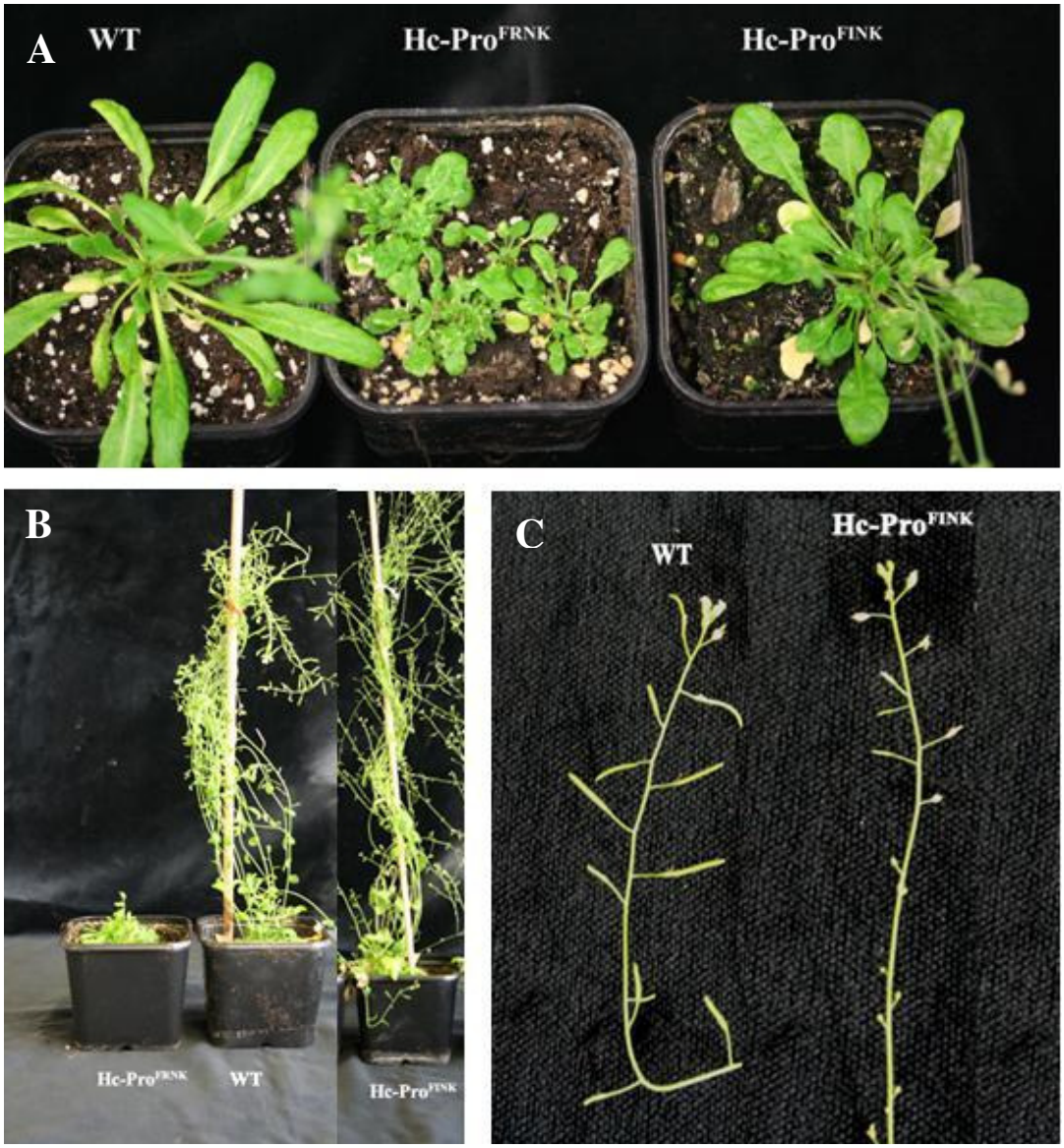

Figure 3.5: Phenotypes observed in *A. thaliana* plants expressing HC-Pro. WT = wild type; **A** = growth form comparison between wild type and HC-Pro$^{FRNK/FINK}$-expressing lines; **B** = flowering of HC-Pro^{FRNK}–expressing line, wild type and HC-Pro^{FINK}-expressing line; **C** = seed production of wild type and HC-Pro^{FINK}-expressing line.

The NLS-HC-Pro proteins appeared to cause severe phenotypes essentially in transgenic *A. thaliana* plants (Table 3.1). The most prominent phenotypes in both plant species expressing NLS-HC-Pro^{FRNK} and NLS-HC-Pro^{FINK} were malformed flowers with reduced seed production and sometimes, flowers that did not fully developed (Fig. 3.6 and 3.7).

In transgenic *A. thaliana* lines, leaves were thick and short and the growth rate of NLS-HC-Pro^{FRNK}-expressing plants was very low. In NLS-HC-Pro^{FINK}-expressing plants, leaf development and growth rate were normal (Fig. 3.6). The most striking phenotype

caused by both NLS-HC-Pro constructs were malformed flowers with reduced seed production (Fig. 3.6).

Figure 3.6: **Phenotypes observed in *A. thaliana* plants expressing HA-NLS-HC-Pro. WT =** wild type*;* **A** = seed production comparison in wild type and HA-NLS-HC-Pro$^{FRNK/FINK}$-expressing lines; **B** = leaf shape comparison between wild type and HA-NLS-HC-Pro$^{FRNK/FINK}$-expressing lines.

Phenotypes observed in *N. benthamiana* plants expressing NLS-HC-Pro transgene constructs are presented in Table 3.1 and Figure 3.7. In all lines, the most notable phenotypes were malformed flowers and reduced seed production. The flowers' petals were short with bent stalks. In addition, some flowers failed to produce capsule. The number of seeds was generally very low when compared to wild type plants. Very few plants showed low growth rate, malformed seedlings and thick malformed leaves (Fig. 3.7). Finally, some of the T0 plant lines were sterile.

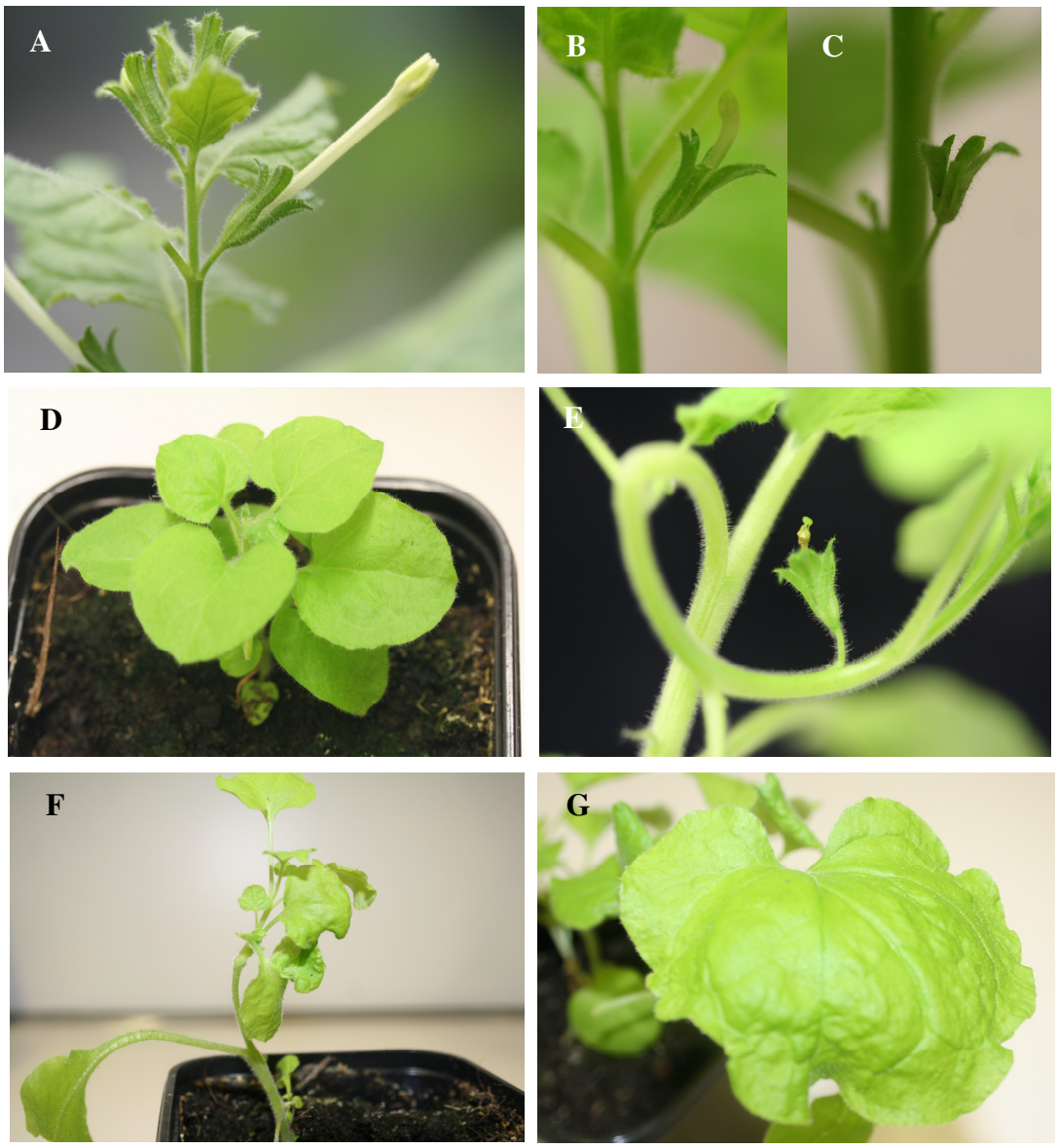

Figure 3.7: Phenotypes observed in *N. benthamiana* plants expressing HA-NLS-HC-Pro$^{FRNK/FINK}$. **A** = *N. benthamiana* wild type; **B-G** = HA-NLS-HC-Pro$^{FRNK/FINK}$–expressing plants **B** = small bent flowers; **C** = undeveloped malformed flowers; **D** = plant dwarfism and low growth rate; **E** = stunting; **F** = malformed seedlings and thick leaves; **G** = blistered leaf epidermis.

3.2.3 Analysis of the RNA silencing suppressor activity of ZYMV HC-Pro^{FRNK} and HC-Pro^{FINK} in transgenic *N. benthamiana* plants

The RSS activity of ZYMV HC-Pro has already been demonstrated through a transient approach in *N. benthamiana* plants (Shiboleth *et al.*, 2007). To test the functionality of HC-Pro^{FRNK} or HC-Pro^{FINK} in *N. benthamiana* plants expressing one of the two genes, the *Agrobacterium*-mediated transient expression procedure (agroinfiltration) was applied. This method is a versatile tool to rapidly introduce genes into plant tissue, and enables gene expression within a short period of time. A useful feature of this method is the ability to introduce multiple genes simultaneously into a patch of leaf tissue. Agroinfiltration has also

been effectively used to deliver RNA silencing inducers and suppressors into transgenic plants expressing a reporter gene (Voinnet *et al*., 1998, 2000; Lleave *et al*., 2000).

To verify the RSS function of HC-Pro^{FRNK} and HC-Pro^{FINK} in transgenic plant lines, a GFP-silencing assay was used. Suppression of gene silencing in transgenic *N. benthamiana* plants constitutively expressing HC-Pro$^{FRNK/FINK}$ was induced by co-infiltration of leaves of three weeks old *N. benthamiana* plants with *Agrobacterium* strains carrying the GFP and the GpG transgene constructs (Dalakouras *et al*., 2009). *N. benthamiana* wild type plants were used as a negative control. Expression of the GpG transgene led to the induction of IR-PTGS. Five and nine dpi, GFP expression was analyzed under UV light. As expected, plants expressing the suppressor maintained green fluorescence even 9 dpi. In contrast, in wild type plants, GFP fluorescence faded in plants infiltrated with GFP and in those that were co-infiltrated with the GFP and GpG constructs due to RNA silencing (Fig. 3.8).

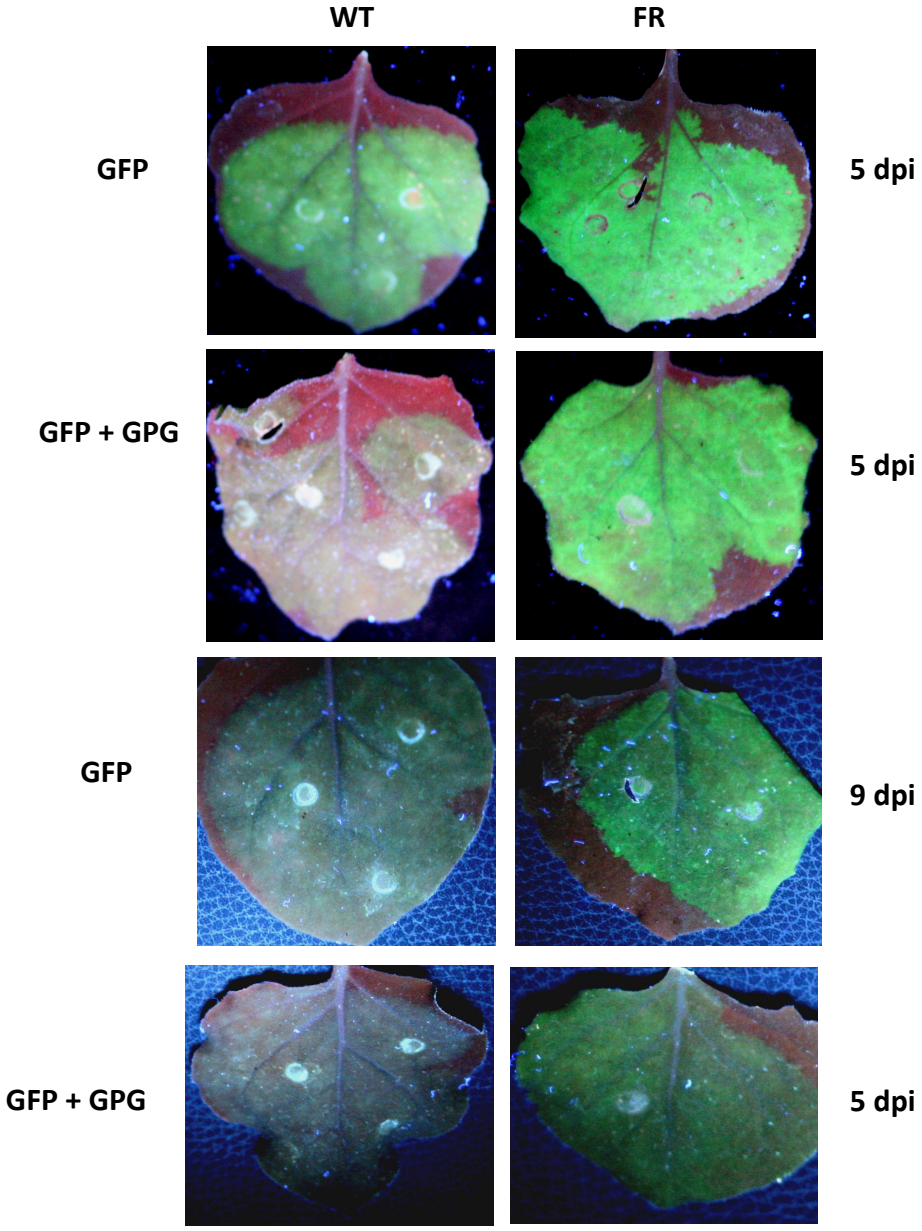

Figure 3.8: RNA silencing suppressor activity in transgenic *N. benthamiana* plants expressing HC-Pro^{FRNK} 5 and 9 dpi. WT = *N. benthamiana* wild type; FR = HC-Pro^{FRNK}–expressing *N. benthamiana* line co-infiltrated with *Agrobacterium* strains harboring the GFP and the silencing-inducing GpG transgene constructs. Images were taken under UV light.

3.2.4 Effects of HC-Pro on miRNA levels in *N. benthamiana* and *A. thaliana*

The influence of ZYMV HC-Pro^{FRNK} and HC-Pro^{FINK} on miRNA accumulation in *N. benthamiana* and *A. thaliana* was examined. The miRNAs of which the accumulation was examined in this study included miRNAs that regulate the expression of transcription factors (miR156c, miR159c, miR162, miR171c, miR160b, miR173), that were associated with miRNA biogenesis (miR168a) and that were involved in the ta-siRNA biogenesis (miR390a). DNA oligonucleotide sequences which were used as probes for miRNA/miRNA* detection,

were based on corresponding miRNA sequences which were available in the *Arabidopsis* MPSS Plus database (Brenner *et al*., 2000).

In RNA samples of ZYMV HC-Pro-expressing plants, miRNA accumulation was detected by Northern blots analysis. Not all of the tested miRNA-strands were detectable and some miRNA-strands differentially accumulated in transgenic and wild type plants. No significant differences were observed for HC-Pro^{FRNK}- and HC-Pro^{FINK}-expressing plants (Fig. 3.9A and B).

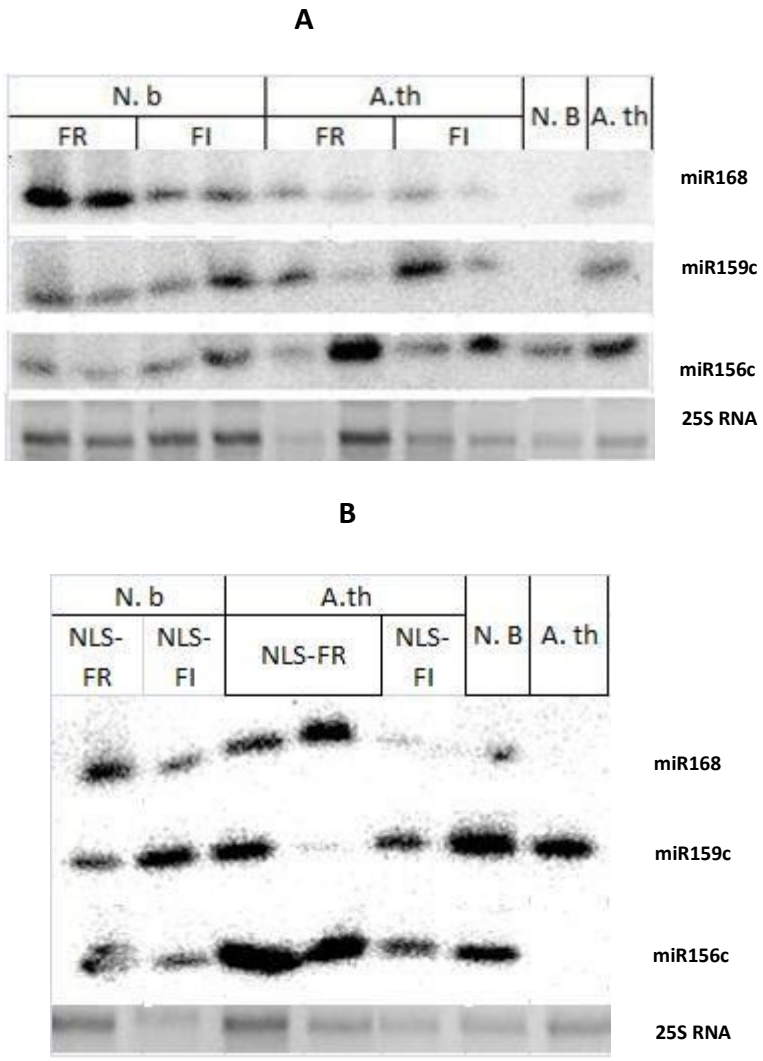

Figure 3.9: Accumulation of miRNA168, 159 and 156 in transgenic *N. benthamiana* and *A. thaliana* plants. A = transgenic *N. benthamiana* (N.b) and *A. thaliana* (A.th) plants expressing HC-Pro^{FRNK} (FR) and HC-Pro^{FINK} (FI); B = transgenic *N. benthamiana* (N.b) and *A. thaliana* (A.th) plants expressing NLS-HC-Pro^{FRNK} (NLS-FR), and NLS-HC-Pro^{FINK} (NLS-FI). *N. benthamiana* and *A. thaliana* wild type were used as controls; 25S rRNA accumulation served as loading control.

3.2.5 Quantitative analysis of calmoduline–related protein (rgs-CaM) expression in *N. benthamiana* plants

In this study, we compared the levels of rgs–CaM mRNA in *N. benthamiana* plants expressing Hc-Pro^{FRNK} (NbFRNK) and Hc-Pro^{FINK} (NbFINK) with the rgs-CaM expression level of wild type plants. RNA was extracted from three weeks old leaves and was subjected to Northern blot analysis. The membrane was probed with an α-^{32}P dCTP-labeled PCR product produced from the rgs-CaM gene using *N. benthamiana* DNA as template. In all transgenic and wild type plants, rgs-CaM mRNA was not detectable. However, to further investigate the rgs-CaM mRNA levels a quantitative RT-PCR (qRT-PCR) analysis was carried out. Specific primers for rgs-CaM were employed and the data obtained from the gene expression analysis of the rgs-CaM gene were normalized on the Eukaryotic translation initiation elongation factor 4A (*eIF4*) and Elongation factor-1 α (*EF1-α*) genes, that are expressed at a constant level in both, the transgenic and wild type plants.

The qRT-PCR analysis was performed using total RNA extracted from leaves of three weeks old *N. benthamiana* plants and was performed in three technical replicates with two repeats per replicate. The primers corresponding to eIF4 and EF1-α performed with comparable efficiency allowing the use of a unique E value for both genes. On the contrary, for the primers targeting the rgs-CaM transcripts it was necessary to calculate their own E value since the performances were significantly different (ANOVA alpha=0.05) compared to those of the control genes. The expression level of rgs-CaM in NbFRNK, NbFINK and *N. benthamiana* wild type plants was normalised for each sample on the level of both the eIF4 and EF1-α controls, respectively. Subsequently, the ratio between normalised rgs-CaM level in the transgenic plants and normalised rgs-CaM level in the wild type was calculated. The T-test analysis was performed between the rgs-CaM expression dataset of the transgenic plants against the rgs-CaM expression dataset of the wild type for the individuation of statistical significant differences in the rgs-CaM expression level.

No significant differences were found when comparing the 3 values of the wild type against the 3 values in each independent transgenic line applying the T-test analysis. In Figure 3.10, the ratio values of the normalized data in each plant line with their standard deviations are shown.

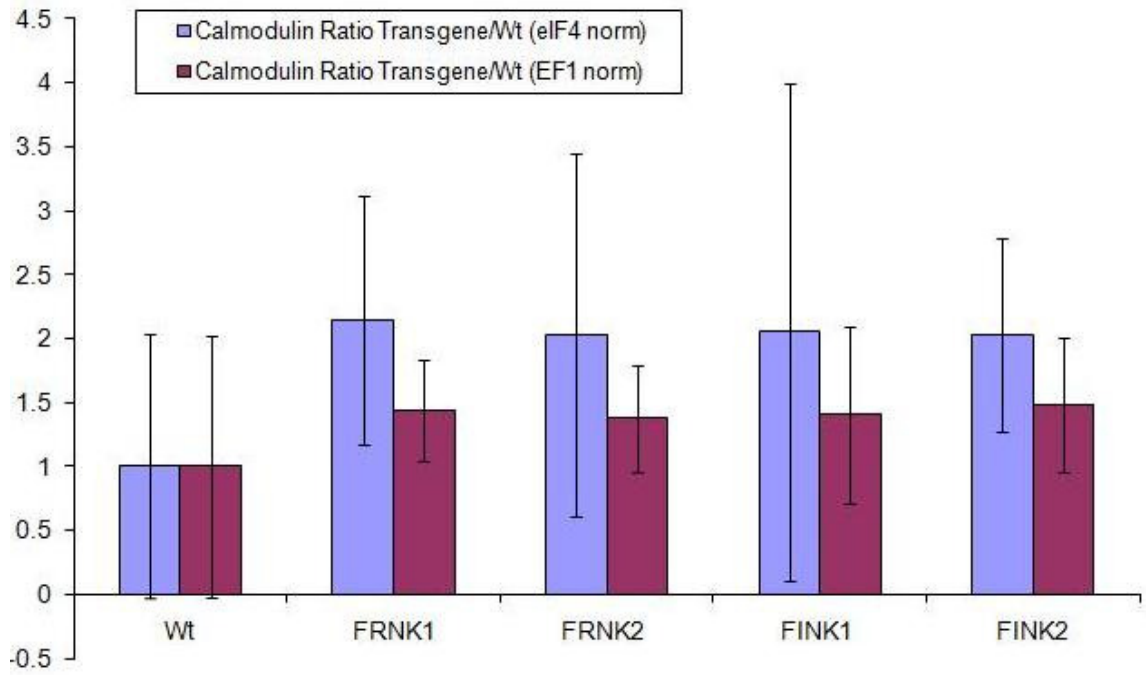

Figure 3.10: rgs-CaM gene expression levels in transgenic and wild type plants; blue = normalized on eIF4; violet = normalized on EF-α; wt = wild type; NbFRNK1 and NbFRNK2 = two independent transgenic plants expressing HC-Pro^{FRNK}; NbFINK1 and NbFINK2 = two independent transgenic plants expressing HC-Pro^{FINK}.

3.2.6 Effect of HC-Pro on PSTVd siRNA in crossed plants

In this study we investigated the effect of HC-Pro on the accumulation of potato spindle tuber viroid (PSTVd) -specific siRNAs. We hypothesized that in PSTVd-infected plants, the siRNA binding activity of HC-Pro may result in altered levels of viroid-derived siRNAs. Genetic crossings between NbFRNK and transgenic *N. benthamiana* plants (Nb-PSTVd) expressing an infectious PSTVd transgene construct (Qi *et al*., 2004) were carried out. DNA of three weeks old progeny plants of these crossings was extracted and analyzed by PCR for the presence of the HC-Pro^{FRNK} and the PSTVd transgenes using the primer pairs Hc-Pro-int-seq-F/Hc-Pro-XbaI–R and PSTVd-for1/PSTVd-rev1 (Table 2.6). Three independent lines (NbFRNK-PSTVd) containing both transgenes were screened (Fig. 3.11).

Total RNA from independent NbFRNK-PSTVd, Nb-PSTVd and NbFRNK lines was extracted and applied to siRNA detection analysis. Using a PSTVd-specific probe, hybridization signals corresponding to PSTVd siRNAs were detectable in NbFRNK-PSTVd and Nb-PSTVd lines (Fig. 3.11). Notably, in the NbFRNK-PSTVd line, the level of PSTVd-derived siRNAs was about 3fold higher than in the Nb-PSTVd line. In contrast, siRNAs could not be detected in the NbFRNK line. In summary, the HC-Pro^{FRNK} proved to increase the accumulation of PSTVd siRNAs which might be attributed to the binding activity of HC-

Pro to siRNA. It should be noted that due to the severe symptoms that are caused by PSTVd in *N. benthamiana*, all NbFRNK-PSTVd and Nb-PSTVd lines died before seed production.

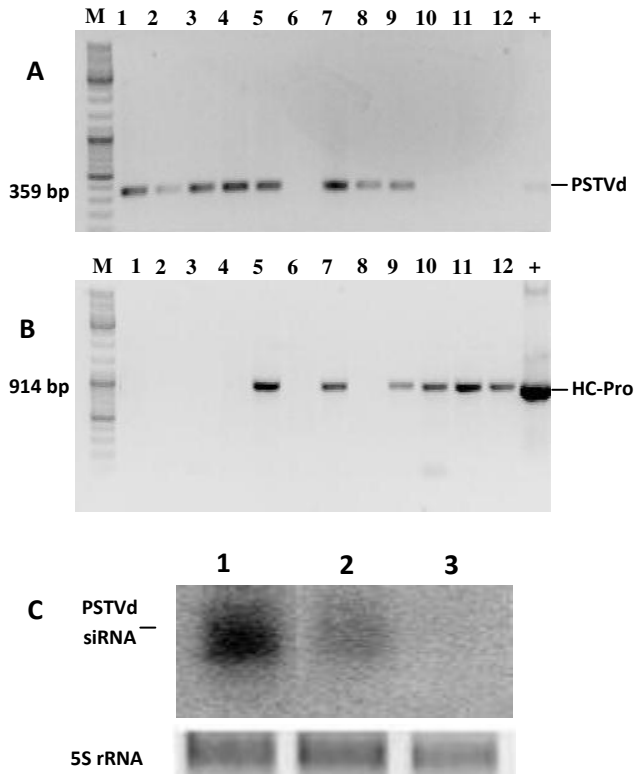

Figure 3.11: Molecular analysis of PSTVd-infected *N. benthamiana* plants expressing a ZYMV HC-Pro transgene. A = PCR to detect the PSTVd transgene in the progeny of genetic crossings; **+** = PSTVd positive control; M = DNA size marker; **B** = PCR to detect the HC-Pro transgene in progeny of genetic crossings; + = HC-Pro positive control; M = DNA size marker; **C** = Northern blot analysis to detect PSTVd siRNAs. The membrane was hybridized against a PSTVd cDNA to visualize the PSTVd siRNAs. 25S rRNA accumulation served as loading control. 1 = NbFRNK-PSTVd; 2 = Nb-PSTVd; 3 = NbFRNK

3.3 Cloning of the Hua enhancer (HEN1) gene from *Solanum lycopersicon*

According to an alignment of HEN1 gene sequences from different plant species (Section 2.2.1.25, Appendix A), two degenerate primers pairs (HEN1-PI-F/HEN1-PI-R and HEN1-P2-F/HEN1-P2-R, Table 2.6) were designed and the SlHEN1 cDNA was amplified from total *S. lycopersicon* RNA by RT-PCR. Amplification of the authentic sequence was confirmed by direct sequencing of PCR products.

In order to obtain the full-length SlHEN1 cDNA, three primers pairs HEN1-EcoRI-PI-F/HEN1-HindIII-PI-R, HEN1-HindIII-P2-F/HEN1-StuI-P2-R and HEN1-StuI-P3-F/HEN1-BamHI-P3-R (Table 2.6) were used. The three amplified fragments were directly cloned into the pJET1/2blunt and pTPCR cloning vectors. Recombinant plasmids were sequenced to confirm that they contained SlHEN1-specific sequences. The three fragments

were linked together and the full length SlHEN1 cDNA was obtained as an *EcoRI*/*BamHI* fragment. Subsequently, the SlHEN1 was cloned into the pPCV702SM and pGADT7 binary vectors.

3.3.1 Subcellular localization of HEN1

In *N. benthamiana*, subcellular localization of SlHEN1 was investigated by agroinfiltration-mediated transient expression of SlHEN1-GFP and SlHEN1-red fluorescent protein (RFP) fusion proteins. From *N. benthamiana* leaves infiltrated with *Agrobacteri*um strains carrying the pPCV702:HEN1-GFP and pPCV702:HEN1-RFP binary vector, protoplasts were produced 3 dpi. Examination of the protoplasts by fluorescence microscopy using a confocal laser-scanning microscope showed that the SlHEN1 was detectable in both, the nucleus and cytoplasm (Fig. 3.12).

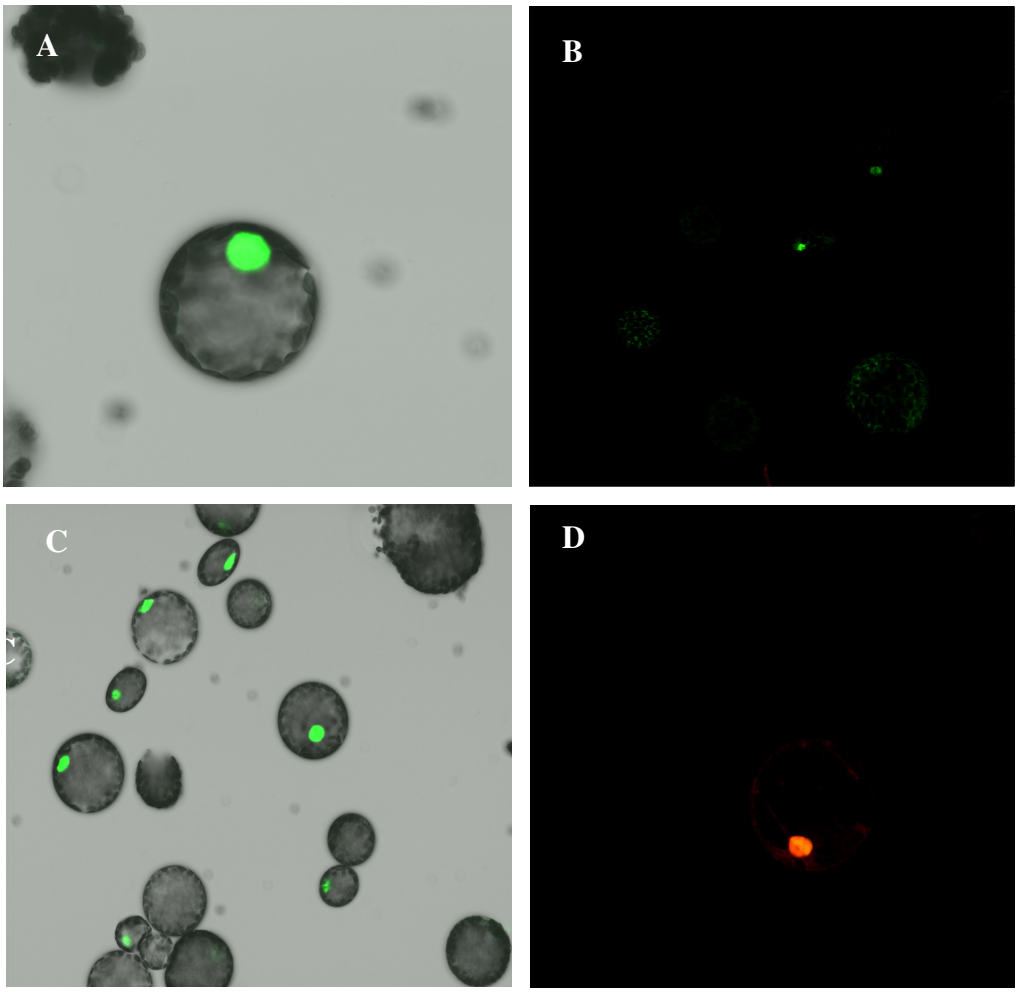

Figure 3.12: Examination by fluorescence microscopy of *N. benthamiana* protoplasts expressing HEN1. *N. benthamiana* leaves were infiltrated with *Agrobacterium* strains carrying the pPCV702:HEN1-GFP (A-C) and pPCV702:HEN1-RFP (D) binary vectors. Protoplasts were produced 3 dpi.

3.4 Protein–protein interaction analysis

Identification of interactions between viral and host proteins is essential to elucidate the molecular mechanisms that underlie the viral infection process and symptom development in plants. Shiboleth and co-workers (2007) reported that in squash, symptoms of ZYMV^{FINK} and ZYMV^{FRNK} infections began with subtle vein clearing on the first true leaf at 5 dpi. In ZYMV^{FRNK}-infected plants, symptoms progressed by time and at later stages. The plants became stunted and exhibited developmental abnormalities that were characterized by filamentous leaves displaying green islands. In contrast, ZYMV^{FINK}-infected plants were similar to healthy plants and exhibited only a few discernible symptoms, including faint discoloration and very slight fanlike folding along veins.

We proposed that differential interactions of HC-Pro^{FRNK} and HC-Pro^{FINK} with host proteins could explain the observed differences in symptom development. In order to investigate this hypothesis, we carried out *in vitro* protein-protein interaction analysis using HC-Pro$^{FRNK/FINK}$ and the two plant proteins, HEN1 and Argonaut 1 (AGO1) that are both involved in the RNAi pathway.

3.4.1 Expression and purification of recombinant ZYMV HC-Pro proteins

To obtain high amounts of purified and functional ZYMV HC-Pro, recombinant proteins were produced in *E. coli*. High-level expression of recombinant proteins in *E. coli* can result in the formation of insoluble aggregates (inclusion bodies). Füllgrabe and co-workers (2011) found that *E. coli*-expressed ZYMV HC-Pro proteins also accumulated mainly in inclusion bodies. To increase protein solubility, the ZYMV HC-Pro proteins were N-terminally fused to a maltose-binding protein (MBP). In addition, a HA-tag was introduced between the MBP and the ZYMV HC-Pro giving the MBP:HA-HC-Pro^{FRNK} and MBP:HA-HC-Pro^{FINK} proteins. Expression at 14^{o}C in the *E. coli* BL21 (DE3) codon plus strain for 16 h produced soluble MBP:HA-HC-Pro^{FRNK} and MBP:HA-HC-Pro^{FINK} proteins which were detectable by immunoblot assays using a monoclonal anti-HA and an anti-MBP antibody, respectively (Fuellgrabe *et al*., 2011).

According to the protein expression procedure described by Füllgrabe and co-workers, the MBP:HA-HC-Pro^{FRNK} and MBP:HA-HC-Pro^{FINK} were produced. In addition, the 53 kDa large MBP protein was expressed in *E. coli* and served as a negative control (see below). Western blot analysis of the purified MBP:HA-HC-Pro proteins with an anti-HA antibody indicated that the major 99 kDa band consisted of the full-length protein (Fig. 3.13). In addition to the full-length protein, some lower molecular mass fragments were immuno-

detected, probably representing proteolytic cleavage products of the MBP:HA-HC-Pro proteins.

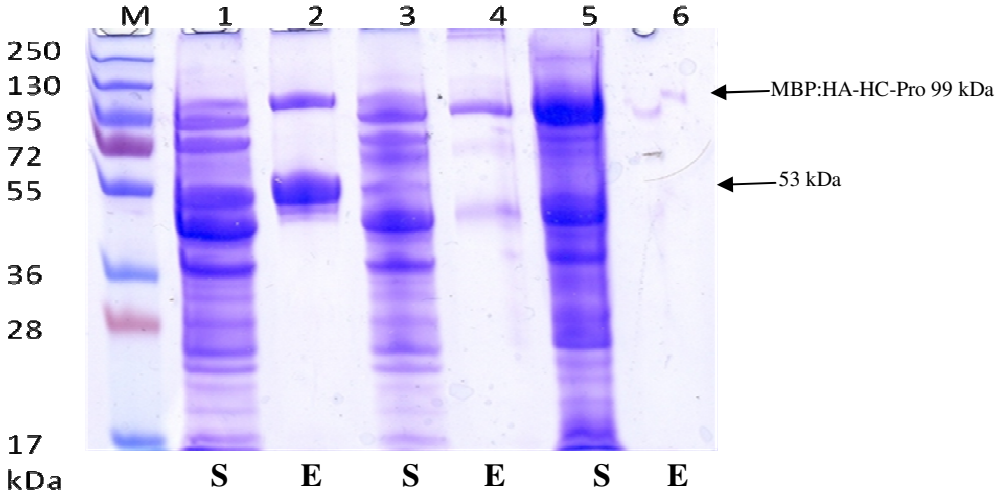

Figure 3.13: Analysis of the purified MBP:HA-HC-Pro fusion proteins by SDS-PAGE and Coomassie blue-staining. Lanes 1 and 2 = maltose binding protein (MBP); lanes 3 and 4 = MBP:HA-HC-Pro^{FRNK}; lanes 5 and 6 = MBP:HA-HC-Pro^{FINK}; M = pre-stained Protein Marker (www.fermentas.com); S = cell supernatant; E = eluate.

3.4.2 ZYMV HC-Pro – HEN1 binding assays

In order to demonstrate direct binding of the ZYMV HC-Pro proteins to AtHEN1, indirect enzyme-linked immunosorbent assays (ELISAs) were applied. A microtiter plate was coated with AtHEN1 (50 U) or with total bacterial soluble proteins as a negative control. Two µg of purified MBP:HA-HC-Pro^{FRNK} and MBP:HA-HC-Pro^{FINK} were added, respectively. MBP was used as negative controls for HC-Pro, while the total bacterial soluble proteins (non-induced BL21 (DE3) codon+) were used as negative controls for AtHEN1. Binding of MBP:HA-HC-Pro proteins to AtHEN1 or to total bacterial soluble proteins was detected using anti-MPB followed by anti-mouse AP detection. Plotting of the plates using a plate reader indicated that MBP:HA-HC-Pro proteins bound AtHEN1. However, MBP:HA-HC-Pro^{FRNK} appeared to bind slightly stronger than MBP:HA-HC-Pro^{FINK} (Fig. 3.14).

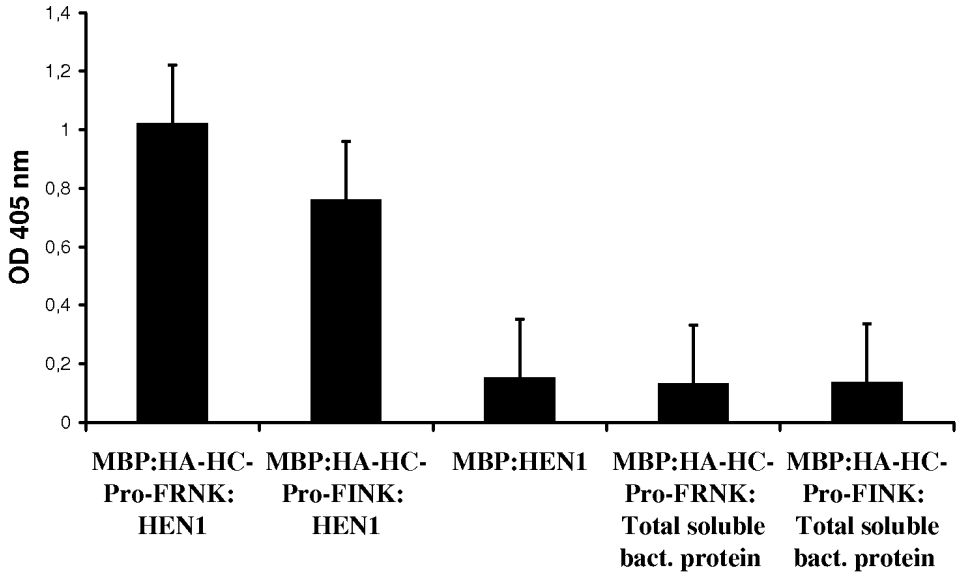

Figure 3.14: Enzyme-linked immunosorbent assays (ELISAs) to analyze interaction between MBP:HA-HC-Pro proteins and AtHEN1 *in vitro*. Bound MBP:HA-HC-Pro proteins were detected after incubation with anti-MBP followed by anti-mouse IgG-conjugated AP-mediated reaction using a plate reader at A405. Values are means of triplicate determination with SD represented by error bars reduced by the mean values of the negative control (MBP).

3.4.3 Epitope mapping of the MBP:HA-HC-Pro to identify the AtHEN1 binding domain

HC-Pro proteins can be schematically divided into three regions: an N-terminal region, a C-terminal region and a central region (Plisson *et al*., 2003). In order to identify the MBP:HA-HC-Pro domain that interacts with AtHEN1 deletions of the N- and C-termini of the MBP:HA-HC-Pro^{FRNK} were generated by site-directed mutagenesis. The MBP:HA:HC-Pro^{FRNK} ΔN2 and MBP:HA:HC-Pro^{FRNK} ΔN3 were generated by PCR using the primer pairs HC-Pro mut N2_F/HC-Pro mut N2_R and HC-Pro mut N3_F/HC-Pro mut N3_R. Restriction analysis using *SacI* was performed for the screening of positive clones resulting in MPB:HA-HC-Pro ΔN2 (comprising the deletion of residues 114 to 456) and MBP:HA-HC-Pro ΔN3 (comprising the deletion of residues 139 to 456) (Fig. 3.15). The generation of the C-terminal mutants, MBP:HA-HC-Pro ΔC7 (comprising the deletion of residues 1 to 322), MBP:HA-HC-Pro ΔC8 (comprising the deletion of residues 1 to 350) and MBP:HA-HC-Pro ΔC9 (comprising the deletion of residues 1 to 372) (Fig. 3.15) was conducted by PCR using the primer pair NcoI delete C-F/NcoI delete C-R. The proteins were produced in *E. coli* as described above and were subsequently analyzed by ELISA. Two micrograms of each protein fraction were used for a HEN1-binding assay. With the exception of MBP:HA-HC-Pro ΔC7, all other deletion mutants exhibited a strongly reduced AtHEN1 binding capacity (Fig. 3.15). Interestingly the MBP:HA-HC-Pro ΔC7 mutant, in which most of the C-terminus was deleted, showed strong binding to AtHEN1. This strong binding could be due to folding of the protein into a structure that would promote an efficient exposition of the domain

interacting with AtHEN1. The above experiments did not enable the identification of a specific binding domain at the amino acid level.

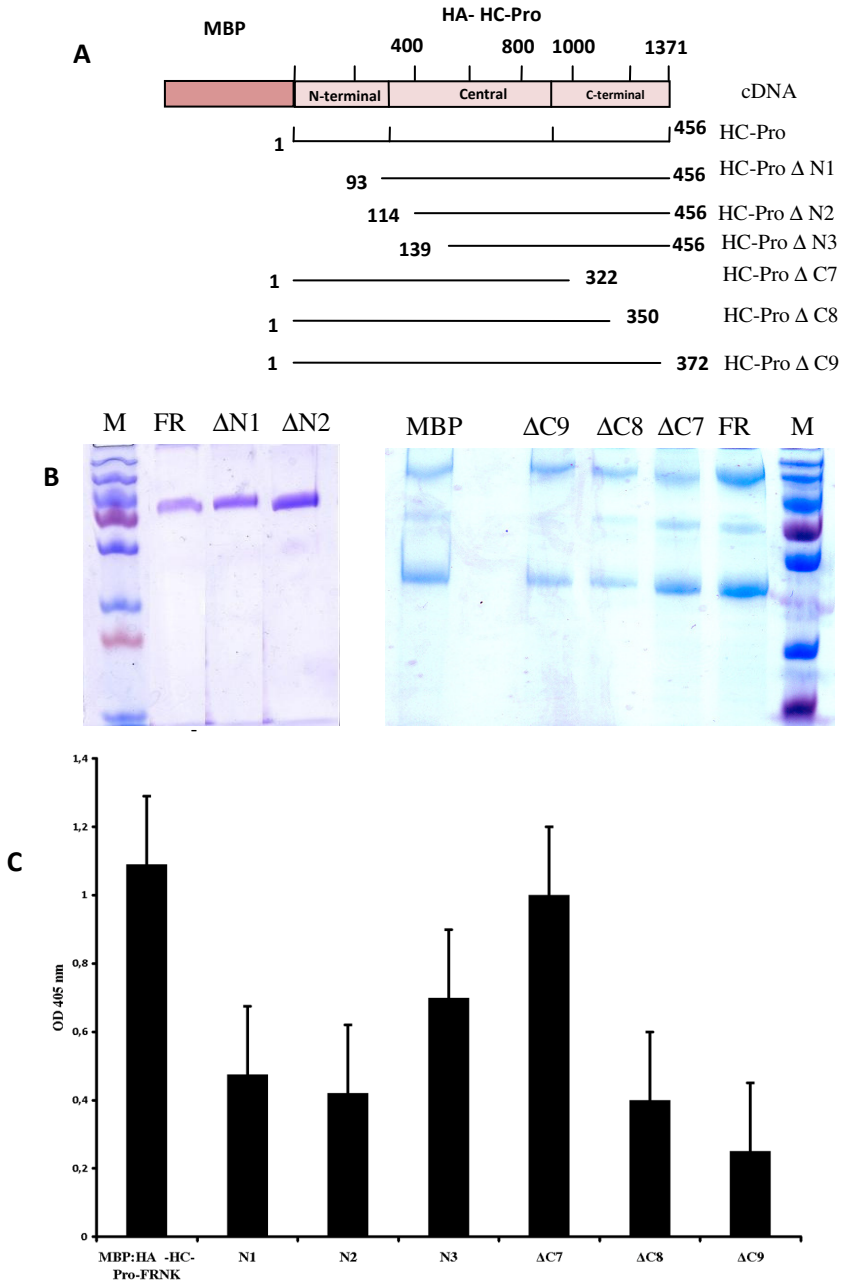

Figure 3.15: Epitope mapping of the HC-Pro to identify domains interacting with AtHEN1 using ELISA. A = Schematic representation of the MBP:HA-HC-Pro^{FRNK} map and of its deletion mutants. The cDNA of MBP:HA-HC-Pro^{FRNK} is indicated by the open box. The scale above the box shows the nucleotide positions. The N-, C-terminal and the central domains of the HC-Pro^{FRNK} are indicated. The full-length and truncated HC-Pro^{FRNK} proteins are presented as solid lines. **B** and **C** = Analysis of the purified MBP:HA-HC-Pro fusion proteins by SDS-PAGE. The purified proteins were subjected to 9% SDS PAGE and the gel was stained with Coomassie blue to show that all proteins were efficiently expressed and purified. M = Protein size marker; FR = MBP:HA-HC-Pro^{FRNK}; ΔN = N-terminal deletions; MBP = Maltose binding protein; ΔC = C terminal deletion. M = pre-stained Protein Marker (www.fermentas.com). **C** = Analysis of the binding activities between AtHEN1 and the N-terminal (ΔN1–ΔN3) and the C-terminal deletion mutants (ΔC7–ΔC9) of MBP:HA-HC-Pro^{FRNK}. Bars in Figure 2D represent the mean of triplicate determinations deducted by SD of the mean value of the negative control (MBP).

3.4.4 Methyltransferase inhibition assay

HEN1 has an S-adenosyl methionine (SAM)-binding pocket and catalyzes 3´-terminal 2´-O-methylation of sRNAs by transferring a methyl group from SAM to the 2'-OH or 3'-OH group of the last nucleotide of miRNA/miRNA* duplexes produced by the nuclease Dicer (Yang *et al*., 2006). This methylation prevents uridylation and subsequent degradation of sRNAs (Li *et al*., 2005).

Our ELISA revealed that MBP:HA-HC-Pro$^{FRNK/FINK}$ can bind to AtHEN1. To test whether this binding inhibits the methyltransferase activity of HEN1 *in vitro*, a methyltransferase inhibition assay was performed. In such an assay, incorporation of ^{14}C-labeled methyl groups into the 3´-end of RNA templates can be detected (Kurth and Mochizuki, 2009). Purified MBP:HA-HC-Pro$^{FRNK/FINK}$ and the truncated proteins MBP:HA-HC-Pro ΔN1 and MBP:HA-HC-Pro ΔC9 were incubated with AtHEN1. To exclude that possible contaminations of the protein preparation, including a co-purified 55 kDa protein, inhibit AtHEN1 activity total soluble bacterial proteins were included in the assay. Subsequently, a synthetic miRNA duplex of 22 bp whose 3´-ends carried a 2´-hydroxyl and SAM [methyl-^{14}C] were added. The methyltransferase inhibition assay showed that MBP:HA-HC-Pro$^{FRNK/FINK}$ clearly inhibited AtHEN1 activity *in vitro* (Fig. 3.16). The total bacterial extracts did not inhibit the AtHEN1 activity. This indicated that no interaction between bacterial proteins and AtHEN1 occurred. This result also argued against any interference of putative protein contaminants with AtHEN1.

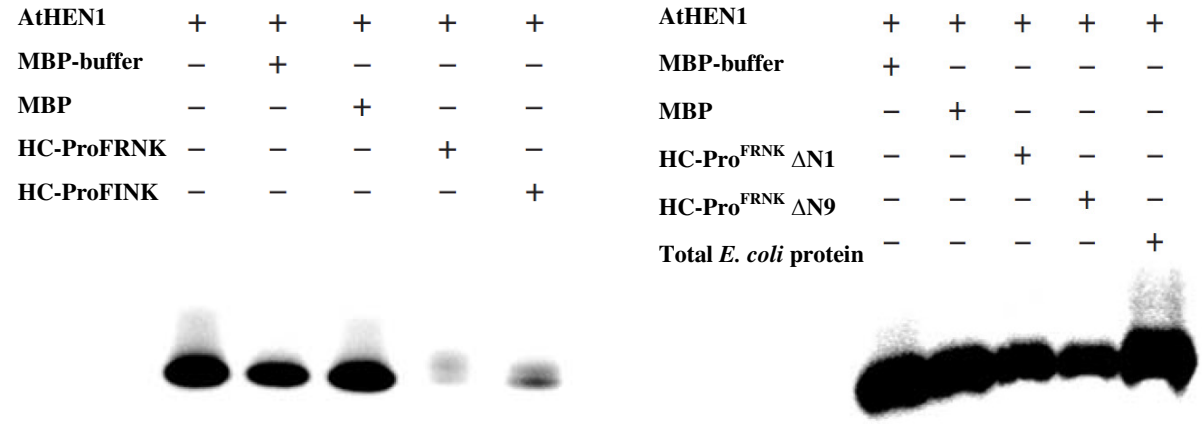

Figure 3.16: Methyltransferase inhibition assay. The methyltransferase inhibition assay was carried out to analyse whether the ZYMV HC-Pro interferes with the activity of AtHEN1. Hc-Pro proteins (MBP:HA-HC-Pro^{FRNK} and MBP:HC-Pro^{FINK}), ΔN1 (N-terminal deletion of MBP:HA-HC-Pro^{FRNK}), ΔC9 (C-terminal deletion of MBP:HA-HC-Pro^{FRNK}), MBP and total soluble bacterial proteins (non-induced BL21(DE3) codon+) as negative controls were mixed with miR173 duplex, AtHEN1 and S-adenosyl-L-[methyl-14C] methionine and incubated for 1 h at 37°C. RNA samples were separated using 20% TBE-polyacrylamide gels. The gels were dried and scanned using PharosFX Plus PhosphorImager.

3.4.5 Cloning of the Argonaute 1 (AGO1) cDNA from *N. benthamiana*

The coding sequence of the *N. benthamiana* AGO1 (NbAGO1) cDNA was generated by RT-PCR using four specific primers, AGO1-EcoRI-P1-F/AGO1-EcoRI-P1-R and AGO1-EcoRI-P2-F/AGO1-BamHI-P2-R (Table 2.6). Reverse transcription reactions were performed with total RNA from *N. benthamiana*. The two PCR products were cloned into the pJET1.2/blunt cloning vector and the corresponding inserts were sequenced. After confirmation of the authentic sequences, the 3' fragment was cloned in the pGADT7 binary vector into the *EcoRI* and *BamHI* sites. After confirmation of the cloning, the 5' fragment was ligated to the 3' fragment into the *EcoRI* site producing pGADT:NbAGO1 plasmid. Following this cloning strategy the NbAGO1 coding region was in frame with the GAL4-DNA activation domain of the pGADT7 yeast expression vector. The corresponding pGADT:NbAGO1 plasmid was used as prey in the yeast-two hybrid system.

3.4.6 The Yeast Two – Hybrid System

Using a yeast two-hybrid system eight tobacco proteins interacting with the Tobacco etch viral (TEV) Hc-Pro were identified (Anandaklakshmi *et al*., 2000). In this work, the yeast two-hybrid approach was accordingly carried out to investigate if the ZYMV HC-Pro^{FRNK} and ZYMV HC-Pro^{FINK} interact with HEN1 or AGO1.

3.4.6.1 Expression of SlHEN1 and NbAGO1 in yeast

In order to express the SlHEN1 and NbAGO1 in yeast cells, the corresponding cDNAs were inserted into the yeast GAL4 activation domain vector pGADT7 as preys. The resulting pGADT:SlHEN1 and pGADT:NbAGO1 vectors were transformed into the yeast Y187 strain. Successful transformation was validated by PCR analysis using specific primers for HEN1 and AGO1, respectively. In addition, Western blot analysis was applied to demonstrate that the proteins were indeed expressed in yeast.

3.4.6.2 Expression of HC-Pro$^{FRNK/FINK}$ in yeast

To examine physical interactions of HC-Pro$^{FRNK/FINK}$ with SlHEN1 or NbAGO1, the coding sequence of HC-Pro^{FRNK} and HC-Pro^{FINK} were fused with the GAL4 DNA-binding domain of the pGBKT7 vector as baits. In addition, the HC-Pro$^{FRNK/FINK}$ cDNAs were inserted into the yeast GAL4 activation domain vector to check any putative HC-Pro self interaction (dimerization).

The coding region of ZYMV HC-Pro$^{FRNK/FINK}$ were generated by PCR using the primers HC-Pro -Y2H NdeI-F and HC-Pro -Y2H XmaI-R (Table 2.6). The resulting plasmids (pGBKT:HC-Pro$^{FRNK/FINK}$ and pGADT:HC-Pro$^{FRNK/FINK}$) were checked by restriction analysis using *NdeI* and *XcmI*. After cloning into *E. coli*, the vectors were isolated and transformed into the yeast Y2H gold strain and the yeast 187 strain, respectively. DNA from selected transformants was extracted and PCR analysis was carried out using the primers Hc-Pro-int-seq-F and HC-Pro -Y2H XmaI-R (Table 2.6) to validate the presence of the corresponding plasmids. Positive yeast clones were checked for expression of the HC-Pro proteins using Western blot analysis.

3.4.6.3 Western blot analysis and Chemiluminescence Immuno Detection

In the pGADT7 and pGBKT7 vectors, recombinant proteins are fused to a HA-tag and a Myc-tag, respectively. Thus, the yeast-expressed proteins could be detected by Western blot analysis using HA- or Myc-specific antibodies. Western blot analysis revealed that the HC-Pro$^{FRNK/FINK}$ proteins were expressed in both yeast strains and the NbAGO1 protein was expressed in the yeast 187 strain (Fig. 3.17). For unknown reasons, the SlHEN1 protein was not detectable by Western blot analysis.

3.4.6.4 HC-Pro self interaction and interaction of HC-Pro with NbAGO1

After selection of positive yeast transformants and validation of protein expression by Western blot analysis, mating between different strains was carried out. Although our ELISA indicated *in vitro* interaction between HC-Pro proteins and AtHEN1, SlHEN1 was excluded from mating experiments, because we were not able to confirm the expression of SLHEN1 in yeast cells.

For mating, single colonies of the yeast Y2H gold and 187 strains expressing the recombinant proteins were picked and placed in a single 2 ml centrifuge tube containing 2X YPDA. The tubes were incubated overnight. Next day, the cultures were examined under the microscope to monitor budding of yeast cells which indicates mating between the strains. The mated yeast strains were then cultured on different medium to examine protein-protein interactions (Table 3.2). All mated strains were able to grow on SD-Leu/Trp or /-Leu-Trp medium which indicates that the mating took place. Y2H gold strain detection demonstrated that only the positive control and *S. cerevisiae* cells carrying the pGBKT:HC-Pro^{FRNK} and pGADT:HC-Pro^{FRNK} plasmids grew on SD/-Leu/-Trp/-His/-Ade/X-a-gal and the colonies turned blue, suggesting that the full-length ZYMV HC-Pro^{FRNK} protein interacted with itself. In other words, the DNA-binding domain and activation domain were brought into sufficient

proximity to drive the transcription of the reporter genes (ADE2, HIS3, lacZ, and MEL1) that allowed the yeast to grow on SD/-Ade/-His/-Leu/-Trp (Fig. 3.18). AGO1 did not interact with HC-Pro$^{FRNK/FINK}$. Mates could not restore auxotrophy in the yeast cells (i.e., transformants were able to grow on SD/-Leu/-Trp but not on SD/-Ade/-His/-Leu/-Trp) (Fig. 3.18). pGBKT7-53 and pGADT7-T were mated as positive controls, while pGBKT7-Lam+ and pGADT7-T were mated as negative controls; the mated transformants were selected on different media (Table 3.2).

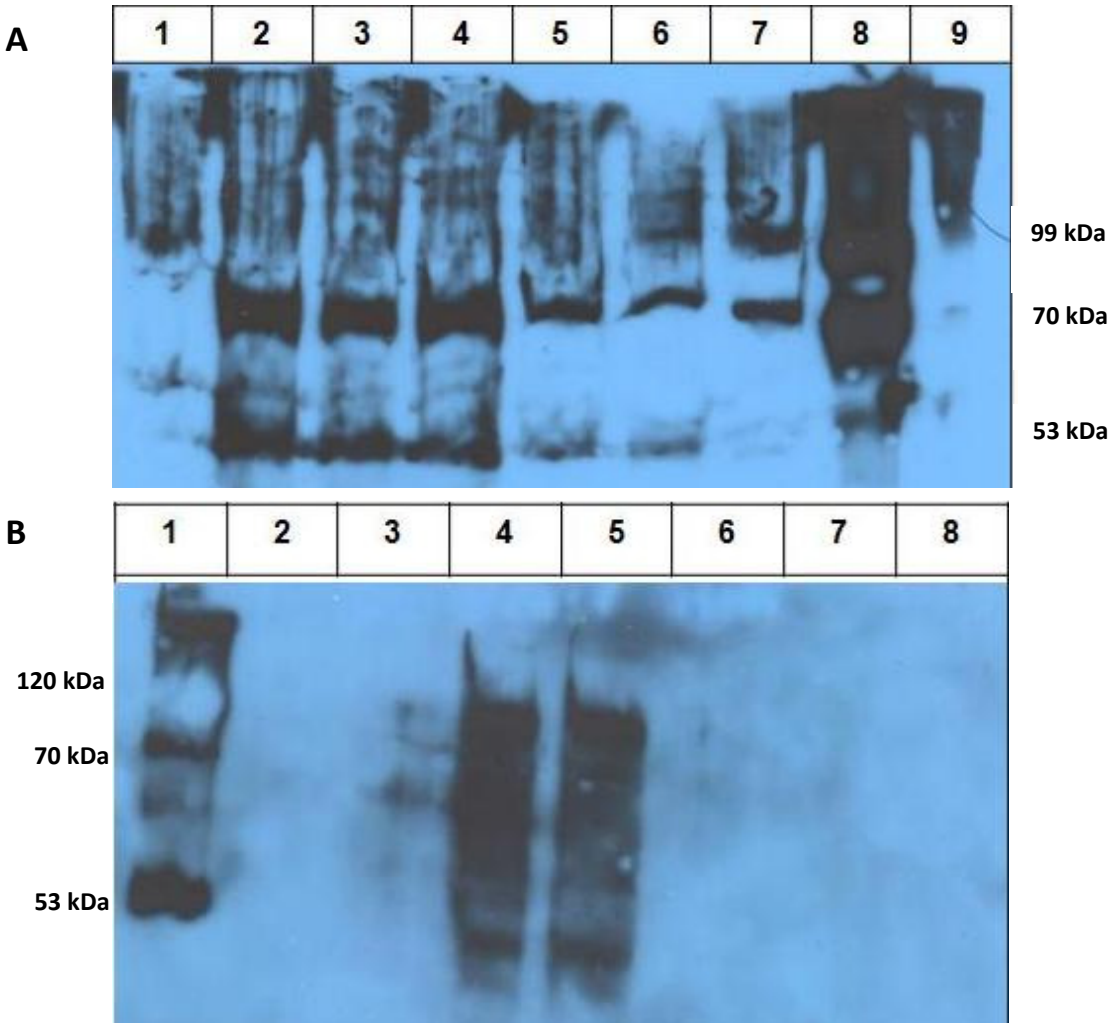

Figure 3.17: Detection of HC-Pro and NbAGO1 proteins by Western blot analysis. Yeast cell cultures were grown at 30°C to an OD600 of approximately 0.5. Total protein samples were separated by 12%SDS-PAGE. Proteins were transferred onto a PVDF membrane. The membrane was incubated with a polyclonal rabbit anti ZYMV-HC antiserum (1:10,000), and then with the AP-IgG anti-rabbit conjugated Hc-Pro anti serum. **A** = Detection of HC-Pro proteins: the Hc-Pro protein was visualized with an anti-rabbit IgG antibody (1:1000) conjugated to horseradish peroxide together with enzyme substrate. **1** = non transformed yeast cells (Y2H); **2-4** = HC-Pro^{FRNK}; **5-7** = HC-Pro^{FINK}; **8** = positive control; **9** = yeast cells transformed with an empty vector (negative control). **B** = Detection of NbAGO1 and SlHEN1 proteins using anti HA-POD (1:1000). **1** = positive control; **2** = yeast cells transformed with an empty vector (negative control); **3** = blank; **4-5** = pGADT:NbAGO1; **6-7** = pGADT:SlHEN1; **8** = non transformed yeast cells (Y187).

Table 3.2: Mating between yeast strains with bait and prey vectors.

No.	Mated strains	Dilution	Selection medium						
			SD-Leu	SD-Trp	DDO	QDO	DDO X-α-Gal /AbA	QDO X-α-Gal/AbA	Conclusion
1	pGBKT7-53 + pGADT7-T	1:10	+	+	+	+	+	+	Positive control mating with interaction
		1 - 100	+	+	+	+	+	+	
2	pGBKT7-Lam + pGADT7-T	1:10	+	+	+	-	-	-	Negative control mating without interaction
		1 - 100	+	+	+	-	-	-	
3	pGBKT:HC-Pro^{FRNK} + pGADT:HC-Pro^{FRNK}	1:10	+	+	+	+	+	+	HC-Pro^{FRNK} self interaction (dimerization)
		1 - 100	+	+	+	+	+	+	
4	pGBKT:HC-Pro^{FINK} + pGADT:HC-Pro^{FINK}	1:10	+	+	+	-	-	-	Mating without interaction
		1 - 100	+	+	+	-	-	-	
5	pGBKT:HC-Pro^{FRNK} + pGADT:NbAGO1	1:10	+	+	+	-	-	-	Mating without interaction
		1 - 100	+	+	+	-	-	-	
6	pGBKT:HC-Pro^{FINK} + pGADT:NbAGO1	1:10	+	+	+	-	-	-	Mating without interaction
		1 - 100	+	+	+	-	-	-	
7	pGBKT7 + pGADT:HC-Pro^{FRNK}	1:10	+	+	+	-	-	-	Mating without interaction
		1 - 100	+	+	+	-	-	-	
8	pGBKT7 + pGADT:HC-Pro^{FINK}	1:10	+	+	+	-	-	-	Mating without interaction
		1 - 100	+	+	+	-	-	-	

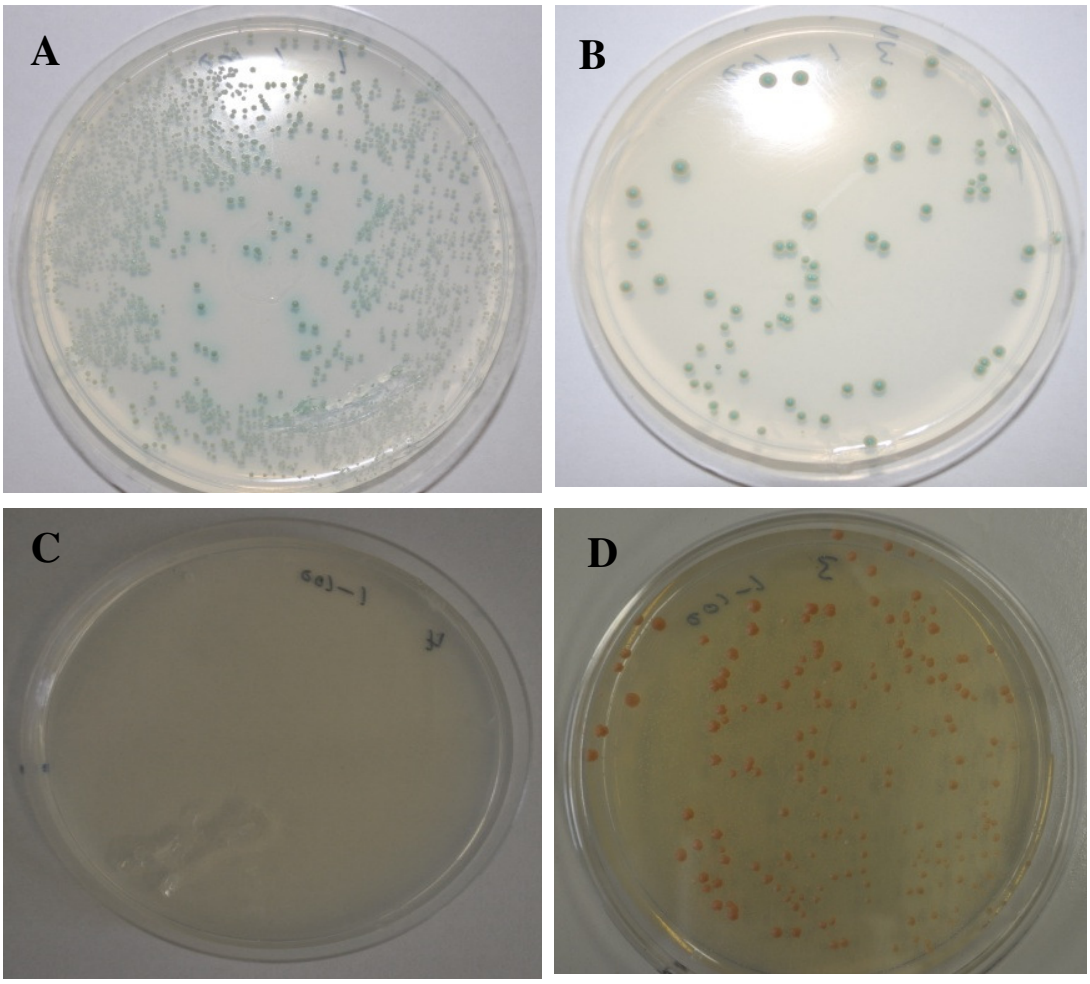

Figure 3.18: Interaction of HC-Pro^{FRNK} in transformed *S. cerevisiae*. **A** = pGBKT7-53 and pGADT7-T mated cells grown on SD/-Ade/-His/-Leu/-Trp/X-α-Gal/AbA (Positive control); **B** = pGBKT:HC-Pro^{FRNK}/pGADT:HC-Pro^{FRNK} grown on SD/-Ade/-His/-Leu/-Trp/X-α-Gal/AbA; **C** = pGBKT:HC-Pro^{FINK}/pGADT:HC-Pro^{FINK} grown on SD/-Ade/-His/-Leu/-Trp/X-α-Gal/AbA; **D** = pGBKT:HC-Pro^{FRNK}/pGADT:HC-Pro^{FRNK} grown on SD/-His/-Leu/-Trp/X-α-Gal/AbA.

4. Discussion

4.1 Subcellular Localization of the ZYMV HC-Pro

The HC-Pro protein is known to play multiple roles in the viral infection cycle (Maia *et al*., 1996). Some of these functions have been mapped to different regions of the protein. The C-terminus is a papain-like proteinase that catalyses autoproteolytic cleavage from the polyprotein and plays a role in virus cell-to-cell movement (Urcuqui-Inchima *et al*., 1999, 2000; Carrington *et al*., 1989; Vargason *et al*., 2003). In this study, we investigated the subcellular location of the ZYMV HC-Pro wild type protein (HC-Pro^{FRNK}) and its mutant HC-Pro^{FINK} in plant cells. In order to enable monitoring of the subcellular location of HC-Pro proteins, they were expressed as N- and C-terminal GFP fusions. To evade the autoproteolytic cleavage of HC-Pro from its C-terminus, a time course protein extraction was carried out after transient expression of the HC-Pro in *N. benthamiana* plants. It was analyzed at which time (dpi) the processing of the full-length HC-Pro-GFP fusion proteins has not efficiently proceeded.

Immunological studies carried out by different researchers (Baunoch *et al*., 1990; De Mejia *et al*., 1985) had shown the association of the Tobacco vein mottling virus (TVMV) and PVY HC-Pro proteins with proteins from the amorphous inclusions. The detection analysis of the HC-Pro of 19 potyviruses has demonstrated that the HC-Pro of TVMV, Plum pox virus (PPV), Pepper mottle virus (PepMV) and Papaya ringspot virus (PRSV) were labeled in amorphous inclusions, the HC-Pro of Bidens mottle virus (BiMoV) was only distributed in cytoplasmic inclusions, the HC-Pro of *Clover yellow vein virus* (CIYVV) and Bean yellow mosaic virus (BYMV) were labeled in pinwheel inclusions, while the HC-Pro of Beet mosaic virus (BtMV) and TEV were only present in nuclear inclusions (Riedel *et al*., 1998). The HC-Pro of Cowpea aphid-borne mosaic virus (CABMV) was diffusely distributed throughout the cytoplasm (Mlotshwa *et al*., 2002). Here we showed that the ZYMV HC-Pro had a diffuse cytoplasmic localization and formed aggregates along the ER (Fig. 3.2). Our results are similar to what was reported for the localization of the TuMV HC-Pro (Zheng *et al*., 2011).

HC-Pro of potyviruses appears to act as a link between virions and aphid mouthparts (Govier and Kassanis, 1974). Potyviruses are transmitted by aphids that feed on the plants and virions can be rapidly adsorbed by aphids and are then released into different plant cells. A model termed the ’bridge’ hypothesis (Pirone and Blanc, 1996) is commonly accepted to explain the mode of action of HC-Pro. The hypothesis describes these nonstructural proteins as molecules capable of engaging two types of interactions: one with the virus CP and the

other with a putative receptor in the vector's mouthparts. HC-Pro acts as a 'bridge' between the aphid and the virus particle which makes it reasonable to assume that HC-Pro would be abundant in the cytoplasm of infected plant cells (Zheng *et al*., 2011). HC-Pro is also involved in virus movement and most viral movement proteins are targeted into the ER (Vogel *et al*., 2007; Samuels *et al*., 2007; Peremyslov *et al*., 2004). The association of ZYMV HC-Pro with the ER may reflect its function in virus movement.

4. 2 Expression of the ZYMV HC-Pro Silencing Suppressors in *N. benthamiana* and *A. thaliana* Plants: their Effects on Plant Development

It is well known that the expression in plants of viral RSS, encoded by different and unrelated RNA and DNA viruses, led to strong developmental defects. In these transgenic plants, the strength of developmental abnormalities was positively correlated with the degree of expression of the RSS (Mallory *et al*., 2002; Kasschau *et al*., 2003; Chapman *et al*., 2004; Dunoyer *et al*., 2004; Mlotshwa *et al*., 2005; Wu *et al*., 2010). In recent years, the interactions of different suppressors with the RNA silencing pathways have been intensively studied (Lakatos *et al*., 2006; Lewsey *et al*., 2007; Yaegashi *et al*., 2007; Zhang *et al*., 2006; Csorba *et al*., 2010). Data from these studies indicate that these interactions are very complex and vary between different suppressor-host combinations. Most of the experimental work has been done in *A. thaliana* and *N. benthamiana*. Thus, it is not clear whether the observed interactions are general phenomena or whether they are specific for the plant species analyzed.

HC-Pro has been extensively studied. Transgenic *A. thaliana, N. benthamiana* and *N. tabacum* harboring either the HC-Pro gene or the P1/HC-Pro gene from different potyviruses were produced (Anandalakshmi *et al*., 2000; Carrington *et al*., 1990; Chapman *et al*., 2004; Dunoyer *et al*., 2004; Kasschau *et al*., 2003; Mallory *et al*., 2001, 2002; Mlotshwa *et al*., 2002, 2005; Shams-Bakhsh *et al*., 2007; Wu *et al*., 2010; Siddiqui *et al*., 2008). In this study, we analyzed and compared if stable expression of the ZYMV HC-Pro produces symptoms. *N. benthamiana* and *A. thaliana* plants were stably transformed with ZYMV HC-Pro^{FRNK} (HC-Pro^{FRNK}) and ZYMV HC-Pro^{FINK} (HC-Pro^{FINK}) transgene constructs possessing and lacking sRNA-binding activity, respectively, and with both transgene constructs fused to a nuclear localization signal (NLS) (NLS-HC-Pro^{FRNK} and NLS-HC-Pro^{FINK}). The ZYMV HC-Pro lacking the P1 was expressed. The P1 protein is considered as a 'mysterious' protein, and its function during virus life cycle has not yet been elucidated (Valli *et al*., 2006). HC-Pro and the P1-related proteins do not share any apparent sequence similarity, but both proteins have protease and RNA binding activity (Rohozkova and Navratil, 2011).

Similar to the expression of other potyviral suppressors in *Arabidopsis*, HC-Pro^{FRNK} caused severe malformations in *A. thaliana*. In contrast, only negligible phenotypic changes were monitored in one transgenic *N. benthamiana* line. HC-Pro^{FINK} did not produce obvious phenotypes in *A. thaliana* plants. Occasionally, reduced numbers of seed sets were observed. If at all, only minimal phenotypic changes were found in *N. benthamiana* plants (Table 3. 1). In *N. benthamiana* and *N. tabacum* plants producing the HC-Pro proteins of PVY-N or PVA, no phenotypic alterations were detected (Mlotshwa *et al*., 2002; Shams-Bakhsh *et al*., 2007; Soitamo *et al*., 2011). However, severe malformations were reported for *N. tabacum* expressing the TEV HC-Pro (Anandalakshmi *et al*., 2000). On the other hand, in transgenic tobacco plants generated by Carrington and co-workers (1990) and by Mallory and co-workers (2001, 2002), no phenotypes were produced by the expression of TEV HC-Pro. A comparative study was carried out by expressing five RSS in *N. benthamiana* and *N. tabacum* plants. Among these suppressors the PVY HC-Pro caused the most striking phenotypes throughout three consecutive generations in both, *N. benthamiana* and *N. tabacum* (Siddiqui *et al*., 2008). Phenotypes caused by this transgene include bending and twisting of the stems, causing a creeping growth habit, the leaves were strongly rolled and hairy, with elongated vein organization. Flowers had very short petals and stamens and protruding pistils, and were sterile. In the HC-Pro-expressing plants, different or lack of phenotypes may be due to variations in the HC-Pro-coding sequences between different potyviruses (Flasinski and Cassidy, 1998) or to different expression levels of the protein in different plants (Siddiqui *et al*., 2008). In our study, HC-Pro-associated phenotypes differed between *A. thaliana* and *N. benthamiana*. This may indicate that the effects of HC-Pro are, at least to some extent, species specific.

This is the first report describing the expression of the ZYMV HC-Pro fused to a NLS sequence. Transgenic *A. thaliana* and *N. benthamiana* lines expressing the NLS-HC-Pro^{FRNK} and NLS-HC-Pro^{FINK} displayed clear phenotypes, including curled leaves, stunting and malformed flowers mainly in *A. thaliana* lines producing NLS-HC-Pro^{FRNK}. Flower malformations were caused by NLS-HC-Pro^{FRNK} and NLS–HC-Pro^{FINK} only in *A. thaliana*. However, seed set was severely reduced in both, *A. thaliana* and *N. benthamiana.* It is worth noting that some phenotypes caused by NLS-HC-Pro were similar to those described for TuMV P1/HC-Pro transgene-expressing *Arabidopsis* (Chapman *et al*., 2004; Dunoyer *et al*., 2004; Kasschau *et al*., 2003; Mlotshwa *et al*., 2005). The P1 protein has a nuclear localization signal (Mukherjee *et al*., 2004). Thus it is expected that the P1 targets the HC-Pro into the nucleus when expressed as a P1/HC-Pro fusion protein. Targeting HC-Pro to the nucleus, either by the P1 protein or by the NLS, enable HC-Pro to be close to host proteins involved in

the silencing machinery, including HEN1 DCL1, and AGOs, and thus, it can physically interact with these proteins and either enhances or suppresses their activities. The development of symptoms in NLS-HC-Pro^{FINK} expressing plants was in accordance with our working hypothesis in which we proposed that targeting of HC-Pro^{FINK} to the nucleus would produce symptoms. HEN1 inhibition in the nucleus may affect miRNA function because miRNAs in contrast to siRNA are likely to be methylated in the nucleus

In the silencing suppressor-expressing plants, the development of phenotypes is likely due to the interference of these suppressors with the endogenous RNA silencing pathways. Previously, it has been reported that viral suppressors interfere with miRNA biosynthesis in *Arabidopsis* thereby inhibiting the cleavage of their target genes (Alvarez *et al*., 2006; Chapman *et al*., 2004; Dunoyer *et al*., 2004; Kasschau *et al*., 2003; Millar and Gubler, 2005). Such interference may target an early step in the silencing pathways and would impair the regulation of multiple miRNA-regulated target genes. Among the known miRNA-regulated genes are the AP2, ARF8 and the ARF10 transcription factors. They are specifically expressed in inflorescence or leaves and are involved in differentiation (Chapman *et al*., 2004; Dunoyer *et al*., 2004; Kasschau *et al*., 2003; Mallory *et al*., 2002; Park *et al*., 2002). However, there is emerging evidence suggesting that the observed phenotypic changes are largely independent of the miRNA pathway (Mlotshwa *et al*., 2005; Diaz-Pendon and Ding, 2008; Diaz-Pendon *et al*., 2007). The data of Endres and coworkers (2010) support this notion; they reported that the ethylene-inducible transcription factor RAV2 is required by two unrelated RSS proteins, HC-Pro of TuMV and P38. It was shown that both viral suppressors require RAV2 to block the activity of primary siRNAs, whereas suppression of transitive silencing is RAV2-independent. Their observations indicated that RAV2 is required for HC-Pro-mediated flower and fertility defects and contributes to the defects in plant size and leaf shape. On the other hand, no difference in miRNA/miRNA* levels were detected in HC-Pro plants in the presence and absence of RAV2. In all cases, the levels of miRNA and miRNA* were independent of RAV2. These results indicate that RAV2 is not required for the HC-Pro-associated developmental defects in miRNA biogenesis. This finding argues against a causative role for miRNAs in most HC-Pro-associated morphological anomalies (Endres *et al*., 2010). However, it seems that HC-Pro-associated phenotypes are more likely related to HC-Pro interference with miRNA biogenesis, no obvious phenotypes were detected in transgenic plants expressing HC-Pro^{FINK}, which lost its sRNA binding activity.

In plants, miRNAs are an important class of endogenous non-coding sRNAs. They play fundamental roles in development by controlling the expression of transcription factors, mainly at the post-transcriptional level (He and Hannon, 2004). Numerous studies with transgenic *N.*

tabacum and *A. thaliana* plants expressing P1/HC-Pro transgene constructs from TEV and TuMV respectively, showed that the presence of P1/HC-Pro proteins leads to an increase in the amounts of miRNA and miRNA target sequences. Expression of HC-Pro did not only change the levels of miRNAs but it also affected miRNA activity. (Mallory *et al*., 2001; Moltshwa *et al*., 2005). These results suggested sequestering of the miRNA duplexes which would prevent their incorporation into RISC. This in turn could influence plant development by affecting miRNA-mediated gene regulation. Thus, the appearance of symptoms could be the result of RSS expression through either viral infection or stable expression (Kasschau *et al*., 2003; Palatnik *et al*., 2003).

Our Northern blots analysis revealed that not all of the selected miRNAs were detectable under the applied conditions (data not shown). However, in the transgenic *N. benthamiana* plants, enhanced accumulation of miR168 and miR159C was found when compared to *N. benthamiana* wild type. Importantly, in ZYMV HC-Pro^{FRNK}- and ZYMV HC-Pro^{FINK}–expressing lines, no significant difference in miR168 and miR159C levels were detectable, both the wild type FRNK and its mutant FINK accumulate almost equal levels of these miRNAs. Our results are in accordance with Wu and co-workers (2010) who reported high accumulation of different miRNAs including miR168 and miR159C in *A. thaliana* lines expressing ZYMV-P1-HC-Pro wild type and diverse ZYMV-P1-HC-Pro mutants. In their experiments, the FINK mutant still retains some activity to suppress miRNA- and ta-siRNA-mediated gene regulation (Wu *et al*., 2010).

ZYMV-infection mainly leads to accumulation of the miR- and the corresponding miR*-strands (Shiboleth *et al*., 2007). MiRNA accumulation appeared to differ between transgenic and virus-infected plants. One reason for this observation could be that plants with different miRNA levels were used (Ehrenreich and Purugganan, 2008). Another consideration is the influence of the P1 protein on the activity of HC-Pro. It has been reported that P1 exerts a reinforcing effect on HC-Pro. It was suggested that this protein acts as a helper protein, improving the expression of the viral genome. On the other hand, P1 could subdue the defense activities of the host plant. P1 has been shown to enhances the RSS activity of HC-Pro when both protein are expressed as a polyprotein (Pruss *et al*., 1997; Rajamaki *et al*., 2005; Valli *et al*., 2006). This would explain the strong effect of the P1/HC-Pro-protein on miRNA accumulation in transgenic or in virus-infected plants. It is possible that in these systems, P1 increases the effect of the HC-Pro and leads to increased miRNA levels by sequestration, thus rendering them inactive and preventing their incorporation into RISC. On the other hand, as mentioned above P1 may target the HC-Pro into the nucleus. In

the nucleus, interference of HC-Pro with miRNA biosynthesis, stability and/or function could be more effective than interference in the cytoplasm.

4.2.1 Functionality of suppressor proteins in transgenic plants

In the highly conserved FRNK box of HC-Pro, a point mutation changing FRNK into FINK resulted in attenuated symptoms in infected host plants. The virus titer, HC-Pro levels and viral siRNA accumulation were similar for the severe (FRNK) and attenuated (FINK) strains. The same mutation in the TEV, TuMV and PVY HC-Pro proteins, however, led to complete loss of the RSS activity in *Agrobacterium*-mediated infiltration experiments of *N. benthamiana*. Moreover, these virus mutants lost infectivity (Gal-On and Raccah, 2000; Shiboleth *et al*., 2007).

In this study, transient expression assays were carried out to verify the functionality of the silencing suppressor activity of HC-Pro^{FRNK} and HC-Pro^{FINK} using transgenic *N. benthamiana* plants. Independent transgenic lines expressing HC-Pro^{FRNK} and HC-Pro^{FINK} were agroinfiltrated with a binary vector harboring a GFP transgenes construct or were co-infiltrated with binary vectors containing a GFP and a GpG (GFP IR) transgene construct. Infiltration of wild type *N. benthamiana* plants was used as a control. Transient expression of GFP in HC-Pro transgenic plants maintained high levels of green fluorescence at 4 and 9 dpi indicating HC-Pro-mediated suppression of GFP silencing. The fact that in the silencing assay, HC-Pro^{FINK}-expressing plants sustained GFP expression indicated that it had not lost its suppressor activity.

From our results it was clear that the HC-Pro^{FRNK} and HC-Pro^{FINK} proteins can be expressed in *N. benthamiana* plants without triggering morphological alterations. Thus, these transgenic *N. benthamiana* plants may serve as a system to over-express transgenes.

4.2.2 HC-Pro$^{FRNK/FINK}$ have no effect on Rgs-Cam levels in *N. benthamiana*

A calmodulin–related protein, the rgs-CaM (regulator of gene silencing-calmodulin-like protein), was shown to interact with TEV HC-Pro using the yeast two-hybrid system (Anandalakshmi *et al*., 2000). It was observed that rgs-CaM mRNA was expressed at low levels in leaves and flowers and at higher levels in stem and roots. In *N. tabacum*, rgs-CaM was induced upon stable expression of the TEV HC-Pro or upon TEV infection (Anandalakshmi *et al*., 2000). Based on these findings it was suggested that HC-Pro directly or indirectly controls rgs-CaM mRNA levels. Transient or over-expression of rgs-CaM in transgenic lines was shown to produce phenotypes that were similar to those observed in HC-Pro-expressing plants. The results of the Vance group (2000) showed that transgenic lines

expressing rgs-CaM are defective in silencing supporting the idea that rgs-CaM is a cellular suppressor of PTGS.

We compared the levels of rgs–CaM mRNA in *N. benthamiana* plants expressing HC-Pro$^{FRNK/FINK}$ with expression in wild type plants. Northern blot analysis revealed that under the applied conditions the rgs-CaM mRNA was not detectable in independent transgenic lines and in wild type plants. Hence, a quantitative analysis was carried out using the qRT-PCR with specific primers for rgs-CaM and two internal controls for the normalization of the results. No significant differences in the rgs-CaM levels were found between the wild type and independent transgenic line. Thus, our results were in contrary to the data of Anandalakshmi and coworkers (2000). However, in contrast to Anandalakshmi and coworkers (2000), we did not express the TEV HC-Pro but the ZYMV HC-Pro. It is reasonable to assume that suppressors from related viruses not necessarily exhibit the same effect on RNA silencing. In addition, different plant species may also differentially respond to specific RSS.

4.2.3 ZYMV HC-Pro^{FRNK} increases the levels of vd-sRNA in PSTVd-infected *N. benthamiana* plants

Viroids are small, closed circular, single-stranded pathogenic RNAs. Viroid genomes do not code for proteins and viroid replication is completely dependent on the host's transcriptional machinery (Flores *et al*., 2005; Ding and Itaya, 2007). As might be expected from their highly base-paired structure and RNA–RNA mode of replication, viroids have been shown to induce RNA silencing. Similar to virus infections, infection of plants by PSTVd leads to the accumulation of viroid-derived small RNAs (vd-sRNA). The detection of vd-sRNA, resembling siRNAs (21-24 nt), in PSTVd-infected plants indicates that viroids are inducers and targets of the host silencing machinery (Di Serio *et al*., 2010).

Accumulation of vd-sRNA was first detected in tomato plants infected with PSTVd (Itaya *et al*., 2001; Papaefthimiou *et al*., 2001). It remains unclear how viroids induce symptoms. It is suggested that vd-sRNAs are able to interfere with host gene regulation thereby causing symptoms (Tessitori *et al*., 2007).

The sRNA binding function of ZYMV HC-Pro implies an effect on plant defense mechanisms and plant development by sequestering siRNAs and miRNAs. This sRNA binding strategy is similar to that of other RSS, such as the tombusvirus P19 protein and the P21 of closteroviruses (Lakatos *et al*., 2004; Ye and Patel, 2005).

N. benthamiana plants expressing PSTVd (Nb-PSTVd) were crossed with *N. benthamiana* expressing HC-Pro^{FRNK} (Nb-HC-Pro^{FRNK}) to examine whether the presence of

this RSS had an effect on PSTVd infection. Northern blot analysis revealed increased accumulation of vd-sRNA in Nb-PSTVd-HC-Pro^{FRNK} plants when compared to Nb-PSTVd plants. The growth rate of the T2 generation of these plants was very low compared to *N. benthamiana* wild type, plants show stunting and they died before flowering. It was reported that HC-Pro enhances the replication of many unrelated viruses, by inhibiting the host defense mechanism (Voinnet, 2005), thus one may speculate that in the Nb-PSTVd-HC-Pro^{FRNK} plants, the HC-Pro proteins also have an enhancing effect on PSTVd replication and infection, which lead to the death of the T2 generation before flowering.

4.3 *SlHEN1* cloning and Cellular Localization

In order to amplify and clone the *HEN1* cDNA from *Solanum lycopersicum*, the full-length *A. thaliana HEN1* sequence was used as query to search the non-redundant protein database using the NCBI–BLAST. Complete homologous sequences with significant similarity to the entire query were found in *Vitis vinifera*, *Solanum lycopersicum*, *Lotus japonicus*, *Oryza sativa japonica*, and *Physcomitrella patens subsp. Patens*. The sequence of *Lotus japonica* was not included because of the uncertainties in position of intron-exon boundaries.

HEN1 was first identified in a genetic screen as a floral pattering gene and was shown to play a role in the specification of stamen and carpel identities during flower development (Chen *et al*., 2002). Later it was found to be essential for *Arabidopsis* miRNA accumulation *in vivo* (Chen *et al*., 2002; Park et al., 2002). In the *Arabidopsis*, sRNAs are methylated at the 2′-hydroxyl group of their 3′-terminal nucleotide by the HEN1 methyltransferase (Yu *et al*., 2005). HEN1 contains a putative nuclear localization signal (NLS) and is thought to exist and function in the nucleus (Park *et al*., 2002; Xie *et al*., 2004). Later it was shown to be also present and functional in the cytoplasm (Fang *et al*., 2007). In addition, Carnation Italian ringspot virus (CIRV) -derived siRNAs were found to be 3′ modified suggesting the presence of HEN1 in the cytoplasm (Lózsa *et al*., 2008).

To determine the cellular localization of the SlHEN1, transient expression and protoplast preparation were carried out. The putative SlHEN1 protein was fused to the N-terminus of GFP/RFP. Our results were in accordance with the observation that HEN1 is present in the nucleus and the cytoplasm.

4.4 Protein-Protein Interactions

Identification of interactions between viral and host proteins is essential to elucidate the molecular mechanisms that underlie the viral infection process and symptom development in plants. Several plant factors have been reported to interact with HC-Pro

including rgs-CaM (Anandalakshmi *et al*., 2000), the 20S proteasome subunits (Jin *et al*., 2007a), the NtMinD (Jin *et al*., 2007b) and the maize ferredoxin-5 (Cheng *et al*., 2008). In this study, we used ELISA and the yeast two-hybrid (Y2H) system to examine interactions of HC-Pro with other plant proteins.

4.4.1 ZYMV HC-Pro interacts *in vitro* with AtHEN1

Our ELISA results indicated that MBP:HA-HC-Pro$^{FRNK/FINK}$ bound AtHEN1. However, MBP:HA-HC-Pro^{FRNK} appeared to bind stronger than MBP:HA-HC-Pro^{FINK}. The lower binding of MBP:HA-HC-Pro^{FINK} implied that the arginine (R) in the FRNK box may play a role in binding not only to siRNAs (Shiboleth *et al*., 2007; Fuellgrabe *et al*., 2011) but also to AtHEN1. The lower binding between HC-Pro and total bacterial proteins (about threefold) indicated the specificity of binding between HC-Pro and AtHEN1.

To identify the minimal motif of HC-Pro for HEN1 binding, six different HC-Pro^{FRNK} deletion mutants were investigated using ELISA. With one exception, the deletion of either the N- or C-terminus of HC-Pro^{FRNK} strongly reduces AtHEN1 binding. Interestingly, ΔC7 in which most of the HC-Pro C-terminus was deleted, showed strong binding to AtHEN1. This strong binding could be due to more favourable folding of the HC-Pro ΔC7 that would promote an efficient exposition of the HC-Pro domain interacting with AtHEN1. This result suggests that the HC-Pro–AtHEN1 interaction requires proper folding more than the structural properties of the HC-Pro protein (Atreya and Pirone, 1993). Our experimental set-up did not enable the identification of the HC-Pro-binding domain at the amino acid level. Due to the observation that all N- and C- terminal deletions, with the exception of HC-Pro ΔC7, led to a loss of interaction with AtHEN1, we conclude that the putative-binding domain of HC-Pro is located close to the centre of the protein between positions 139 and 320 of ZYMV HC-Pro. Alternatively, one may speculate that N- and C-terminal domains of HC-Pro are both required for AtHEN1 binding. However, the observation that HC-Pro ΔC7 strongly bound to AtHEN1 argues against this hypothesis. We have not identified the exact binding sites or the mode of interaction between HC-Pro and AtHEN1. Crystal structure analysis may help resolve these issues.

4.4.2 HC-Pro inhibits HEN1 activity *in vitro*

The central region of HC-Pro which is highly conserved among all sequenced members of the genus Potyvirus is involved in viral long-distance movement and in maintenance of virus replication (Cronin *et al*., 1995). The FRNK box within the central domain is required for binding of dsRNA and replacement of R180 by leucine (I) within this sequence impaired sRNA binding and led to the attenuation of ZYMV infection symptoms

(Shiboleth *et al*., 2007). In addition, there is evidence suggesting that HC-Pro affected HEN1 activity *in vivo* resulting in the suppression of RNA mediated silencing (Yu *et al*., 2006; Lózsa *et al*., 2008). However, the mechanism of HC-Pro interference with HEN1 has not yet been demonstrated. The finding that mutating the FRNK box of HC-Pro results in loss of its sRNA-binding activity, even though silencing suppression is retained (Shiboleth *et al*., 2007) prompted us to further investigate the silencing suppression function(s) of HC-Pro.

Our results showed that HC-Pro$^{FRNK/FINK}$, but not the truncated proteins (ΔN1 and ΔC9) displaying decreased *in vitro* affinity for AtHEN1 binding, inhibited the methyltransferase activity of AtHEN1 *in vitro*. It was proposed that sRNAs that were bound by HC-Pro could be protected against HEN1-mediated methylation (Yu *et al*., 2006). In CIRV- and TEV-infected *N. benthamiana* plants, varying effects of their RSS proteins, p19 and HC-Pro, on siRNA 3′ modifications were observed (Lózsa *et al*., 2008). The effects ranged from slight modification by CIRV to significant inhibition of si/miRNA modifications by TEV. Similar to the suggestion of Yu and co-workers (2006), Lózsa and co-workers (2008) proposed that HC-Pro covers the 3′-overhangs of sRNAs resulting in the inhibition of 3′ modifications by blocking HEN1 accessibility to sRNAs. Alternatively, they speculated that HC-Pro competes with HEN1. Two independent studies revealed that the 126 kDa replicase protein of TMV exhibits suppressor activity (Takeda *et al*., 2008; Ding *et al*., 2004). The mechanism of suppression was linked to its interference with HEN1 methylation of siRNAs (Vogler *et al*., 2007). Since the TMV replicase possesses a methyltransferase activity it was hypothesized that it could be involved in de-methylation of sRNAs. Alternatively, the TMV replicase may bind to siRNAs thereby protecting them from HEN1 methylation (Vogler *et al*., 2007). However, the HC-Pro^{FINK} lost sRNA binding activity *in vitro* and *in vivo* but it retained its silencing suppressor activity (Fuellgrabe *et al*., 2011; Shiboleth *et al*., 2007). Thus, our results strongly indicate that inhibition of the AtHEN1 activity by HC-Pro$^{FRNK/FINK}$ is probably due to direct interaction between both proteins. It can therefore be concluded that HEN1 inhibition and sRNA-binding activities of HC-Pro are independent of each other.

In this study, we show that HC-Pro interacted with AtHEN1 and inhibited its methyltransferase activity. This interaction might explain the flower deformation, low seed set and infertility in the transgenic plants expressing HC-Pro and in particular in those expressing the NLS-HC-Pro fusion proteins. This view would be in accordance with the finding that HEN1 plays a role in the specification of stamen and carpel identities during flower development (Chen *et al*., 2002).

4.4.3 ZYMV HC-Pro$^{FRNK/FINK}$ do not interact with AGO1

In addition to AtHEN1, we intended to examine the interaction between HC-Pro$^{FRNK/FINK}$ and AGO1, one of the most essential enzymes of the RNAi machinery. It should be noted that we could not validate our ELISA data which indicated that HC-Pro interacts with HEN1 using the Y2H system. We failed to detect the SlHEN1 protein in yeast cells. It was not clear whether SlHEN1 was not expressed or whether the protein extraction method that we applied was not adequate for the extraction of SlHEN1.

In contrast, we succeeded to express the NbAGO1 in yeast. However, we found that HC-Pro$^{FRNK/FINK}$ did not interact with NbAGO1. From the mating experiments it was clear that mating between the two yeast strains harboring HC-Pro^{FRNK} or HC-Pro^{FINK} and NbAGO1 was successful. The mated strains were able to grow on SD–Leu/-Trp/-His but they did not grow on SD-Leu/-Trp/-His/-Ade. Although interaction between AGO1 and RSS proteins has been reported the ZYMV HC-Pro did obviously not belong to this class of RSS (Bortolamiol *et al*., 2007; Chiu *et al*., 2010; Csorba *et al*., 2010).

4.4.4 Self interaction of HC-Pro^{FRNK} in the Y2H

It has been reported that the HC-Pro interacts with itself (Urcuqui-Inchima *et al*., 2000; Lin *et al*., 2009). Size exclusion chromatography (SEC) suggested that the functional HC-Pro proteins of TVMV, PVY and TuMV form dimers or trimers (Thornbury *et al*., 1985; Wang and Pirone, 1999). Data from electron microscopy, biochemical analysis and secondary structure predictions suggested that soluble HC-Pro of Lettuce mosaic virus (LMV) is present as dimers (Plisson *et al*., 2003). In addition, structural analysis of TEV HC-Pro revealed dimeric, tetrameric and hexameric forms (Ruiz-Ferrer *et al*., 2005). Y2H assays also demonstrated self-interactions of HC-Pro. However, all of the studies described above indicated different regions of the proteins as key domains for the self-interactions. Urcuqui-Inchima and coworkers (2000) suggested that only the N-terminus was involved in HC-Pro self-interaction. Guo and co-workers (1999) identified a 24 amino acids (aa) long N-terminal domain and the C-terminal proteinase part to be required for self interaction of *Potato A potyvirus* (PAV) HC-Pro. Using SEC, cross-linking and crystallization analysis, Plisson and co-workers (2003) found that a mutant of the LMV HC-Pro lacking aa 4–102 was still organized as tetramers. These data demonstrated that the N-terminal 102 aa of HC-Pro were not essential for dimerisation and that an essential self-interaction domain was located in the remaining part of the molecule. Crosslinking studies with a 32-kDa trypsin digestion product of LMV HC-Pro further defined a dimerisation domain to the C-terminal 282 aa (Plisson *et al*., 2003). The TuMV HC-Pro was studied to investigate the domain required for self interaction using the Y2H and bimolecular fluorescence complementation (BiFC) (Zheng *et*

al., 2011). The central and C-terminal regions of the HC-Pro were clearly involved in self-interaction and HC-Pro homodimerization. The N-terminus appeared to have a very weak effect on self-interaction. These results suggest that the self-interacting domains differ among potyviral HC-Pro proteins (Zheng *et al*., 2011).

Our studies showed that HC-Pro^{FRNK} was able to self-interact. Using the Y2H system, the 4 reporter genes became activated and cells turned blue. In contrast, no self-interaction was detectable when HC-Pro^{FINK} was analyzed. It is reasonable to assume that the FRNK to FINK mutation accounted for the failure of HC-Pro^{FINK} to form dimers since HC-Pro^{FRNK} and HC-Pro^{FINK} only differ in the replacement of R by I. This would be also in agreement with the observation that the central domain of the TuMV HC-Pro is involved in the self-interaction (Zheng *et al*., 2011). It has been proposed that the active form of HC-Pro is a dimer which would be functional in many biological processes (Thornbury *et al*., 1985). Hence, the inability of HC-Pro^{FINK} to form dimers may explain the loss of its sRNA binding activity.

5. References

Ahlquist, P. 2002. RNA-dependent RNA polymerases, viruses, and RNA silencing. Science 296: 270-273.

Akbergenov, R., A. Si-Ammour, T. Blevins, I. Amin, C. Kutter, H. Vanderschuren, P. Zhang, W. Cruissem, F. Jr. Meins, T. Hohn and M. M. Pooggin. 2006. Molecular characterization of geminivirus-derived small RNAs in different plant species. Nucleic Acids Res. 34: 462-471.

Alcazar, R. M., R. Lin and A. Z. Fire. 2008. Transmission dynamics of heritable silencing induced by double-stranded RNA in *Caenorhabditis elegans*. Genetics 180:1275–1288.

Alvarado, V. and H. B. Scholthof. 2009. Plant responses against invasive nucleic acids: RNA silencing and its suppression by plant viral pathogens. Semin. Cell Dev. Biol. 209: 1032–1040.

Alvarez, J., P. I. Pekker, A. Goldshmidt, E. Blum, Z. Amsellem and Y. Eshed. 2006. Endogenous and synthetic MicroRNAs stimulate simultaneous, efficient, and localized regulation of multiple targets in diverse species. Plant Cell 18: 1134-1151.

Ambros, V. 2003. MicroRNA pathways in flies and worms: growth, death, fat, stress and timing. Cell 113: 673-676.

Anandalakshmi, R., G. J. Pruss, X. Ge, R. Marathe, A. C. Mallory, T. H. Smith and V. B. Vance. 1998. A viral suppressor of gene silencing in plants. Proc. Natl. Acad. Sci. USA 95:13079–13084.

Anandalakshmi, R., R. Marathe, X. Ge, J. M., Jr. Herr, C. Mau, A. Mallory, G. Pruss, L. Bowman and V. B. Vance. 2000. A calmodulin-related protein that suppresses posttranscriptional gene silencing in plants. Science 290: 142-144.

Astier-Manifacier, S. and P. Cornuet. 1971. RNA-dependent RNA polymerase in Chinese cabbage. Biochim. Biophys. Acta 232: 484–493.

Atreya, C. D. and T. P. Pirone. 1993. Mutational analysis of the helper component-proteinase gene of a potyvirus: effects of amino acid substitutions, deletions, and gene replacement on virulence and aphid transmissibility. Proc. Natl. Acad. Sci. USA 90: 11919-11923.

Aufsatz, W., M. F. Mette, J. van der Winden, M. Matzke and A. J. Matzke. 2002. HDA6, a putative histone deacetylase needed to enhance DNA methylation induced by double stranded RNA. EMBO J. 21: 6832-6841.

Aufsatz, W., M. F. Mette, A. J. Matzke and M. Matzke. 2004. The role of MET1 in RNA-directed de novo and maintenance methylation of CG dinucleotides. Plant Mol. Biol. 54: 793-804.

Aukerman, M. J. and H. Sakai. 2003. Regulation of flowering time and floral organ identity by a MicroRNA and its APETALA2-like target genes. Plant Cell 15: 2730-2741.

Azevedo, J., D. Garcia, D. Pontier, S. Ohnesorge, A. Yu, S. Garcia, L. Braun, M. Bergdoll, M. A. Hakimi, T. Lagrange and O. Voinnet. 2010. Argonaute quenching and global changes in Dicer homeostasis caused by a pathogen-encoded GW repeat protein. Genes Dev. 24: 904-915.

Baltimore, D. 1970. RNA-dependent DNA polymerase in virions of RNA tumour viruses. Nature 226: 1209-1211.

Bartel, B. and D. P. Bartel. 2003. MicroRNAs: at the root of plant development. Plant Physiol. 132: 709-717.

Bartel, D. P. 2004. MicroRNAs: genomics, biogenesis, mechanism, and function. Cell 116: 281-297.

Baulcombe, D. C. 1996. RNA as a target and an initiator of post-transcriptional gene silencing in transgenic plants. Plant Mol. Biol. 32: 79–88.

Baulcombe, D. 2004. RNA silencing in plants. Nature 431: 356–363.

Baumberger, N. and D. C. Baulcombe. 2005. *Arabidopsis* ARGONAUTE1 is an RNA slicer that selectively recruits microRNAs and short interfering RNAs. Proc. Natl. Acad. Sci. USA 102: 11928-11933.

Baunoch, D., P. Das and V. Hari. 1990. Potato virus Y helper component protein is associated with amorphous inclusions. J. Gen. Virol. 71: 2479–2482.

Bayne, E. H., D. V. Rakitina, S. Y. Morozov and D. C. Baulcombe. 2005. Cell-to-cell movement of Potato Potexvirus X is dependent on suppression of RNA silencing. Plant J. 44: 471–482.

Bender, J. 2004. Chromatin-based silencing mechanisms. Curr. Opin. Plant Biol. 7: 521-526.

Bernstein, E., A. A. Caudy, S. M., Hammond and G. J. Hannon. 2001. Role for a bidentate ribonuclease in the initiation step of RNA interference. Nature 409: 363-366.

Birnboim, H. C. and J. Doly. 1979. A rapid alkaline extraction procedure for screening recombinant plasmid DNA. Nucleic Acids Res. 7: 1513-1523.

Bisaro, D. M. 2006. Silencing suppression by geminivirus proteins. Virology 344: 158-168.

Blanc, S., J. J. Lopez-Moya, R. Wang, S. Garcia-Lampasona, D. W. Thornbury and T. P. Pirone. 1997. A specific interaction between coat protein and helper component correlates with aphid transmission of a potyvirus. Virology 231: 141–147.

Blevins, T., R. Rajcswaran, P. V. Shivaprasad, D. Bekriazariants, A. Si-Ammour, H. S. Park, F. Vazqucz, D. Robertson, F. Jr. Meins, T. Hohn and M. M. Pooggin. 2006. Four plant Dicers mediate viral small RNA biogenesis and DNA virus induccd silencing. Nucleic Acids Res. 34: 6233-6246.

Boonrod, K., D. Galetzka, P. D. Nagy, U. Conrad and G. Krczal. 2004. Single-chain antibodies against a plant viral RNA-dependent RNA polymerase confer virus resistance. Nat. Biotechnol. 22: 856–862.

Borsani, O., J. Zhu, P. E. Verslues, R. Sunkar and J. K. Zhu. 2005. Endogenous siRNAs derived from a pair of natural cis-antisense transcripts regulate salt tolerance in *Arabidopsis*. Cell 123: 1279-1291.

Bortolamiol, D., M. Pazhouhandeh, K. Marrocco, P. Genschik and V. Ziegler-Graff. 2007. The polerovirus F box protein P0 targets ARGONAUTE1 to suppress RNA Silencing. Curr. Biol. 17: 1615–1621.

Bouche, N., D. Lauressergues, V. Gasciolli and H. Vaucheret. 2006. An antagonistic function for *Arabidopsis* DCL2 in development and a new function for DCL4 in generating viral siRNAs. EMBO J. 25: 3347-3356.

Boutet, S., F. Vazquez, J. Liu, C. Beclin, M. Fagard, A. Gratias, J. B. Morel, P. Crete, X. Chen and H. Vaucheret. 2003. *Arabidopsis* HEN1: a genetic link between endogenous miRNA controlling development and siRNA controlling transgene silencing and virus resistance. Curr. Biol. 13: 843-848.

Bradford, M. M. 1976. A rapid and sensitive method for the quantitation of microgram quantities of protein utilizing the principle of protein-dye binding. Anal. Biochem. 72: 248-254.

Bragg, J. N. and A. O. Jackson. 2004. The C-terminal region of the Barley stripe mosaic virus γb protein participates in homologous interactions and is required for suppression of RNA silencing. Mol. Plant Pathol. 5: 465–481.

Brenner, S., M. Johnson, J. Bridgham, G. Golda, D. H. Lloyd, D. Johnson, S. Luo, S. McCurdy, M. Foy, M., Ewan, R. Roth, D. George, S. Eletr, G. Albrecht, E. Vermaas, S. R. Williams, K. Moon, T. Burcham, M. Pallas, R. B. DuBridge, J. Kirchner, K. Fearon, J. Mao and K. Corcoran. 2000. Gene expression analysis by massively parallel signature sequencing (MPSS) on microbead arrays. Nature biotechnology 18: 630-634.

Brigneti, G., O. Voinnet, W. X. Li, L. H. Ji, S. W. Ding and D. C. Baulcombe. 1998. Viral pathogenicity determinants are suppressors of transgene silencing in *Nicotiana benthamiana*. EMBO J. 17: 6739–6746.

Brodersen, P. and O. Voinnet. 2006. The diversity of RNA silencing pathways in plants. Trends Genet. 225: 268-280.

Brodersen, P., L. Sakvarelidze-Achard, M. Bruun-Rasmussen, P. Dunoyer, Y. Y. Yamamoto, L. Sieburth and O. Voinnet. 2008. Widespread translational inhibition by plant miRNAs and siRNAs. Science 320: 1185–1190.

Bucher, E., T. Sijen, P. de Haan, R. Goldbach and M. Prins. 2003. Negative-strand tospoviruses and tenuiviruses carry a gene for a suppressor of gene silencing at analogous genomic positions. J. Virol. 77: 1329–1336.

Burgyán, J. and Z. Havelda. 2011. Viral suppressors of RNA silencing. Trends Plant Sci. 16: 265-272.

Burnette, W. N. 1981. Western blotting: electrophoretic transfer of proteins from sodium dodecyl sulfate - polyacrylamide gels to unmodified nitrocellulose and radiographic detection with antibody and radioiodinated protein A. Anal. Biochem. 112: 195-203.

Burton, N. O., K. B. Burkhart and S. Kennedy. 2011. Nuclear RNAi maintains heritable gene silencing in *Caenorhabditis elegans*. PNAS 108: 19683-19688.

Cao, X. and S. Jacobsen. 2002. Role of the *Arabidopsis* DRM methyltransferases in de novo DNA methylation and gene silencing. Curr. Biol. 12: 1138–1144.

Carmell, M. A., Z. Xuan, M. Zhang and G. J. Hannon. 2002. The Argonaute family: tentacles that reach into RNAi, developmental control, stem cell maintenance, and tumorigenesis. Genes Dev. 16: 2733-2742.

Carrington, J. C., S. M. Cary, T. D. Parks and W. G. Dougherty. 1989. A second proteinase encoded by a plant potyvirus genome. EMBO J. 8: 365-370.

Carrington, J. C., D. O. Freed and C. S. OH. 1990. Expression of potyviral polyproteins in transgenic plants reveals three proteolytic activities required for complete processing. EMBO J. 9: 1347-1353.

Carrington J. C. and V. Ambros. 2003. Role of microRNAs in plant and animal development. Science 301: 336-338.

Chan, S. W., I. R. Henderson and S. E. Jacobsen. 2005. Gardening the genome: DNA methylation in *Arabidopsis thaliana*. Nat. Rev. Genet. 6: 351–360.

Chapman, E. J., A. I. Prokhnevsky, K. Gopinath, V. V. Dolja and J. C. Carrington. 2004. Viral RNA silencing suppressors inhibit the microRNA pathway at an intermediate step. Genes Dev. 18: 1179-1186.

Chen J., W. X. Li, D. Xie, J. R. Peng and S. W. Ding. 2004. Viral virulence protein suppresses RNA silencing-mediated defense but upregulates the role of microRNA in host gene expression. Plant Cell 16: 1302-1313.

Chen, X. 2004. A microRNA translational repressor of APETALA2 in *Arabidopsis* flower development. Science 303: 2022-2025.

Chen, X. 2005. MicroRNA biogenesis and function in plants. FEBS Lett. 579: 5923-5931.

Chen, X. 2007. A marked end. Nat. Struct. Mol. Biol. 14: 259–260.

Chen, X., J. Liu, Y. Cheng and D. Jia. 2002. HEN1 functions pleiotropically in *Arabidopsis* development and acts in C function in the flower. Develop. 129: 1085–1094.

Cheng, Y. Q., Z. M. Liu, J. Xu, T. Zhou, M. Wang, Y. T. Chen, H. F. Li and Z. F. Fan. 2008. HC-Pro protein of sugar cane mosaic virus interacts specifically with maiz ferredoxin-5 in vitro and in plants. J. Gen. Virol. 89: 2046-2054.

Chien, C. T., P. L. Bartel, R. Sternglanz and S. Fields. 1991 The two-hybrid system: A method to identify and clone genes for proteins that interact with a protein of interest. Proc. Nat. Acad. Sci. USA 88: 9578–9582.

Chiu, M. H., I. H. Chen, D. C. Baulcombe and C. H. Tsai. 2010. The silencing suppressor P25 of Potato virus X interacts with Argonaute1 and mediates its degradation through the proteasome pathway. Mol. Plant Pathol. 11: 641-649.

Chomczynski, P. and N. Sacchi. 1987. Single-step method of RNA isolation by acid guanidinium thiocyanate-phenol-chloroform extraction. Anal. Biochem. 162: 156-159.

Clontech. 2008. YeastmakerTM Yeast Transformation System 2 User Manual.

Clough, S. J. and A. F. Bent. 1998. Floral Dip: a simplified method for Agrobacterium-mediated transformation of *Arabidopsis thaliana*. Plant J. 16: 735-743.

Cronin, S., J. Verchot, R. Haldeman-Cahill, M. C. Schaad and J. C. Carrington. 1995. Long-distance movement factor: a transport function of the potyvirus helper component-proteinase. Plant Cell 7: 549–559.

Csorba, T., A. Bovi, T. Dalmay and J. Burgyan. 2007. The p122 subunit of tobacco mosaic virus replicase is a potent silencing suppressor and compromises both siRNA and miRNA mediated pathways. J. Virol. 81: 11768–11780.

Csorba, T., R. Lozsa, G. Hutvagner and J. Burgyan. 2010. Polerovirus protein P0 prevents the assembly of small RNA-containing RISC complexes and leads to degradation of Argonaute1. Plant J. 62: 463–472.

Cuellar, W. J., J. F. Kreuze, M. L. Rajamak, K. R. Cruzado, M. Untiveros and J. P. T. Valkonen. 2009. Elimination of antiviral defense by viral RNase III. Proc. Natl. Acad. Sci. USA 106: 10354–10358.

Dalakouras A., M. Moser, K. Boonrod, G. Krczal and M. Wassenegger. 2011. Diverse spontaneous silencing of a transgene among two *Nicotiana* species. Planta 234: 699-707.

Dalakouras, A., M. Moser, M. Zwiebel, G. Krczal, R. Hell and M. Wassenegger. 2009. A hairpin RNA construct residing in an intron efficiently triggered RNA-directed DNA methylation in tobacco. Plant J. 60: 840-851.

De Mejia, M., E. Hiebert, D. Purcifull, D. Thornbury and T. Pirone. 1985. Identification of potyviral amorphous inclusion protein as a nonstructural, virus-specific protein related to helper component. Virology 142: 34–43.

Deleris, A., J. Gallego-Bartolome, J. Bao, K. D. Kasschau, J. C. Carrington and O. Voinnet. 2006. Hierarchical action and inhibition of plant DICER-LIKE proteins in antiviral defense. Science 313: 68–71.

Di Guan, C., P. Li, P. D. Riggs and H. Inouye. 1988. Vectors that facilitate the expression and purification of foreign peptides in *Escherichia coli* by fusion to maltose-binding protein. Gene 67: 21-30.

Di Serio, F., A. E. Martínez de Alba, B. Navarro, A. Gisel and R. Flores. 2010. RNA-Dependent RNA polymerase 6 delays accumulation and precludes meristem invasion of a viroid that replicates in the nucleus. J. Virol. 84: 2477–2489.

Díaz-Pendón, J. A., F. L. Li, W. X. Li and S. W. Ding. 2007. Suppression of antiviral silencing by Cucumber mosaic virus 2b protein in *Arabidopsis* is associated with drastically reduced accumulation of three classes of viral small interfering RNAs. Plant Cell 19: 2053-2063.

Diaz-Pendon, J. A. and S. W. Ding. 2008. Direct and indirect roles of viral suppressors of RNA silencing in pathogenesis. Annu. Rev. Phytopathol. 46: 303–326.

Ding, B. and A. Itaya. 2007. Viroid: a useful model for studying the basic principles of infection and RNA biology. Mol. Plant Microbe Interact. 20: 7-20.

Ding, S.W. 2010. RNA-based antiviral immunity. Nat. Rev. Immunol 10:632–644.

Ding, S. W. and O. Voinnet. 2007. Antiviral immunity directed by small RNAs. Cell130: 413–426.

Ding, S. W., B. J. Anderson, H. R. Haase and R. H. Symons. 1994. New overlapping gene encoded by the Cucumber mosaic virus genome. Virology 198: 593-601.

Ding, S. W., B. J. Shi, W. X. Li and R. H. Symons. 1996. An interspecies hybrid RNA virus is significantly more virulent than either parental virus. Proc. Natl. Acad. Sci. USA 93: 7470-7474.

Ding, X. S., J. Liu, N. H. Cheng, A. Folimonov, Y. M. Hou, Y. Bao, C. Katagi, S. A. Carter and R. S. Nelson. 2004. The Tobacco mosaic virus 126-kDa protein associated with virus replication and movement suppresses RNA silencing. Mol. Plant Microbe Interact. 17: 583–592.

Dong, X., R. van Wezel, J. Stanley and Y. Hong. 2003. Functional characterization of the nuclear localization signal for a suppressor of posttranscriptional gene silencing. J. Virol. 77: 7026–7033.

Dugas, D. V. and B. Bartel. 2004. MicroRNA regulation of gene expression in plants. Curr. Opin. Plant Biol. 7: 512-520.

Dunoyer, P., C. H. Lecellier, E. A. Parizotto, C. Himber and O. Voinnet. 2004. Probing the microRNA and small interfering RNA pathways with virus-encoded suppressors of RNA silencing. Plant Cell 16: 1235–1250.

Dunoyer, P., S. Pfeffer, C. Fritsch, O. Hemmer, O. Voinnet and K. E. Richards. 2002. Identification, subcellular localization and some properties of a cysteine-rich suppressor of gene silencing encoded by peanut clump virus. Plant J. 29: 555-567.

Dunoyer, P., C. Himber and O. Voinnet. 2006 Induction, suppression and requirement of RNA silencing pathways in virulent Agrobacterium tumefaciens infections. Nat. Genet. 38: 258–263.

Dunoyer, P., C. Himber, V. Ruiz-Ferrer, A. Alioua and O. Voinnet. 2007. Intra- and intercellular RNA interference in *Arabidopsis thaliana* requires components of the microRNA and heterochromatic silencing pathways. Nat. Genet. 39: 848-856.

Edwards, K., C. Johnstone and C. Thompson. 1991. A simple and rapid method for the preparation of plant genomic DNA for PCR analysis. Nucleic Acids Res. 19: 1349.

Ehrenreich, I. M. and M. Purugganan. 2008. MicroRNAs in plants: Possible contributions to phenotypic diversity. Plant Signal. Behav. 3: 829-830.

Endres, M. W., B. D. Gregory, Z. Gao, A. W. Foreman, S. Mlotshwa, X. Ge, G. J. Pruss, J. R. Ecker, L. H. Bowman and V. Vance. 2010. Two plant viral suppressors of silencing require the ethylene-inducible host transcription factor RAV2 to block RNA silencing. PLoS Pathog. 6: e1000729.

English, J. J., E. Mueller and D. C. Baulcombe. 1996. Suppression of virus accumulation in transgenic plants exhibiting silencing of nuclear genes. Plant Cell 8: 179-188

Eun,Ch., Z. J. Lorkovic, U. Naumann, Q. Long, E. R. Havecker, S. A. Simon, B. C. Meyers, A. J. M. Matzke and M. Matzke. 2011. AGO6 Functions in RNA-mediated transcriptional gene silencing in shoot and root meristems in *Arabidopsis thaliana*. PLoS ONE 6 (10): e25730.

Fang, Y. and D. L. Spector. 2007. Identification of nuclear dicing bodies containing proteins for microRNA biogenesis in living *Arabidopsis* plants. Curr. Biol. 17: 818-823.

Fields, S. and O. Song. 1989. A novel genetic system to detect protein-protein interactions. Nature 340: 245–247.

Finnegan, E. J., R. Margis and P. M. Waterhouse. 2003. Posttranscriptional gene silencing is not compromised in the *Arabidopsis* CARPEL FACTORY DICER-LIKE1 mutant, a homolog of Dicer-1 from Drosophila. Curr. Biol. 13: 236-240.

Fire, A., S. Xu, M. K. Montgomery, S. A.Kostas, S. E. Driver and C. C. Mello. 1998. Potent and specific genetic interference by double-stranded RNA in *Caenorhabditis elegans*. Nature 391: 806-811.

Flasinski, S. and B. G. Cassidy. 1998. Potyvirus aphid transmission requires helper component and homologous coat protein for maximal efficiency. Arch. Virol. 143: 2159-2172.

Flores, R., C. Hernández, A. E. Martínez de Alba, J. A. Daròs and F. Di Serio. 2005. Viroids and viroid-host interactions. Annu. Rev. Phytopathol. 43: 117–139.

Fuellgrabe, M. 2010. Funktionelle Analyse der Helper-Component Proteinase (HC-Pro) aus Zucchini Yellow Mosaic Virus. Dissertation, Johann Wolfgang Goethe-University, Frankfurt am Main, Germany.

Fuellgrabe, M. F., K. Boonrod, R. Jamous, M. Moser, Y. Shiboleth, G. Krczal and M. Wassenegger. 2011. Expression, purification and functional characterization of recombinant Zucchini yellow mosaic virus HC-Pro. Protein Expr. Purif. 75: 40–45.

Fukunaga, R. and J. A. Doudna. 2009. dsRNA with 5' overhangs contributes to endogenous and antiviral RNA silencing pathways in plants. EMBO J. 28: 545–555.

Gal-On, A. and B. Raccah. 2000. A point mutation in the FRNK motif of the potyvirus helper component-protease gene alters symptom expression in cucurbits and elicits protection against the severe homologous virus. Phytopathol. 90: 467–473.

Garcia-Ruiz, H., A. Takeda, E. J. Chapman, C. M. Sullivan, N. Fahlgren, K. J. Brempelis and J. C. Carrington. 2010. *Arabidopsis* RNA-dependent RNA polymerases and dicer-like proteins in antiviral defense and small interfering RNA biogenesis during Turnip Mosaic Virus infection. Plant Cell 22: 481–496.

Gazzani, S., T. Lawrenson, C. Woodward, D. Headon and R. Sablowski. 2004. A link between mRNA turnover and RNA interference in *Arabidopsis*. Science 306: 1046-1048.

Ghazala, W., A. Waltermann, R. Pilot, S. Winter and M. Varrelmann. 2008. Functional characterization and subcellular localization of the 16K cysteine-rich suppressor of gene silencing protein of Tobacco rattle virus. J. Gen. Virol. 89: 1748–1758.

Glick, E., A. Zrachya Y. Levy, A. Mett, D. Gidoni, E. Belausov, V. Citovsky and Y. Gafni. 2008. Interaction with host SGS3 is required for suppression of RNA silencing by Tomato yellow leaf curl virus V2 protein. Proc. Natl. Acad. Sci. USA 105: 157–161.

González, I., L. Martínez, D. V. Rakitina, M. G. Lewsey, F. A. Atencio, C. Llave, N. O. Kalinina, J. P. Carr, P. Palukaitis and T. Canto. 2010. Cucumber Mosaic Virus 2b protein subcellular targets and interactions: Their significance to RNA silencing suppressor activity. Mol. Plant Microbe Interact. 23: 294–303.

Gonzalez-Jara, P., F. A. Atencio, B. Martinez-Garcia, D. Barajas, F. Tenllado and J. R. Diaz-Ruiz. 2005. A single amino acid mutation in the Plum pox virus helper component-proteinase gene abolishes both synergistic and RNA silencing suppression activities. Phytopathol. 95: 894-901.

Goto, K., T. Kobori, Y. Kosaka, T. Natsuaki and C. Masuta. 2007. Characterisation of silencing suppressor 2b of Cucumber mosaic virus based on examination of its small RNA-binding abilities. Plant Cell Physiol. 48: 1050-1060.

Govier, D. and B. Kassanis. 1974. A virus-induced component of plant sap needed when aphids acquire potatovirus Y from purified preparations. Virology 61: 420–426.

Grumet, R., J. C. Sanford and S. A. Johnston. 1987. Pathogen-derived resistance to viral infection using a negative regulatory molecule. Virology 161: 561-569.

Guo, D., A. Merits and M. Saarma. (1999). Self-association and mapping of interaction domains of helper component-proteinase of potato A potyvirus. J. Gen. Virol. 80: 1127-1131.

Guo, H. S. and S. W. Ding. 2002. A viral protein inhibits the long range signaling activity of the gene silencing signal. EMBO J. 21: 398-407.

Haas, G., J. Azevedo, G. Moissiard, A. Geldreich, C. Himber, M. Bureau, T. Fukuhara, M. Keller and O. Voinnet. 2008. Nuclear import of CaMV P6 is required for infection and suppression of the RNA silencing factor DRB4. EMBO J. 27: 2102–2112.

Hamera, S., X. Song, L. Su, X. Chen and R. Fang. 2011. Cucumber Mosaic Virus suppressor 2b binds to AGO4-related small RNAs and impairs AGO4 activities. Plant J., doi:10.1111/j.1365-313X.2011.04774.x

Hamilton, A. J. and D. C. Baulcombe.1999. A species of small antisense RNA in posttranscriptional gene silencing in plants. Science 286: 950–952.

Hamilton, A., O. Voinnet, L. Chappell and D. Baulcombe. 2002. Two classes of short interfering RNA in RNA silencing. EMBO J. 21: 4671-4679.

Hammond, S. M., E. Bernstein, D. Beach and G. J. Hannon. 2000. An RNA-directed nuclease mediates post-transcriptional gene silencing in Drosophila cells. Nature 404: 293-296.

Han, Y. and D. Grierson. 2002. Relationship between small antisense RNAs and aberrant RNAs associated with sense transgene mediated gene silencing in tomato. Plant J. 29: 509-519.

Hannon, G. J. 2002. RNA interference. Nature 418: 244-251.

Harper, J. W., G. R. Adami, N. Wei, K. Keyomarsi and S. J. Elledge. 1993. The p21 Cdk-interacting protein Cip1 is a potent inhibitor of G1 cyclin-dependent kinases. Cell 75: 805–816.

Harvey, J. J. W., M. G. Lewsey, K. Patel, J. Westwood, S. Heimsta, J. P. Carr and D. C. Baulcombe. 2011. An antiviral defense role of AGO2 in plants. PLoS ONE 6: (1): e14639.

Havecker, E. R., L. M. Wallbridge, T. J. Hardcastle, M. S. Bush, K. A. Kelly, R. M. Dunn, F. Schwach, J. H. Doonan and D. C. Baulcombe. 2010. The *Arabidopsis* RNA-directed DNA methylation argonautes functionally diverge based on their expression and interaction with target loci. Plant Cell 22: 321–334.

He, L. and G. J. Hannon. 2004. MicroRNAs: small RNAs with a big role in gene regulation. Nat. Rev. Genet. 5: 522-531.

He, X. J., T. Chen and K. Zhu. 2011. Regulation and function of DNA methylation in plants and animals. Cell Res. 21: 442–465.

Hellens, R., P. Mullineax and H. Klee. 2000. A guide to *Agrobacterium* binary Ti vectors, Trends Plant Sci. 5: 446-451.

Hemmes, H., L. Lakatos, R. Goldbach, J. Burgyan and M. Prins. 2007. The NS3 protein of Rice hoja blanca tenuivirus suppresses RNA silencing in plant and insect hosts by efficiently binding both siRNAs and miRNAs. RNA 13: 1079–1089.

Henderson, I. R., X. Zhang, C. Lu, L. Johnson, B. C. Meters, P. J. Green and S. E. Jacobsen. 2006. Dissecting *Arabidopsis thaliana* DICER function in small RNA processing, gene silencing and DNA methylation patterning. Nat. Genet. 38: 721-725.

Herr, A. J., M. B. Jensen, T. Dalmay and D. C. Baulcombe. 2005. RNA polymerase IV directs silencing of endogenous DNA. Science 308: 118–120.

Horsch, R. B., J. E. Fry, N. L. Hoffman, D. Eichholz, S. G. Rogers and R. T. Fraley. 1985. A simple and general method for transferring genes into plants. Science 227: 1229-1231.

Horwich, M. D., C. Li, C. Matranga, V. Vagin, G. Farley, P. Wang and P. D. Zamore. 2007. The Drosophila RNA methyltransferase, DmHen1, modifies germline piRNAs and single-stranded siRNAs in RISC. Curr. Biol. 17: 1265–1272.

Howard, A. R., M. L. Heppler, H. J. Ju, K. Krishnamurthy, M. E. Payton and J. Verchot-Lubicz. 2004. Potato virus X TGBp1 induces plasmodesmata gating and moves between cells in several host species whereas CP moves only in N. benthamiana leaves. Virology 328: 185–197.

Inoue, H., H. Nojima and H. Okayama. 1990. High efficiency transformation of *Escherichia coli* with plasmids. Gene 96: 23-28.

Itaya, A., A. Folimonov, Y. Matsuda, R. S. Nelson and B. Ding. 2001. Potato spindle tuber viroid as inducer of RNA silencing in infected tomato. Mol. Plant Microbe Interact. 14: 1332–1334.

Jin Y., D. Ma, J. Dong, J. Jin, D. Li, C. Deng and T. Wang. 2007a. HC-Pro protein of Potato virus Y can interact with three Arapidopsis 20S proteasome subunits in planta. J. Virol. 81: 12881-12888.

Jin Y., D. Ma, J. Dong, D. Li, C. Deng, J. Jin and T. Wang. 2007b. The HC-Pro protein of Potato virus Y interacts with NtMinD of tobacco. Mol. Plant Microbe Interact. 20: 1505-1511.

Johansen, L. K. and J. C. Carrington. 2001. Silencing on the spot. Induction and suppression of RNA silencing in the Agrobacterium-mediated transient expression system. Plant Physiol. 126: 930-938.

Jones-Rhoades, M. W. and D. P. Bartel. 2004. Computational identification of plant miRNAs and their targets, including a stress-induced miRNA. Mol. Cell 14: 787-799.

Johnes-Roades, M. W., D. P. Bartel and B. Bartel. 2006. MicroRNAs and their regulatory roles in plants. Annu. Rev. Plant Biol. 57: 19-53.

Jyothishwaran, G., D. Kotresha, T. Selvaraj, S. H. Srideshikan and C. Jayabaskaran. 2007. A modified freeze–thaw method for efficient transformation of *Agrobacterium tumefaciens.* Curr. Sci. 93: 770-772.

Kalinina, N. O., D. V. Rakitina, A. G. Solovyev, J. Schiemann and S. Y. Morozov. 2002. RNA helicase activity of the plant virus movement proteins encoded by the first gene of the triple gene block. Virology 296: 321–329.

Kanazawa, A., J. Inaba, H. Shimura, S. Otagaki, S. Tsukahara, A. Matsuzawa, B. M. Kim, K. Goto and C. Masuta. 2011. Virus-mediated efficient induction of epigenetic modifications of endogenous genes with phenotypic changes in plants. Plant J. 65:156-168.

Kang, C. B., S. Dhe-Paganon and H. S. Yoon. 2008. FKBP family proteins: immunophilins with versatile biological functions. Neurosignals 16: 318–325.

Kasschau, K. D. and J. C. Carrington. 1995. Requirement for HC-Pro processing during genome amplification of tobacco etch potyvirus. Virology 209: 268–273.

Kasschau, K. D. and J. C. Carrington. 1998. A counter defensive strategy of plant viruses: suppression of posttranscriptional gene silencing. Cell 95: 461–470.

Kasschau, K. D., Z. Xie, E. Allen, C. Llave, E. J. Chapman, K. A. Krizan and J. C. Carrington. 2003. P1/HC-Pro, a viral suppressor of RNA silencing, interferes with Arabidopsis development and miRNA function. Dev. Cell 4: 205–217.

Khan, Z.A., K. T. Hiriyanna, F. Chavez and H. Fraenkel-Conrat. 1986. RNA-directed RNA polymerases from healthy and from virus-infected cucumber. Proc. Natl. Acad. Sci. USA 83: 2383–2386.

Kirino, Y. and Z. Mourelatos. 2007. The mouse homolog of HEN1 is a potential methylase for Piwi-interacting RNAs. RNA 13: 1397–1401.

Koncz, C. and J. Schell. 1986. The promoter of the TL-DNA gene 5 controls the tissue-specific expression of chimeric genes carried by a novel type of *Agrobacterium* binary vector. Mol. Gen. Genet. 204: 383–396.

Kreuze, J. F., E. I. Savenkov, W. Cuellar, X. Li and J. P. Valkonen. 2005. Viral class 1 RNase III involved in suppression of RNA silencing. J. Virol. 79: 7227-7238.

Kricka, L. J. and T. P. Whitehead. 1987. Chemiluminescent and bioluminescent immunoassays. J. Pharm. Biomed. Anal. 5: 829-833.

Kurth, H. M. and K. Mochizuki. 2009. 2′-O-methylation stabilizes Piwi-associated small RNAs and ensures DNA elimination in Tetrahymena. RNA 15: 675–685.

Labjournal. http://www.laborjournal.de/rubric/tricks/tricks/trick81.html

Laemmli, U. K. 1970. Cleavage of structural proteins during the assembly of the head of bacteriophage T4. Nature 227: 680-685.

Laible, M. and K. Boonrod. 2009. Homemade site directed mutagenesis of whole plasmids. J. visual. exper. 27.

Lakatos, L., G. Szittya and D. J. B. Silhavy. 2004. Molecular mechanisms of RNA silencing suppression mediated by p19 protein of tombusviruses. EMBO J. 23: 876-884.

Lakatos, L., T. Csorba, V. Pantaleo, E. J. Chapman, J. C. Carrington, Y. P. Liu, V. V. Dolja, L. F. Calvino, J. J. Lopez-Moya and J. Burgyan. 2006. Small RNA binding is a common strategy to suppress RNA silencing by several viral suppressors. EMBO J. 25: 2768-2780.

Lau, N. C., L. P. Lim, E. G. Weinstein and D. P. Bartel. 2001. An abundant class of tiny RNAs with probable regulatory roles in *Caenorhabditis elegans*. Science 294: 858-862.

Lee, R. C., R. L. Feinbaum and V. Ambros. 1993. The *Caenorhabditis elegans* heterotrophic gene lin-4 encodes small RNAs with antisense complementarity to lin-14. Cell 75: 843-854.

Lee, R. C. and V. Ambros. 2001. An extensive class of small RNAs in *Caenorhabditis elegans*. Science 294: 862-864.

Lee, Y. S., K. Nakahara, J. W. Pham, K. Kim, Z. He, E. J. Sontheimer and R. W. Carthew. 2004. Distinct roles for Drosophila Dicer-1 and Dicer-2 in the siRNA/miRNA silencing pathways. Cell 117: 69-81.

Levy, A., M. Dafny-Yelin and T. Tzfira. 2008. Attacking the defenders: plant viruses fight back. Trends Microbiol. 16: 194–197.

Lewsey, M., F. C. Robertson, T. Canto, P. Palukaitis and J. P. Carr. 2007. Selective targeting of miRNA-regulated plant development by a viral counter-silencing protein. Plant J. 50: 240-252.

Li, F. and S. W. Ding. 2006. Virus counterdefense: diverse strategies for evading the RNA silencing immunity. Annu. Rev. Microbiol. 60: 503-531.

Li, H. W., A. P. Lucy, H. S. Guo, W. X. Li, L. H. Ji, S. M. Wong and S. W. Ding. 1999. Strong host resistance targeted against a viral suppressor of the plant gene silencing defence mechanism. EMBO J. 18: 2683–2691.

Li, H., W. X. Li and S. W. Ding, 2002. Induction and suppression of RNA silencing by an animal virus. Science 296: 1319–1321.

Li, J., Z. Yang, B. Yu, J. Liu and X. Chen. 2005. Methylation protects miRNAs and siRNAs from a 3′-end uridylation activity in *Arabidopsis*. Curr. Biol. 15: 1501–1507.

Lin, L. , Y. Shi, Z. Luo, Y. Lu, H. Zheng, F. Yan, J. Chen, M. Adams and Y. Wu. 2009. Protein-protein interactions in two potyviruses using the yeast two-hybrid system. Virus Res. 142: 36–40.

Lindbo, J. A., L. Silva-Rosales, W. M. Proebsting and W. G. Dougherty. 1993. Induction of a highly specific antiviral state in transgenic plants: implications for regulation of gene expression and virus resistance. Plant Cell 5: 1749–1759.

Liu, Q., T. A. Rand, S. Kalidas, F. Du, H. E. Kim, D. P. Smith and X. Wang. 2003. R2D2, a bridge between the initiation and effector steps of the Drosophila RNAi pathway. Science 301: 1921-1925.

Llave C. 2010. Virus-derived small interfering RNAs at the core of plant-virus interactions. Trends Plant Sci. 15: 701–707.

Lleave, C., K. D. Kasschau and J. C. Carrington. 2000. Virus-encoded suppressor of posttranscriptional gene silencing targets a maintenance step in the silencing pathway. Proc. Natl. Acad. Sci. USA 97: 13401-13406.

Lleave, C., K. D. Kasschau, M. A. Rector and J. C. Carrington. 2002a. Endogenous and silencing associated small RNAs in plants. Plant Cell 14: 1605-1619.

Lleave, C., Z. Xie, K. D. Kasschau and J. C. Carrington. 2002b. Cleavage of Scarecrow-like mRNA targets directed by a class of Arabidopsis miRNA. Science 297: 2053-2056.

Lózsa, R., T. Csorba, L. Lakatos and J. Burgyan. 2008. Inhibition of 3' modification of small RNAs in virus infected plants require spatial and temporal co-expression of small RNAs and viral silencing suppressor proteins. Nucleic Acids Res. 36: 4099–4107.

Lu, R., A. M. Martin-Hernandez, J. R. Peart, I. Malcuit and D. C. Baulcombe. 2003. Virus-induced gene silencing in plants. Methods 30: 296-303.

Lucy, A. P., H. S. Guo, W. X. Li and S. W. Ding. 2000. Suppression of posttranscriptional gene silencing by a plant viral protein localized in the nucleus. EMBO J. 7: 1672-1680.

Maia, I. G. and F. Bernardi. 1996. Nucleic acid-binding properties of a bacterially expressed potato virus Y helper component-proteinase. J. Gen. Virol. 77: 869–877.

Mallory, A. C., L. Ely, T. H. Smith, R. Marathe, R. Anandalakshmi, M. Fagard, H. Vaucheret, G. Pruss, L. Bowman and V. B. Vance. 2001. HC-Pro suppression of transgene silencing eliminates the small RNAs but not transgene methylation or the mobile signal. Plant Cell 13: 571–583.

Mallory, A.C., A. Hinze, M. R. Tucker, N. Bouche´, V. Gasciolli, T. Elmayan, D. Lauressergues, V. Jauvion, H. Vaucheret and T. Laux. 2009. Redundant and specific roles of the ARGONAUTE proteins AGO1 and ZLL in development and small RNA-directed gene silencing. PLoS Genet. 5: e1000646.

Mallory, A. C., B. J. Reinhart, D. Bartel, V. B. Vance and L. H. Bowman. 2002. A viral suppressor of RNA silencing differentially regulates the accumulation of short interfering RNAs and microRNAs in tobacco. Proc. Natl. Acad. Sci. USA 99: 15228-15233.

Mallory, A. C., S. Mlotshwa, L. H. Bowman and V. B. Vance. 2003. The capacity of transgenic tobacco to send a systemic RNA silencing signal depends on the nature of the inducing transgene locus. Plant J. 35: 82-92.

Mallory, A. C., D. V. Dugas, D. B. Bartel and E. Bartel. 2004. MicroRNA regulation of NAC-domain targets is required for proper formation and separation of adjacent embryonic, vegetative, and floral organs. Curr. Biol. 14: 1035-1046

Mallory, A. C. and H. Vaucheret. 2004. MicroRNAs: something important between the genes. Curr. Opin. Plant Biol. 7: 120-125.

Mallory, A. and H. Vaucheret. 2010. Form, function, and regulation of ARGONAUTE proteins. Plant Cell 22: 3879–3889.

Margis, R., A. F. Fusaro, N. A. Smith, S. J. Curtin, J. M. Watson, E. J. Finnegan and P. M. Waterhouse. 2006. The evolution and diversification of Dicers in plants. FEBS Lett. 580: 2442–2450.

Martínez-Priego, L., L. Donaire, D. Barajas and C. Llave. 2008. Silencing suppressor activity of the Tobacco rattle virus-encoded 16-kDa protein and interference with endogenous small RNA-guided regulatory pathways. Virology 376: 346–356.

Matzke, M., W. Aufsatz, T. Kanno, L. Daxinger, I. Papp, M. F. Mette and A. J. Matzke. 2004. Genetic analysis of RNA mediated transcriptional gene silencing. Biochim. Biophys. Acta 1677: 129-141.

Mérai, Z., Z. Kerenyi, A. Molnar, A. Barta, A. Valoczi, G. Bisztray, Z. Havelda, J. Burgyán and D. Silhavy. 2005. Aureusvirus P14 is an efficient RNA silencing suppressor that binds double-stranded RNAs without size specificity. J. Virol. 79: 7217-7226

Mérai, Z., Z. Kerényi, S. Kertész, M. Magna, L. Lakatos and D. Silhavy. 2006. Double-stranded RNA binding may be a general plant RNA viral strategy to suppress RNA silencing. J. Virol. 80: 5747-5756.

Mette, M. F., W. Aufsatz, J. van der Winden, M. A. Matzke and A. J. Matzke. 2000. Transcriptional silencing and promoter methylation triggered by double-stranded RNA. EMBO J. 19: 5194- 5201.

Mi, S., T. Cai, Y. Hu, Y. Chen, E. Hodges, F. Ni, L. Wu, S. Li, H. Zhou, C. Long, S. Chen, G. J. Hannon and Y. Qi. 2008. Sorting of small RNAs into *Arabidopsis* Argonaute complexes is directed by the 5´terminal nucleotide. Cell 133: 116-127.

Millar, A. A. and F. Gubler. 2005. The *Arabidopsis* GAMYB -like genes, MYB33 and MYB65, are microRNA-regulated genes that redundantly facilitate anther development. Plant Cell 17: 705-721.

Mlotshwa, S. W., J. Verver, I. Sithole-Niang, K. Gopinath, J. Carette, A. V. Kammen, and J. Wellink. 2002. Subcellular location of the helper component–proteinase of Cowpea aphid–borne mosaic virus. Virus Genes 25: 207-216.

Mlotshwa, S., S. E. Schauer, T. H. Smith, A. C. Mallory, J. M. Herr Jr., B. Roth, D. S. Merchant, A. Ray, L. H. Bowman and V. B. Vance. 2005. Ectopic DICER-LIKE1 expression in P1/HC-Pro *Arabidopsis* rescues phenotypic anomalies but not defects in microRNA and silencing pathways. Plant Cell 17: 2873-2885.

Mlotshwa, S., G. J. Pruss, A. Peragine, M. W. Endres, J. Li, X. Chen, R. S. Poethig, L. H. Bowman and V. Vance. 2008. DICER-LIKE2 plays a primary role in transitive silencing of transgenes in *Arabidopsis*. PLoS ONE 3: e1755.

Montgomery, T.A., M. D. Howell, J. T. Cuperus, D. Li, J. E. Hansen, A. L. Alexander, E. J. Chapman, N. Fahlgren, E. Allen and J. C. Carrington. 2008. Specificity of ARGONAUTE7-miR390 interaction and dual functionality in TAS3 trans-acting siRNA formation. Cell 133: 128–141.

Morel, J. B., C. Godon, P. Mourrain, C. Beclin, C. Boutet, F. Feuerbach, F. Proux and H. Vaucheret. 2002. Fertile hypomorphic ARGONAUTE ago1 mutants impaired in post-transcriptional gene silencing and virus resistance. Plant Cell 14: 629-639.

Morris, K. V. 2009. RNA-directed control of transcription in human cells: specifically turning genes on or off. Gene Therapy and Regulation 4: 1–10.

Moser, M. 2010. Gene expression analysis in *Candidatus* phytoplasma mali-resistant and -susceptible Malus genotypes. Dissertation, University of Mainz, Germany.

Mourrain, P., C. Beclin, T. Elmayan, F. Feuerbach, C. Godon, J. B. Morel, D. Jouette, A. M. Lacombe, S. Nikic, N. Picault, K. Rémoué, M. Sanial, T. A. Vo and H. Vaucheret. 2000. Arabidopsis SGS2 and SGS3 genes are required for posttranscriptional gene silencing and natural virus resistance. Cell 101: 533-542.

Mukherjee, K., Y. Verma, S. K. Chakrabarti, S. M. P. Khurana. 2004. Phylogenetic analysis of 5′-UTR and P1 protein of Indian common strain of potato virus Y reveals its possible introduction in India. Virus Genes 29: 229–237.

Nayak, A., B. Berry, M. Tassetto, M. Kunitomi, A. Acevedo, C. Deng, A. Krutchinsky, J. Gross, C. Antoniewski and R. Andino. 2010. Cricket paralysis virus antagonizes Argonaute 2 to modulate antiviral defense in Drosophila. Nat. Struct. Mol. Biol. 17: 547- 554.

Nykänen, A., B. Haley and P. D. Zamore. 2001. ATP requirements and small interfering RNA structure in the RNA interference pathway. Cell 107: 309-321.

Okamura, K., A. Ishizuka, H. Siomi, M. C. Siomi. 2004. Distinct roles for Argonaute proteins in small RNA directed RNA cleavage pathways. Genes Dev. 18: 1655-1666.

Omarov, R. T., J. J. Ciomperlik and H. B. Scholthof. 2007. RNAi-associated ssRNA-specific ribonucleases in Tombusvirus P19 mutant-infected plants and evidence for a discreate srRNA-containing effector complex. Proc. Natl. Acad. Sci. USA 104: 1714-1719.

Omer, A. D., S. Ziesche, H. Ebhardt and P. P. Dennis. 2002. In vitro reconstitution and activity of a C/D box methylation guide ribonucleoprotein complex. Proc. Natl. Acad. Sci. USA 99: 5289-5294.

Palatnik, J. F., E. Allen, X. Wu, C. Schommer, R. Schwab, J. C. Carrington and D. Weigel. 2003. Control of leaf morphogenesis by microRNAs. Nature 425: 257-263.

Palauqui, J. C., T. Elmayan, J. M. Pollien and H. Vaucheret. 1997. Systemic acquired silencing: transgene-specific post-transcriptional silencing is transmitted by grafting from silenced stocks to nonsilenced scions. EMBO J. 16: 4738-4745.

Pantaleo, V., G. Szittya and J. Burgyan. 2007. Molecular bases of viral RNA targeting by viral small interfering RNA-programmed RISC. J. Virol. 81: 3797-3806.

Papaefthimiou, I., A. J. Hamilton, M. A. Denti, D. C. Baulcombe, M. Tsagris and M. Tabler. 2001. Replicating potato spindle tuber viroid RNA is accompanied by short RNA fragments that are characteristic of posttranscriptional gene silencing. Nucleic Acids Res. 29: 2395–2400.

Parizotto, E. A., P. Dunoyer, N. Rahm, C. Himber and O. Voinnet. 2004. In vivo investigation of the transcription, processing, endonucleolytic activity, and functional relevance of the spatial distribution of a plant miRNA. Genes Dev. 18: 2237-2242.

Park, W., J. Li, R. Song, J. Messing and X. Chen. 2002. CARPEL FACTORY, a Dicer homolog, and HEN1, a novel protein, act in microRNA metabolism in Arabidopsis thaliana. Curr. Biol. 12: 1484–1495.

Pazhouhandeh, M., M. Dieterle, K. Marrocco, E. Lechner, B. Berry, V. Brault, O. Hemmer, T. Kretsch, K. E. Richards, P. Genschik and V. Ziegler-Graff. 2006. F-box-like domain in the polerovirus protein P0 is required for silencing suppressor function. Proc. Natl. Acad. Sci. USA 103: 1994–1999.

Peirson, S. N., J. N. Butler and R. G. Foster. 2003. Experimental validation of novel and conventional approaches to quantitative real-time PCR data analysis. Nucleic Acids Res. 31: e73.

Peragine, A., M. Yoshikawa, G. Wu, H. L. Albrecht and R. S. Poething. 2004. SGS3 and SGS2/SDE1/RDR6 are required for juvenile development and the production of trans-acting siRNAs in *Arabidopsis*. Genes Dev. 18: 2368-2379.

Peremyslov, V. V., Y. W. Pan and V. V. Dolja. 2004. Movement protein of a closterovirus is a type III integral transmembrane protein localized to the endoplasmic reticulum. J. Virol. 78: 3704–3709.

Petty, I. T., R. French, R. W. Jones and A. O. Jackson. 1990. Identification of Barley stripe mosaic virus genes involved in viral RNA replication and systemic movement. EMBO J. 9: 3453–3457.

Pfeffer, S., P. Dunoyer, F. Heim, K. E. Richards, G. Jonard and V. Ziegler-Graff. 2002. P0 of beet Western yellows virus is a suppressor of posttranscriptional gene silencing. J. Virol. 76: 6815–6824.

Pirone, T. and S. Blanc. 1996. Helper-dependent vector transmission of plant viruses. Annu. Rev. Phytopathol. 34: 227-247.

Plisson, C., M. Drucker, S. Blanc, S. German-Retana, O. Le Gall, D. Thomas and P. Bron. 2003. Structural characterization of HC-Pro, a plant virus multifunctional protein. J. Biol. Chem. 278: 23753–23761.

Pruss, G., X. Ge, X. M. Shi, J. C. Carrington and V. B. Vance. 1997. Plant viral synergism: the potyviral genome encodes a broad-range pathogenicity enhancer that transactivates replication of heterologous viruses. Plant Cell 9: 859-868.

Qi, Y., X. He, X. J. Wang, O. Kohany, J. Jurka and G. J. Hannon. 2006. Distinct catalytic and noncatalytic roles of ARGONAUTE4 in RNA-directed DNA methylation. Nature 443: 1008-1012.

Qu, F., T. Ren and T. J. Morris. 2003. The coat protein of Turnip crinkle virus suppresses posttranscriptional gene silencing at an early initiation step. J. Virol 77: 511–522.

Qu, F., X. Ye and T. J. Morris. 2008. Arabidopsis DRB4, AGO1, AGO7, and RDR6 participate in a DCL4-initiated antiviral RNA silencing pathway negatively regulated by DCL1. Proc. Natl. Acad. Sci. USA 105: 14732-14737.

Rajamaki, M. L., J. Kelloniemi, A. Alminaite, T. Kekarainen, F. Rabenstein and J. P. Valkonen. 2005. A novel insertion site inside the potyvirus P1 cistron allows expression of heterologous proteins and suggests some P1 functions. Virology 342: 88-101.

Rakesh, C. 1996. Preparation of electro-competent E. coli using salt-free growth medium. Biotechniques 20: 42-44.

Ramachandran, V. and X. Chen. 2008. Degradation of microRNAs by a family of exoribonucleases in Arabidopsis. Science 321: 1490–1492.

Ratcliff, F. G., S. A. MacFarlane and D. C. Baulcombe. 1999. Gene silencing without DNA. RNA-mediated cross-protection between Posttranscriptional gene silencing viruses. Plant Cell 11: 1207–1216.

Reed, J.C., K. D. Kasschau, A. I. Prokhnevsky, K. Gopinath, G. P. Pogue, J. C. Carrington and V. V. Dolja. 2003. Suppressor of RNA silencing encoded by Beet yellows virus. Virology 306: 203–209.

Reinhart, B., E. G. Weinstein, M. W. Rhoades, B. Bartel and D. P. Bartel. 2002. MicroRNAs in plants. Genes Dev. 16: 1616-1626.

Riedel, D., D. Lesemann and E. Maiss. 1998. Ultrastructural localization of nonstructural and coat proteins of 19 potyviruses using antisera to bacterially expressed proteins of plum pox potyvirus. Arch. Virol. 143: 2133–2158.

Rivas, F. V., N. H. Tolia, J. J. Song, J. P. Aragon, J. Liu, G. J. Hannon and L. Joshua-Tor. 2005. Purified Argonaute2 and an siRNA form recombinant human RISC. Nat. Struct. Mol. Biol. 12: 340-349.

Rohožková J. and M. Navrátil. 2011. P1 peptidase – a mysterious protein of family Potyviridae. J. Biosci. 36: 189–200.

Roth, B. M., G. J. Pruss and V. B. Vance. 2004. Plant viral suppressors of RNA silencing. Virus Research 102: 97–108.

Ruijter, J. M., C. Ramakers, W. M. Hoogaars, Y. Karlen, O. Bakker, M. J. van den Hoff and A. F. Moorman. 2009. Amplification efficiency: linking baseline and bias in the analysis of quantitative PCR data. Nucleic Acids Res 37: e45

Ruiz, F., L. Vavssie, C. Klotz, L. Sperling and L. Madeddu. 1998. Homology dependent gene silencing in *Paramecium*. Mol. Biol. Cell 9: 931-943.

Ruiz-Ferrer, V. and O. Voinnet. 2009. Roles of plant small RNAs in biotic stress responses. Annu Rev Plant Biol 60: 485–510.

Ruiz-Ferrer, V., J. Boskovic, C. Alfonso, G. Rivas, O. Llorca, D. Lopez-Abella and J. J. Lopez-Moya. 2005. Structural analysis of tobacco etch potyvirus HC-Pro oligomers involved in aphid transmission. J. Virol. 79: 3758–3765.

Saenz, P., B. Salvador, C. Simon-Mateo, K. D. Kasschau, J. C. Carrington and J. A. Garcia. 2002. Host-specific involvement of the HC protein in the long-distance movement of Potyviruses. J. Virol. 76: 1922–1931.

Samuels, T. D., H. J. Ju, C. M. Ye, C. M. Motes, E. B. Blancaflor and J. Verchot-Lubicz. 2007. Potato virus X TGBp1 protein accumulates independently of TGBp2 and TGBp3 to promote virus cell-to-cell movement. Virology 367: 375–389.

Schiebel, W., B. Haas, S. Marinkovic, A. Klanner and H. L. Sänger. 1993. RNA-directed RNA polymerase from tomato leaves. I. Purification and physical properties. J. Biol. Chem. 268: 11851-11857.

Schob, H., C. Kunz and F. Jr. Meins. 1997. Silencing of transgenes introduced into leaves by agroinfiltration: a simple, rapid method for investigation of sequence requirements for gene silencing. Mol. Gen. Genet. 256: 581-585.

Schwach, F., F. E. Vaistij, L. Jones and D. Baulcombe. 2005. An RNA-dependent RNA-polymerase prevents meristem invasion by Potato virus X and is required for the activity but not the production of a systemic silencing signal. Plant Physiol. 138: 1842-1852.

Shams-Bakhsh, M., T. Canto and P. Palukaitis. 2007. Enhanced resistance and neutralization of defence responses by suppressors of RNA silencing. Virus Res. 130: 103–109.

Shen, D., Sh. Wang, H. Chen, Q-H. Zhu, Ch. Helliwell and L. Fan. 2009. Molecular phylogeny of miR390-guided trans-acting siRNA genes (*TAS3*) in the grass family Plant Syst Evol 283: 125-132.

Shi, H., C. Tschudi and E. Ullu. 2006. Functional replacement of *Trypanosoma brucei* Argonaute by the human slicer Argonaute2. RNA 12: 943–947.

Shi, X. M., H. Miller, J. Verchot, J. C. Carrington and V. B. Vance. 1997. Mutations in the region encoding the central domain of helper componentproteinase HC-Pro eliminate potato virus X/potyviral synergism. Virology 231: 35–42.

Shiboleth, Y. M., E. Haronsky, D. Leibman, T. Arazi, M. Wassenegger, S. A. Whitham, V. Gaba and A. Gal-On. 2007. The Conserved FRNK box in HC-Pro, a plant viral suppressor of gene silencing, is required for small RNA binding and mediates symptom development. J. Virol. 81: 13135–13148.

Siddiqui, S. A., C. Sarmiento, E. Truve, H. Lehto and K. Lehto. 2008. Phenotypes and functional effects caused by various viral RNA silencing suppressors in transgenic *Nicotiana benthamiana* and *N. tabacum*. Mol. Plant Microbe Interact. 21: 178-187.

Sijen, T. and R. H. Plasterk. 2003. Transposon silencing in the *Caenorhabditis elegans* germ line by natural RNAi. Nature 426: 310-314.

Silhavy, D., A. Molnar, A. Lucioli, G. Szittay, C. Hornyik, M. Tavazza and J. Burgyan. 2002. A viral protein suppresses RNA silencing and binds silencing-generated, 21- to 25-nucleotide doublestranded RNAs. EMBO J. 21: 3070-3080.

Smith N. A., S. P. Singh, M. B. Wang, P. A. Stoutjesdijk, A. G. Green and P. M. Waterhouse. 2000. Total silencing by intron-spliced hairpin RNAs. Nature 407: 319-320.

Soitamo, A. J., B. Jada and K. Lehto. 2011. HC-Pro silencing suppressor significantly alters the gene expression profile in tobacco leaves and flowers. BMC Plant Biol. 11: 68.

Song, J. J. and L. Joshua-Tor. 2006. Argonaute and RNA-getting into the groove. Curr. Opin. Struct. Biol. 16: 5-11.

Stenger, D. C., R. French and F. E. Gildow. 2005. Complete deletion of wheat streak mosaic virus HC-Pro: a null mutant is viable for systemic infection. J. Virol. 79: 12077–12080.

Syller, J. 2006. The roles and mechanisms of helper component proteins encoded by potyviruses and caulimoviruses. Physiol. Mol. Plant Pathol. 67: 119-130.

Szittya, G., D. Silhavy, T. Dalmay and J. Burgyan. 2002. Sizedependent cell-to-cell movement of defective interfering RNAs of Cymbidium ringspot virus. J. Gen. Virol. 83: 1505–1510.

Takeda, A., M. Tsukuda, H. Mizumoto, K. Okamoto., M. Kaido, K. Mise and T. Okuno. 2008. A plant RNA virus suppresses RNA silencing through viral RNA replication. EMBO J. 24: 3147–3157.

Tang, G., B. J. Reinhart, D. Bartel and P. D. Zamore. 2003. A biochemical framework for RNA silencing in plants. Genes Dev. 17: 49-63.

Temin, H. M. and S. Mizutani. 1970. RNA-dependent DNA polymerase in virions of Rous sarcoma virus. Nature 226: 1211-1213.

Tessitori, M., G. Maria, C. Capasso, G. Catara, S. Rizza, V. De Luca, A. Catara, A. Capasso and V. Carginale. 2007. Differential display analysis of gene expression in Ertog citron leaves infected by Citrus Viroid III. Biochim. Biophys. Acta 1769: 228-235.

Thornbury, D., G. Hellmann, R. Rhoads and T. Pirone. 1985. Purification and characterization of potyvirus helper component. Virology 14: 260–267.

Thorpe, G. H. and L. J. Kricka. 1986. Enhanced chemiluminescent reactions catalyzed by horseradish peroxidase. Methods Enzymol. 133: 331-353.

Tijsterman, M., R. F. Ketting, K. L. Okihara, T. Sijen and R. H. Plasterk. 2002. RNA helicase MUT-14-dependent gene silencing triggered in *C. elegans* by short antisense RNAs. Science 295: 694–697.

Tkaczuk, K., A. Obarska and J. Bujnicki. 2006. Molecular phylogenetics and comparative modeling of HEN1, a methyltransferase involved in plant microRNA biogenesis. BMC Evol. Biol. 6: 6.

Torres-Barcelo, C., S. Martin, J. A. Daros and S. F. Elena. 2008. From hypo- to hypersuppression: effect of amino acid substitutions on the RNA-silencing suppressor activity of the Tobacco etch potyvirus HCPro. Genetics 180: 1039-1049.

Trinks, D., R. Rajeswaran, P. V. Shivaprasad, R. Akbergenov, E. J. Oakeley, K. Veluthambi, T. Hohn and M. M. Pooggin. 2005. Suppression of RNA silencing by a geminivirus nuclear protein, AC2, correlates with transactivation of host genes. J. Virol. 79: 2517–2527.

Urcuqui-Inchima, S., J. Walter, G. Drugeon, S. German-Retana, A. L. Haenni, T. Candresse, F. Bernardi and O. Le Gall. 1999. Potyvirus helper component-proteinase self-interaction in the yeast two-hybrid system and delineation of the interaction domain involved. Virology 258: 95–99.

Urcuqui-Inchima, S., I. G. Maia, P. Arruda, A. L. Haenni and F. Bernardi. 2000. Deletion mapping of the potyviral helper component-proteinase reveals two regions involved in RNA binding. Virology 268: 104–111.

Vaistij, F. E., L. Jones and D. C. Baulcombe. 2002. Spreading of RNA targeting and DNA methylation in RNA silencing requires transcription of the target gene and a putative RNA-dependent RNA polymerase. Plant Cell 14: 857-867.

Valli, A., A. M. Martin-Hernandez, J. J, Lopez-Moya and J. A. Garcia. 2006. RNA silencing suppression by a second copy of the P1 serine protease of Cucumber vein yellowing ipomovirus, a member of the family Potyviridae that lacks the cysteine protease HCPro. J. Virol. 80: 10055-10063.

Valoczi, A., E. Varallyay, S. Kauppinen, J. Burgyan and Z. Havelda. 2006. Spatio-temporal accumulation of microRNAs is highly coordinated in developing plant tissues. Plant J. 47: 140-151.

Valverde, R. A., C. A. Clark and J. P. T. Valkonen. 2007. Viruses and Virus Disease Complexes of Sweetpotato. Plant Viruses ©2007 Global Science Books .

van der Krol, A. R., L. A. Mur, M. Beld, J. N. Mol and A. R. Stuitje. 1990. Lavonoid genes in petunia: addition of a limited number of gene copies may lead to a suppression of gene expression. Plant Cell 2: 291-299.

van Engelen, F. A., J. W. Molthoff, A. J. Conner, J. P. Nap, A. Peereira and W. J. Stiekema. 1995. pBINPLUS: an improved plant transformation vector based on pBIN19. Transgenic Res. 4: 288-290.

Vargason, J. M., G. Szittya, J. Burgyán and T. M. T. Hall. 2003. Size selective recognition of siRNA by an RNA silencing suppressor. Cell 115: 799–811.

Vastenhouw, N. L., K. Brunschwig K. L. Okihara, F. Muller, M. Tijsterman and R. H. Plasterk. 2006. Gene expression: Long-term gene silencing by RNAi. Nature 442:882.

Vaucheret, H., F. Vazquez, P. Crete and D. P. Bartel. 2004. The action of ARGONAUTE1 in the miRNA pathway and its regulation by the miRNA pathway are crucial for plant development. Genes Dev. 18: 1187-1197.

Vaucheret, H. 2006. Post-transcriptional small RNA pathways in plants: mechanisms and regulations. Genes Dev. 20: 759-771.

Vaucheret, H., A. C. Mallory and D. P. Bartel. 2006. AGO1 homeostasis entails coexpression of MIR168 and AGO1 and preferential stabilization of miR168 by AGO1. Mol. Cell 22: 129–136.

Verchot, J., K. L. Herndon and J. C. Carrington. 1992. Mutational analysis of the tobacco etch potyviral 35-kDa proteinase: identification of essential residues and requirements for autoproteolysis. Virology 190: 298–306.

Vogel, F., D. Hofius and U. Sonnewald. 2007. Intracellular Trafficking of Potato Leafroll Virus Movement Protein in Transgenic Arabidopsis. Traffic. 8: 1205–1214.

Vogler, H., R. Akbergenov, P. V. Shivaprasad, V. Dang, M. Fasler, M. O. Kwon, S. Zhanybekova, T. Hohn and M. Heinlein. 2007. Modification of small RNAs associated with suppression of RNA silencing by Tobamovirus replicase protein. J. Virol. 81: 10379–10388.

Vogt, U., T. Pélissier, A. Pütz, F. Razvi, R. Fischer and M. Wassenegger. 2004. Viroid-induced RNA silencing of GFP-viroid fusion transgenes does not induce extensive spreading of methylation or transitive silencing. Plant J. 38: 107-118.

Voinnet, O., Y. M. Pinto and D. C. Baulcombe. 1998. Systemic spread of sequence-specific transgene RNA degradation is inititated by localized introduction of ectopic promoterless DNA. Cell 95: 177-187.

Voinnet, O., Y. M. Pinto and D. C. Baulcombe. 1999. Suppression of gene silencing: a general strategy used by diverse DNA and RNA viruses of plants. Proc. Natl. Acad. Sci. USA 96: 14147–14152.

Voinnet, O., C. Lederer and D. C. Baulcombe. 2000. A viral movement protein prevents spread of the gene silencing signal in *Nicotiana benthamiana*. Cell 103: 157-167.

Voinnet, O. 2001. RNA silencing as a plant immune system against viruses. Trends Genet. 17: 449- 459.

Voinnet, O. 2009. Origin, biogenesis, and activity of plant microRNAs. Cell 136: 669-687

Voinnet, O., S. Rivas, P. Mestre and D. Baulcombe. 2003. An enhanced transient expression system in plants based on suppression of gene silencing by the p19 protein of tomato bushy stunt virus. Plant J. 33: 949–956.

Voinnet, O. 2005. Induction and suppression of RNA silencing: insights from viral infections. Nat. Rev. Genet. 6: 206-220.

Wang, H., L. Hao, C. Y. Shung, G. Sunter and D. M. Bisaro. 2003. Adenosine kinase is inactivated by geminivirus AL2 and L2 proteins. Plant Cell 15: 3020–3032.

Wang, H., K. J. Buckley, X. Yang, R. C. Buchmann and D. M. Bisaro.2005. Adenosine kinase inhibition and suppression of RNA silencing by geminivirus AL2 and L2 proteins. J. Virol. 79: 7410–7418.

Wang, R. Y. and T. P. Pirone. 1999. Purification and characterization of turnip mosaic virus helper component protein. Phytopathology 89: 564–567.

Wang, Y., V. Gaba, J. Yang, P. Palukaitis and A. Gal-On. 2002. Characterization of synergy between cucumber mosaic virus and potyviruses in cucurbit hosts. Phytopathology 92: 51–58.

Wang, Y., T. Tzfira, V. Gaba, V. Citovsky, P. Palukaitis and A. Gal-On. 2004. Functional analysis of the Cucumber mosaic virus 2b protein: Pathogenicity and nuclear localization. J. Gen. Virol. 85: 3135-3147.

Wang, X. B., Q. Wu, T. Ito, F. Cillo, W. X. Li, X. Chen, J. L. Yu and S. W. Ding. 2010. RNAi-mediated viral immunity requires amplification of virus-derived siRNAs in Arabidopsis thaliana. Proc. Natl. Acad. Sci. USA 107: 484–489.

Wassenegger, M., S. Heimes, L. Riedel and H. L. Sanger. 1994. RNA-directed de novo methylation of genomic sequences in plants. Cell 76: 567–576.

Wassenegger, M. 2000. RNA-directed DNA methylation. Plant Mol. Biol. 43: 203–220.

Wassenegger, M. and G. Krczal. 2006. Nomenclature and functions of RNA-directed RNA polymerases. Trends Plant Sci. 113: 142-151.

Waterhouse, P. M., M. B. Wang and E. J. Finnegan. 2001. Role of short RNAs in gene silencing. Trends Plant Sci. 6: 297-301.

Weiner, M. P., G. L. Costa, W. Schoettlin, J. Cline, E. Mathur and J. C. Bauer. 1994. Site-directed mutagenesis of double-stranded DNA by the polymerase chain reaction. Gene 151: 119-123.

Wicker, T. 1950. The origin and behavior of mutable loci in maize. Proc. Natl. Acad. Sci. USA 366: 344–355.

Wu, H. W., S. S. Lin, K. C. Chen, S. D. Yeh and N. H. Chua. 2010. Discriminating mutations of HC-Pro of Zucchini yellow mosaic virus with differential effects on small RNA pathways involved in viral pathogenicity and symptom development. Mol. Plant Microbe Interact. 23: 17-28.

Xie, Z., K. D. Kasschau and J. C. Carrington. 2003. Negative feedback regulation of Dicer-Like1 in Arabidopsis by microRNA-guided mRNA degradation. Curr. Biol. 13: 784-789.

Xie, Z., L. K. Johansen, A. M. Gustafson, K. D. Kasschau, A. D. Lellis, D. Zilberman, S. E. Jacobsen and J. C. Carrington. 2004. Genetic and functional diversification of small RNA pathways in plants. PLoS Biol. 2: e104.

Yaegashi, H., T. Takahashi, M. Isogai, T. Kobori, S. Ohki and N. Yoshikawa. 2007. Apple chlorotic leaf spot virus 50 kDa movement protein acts as a suppressor of systemic silencing without interfering with local silencing in Nicotiana benthamiana. J. Gen. Virol. 88: 316-324.

Yambao, M. L., H. Yagihashi, H. Sekiguchi, T. Sekiguchi, T. Sasaki, M. Sato,G. Atsumi, Y. Tacahashi, K. S. Nakahara and I. Uyeda. 2008. Point mutations in helper component protease of Clover yellow vein virus are associated with the attenuation of RNA-silencing suppression activity and symptom expression in broad bean. Arch. Virol. 153: 105-115.

Yang, Z., Y. W. Ebright, B. Yu and X. Chen. 2006. HEN1 recognizes 21-24 nt small RNA duplexes and deposits a methyl group onto the 2′ OH of the 3′ terminal nucleotide. Nucleic Acids Res. 34: 667-675.

Ye, K. and D. J. Patel. 2005. RNA silencing suppressor p21 of beet yellows virus forms an RNA binding octameric ring structure. Structure 13: 1375–1384.

Ye, K., L. Malinina and D. J. Patel. 2003. Recognition of small interfering RNA by a viral suppressor of RNA silencing. Nature 426: 874–878.

Yekta, S., I. h. Shih and D. P. Bartel. 2004. MicroRNA-directed cleavage of *HOXB8* mRNA. Science 304: 594-596.

Yelina, N. E., E. I. Savenkov, A. G. Solovyev, S. Y. Morozov and J. P. Valkonen. 2002. Long-distance movement, virulence and RNA silencing suppression controlled by a single protein in hordei- and potyviruses: complementary functions between virus families. J. Virol. 76: 12981–12991.

Yu, B., E. J. Chapman, Z. Yang, J. C. Carrington and X. Chen. 2006. Transgenically expressed viral RNA silencing suppressors interfere with microRNA methylation in *Arabidopsis*. FEBS Lett. 580: 3117–3120.

Yu, B., Z. Yang, J. Li, S. Minakhina, M. Yang, R. W. Padgett, R. Steward and X. Chen. 2005. Methylation as a crucial step in plant microRNA biogenesis. Science 307: 932–935.

Yu, D., B. Fan, S. A. MacFarlane and Z. Chen. 2003. Analysis of the involvement of an inducible Arabidopsis RNA-dependent RNA polymerase in antiviral defense. Mol. Plant Microbe Interact. 16: 206-216.

Zamore, P. D. 2002. Ancient pathways programmed by small RNAs. Science 296: 1265-1269.

Zamore, P. D., T. Tuschl, P. A. Sharp and D. P. Bartel. 2000. RNAi: Double-stranded RNA directs the ATP-dependent cleavage of mRNA at 21 to 23 nucleotide intervals. Cell 101: 25–33.

Zhang, X., Y. R. Yuan, S. S. Lin, T. Tuschl, D. J. Patel and N. H. Chua. 2006. Cucumber mosaic virus-encoded 2b suppressor inhibits *Arabidopsis* Argonaute1 cleavage activity to counter plant defense. Genes Dev. 20: 3255-3268.

Zheng, H., F. Yan, Y. Lu, L. Sun, L. Lin, L. Cai, M. Hou and M. Chen. 2011. Mapping the self-interacting domains of TuMV HC-Pro and the subcellular localization of the protein. Virus gene 42: 110-116.

Zilberman, D., X. Cao and S. E. Jacobsen. 2003. ARGONAUTE4 control of locus-specific siRNA accumulation and DNA and histone methylation. Science 299:716-719.

Zilberman, D., X. Cao, L. K. Johansen, Z. Xie, J. C. Carrington and S. E. Jacobsen. 2004. Role of *Arabidopsis* ARGONAUTE4 in RNA-directed DNA methylation triggered by inverted repeats. Curr. Biol. 14: 1214-1220.

6. Summary

The helper component-proteinase (HC-Pro) is a multifunctional protein found among potyviruses. It plays multiple roles in the viral infection cycle and some of these functions have been mapped to different regions of the protein. The subcellular localization of several viral RNA silencing suppressor (RSS) proteins was identified. In this study, we have shown that the Zucchini yellow mosaic virus (ZYMV) HC-Pro wild type (HC-Pro^{FRNK}) and its mutant, HC-Pro^{FINK}, had a diffuse cytoplasmic localization and formed aggregates along the endoplasmic reticulum (ER).

HC-Pro^{FRNK} and HC-Pro^{FINK} were stably expressed in *N. benthamiana* and *A. thaliana* plants. In addition, the HC-Pro^{FRNK} and HC-Pro^{FINK} were fused to a nuclear localization signal (NLS) sequence (NLS-HC-Pro^{FRNK} and NLS-HC-Pro^{FINK}) and these transgenes constructs were also stably transformed into *N. benthamiana* and *A. thaliana*. Expression of all four transgenes caused different effects in the two plant species. HC-Pro^{FRNK}–producing *A. thaliana* plants displayed severe phenotypic alterations. In *A. thaliana*, the HC-Pro^{FINK} led to a reduced number of seed set. In *N. benthamiana* expressing HC-Pro$^{FRNK/FINK}$, generally no or only slight phenotypic changes were monitored. The NLS-HC-Pro$^{FRNK/FINK}$-producing plants displayed clear phenotypes. Flower malformations and severe reduction of seed set were the most conspicuous observations made. In general, more severe developmental disturbances were observed in transgenic *A. thaliana* than in *N. benthamiana* plants.

ZYMV HC-Pro RSS activity was previously demonstrated in *N. benthamiana* plants by transient expression experiments. In this study, RSS activity was confirmed in *N. benthamiana* lines stably expressing ZYMV HC-Pro$^{FRNK/FINK}$. Notably, these plants did not show significant morphological alterations. Because the RSS activity of HC-Pro leads to enhanced transgene expression, our “symptom-free” transgenic *N. benthamiana* plants may serve as a platform for over-expression of foreign genes.

In tobacco, transient or over-expression of rgs-CaM mimicked the phenotypic effects of Tobacco etch virus (TEV) HC-Pro, indicating that TEV HC-Pro may up-regulate rgs-CaM expression. However, our data revealed no significant difference in the levels of rgs–CaM mRNA in *N. benthamiana* plants expressing HC-Pro$^{FRNK/FINK}$ when compared with the steady-state mRNA level found in the wild type plants. It is likely that RSS proteins from related viruses do not necessarily exhibit identical effects on RNA silencing. In addition, plant species might also differentially respond to identical RSS proteins.

The small RNA (sRNA) binding activity of HC-Pro was evident in *N. benthamiana* plants co-expressing the HC-Pro^{FRNK} and an infectious transgene construct of Potato spindle tuber viroid (PSTVd). In comparison to PSTVd-infected *N. benthamiana* plants, Northern

blot analysis showed increase accumulation of viroid-derived sRNAs in the double transformed plants.

There is indirect evidence showing that in plants, transient or stable expression of HC-Pro results in decreased accumulation of methylated sRNAs. In this study, we demonstrated that recombinant ZYMV HC-Pro inhibited the methyltransferase activity of the *A. thaliana* Hua enhancer 1 (AtHEN1) *in vitro*. Moreover, we found that HC-Pro^{FINK} lacking sRNA-binding activity, also inhibited AtHEN1 activity. In contrast, truncated HC-Pro and total soluble bacterial proteins did not affect AtHEN1 activity. Using enzyme-linked immunosorbent assays, we provided evidence that the HC-Pro$^{FRNK/FINK}$, both bound to AtHEN1. Our results strongly indicated that inhibition of the AtHEN1 activity by HC-Pro is probably due to direct interactions between both proteins. We concluded that AtHEN1 inhibition and sRNA-binding activities of HC-Pro are independent of each other. Using the yeast two-hybrid (Y2H) system, we could show that in contrast to RSS proteins from some other viruses, the HC-Pro$^{FRNK/FINK}$ proteins did not interact with the Argonaute 1 (AGO1) protein.

Similar to previous reports our data confirmed that HC-Pro interacts with itself to form homodimers. Notably, only HC-Pro^{FRNK} but not HC-Pro^{FINK} was able to interact with itself. The conserved FRNK box is located in the central domain of HC-Pro and this domain has been previously shown to be involved in self-interaction.

It should be noted that parts of the work have been published in:

- Jamous R. M., Boonrod K., Fuellgrabe M. W., Ali-Shtayeh M. S., Krczal G. and Wassenegger M. (2011). The HC-Pro of the *Zucchini Yellow Mosaic Virus* (ZYMV) inhibits HEN1 methytransferase activity *in vitro*. J. Gen. Virol. 92, 2222-2226.

- Fuellgrabe M., Boonrod K., Jamous R., Moser M., Shiboleth Y., Krczal G. and Wassenegger M. (2011). Expression, purification and functional characterization of recombinant Zucchini yellow mosaic virus HC-Pro. Protein Expr. Purif. 75: 40-45.

7. Zusammenfassung

Bei der „helper component-proteinase“ (HC-Pro) handelt es sich um ein multifunktionales Protein, das bei alle Potyviren nachgewiesen wurde. Dieses Protein übernimmt verschiedene Aufgaben im Infektionszyklus der Viren. Einige dieser Funktionen konnten bestimmten Regionen des Proteins zugeordnet werden. Die subzelluläre Lokalisation zahlreicher viraler „RNA silencing suppressor“ (RSS) Proteine konnte bestimmt werden. In der vorliegenden Arbeit wurde gezeigt, dass die natürliche Form der „Zucchini yellow mosaic virus“ (ZYMV) HC-Pro (HC-Pro^{FRNK}) sowie die mutierte Variante, HC-Pro^{FINK}, diffuse im Zytoplasma verteilt sind. Beide Formen bilden entlang des endoplasmatischen Retikulums Aggregate.

HC-Pro^{FRNK} und HC-Pro^{FINK} wurden stabil in *N. benthamiana* und *A. thaliana* Pflanzen exprimiert. Darüber hinaus wurden beide Proteine jeweils mit einer „nuclear localization signal“ (NLS) Sequenz verknüpft. Die daraus resultierenden NLS-HC-Pro^{FRNK} und NLS-HC-Pro^{FINK} Transgene wurden ebenfalls stabil in *N. benthamiana* und *A. thaliana* transformiert. Die Expression dieser vier Transgene löste unterschiedliche Effekte in den beiden Pflanzenarten aus. HC-Pro^{FRNK}-produzierende *A. thaliana* Pflanzen zeigten starke phänotypische Veränderungen. In *A. thaliana* führte HC-Pro^{FINK} zu einer reduzierten Anzahl von Samenansätzen. In *N. benthamiana* Pflanzen, die HC-Pro$^{FRNK/FINK}$ exprimierten, wurden generell keine oder nur sehr schwache phänotypische Veränderungen festgestellt. NLS-HC-Pro$^{FRNK/FINK}$-produzierende Pflanzen zeigten hingegen deutliche Phänotypen. Dabei wurden Missbildungen der Blüten und drastische Verringerung der Samenansätze am häufigsten beobachtet. Grundsätzlich wurden bei *A. thaliana* stärkere Entwicklungsstörungen gefunden als bei *N. benthamiana*.

Für *N. benthamiana* wurde bereits früher mittels transienter Expression nachgewiesen, dass die ZYMV HC-Pro eine RSS-Aktivität besitzt. Mit *N. benthamiana* Pflanzen, die die ZYMV HC-Pro$^{FRNK/FINK}$ Proteine stabil exprimieren, wurde in der hier vorliegenden Studie die Existenz dieser Aktivität bestätigt. Bemerkenswerterweise zeigten diese Pflanzen keine auffälligen morphologischen Veränderungen. Da die RSS-Aktivität der HC-Pro zu einer erhöhten Transgenexpression führen kann, würden sich diese „symptomfreien“, transgenen *N. benthamiana* Pflanzen gut für die Entwicklung einer Plattform zur Überexpression von fremden Genen eignen.

In Tabak täuscht die Überexpression des rgs-CaM die phänotypischen Effekte der „Tobacco etch virus“ (TEV) HC-Pro vor. Dies deutet darauf hin, dass die TEV HC-Pro die Expression der rgs-CaM hoch reguliert. Unsere Daten zeigten allerdings keine signifikanten Konzentrationsunterschiede an rgs-CaM mRNA in den HC-Pro$^{FRNK/FINK}$-exprimierenden *N.*

benthamiana Pflanzen. Es ist durchaus wahrscheinlich, dass die RSS Proteine selbst von verwandten Viren unterschiedliche Auswirkungen auf das „RNA silencing“ haben. Zudem wird vermutlich die Reaktion jeder Pflanzenart auf identische RSS Proteine unterschiedlich ausfallen.

Die Bindungsaktivität von HC-Pro für kleine RNA Moleküle (sRNAs) wurde in *N. benthamiana* Pflanzen, die gleichzeitig die HC-Pro^{FRNK} und ein infektiöses Potato spindle tuber viroid (PSTVd) Transgenkonstrukt exprimierten, eindeutig nachgewiesen. Im Vergleich zu PSTVd-infizierten *N. benthamiana* Pflanzen, zeigten „Northern blot“ Analysen mit Proben aus diesen Pflanzen eine erhöhte Akkumulation viroid-spezifischer sRNAs.

Einige Indizien sprachen dafür, dass in Pflanzen, welche die HC-Pro transient oder stabil exprimierten, geringere Mengen an methylierten sRNAs akkumulierten. Mit den hier durchgeführten *in vitro* Experimenten konnte gezeigt werden, dass die rekombinante HC-Pro die Methyltransferaseaktivität der *A. thaliana* Hua enhancer 1 (AtHEN1) inhibiert. Darüber hinaus haben wir herausgefunden, dass auch die HC-Pro^{FINK}, die keine sRNA Bindungsaktivität mehr besitzt, AtHEN1 inhibiert. Im Gegensatz dazu hatten verkürzte HC-Pro Proteine und eine Fraktion löslicher Bakterienproteine keinen Effekt auf die AtHEN1 Aktivität. Mit Hilfe von”enzyme-linked immunosorbent assays” (ELISAs) wurde der Nachweis erbracht, dass beide HC-Pro$^{FRNK/FINK}$ Proteine an die AtHEN1 binden. Unsere Ergebnisse sprechen dafür, dass die Inhibierung der AtHEN1-Aktivität durch HC-Pro auf einer direkten Interaktion zwischen den beiden Proteinen basiert. Aus diesen Resultaten lässt sich schließen, dass die Inhibierung der AtHEN1 und die sRNA-Bindungsaktivität voneinander unabhängig Eigenschaften der HC-Pro sind. Mit dem “yeast two-hybrid (Y2H) system“ konnten wir zeigen, dass die HC-Pro$^{FRNK/FINK}$ Proteine im Gegensatz zu einigen anderen viralen RSS Proteinen nicht mit Argonaute 1 (AGO1) interagieren.

Wie frühere Arbeiten, so haben auch unsere Daten gezeigt, dass HC-Pro Moleküle untereinander eine Bindung eingehen können und Homodimere bilden. Interessanterweise konnte aber nur die HC-Pro^{FRNK} nicht aber die HC-Pro^{FINK} mit sich selbst interagieren. Die konservierte FRNK Box befindet sich in der zentralen Domäne der HC-Pro, und eine Bedeutung diese Domäne für Selbstinteraktionen wurde bereits beschrieben.

Es sei erwähnt, dass Teile dieser Arbeit publiziert wurden:

- Jamous R. M., Boonrod K., Fuellgrabe M. W., Ali-Shtayeh M. S., Krczal G. and Wassenegger M. (2011). The HC-Pro of the *Zucchini Yellow Mosaic Virus* (ZYMV) inhibits HEN1 methytransferase activity *in vitro*. J. Gen. Virol. 92, 2222-2226.

- Fuellgrabe M., Boonrod K., Jamous R., Moser M., Shiboleth Y., Krczal G. and Wassenegger M. (2011). Expression, purification and functional characterization of recombinant Zucchini yellow mosaic virus HC-Pro. Protein Expr. Purif. 75: 40-45.

Appendix A: Sequence Alignment of Plant HEN1

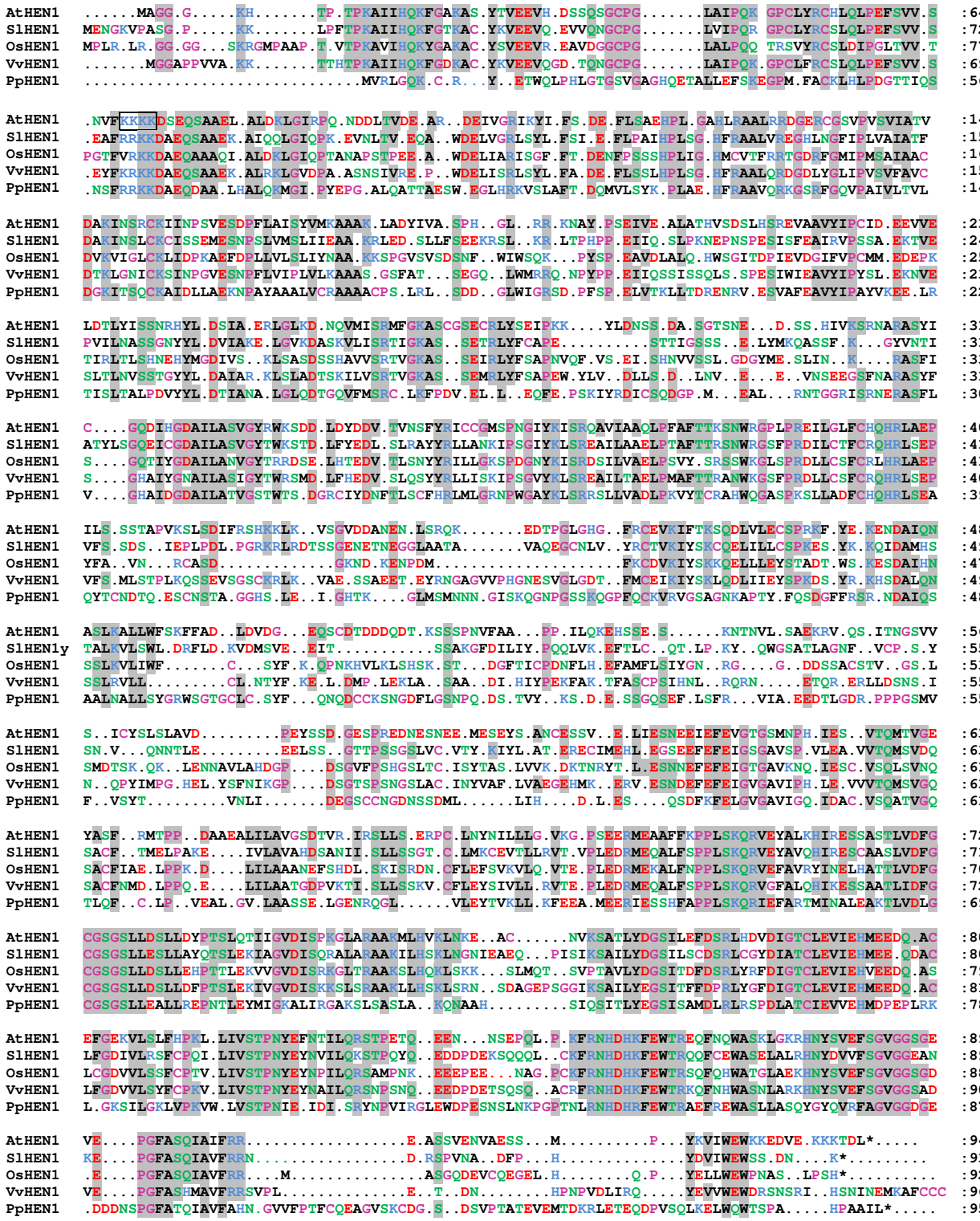

Figure A-1: Sequence alignment of plant HEN1 proteins using *A. thaliana* HEN1 sequence as proframe: At = *Arabidopsis thaliana*; Sl = *Solanum lycopersicon*; Os = *Oryza sativa*; Vv = *Vitis vinifera*; Pp = *Physcomitrella patens* subsp *Patens*. Amino acids are colored according to the physico-chemical properties of their side-chains (negatively charged in red, positively charged in blue, polar in green, hydrophobic in black, nonpolar in pink). Risidues conserved in >50% of all sequences are highlighted. A putative nuclear localization signal (NLS) is boxed.

Appendix B: Plasmid Maps

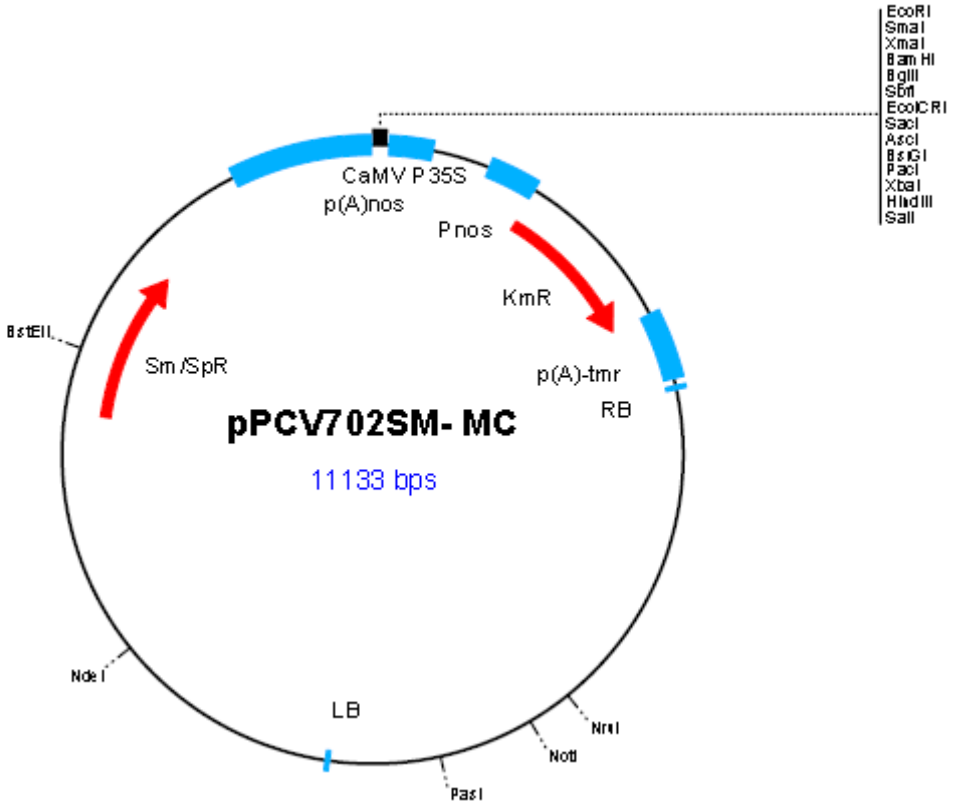

Figure B-1: Map of the pPCV702SM-MC binary vector. RB = right border; CaMV P35S = cauliflower mosaic virus (CaMV) 35S promoter; p(A)nos = nopaline synthase gene (nos) polyadenylation signal sequence; P nos = nos promoter; KmR = Kanamycine resistance; p(A)-tmr = *Agrobacterium* tumor morphology gene polyadenylation signal sequence; LB = left border; Sm/SpR = streptomycin/spectinomycin resistance.

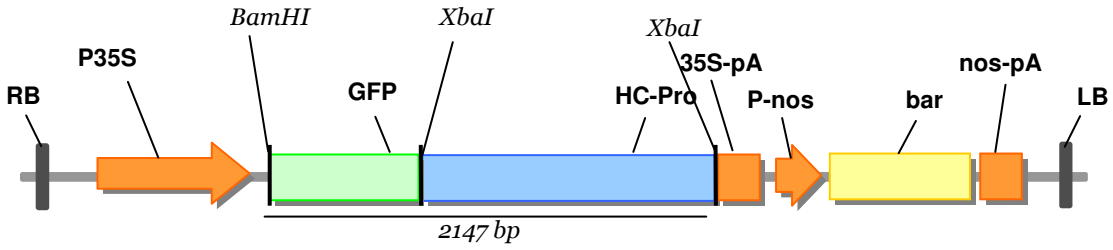

pPCV702SM:GFP-HC-Pro

Figure B-2: Schematic overview of the pPCV702SM:GFP-HC-Pro construct. RB = right border; P35S = cauliflower mosaic virus (CaMV) 35S promoter; GFP = green fluorescent protein, HC-Pro = helper component protease; 35S-pA = CaMV 35S polyadenylation signal sequence; P-nos = nopaline synthase (nos) promoter; bar = bialaphos resistance gene; nos-pA = nos polyadenylation signal sequence; LB = left border

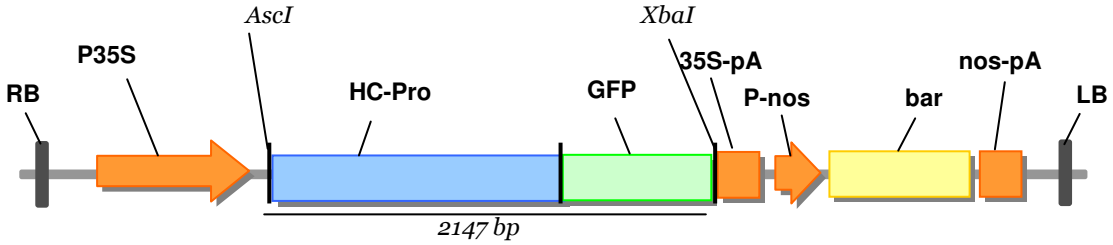

pPCV702SM-MC:HC-Pro-GFP

Figure B-3: Schematic overview of the pPCV702SM-MC:HC-Pro-GFP construct. RB = right border; P35S = cauliflower mosaic virus (CaMV) 35S promoter; HC-Pro = helper component protease; GFP = green fluorescent protein; 35S-pA = CaMV 35S polyadenylation signal sequence; P-nos = nopaline synthase gene (nos) promoter; bar = bialaphos resistance gene; nos-pA = nos polyadenylation signal sequence; LB = left border

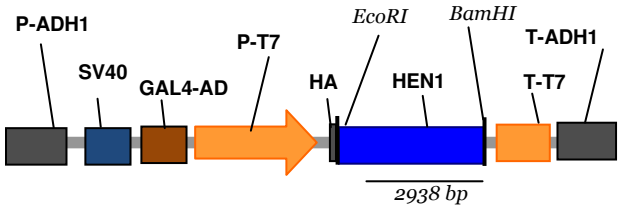

pGADT:SlHEN1

Figure B-4: Schematic overview of the pGADT:SlHEN1 construct. P-ADH1 = *Saccharomyces cervisiae* ADH1 promotor; SV40 = Simian-virus 40 nuclear localization signal; GAL4-AD = GAL4 DNA binding domain; P-T7 = T7 RNA polymerase promotor; HA = hemagglutinin epitop tag; HEN1 = Hua Enhancer 1 cDNA; T-T7 = T7 RNA polymerase transcription termination signal; T-ADH1 = *S. cervisiae* ADH1 transcription termination signal.

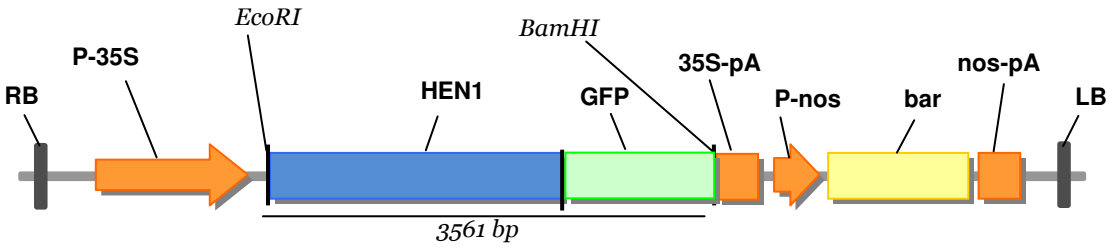

pPCV702SM:HEN1-GFP

Figure B-5: Schematic overview of the pPCV702SM:HEN1-GFP construct. RB = right border; P35S = cauliflower mosaic virus (CaMV) 35S promoter; HEN1= Hua Enhancer 1; GFP = green fluorescent protein; CaMV 35S polyadenylation signal sequence; P-nos = nopaline synthase gene promoter; bar = bialaphos resistance gene; nos-pA = nos polyadenylation signal sequence; LB = left border

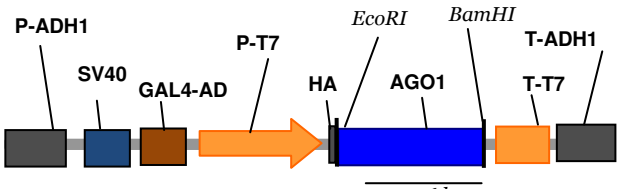

pGADT:NbAGO1

Figure B-6: Schematic overview of the pGADT:NbAGO1 construct. P-ADH1 = *Saccharomyces cervisiae* ADH1 promotor; SV40 = Simian-virus 40 nuclear localization signal; GAL4-AD= GAL4 DNA activation domain; P-T7 promotor= T7 RNA polymerase promotor; HA = hemagglutinin epitop tag; AGO1 = Nicotiana benthamiana Argonaute 1 coding region; T-T7 = T7 RNA polymerase transcription termination signal; T-ADH1 = *S. cervisiae* ADH1 terminator.

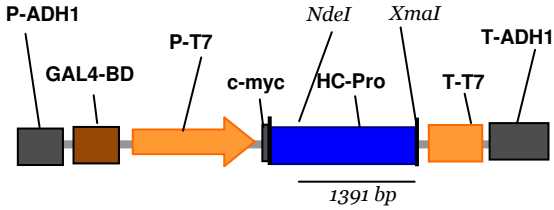

pGBKT:HC-Pro$^{FRNK/FINK}$

Figure B-7: Schematic overview of the pGBKT:HC-Pro$^{FRNK/FINK}$ constructs. P-ADH1 = *Saccharomyces cervisiae* ADH1 promotor; GAL4-BD= GAL4 DNA binding domain; P-T7 = T7 RNA polymerase promotor; c-myc = Transcription factor c-myc epitop tag; HC-Pro = Helper component protein (HC-Pro^{FRNK} or HC-Pro^{FINK}); T-T7 = T7 RNA polymerase transcription termination signal; T-ADH1 = *S. cervisiae* ADH1 transcription termination signal.

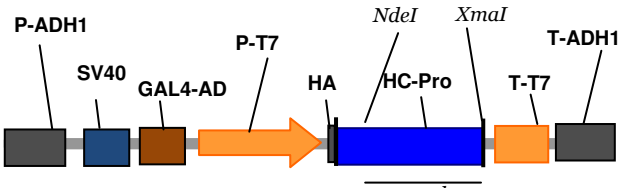

pGADT:HC-Pro$^{FRNK/FINK}$

Figure B-8: Schematic overview of the pGADT: HC-Pro$^{FRNK/FINK}$ constructs. P-ADH1 = *Saccharomyces cervisiae* ADH1 promotor; SV40 = Simian-virus 40 nuclear localization signal; GAL4-AD= GAL4 DNA activation domain; P-T7 = T7 RNA polymerase promotor; HA = hemagglutinin epitop tag; HC-Pro = Helper component protein (HC-Pro^{FRNK} or HC-Pro^{FINK}); T-T7 = T7 RNA polymerase transcription termination signal; T-ADH1 = *S. cervisiae* ADH1 transcription termination signal.

Appendix C: Solutions, Buffers and Media

Buffer and solutions for Western blot analysis

• Total protein extraction buffer	1	ml	Glycerol (10%)
	1.4	ml	Tris-HCl (1,5 M), pH = 8.0
	0.5	ml	ß-mercaptoethanol
	2	ml	SDS (10%)
	10	ml	ddH_2O
• Protein loading buffer	1	ml	Glycerol (10%)
	1	mM	Tris-HCl, pH = 6.8
	0.5	ml	ß-mercaptoethanol
	2	ml	SDS (10%)
	10	ml	ddH_2O
	0.01%	(w/v)	Bromphenol blue
• Protein running buffer (1x for SDS-PAGE)	25	mM	Tris-HCl, pH = 6.8
	200	mM	Glycin
	0.1	% (w/v)	SDS
	1	L	ddH_2O
• Transfer buffer (1x for Western blot)	300	mM	Tris-HCl, pH = 8.0
	2.4	M	Glycin
	20	% (v/v)	Methanol
	Ad to 1 l		ddH_2O
• Marvel buffer (1x)	20	mM	Tris-HCl, pH = 7.8
	80	mM	NaCl
• PBS (10x)	80	g	NaCl
	2	g	KCl
	26.8	g	Na_2HPO_4
	2.4	g	K_2HPO_4
pH 7.4	Ad to 1 l		ddH_2O
• PBST (1x)	0.1	% (v/v)	Tween20
	1	l	1x PBS
• Coomassie blue straining solution	0.1	% (w/v)	CBB G250
	10	% (v/v)	Acetic acid
	40	% (v/v)	Methanol
	Ad to 100 ml		ddH_2O
• Destraining solution	37.5	ml	Methanol
	25	ml	Acetic acid
	Ad to to 500 ml		ddH_2O

Solutions for Chemiluminescence detection

• Chemiluminescence detection substrate	500	µl	Solution A
	50	µl	Solution B
	0.15	µl	H_2O_2 (30%)
• Solution A	5	ml	Tris-HCl (0.1 M), pH = 8.5
	1.25	mM	Luminole
	0.2	mM	Coumaric acid
	Ad to 50 ml		dH_2O
• Solution B	11	mg	Para-hydroxy-coumarine-acid
	10	ml	DMSO
• Developing solution	103	ml	Developer and replenisher®
	370	ml	ddH_2O
• Fixing solution	103	ml	Fixer and replenisher®
	370	ml	ddH_2O

Solutions for protoplast preperation from plants

• Enzyme solution (Protoplast)	1.2	% (w/v)	Cellulose R10
	3	% (w/v)	Macerozyme R10
	14	% (w/v)	Sucrose
	10	mM	$CaCl_2$
	20	mM	KCl
	20	mM	MES
	0.1	% (w/v)	BSA
Adjust pH 5.7	Ad to 20 ml		ddH_2O
• W5 solution	154	mM	NaCl
	125	mM	$CaCl_2$
	5	mM	KCl
	2	mM	MES pH 5.7

Solutions and medium for transformation of yeast cells

YPDA medium	20	g/l	Peptone
	10	g/l	Yeast extract
	20	g/l	Agar
	2	% (W/V)	Dextrose (Glucose)
• 1.1x TE/LiAc	1	ml	10x TE (pH = 7.5)
	1	ml	LiAc
	Ad to 10 ml		ddH_2O
• PEG/LiAc	8	ml	PEG 4000 (50%)
	1	ml	TE buffer 10x (pH = 7.5)
	1	ml	LiAc

• TE buffer 10x	100	mM	Tris-HCl, pH = 7.5
Adjust pH 7.5	10	mM	EDTA
• SD medium	6.7	g	Yeast nitrogen base without amino acids
	20	g	Agar (for plates only)
	850	ml	ddH_2O
	100	ml	10x dropout solution
• 10x dropout solution	200	mg	L-Adenine hemisulfate salt
	200	mg	L-Arginine HCl
	200	mg	L-Histidine HCl monohydrate
	300	mg	L-Isoleucine
	1	g	L-Leucine
	300	mg	L-Lysine HCl
	200	mg	L-Methionine
	500	mg	L-Phenylalanine
	2	g	L-Threonine
	200	mg	L-Tryptophan
	300	mg	L-Tyrosine
	200	mg	L-Uracil
	1.5	g	L-Valine
	Ad to 1 l		ddH_2O

Solutions for protein extraction from yeast

• Cracking buffer	48	g	Urea 8 M
	5	% (w/v)	SDS
	40	mM	Tris-HCl, pH = 6.8
	0.1	mM	EDTA
	40	mg	Bromophenol blue
	Ad to 100ml		ddH_2O
• Cracking buffer (complete)*	1	ml	Cracking buffer stock solution
	10	µl	β-mercaptoethanol
	70	ul	Protease inhibitor solution
	50	ul	PMSF 100x
	Ad to 1.13 ml		ddH_2O

**Prepare only the nedded volume just before use*

Buffers for gel electrophoresis

• TAE buffer (10x)	48.4	g	Tris-HCl, pH = 8.0
	11	ml	Acetic acid
	25	500 mM	EDTA
	1	l	ddH_2O

• TBE buffer (10X)	108	g	Tris-HCl, pH = 8.3
	55	g	Boric acid
	40	ml	EDTA (0.5M), pH = 8.0
	Ad to 1 l		ddH_2O

Medium and solutions for cloning and transformation

• LB-Medium (pH = 7.5)	1	% (w/v)	Trypton
	0.5	% (w/v)	Yeast extract
	1	% (w/v)	NaCl
On LB plates	1.5	% (w/v)	Agar
• SOB-Medium	0.5	% (w/v)	Yeast extract
Sterile $MgCl_2$ and $MgSO_4$ were added after autoclaving	2	% (w/v)	Trypton
	10	mM	NaCl
	2.5	mM	KCl
	10	mM	$MgCl_2$
	10	mM	$MgSO_4$
• SOC-Medium	20	mM	Glucose in SOB-Medium
• Agrobacterium induction medium	100	µl	MES (1 M)
	10	µl	Acetosyringone (200 mM)
	180	mg	D-glucose
	43	mg	MS salts
	10	ml	ddH_2O
• Medium for floral dip of *A. thaliana*	2.165	g	MS salts
	5	% (w/v)	sucrose
	500	µl	Silvet L-77
	1	ml	Acetosyringone (200 mM)
	Ad to 1 l		ddH_2O
½ MS-agar plates for regeneration	1.1	g	Sucrose
	5	g	MS salts
	4	g	Plant-Agar
Adjust pH 7.0 with KOH	Ad to 500 ml		ddH_2O

Solutions for northern blot

• MOPS 10x	41.85	g	MOPS
	6.80	mM	$NaOAc - 3H_2O$
	20	ml	EDTA
	Ad to 1 l		ddH_2O

Adjust pH to 7.0 with 10 M NaOH. Store at 4°C / dark

• RNA-loading dye	30	% (w/v)	Ficoll
	10	mM	EDTA (pH = 8)
	0.25	% (w/v)	Bromophenol blue
	0.25	% (w/v)	Xylene cyanol
• Denaturating buffer	500	µl	Deionized formamide
	120	µl	Formaldehyde (37%)
	200	µl	MOPS 10x
	120	µl	ddH_2O
	1	µl	EtBr
• 20x SSC	173.3	g	NaCl
	88.2	g	Sodium citrate - $2H_2O$
Adjust pH to 7.0 with HCl	Ad to 1 l		ddH_2O
• 2 x TBE-urea buffer	0.5	1x	TBE buffer
	12	% (w/v)	Ficoll 400
	0.01	% (w/v)	Bromophenol blue
	0.05	% (w/v)	Xylene cyanol
	7	M	Urea
• Wash buffer	2	x	SSC
	2	% (w/v)	SDS

General statement

I declare that I am the sole author of this submitted dissertation and that I did not make use of any sources or help apart from those specifically referred to. Experimental data or material collected from or produced by other persons is made easily identifiable.

I also declare that I did not apply for permission to enter the examination procedure at another institution and that the dissertation is neither presented to another faculty nor used in its current or any other form in other examination.

Curriculum Vitae

Personal Information

Name: Rana M. Jamoos
Place & Date of Birth: Nablus, 1967
Nationality: Palestinian

Honors/ Awards

The Hisham Hijjawi Award for Applied Sciences in the Field of Industry and Environment for the Year 1999. Awarded in recognition of the distinguished applied scientific value of research article entitled: "Ecology of cycloheximide-resistant fungi in field soils receiving raw city wastewater or normal irrigation water." *Mycopathologia* 144:39-54.

Education

B.Sc. Biology, (1992). ***An-Najah Univ***, Dept Biological Sci, Nablus, Palestine.

MSc., Biological Sciences, (1998). ***An-Najah Univ***, Dept Biological Sci, Nablus, Palestine.

Title of MSc Thesis: *"Ecology of cycloheximide-resistant fungi in field soils receiving raw city waste water or normal irrigation water in nablus area."*

Work Experience

2001-2007: **Coordinator and Researcher** of Biodiversity and Biotechnology Research Unit, (BBRU). Biodiversity & Environmental Research Center (BERC*),* Til, Nablus, West Bank.

2010-now Researcher and Head of BBRU, BERC.

Publications

Ali-Shtayeh, M.S., **JAMOUS, R.M**., Hussein, E.Y., Mallah, O.B. & Abu-Zaitoun, S.Y. (2011). First Report of watermelon chlorotic stunt virus (WmCSV) in watermelon (*Citrullus lanatus*), and cucumber (*Cucumis sativa*) in the Palestinian Authority. *Plant Disease* (accepted), available online – First Look. (http://apsjournals.apsnet.org/toc/pdis/0/ja).

JAMOUS, R.M., Boonrod, K., Fuellgrabe, M.W., Ali-Shtayeh, M.S., Krczal, G. & Wassenegger, M. (2011). The HC-Pro of the *Zucchini Yellow Mosaic Virus* (ZYMV) inhibits HEN1 methytransferase activity *in vitro*. *J Gen Virol* 92: 2222-2226. doi:10.1099/vir.0.031534-0.

Fuellgrabe, M.W., Boonrod, K., **JAMOUS, R**., Moser, M., Shiboleth, Y., Krczal, G. & Wassenegger, M. (2011). Expression, purification and functional characterization of recombinant Zucchini yellow mosaic virus HC-Pro. *Protein Expr Purif* 75: 40–45. doi:10.1016/j.pep.2010. 07.008.

Ben-Arye, E., Ali-Shtayeh, M.S., Nejmi, M., Schiff, E., Hassan, E., Mutafoglu, K., Afifi, F., **JAMOUS, R.M**., Lev, E. & Silbermman, M. (2011). Integrative oncology research in the Middle-East: Weaving traditional and complementary medicine in supportive care. *Supportive Care* Cancer DOI 10.1007/s00520-011-1121-0 (Manuscript No: JSCC-D-10-00476R2, Published online: 01 March 2011).

Ali-Shtayeh M.S., **JAMOUS, R.M**. & Jamous, R.M. (2011). Complementary and Alternative Medicine use amongst Palestinian diabetic patients. *Complementary Therapies in Clinical Practice*, doi:10.1016/j.ctcp.2011.09.001.

Ali-Shtayeh M.S., **JAMOUS, R.M.** & Jamous, R.M. (2011). Herbal preparation use by patients suffering from cancer in Palestine. *Complementary Therapies in Clinical Practice*,17: 235-240. http://dx.doi.org/10.1016/j.ctcp.2011.06.002.

Ali-Shtayeh, M.S., Deeb Ali, W.M. & **JAMOUS, R.M**. (2010). Ecological investigations on terrestrial arthropod biodiversity under different grassland ecosystems in El-Fara'a area (Palestine). *Biodiversity and Environmental Sciences Studies* 5: 19-34.

Ali-Shtayeh, M.S., **JAMOUS, R.M.** *et al.* (2008). Traditional knowledge of wild edible plants used in Palestine (Northern West Bank): A comparative study. *Journal of Ethnobiology and Ethnomedicine*, 4:13. (Highly accessed)

Ali-Shtayeh, M.S. & **JAMOUS, R.M.** (2008). Traditional Arabic Palestinian Herbal Medicine, TAPHM. Til, Nablus, Palestine, Biodiversity and Environmental Research Center, BERC.

Ali-Shtayeh, M.S. & **JAMOUS, R.M**. (2006). Field Guide on the Production and Storage Techniques of Seeds of Indigenous (Baladi) Varieties of Vegetables. Til, Nablus: Biodiversity & Environmental Research Center.

Ali-Shtayeh, M.S., **JAMOUS, R.M**. & AL-Khader, M.Y. (2006). Field guide to the "New

Hakooreh". Til, Nablus: Biodiversity & Environmental Research Center. (In Arabic).

Ali-Shtayeh, M.S., & **JAMOUS, R.M**. (2006). Ethnobotany of Palestinian Herbal Medicine in the Northern West Bank and Gaza Strip: A Review and a Comprehensive Field Study. *Biodiversity and Environmental Sciences Studies 4*: 1-128.

Ali-Shtayeh, M.S. & **JAMOUS, R.M**. (2005). Establishing a community seed bank for semi-arid agriculture in Palestine: Structure, management, and function**.** *Biodiversity and Environmental Sciences Studies* 3: 1-42

Ali-Shtayeh, M.S, Zayed R.A & **JAMOUS, R.M.** (2003). Palestinian plants as a source of antimycotics. In: M.K. Rai and D. Mares (Editors) *Plant derived antimycotics*. Binghamton: The Haworth Press.

Ali-Shtayeh, M.S., Salah , A.A. & **JAMOUS, R.M.** (2003). Ecology of hymexazol-insensitive *Pythium* species in field soils. *Mycopathlogia* 156: 333-342.

Ali-Shtayeh, M.S., **JAMOUS, R.M**. & Hamad, A.K.H. (2003). Guide to trees and shrubs from Palestine. Til, Nablus: Biodiversity & Environmental Research Center.

Ali-Shtayeh, M.S. & **JAMOUS, R.M.** (2003). BERC-TIL botanic gardens newsletter. Til, Nablus: Biodiversity and Environmental Research Center (BERC). In Arabic**.**

Ali-Shtayeh, M.S., Mari', A.B. & **JAMOUS, R.M.** (2003). Distribution, occurrence and characterization of entomopathogenic fungi in agricultural soil in the Palestinian Area. *Mycopathologia* 156: 235-244.

Ali-Shtayeh, M..S., Khaleel, T.Kh. & **JAMOUS, R.M**. (2002). Ecology of dermatophytes and other keratinophilic fungi in swimming pools and polluted and unpolluted streams. *Mycopathologia* 156: 193-205.

Ali-Shtayeh, M.S. & **JAMOUS, R.M.** (2002). "Red list of threatened plants" of the West Bank and Gaza Strip and role of botanic gardens in their conservation. *Biodiversity and Environmental Sciences Studies 2*: 1-47.

Ali-Shtayeh, M.S. & **JAMOUS, R.M.** (2002). Biodiversty: Value and conservation. *Biodiversity and Environmental Sciences Studies 1*: 1-38.

Ali-Shtayeh, M.S., Salameh, A.A.M., Abu-Ghdeib, S.I., **JAMOUS, R.M.** & Khraim, H. (2002). Prevalence of asymptomatic tinea capitis carriers in school children in Nablus area (Palestine). *Mycoses* 45: 188-194 .

Ali-Shtayeh, M.S., Salameh, A.A.M., Abu-Ghdeib, S.I. & **JAMOUS, R.M.** (2001). Hair and scalp mycobiota in school children in Nablus area. *Mycopathologia* 150: 127-135.

Ali-Shtayeh, M.S. & **JAMOUS, R.M.** (2000). Keratinophilic fungi and related dermatophytes in polluted soil and water habitats. In: Kushwaha, RKS, & Guarro, J. (Eds.) Biology of Dermatophytes and other Keratinophilic Fungi. Revista Iberoamericana de Micologia (pp. 51-59). Bilbao.

Ali-Shtayeh, M.S., **JAMOUS, R.M.** & Abu-Ghdeib, S.I. (1999). Ecology of cycloheximide-resistant fungi in field soils receiving raw city wastewater or normal irrigation water. *Mycopathologia* 144:39-54.

Rana M. Jamoos